Physicochemical Study of Nano-structuring Within Ionic Liquids Using Photoswitchable Spirocyclic Compounds

Simon Coleman B.Sc.

Thesis submission for the Degree of Doctor of Philosophy

Supervisors: Professor Dermot Diamond
Dr. Robert Byrne

School of Chemical Sciences

Dublin City University

January 2011

I may, I might, I must

If you will tell me why the fen appears impassable,
I then will tell you why I think that I can get across it if I try

Marriane Moore

Declaration

I hereby certify that this material, which I now submit for assessment on the programme of study leading to the award of Doctor of Philosophy is entirely my own work, that I have exercised reasonable care to ensure that the work is original, and does not to the best of my knowledge breach any law of copyright, and has not been taken from the work of others save and to the extent that such work has been cited and acknowledged within the text of my work.

Signed: ________________________

Simon Coleman

ID No.: 52598191

Date: _____________

Acknowledgements

I'd like to thank everyone who believed in me and supported me throughout my entire studies. Firstly, to Prof. Dermot Diamond for seeing the potential and taking a chance on me. Without the opportunity you offered I wouldn't be where I am today! To Dr. Robert Byrne, I owe the same sentiment. I'd heard so many glowing reviews of how he was a natural at this research lark and one to watch. My project was somewhat turbulent to start and your focus and foresight gave me the guidance I needed to get my own career off the ground. We are flying high now! I feel uniquely fortunate that I can also call you a friend as well as a colleague. The informal meetings on the surf boards certainly allowed for abstract project discussions! Seriously owe you! To all of the guys in the group for all your help over the years. Its great to have such a diverse group with so many different areas of expertise. A special thanks goes out to Dr. Stephen Beirne for all his help fabricating my gadgets. Dr. Martina O'Toole who sat next to me for a year in SG03 and listened to my constant ramblings of frustration and offering her advice with the benefit of hindsight! Andy Kavanagh, who spent two months living in a shoe box in Melbourne with me and didn't kill me! The best person you could ever share a desk with (SG03 always had good music!) and good for discussions on all things ionic!! The two Johns, Breda, Emer, Daniel, Damien, Dylan, Cormac in N205 and Silvia, Michele, XuYuan, Caroline, Larisa and Bartosz in SG03. Thanks for all the help, even if it was just be bouncing ideas off you! Lastly I want to say my deepest thanks to my family. They have always supported me in everything I have chosen to do and have been a source of strength when times were tough. This is as much for you as it is for me; I am who I am because of you guys! Now… time to get a job and leave you alone!!!

Publication List

Thermal reversion of Spirooxazine in ionic liquids containing the $[NTf_2]^-$ anion

Simon Coleman, Robert Byrne, Stela Minkovska and Dermot Diamond
Physical Chemistry Chemical Physics, **2009**,11,*5609*

Photochromism of nitrobenzospiropyran in phosphonium based ionic liquids

Robert Byrne, Simon Coleman, Kevin J Fraser, Ana Raduta, Douglas R. MacFarlane and Dermot Diamond
Physical Chemistry Chemical Physics, **2009**, 11*, 7286*

Investigating nano-structuring within imidazolium ionic liquids:
A thermodynamic study using photochromic molecular probes

Simon Coleman, Robert Byrne, Stela Minkovska and Dermot Diamond
Journal of Physical Chemistry B, **2009**, 47,*113*

Designer Molecular Probes for Phosphonium Ionic Liquids

Robert Byrne, Simon Coleman, Simon Gallagher and Dermot Diamond.
Physical Chemistry Chemical Physics,**2010**, 12, *1895*

Photo-functional Imidazolium Ionic Liquids containing a novel spiropyran cation

Simon Coleman, Robert Byrne, Nameer Alhashimy, Kevin J Fraser, Douglas R MacFarlane and Dermot Diamond
Physical Chemistry Chemical Physics,**2010**, 12, 7009

Physicochemical experiments and electronic structure calculations reveal competitive, tuneable ion-pair and ion-probe interactions for nitrobenzospiropyran in phosphonium-based ionic liquids.

Damien Thompson, Simon Coleman, Dermot Diamond, and Robert Byrne
Physical Chemistry Chemical Physics, **2010**, *In review*

Conference contributions

Posters

Investigating nano-structured domains within ionic liquids: the effect of cation change on thermal equilibrium and relaxation of spiropyran and spirooxazine.
Simon P Coleman, Robert Byrne, Stella Minkovska and Dermot Diamond

COIL-3: 3rd Congress on Ionic Liquids, Cairns Convention Centre, Cairns, Queensland, Australia, May 31st- June 4th 2009.

Structural analysis of photoswitchable imidazolium ionic liquids based on the [NTf $_2$***]*** $^-$ ***anion***
Simon Coleman, Robert Byrne Kevin J Fraser, Douglas R MacFarlane and Dermot Diamond

42nd IUPAC World Chemistry Congress: Chemistry Solutions, Scottish Exhibition and Conference Centre, Glasgow, Scotland, August 2nd – August 7th 2009.

Oral Presentations

Structural analysis of photoswitchable imidazolium ionic liquids based on the [NTf $_2$***]*** $^-$ ***anion***
Simon Coleman, Robert Byrne Kevin J Fraser, Douglas R MacFarlane and Dermot Diamond

Oral poster preview presentation

42nd IUPAC World Chemistry Congress: Chemistry Solutions, Scottish Exhibition and Conference Centre, Glasgow, Scotland, August 2nd – August 7th 2009.

Project collaborations

Investigation of nano-structuring within Ionic Liquids
Collaboration with Prof. Douglas MacFarlane

MacFarlane Ionic Liquids Group, Monash University, Melbourne, Australia
June- August 2009 (8 weeks)

Theoretical studies of liquid ion pair formation in ionic liquids
Collaboration with Dr. Damien Thompson

Tyndall National Institute, Lee Maltings, Cork, Ireland
January-February 2010 (5 weeks)

Abbreviations

ACN	Acetonitrile
$[bmPy]^+$	1-butyl-1-methylpyrrolidinium cation
BSP	2,3-dihydro-1’,3’,3’-trimethyl-6-nitrospiro[1-benzopyran-2,2’-1H-indole]
BSP-1	BSP Hydroxyl derivative
BSP-2	BSP Carboxylic acid derivative
BSP-3	BSP Tetradecane derivative
$[C_nmIm]^+$	3-alkyl-1-methylimidazolium cation (n = carbon chain length)
$[Cl]^-$	Chloride anion
$[dbsa]^-$	dodecylbenzylsulfonic acid anion
$[dca]^-$	dicyanamide anion
DCM	Dichloromethane
DSC	Differential Scanning Calorimetry
E_a	Activation energy
EPD	Electron pair dononation
EPA	Electron pair acceptance
EtOH	Ethanol
H-Bond	Hydrogen bond
HOMO	Highest occupied molecular orbital
IL	Ionic Liquid (typically used to following description of system: “imidazolium based IL”)
$K^‡$	Equilibrium of activation
K_e	Ground state equilibrium constant
LED	Light emitting diode
LUMO	Lowest unoccupied molecular orbital

MC_x	Merocyanine (spirocyclic compound open form). x denotes the parent compound that is in its open form (BSP/SO/SP_{Im})
MeOH	Methanol
NIR	Near infrared
$[NTf_2]^-$	Bis(trifluorosulfonyl)imide anion
$[P_{6,6,6,14}]^+$	Trihexyltetradecylphosphonium cation
QM	Quantum mechanics
SO	1,3,3-trimethyl-5’-(2-benzothiazolyl)-spiroindoline-2,3’-naphtho(2,1-b)(1,4) oxazine
SP	Spiro (spirocyclic compound closed from)
SP_{Im}	1́ - (3″-methylimidazolioethyl)-3́,3́–dimethyl-6 -nitrospiro–[2*H*-1-benzopyran-2,2́-indoline] bromide
TGA	Thermogravimetric analysis
$[tos]^-$	tosylate anion
UV/Vis	Ultraviolet/visible spectrometry
ΔE	binding energy
$\Delta G^\ddagger$	Gibbs energy of activation
$\Delta H^\ddagger$	Enthalpy of activation
Δq	difference in charge distribution
$\Delta S^\ddagger$	Entropy of activation
α	Hydrogen bond acidity
β	Hydrogen bond basicity
π^*	Polarisability
‡	Double dagger (transition state)

ABSTRACT

1. INTRODUCTION

2. NOVEL ENVIRONMENTS FOR SOLUTION BASED PHOTOCHEMISTRY: THERMODYNAMIC AND KINETIC STUDY OF SPIROCYCLIC COMPOUNDS IN IONIC LIQUIDS

3. INVESTIGATION OF STRUCTURING IN IONIC LIQUIDS BASED ON THE $[NTf_2]$ ANION

4. SPECIFIC PROBING OF IONIC LIQUID DOMAINS USING FUNCTIONALISED SPIROPYRAN DERIVATIVES

5. PHYSICOCHEMICAL AND THEORETICAL STUDY OF 'IONICITY' BASED UPON LIQUID ION PAIR FORMATION IN IONIC LIQUIDS USING SPIROPYRAN

6. INTEGRATION EFFECTS OF A NOVEL PHOTO-FUNCTIONAL SPIROPYRAN CATION UPON IMIDAZOLIUM BASED IONIC LIQUID NANOSTRUCTURE

7. CONCLUSIONS AND FUTURE WORK

A. APPENDIX

Abstract

Ionic liquids (ILs) are presented as novel solvents for the replacement of organic solvents and the formation of smart liquids. The following thesis investigates the proposed nano- and atom-scale structuring of ionic liquids, a feature that appears to totally underpin their unique behavioural characteristics and facilitate accurate predictions of trends. Solvent organisation is one of the most fundamental properties of any liquid as it determines more complex processes such as solvation and reaction dynamics. It is believed that unique ordering in ionic liquids results form a balance between *anion-cation*, *cation-cation* and most importantly, *ion-pair* formation. The final parameter has been found to be critical to the 'ionicity' or transport properties of the liquids and these atom-atom interactions mediate the dissociation of the ions and thus the ability to form solvation shells associated with the 'ionic liquid effect'. To probe ionic liquid behaviour, the effect of cation changes were examined experimentally and compared to that of model systems drawn for conventional molecular solvents.

Initial studies (Chapter 2) involved the addition of photochromic spirocyclic compounds to ionic liquids which interact with both nano-domains within the liquid structure and report the environment present based upon the rates of thermal relaxation of the compounds from their open merocyanine (**MC**) form to their closed (**SP**) form and the equilibrium effects upon the **MC-SP** inter-conversion and the dependence of cation and anion choice while optimising the choice of probe molecule by establishing whether spiropyran (**BSP**) or spirooxazine (**SO**) met the required sensitivity to effectively probe the ionic liquids.

Subsequent studies (Chapter 3-4) focus upon the effects of nano-structuring in imidazolium and phosphonium based ionic liquids through kinetic and thermodynamic analysis and attempt to rationalise the formation for these distinct nano-domains. Such formations produce complex solvent systems which current methods of charactertisation appear unable to quantify sufficiently, in particular, the 'polarity' of ionic liquids. The dynamic nature of the **BSP/SO-MC$_{\mathbf{BSP/SO}}$** interconversion allows for the unique ability of the compound to examine both regions through migration and solvent reorganisation and thus report parameters previously incomprehensible to traditional probe dyes. Derivatives of spiropyran were subsequently added to ionic liquids to preposition them within the specific regions of the liquids defined by previous experiments to allow for more specific characterisation of the properties of each nano-domain.

Final investigations (Chapter 5) examine the novel theory that the unique properties ionic liquids and indeed the nano-structuring observed may be due to liquid organisation occurring at the atomic level. Studies involved the comparison of experimental data based upon thermodynamic and kinetic parameters to quantum mechanical models of ionic liquid ion pairs and their interaction with the **MC** form of the probe molecule. The formation of Liquid Ion Pairs (LIPs) is believed to be the precursor to the nano-structures which in turn mediate the unique bulk properties of the liquids such as their transport properties. Future work outlines the integration of spiropyran into the ionic liquid nanostructure and the possibility of manipulating the ion pair interactions to produce ionic liquids with photoswitchable rheological properties and possible application in light mediated sensing.

1

Introduction

1.1 Liquids: solutions and solvation

According to the states of matter, liquids lie as an intermediate between solids and gases. Where solids possess strong inter-molecular interactions that result in a rigid, highly structured system, gases lack these associations and the molecules are free to disperse infinitely to fill the container they are placed in. Liquids have properties of both of these states whereby a liquid contains sufficient inter-molecular interactions to retain a set volume but these interactions remain weak enough for the material to flow freely and conform to the shape of the container it is placed within (providing sufficient volume of liquid).

It is these intermediate properties that make liquids particularly interesting as they allow liquids to dissolve both solids and gasses within them to form solutions. The ability of a liquid to dissolve a solute is known as solvation and is a distinct property in each individual solvent. Traditionally solvation has been determined by the use of parameters which determine the 'polarity' of a solvent. By definition, 'like dissolves like' polar solvents are highly solvating to solutes composed of charged groups such as ions/salts while non-polar solvents dissolve neutral aliphatic hydrocarbon chain based materials. The ability of a liquid to dissolve various solutes is important as this allows for a vast quantity of chemical reactions to proceed. The primary issue with current solvents (molecular solvents/volatile organic solvents) is the waste they generate and the hazard they pose due to their volatility. For this reason 'green' alternatives have been actively sought after. A relatively new class of solvents known as ionic liquids (ILs) are becoming increasing popular as viable replacement solvents to molecular solvents due to their favourable inherent properties. However, for effective implementation of these novel solvents, extensive studies must be carried out into their physical properties to ensure they can compete with or improve upon similar processes in molecular solvents.

1.2 Ionic liquids

1.2.1 History of ionic liquids

The reported discovery of ionic liquids dates back to the mid-late nineteenth century with the formation of a by-product of $AlCl_3$-catalysed Friedel-Crafts reaction which produced a ‘red oil,[1] later found to be composed of a carbocation and tetrachloroaluminate anion.[2] In 1914, Paul Walden is widely acknowledged as synthesising the first truly ionic liquid with the formation of ethylammonium nitrate.[3] Detailed analysis of ionic liquids began to emerge in the 1980s when the focus of their application as electrolytes in batteries[4, 5] and subsequently electroplating of metals (1992)[6,7] was initiated. Application of ionic liquids subsequently suffered from very little investigation until the 1990s when the formation of water and air stable ionic liquids was reported and opened up new application possibilities.[8] Interest in ionic liquids continued to grow since then with investigations of ionic liquids being applied to techniques including catalysis,[9] elemental analysis[10], synthesis[11] and supercritical fluids.[12, 13] In recent years, with global recognition of the effects of pollution upon climate change, the requirement for ‘green’ solvents has become paramount and ionic liquids now show great promise as replacement solvents in the chemical processes due to their lack of volatility and thermal stability. In addition to this, the use of ionic liquids as dual role solvents is also under consideration whereby the solvent acts as both the solvent system and reactant/catalyst in the reaction process.[14]

1.2.2 Chemical properties of ionic liquids

Ionic liquids are materials, composed entirely of ions, which have melting points below 100 ºC.[15] Ionic liquids are a complex network ions which are mediated by non-specific interactions (electrostatic charges) and specific interactions (hydrogen bonding). The asymmetric form of the ions and their bulky/non-linear association creates a reduction in bond strength between the ions and a corresponding reduction in the coulombic interactions which results in a lowering of the salt melting points.[16] A subclass of these materials known as '*room temperature ionic liquids*' (RTILs) have moved to the forefront of ionic liquid research due to their melting temperatures being below 30°C. These liquids exhibit the most favourable properties for solvent use due to their formation of stable, non-volatile liquids in ambient room conditions while also maintaining their stability over large temperature ranges. Ionic liquids differ from other classes of solvents due to the binary, charged nature of the liquids when compared to atomic or molecular solvents (figure 1.1).

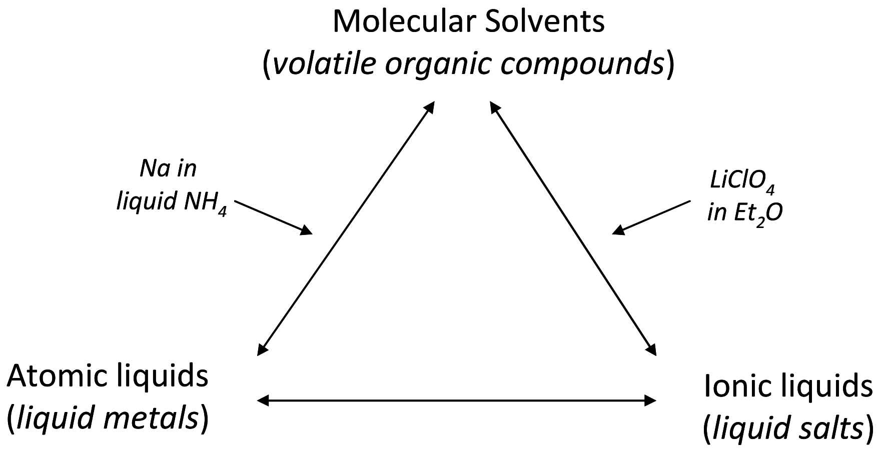

Fig 1.1 Classification of solvents based on their characteristic chemical bonds.[17]

Atomic liquids such as liquid mercury or sodium contain individual atoms of the element and consist of single components which weakly associate to form liquids. Similarly, molecular solvents, such as ethanol, consist of single molecules whose associations, such as hydrogen bonding, create common organic solvents. Ionic liquids present themselves as binary components whereby each liquid 'unit' of the liquid consists of two ionic molecules and a completely charged system (figure 1.2). Although several molecular solvents such as H_2O can undergo autoprotolysis (formation of charged species, in this case H_3O^+) which produces small but not insignificant numbers of ions,[17] molecular solvents are considered to consist of neutral molecules (slight charges associated with dipoles neutralise one another in each molecule). Intermediates between each class of liquid can also exist. Certain mixtures of salts and molecular solvents can be considered dilute ionic liquids such as 5M lithium perchlorate in diethyl ether. However the extensive diffusion of the lithium ions resulting from a ratio of approximately 2:1 ether : lithium which is not fully coordinated and not a true ionic liquid. Structurally, ionic liquids ions contain permanent charges, which unlike the diffuse and temporary dipoles of molecular solvents, present a far more complex system. The solvent-solvent interactions, which as a consequence results in low vapour pressures, reduces the risk of exposure through inhalation as observed with molecular solvents with boiling points close to that of room temperature and so removes the requirement for ventilation and/or fumehood confinement to prevent exposure to personnel and solvent loss during experimental procedures due to evaporation.

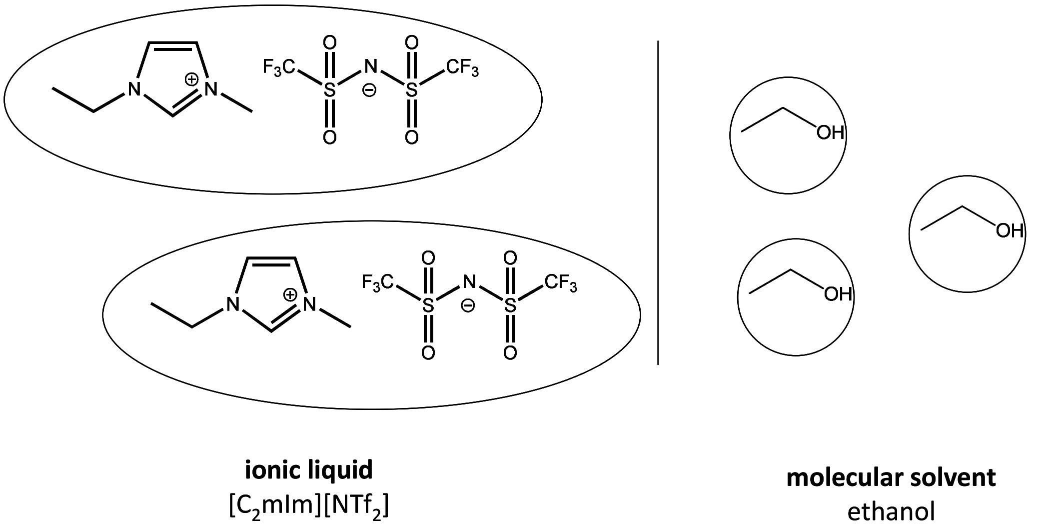

Fig 1.2 Encircled molecules represents solvent ‘unit’. Simple single molecule units produce common molecular solvents (each unit is a single atom in atomic liquids) while ionic liquids consist of binary systems with permanent charges.

Ionic liquids can be recycled, reducing chemical waste and increasing the lifetime of the liquids, further adding to the ‘green’ aspects of ionic liquids.[18] For example, the hydrophobic nature of certain ionic liquids allows for the addition of hydrophobic compounds that, once reacted, form hydrophilic products. The addition of water then allows for the removal of pure products and the removal of the ionic liquid for use once again a reaction medium. The vast numbers of available ions results in a theorised number of possible ionic liquids to be over 10^{14} combinations.[19] For this reason, ionic liquids have become known as ‘designer solvents’[20] whose customisability allows for the ability to endow specific properties upon the final liquid product. Recent innovations in ionic liquid development has produced the popular air and water stable liquids. To minimise water contamination, during metathesis and upon exposure to the environment, perfluorinated anions are commonly used to produce hydrophobic liquids. The anions $[BF_4]^-$ and $[PF_6]^-$ were initially chosen to form ILs but have been found to be of lower thermal stability and undergo spontaneous hydrolysis reactions resulting in the production of HF.[21] Research into more stable fluorine based anions resulted in the discovery of bis(trifluorosulfonyl)imide ($[NTf_2]^-$). The stability of this anion is well established with little or no interaction/reaction found for the ion itself.[22] Lewis acid ionic liquids have been synthesised by the reaction of a halide salt with a lewis acid, most commonly ($AlCl_3$) with the acid in excess (approximate mole ratio of 1:2 salt:acid).[16] The result of this is liquids with inherent catalytic effects.[23] for organic reactions and also be used as the solvent media within which the reaction can take place. The functionalisation of ionic liquid ions has also been extended to pharmaceutical applications. Recent developments has seen the conceptual design of salicylate functionalised cations in an effort to produce 'liquid aspirin' by Rodgers *et al*.[24]

The charged nature of the ions within each ionic liquid creates an inherent conductivity due to ion conduction and thus measurable currents.[25] The result of this has been their increased use in electrochemistry[26] and the evolution of wide electrochemical windows (around 3.7 V for $[C_2mIm][PF_6]$ in ethylene carbonate[27] versus ~2 V in 1M KCL[28]) means that a single ionic liquid can be used for several different experimental conditions without the traditional requirement of changing electrolytes depending on the potential limit required. High thermal stabilities (450 ºC for $[C_2mIm][BF_4]$[29]) and tuneable transport and rheological properties enforce the fact that ionic liquids are durable, customisable materials which show great promise as replacement solvents.[16] The limitation to ionic liquids replacing conventional solvents is the lack of a more precise understanding of the processes occurring within the materials which mediate their unique properties.

Synthetic processes in ionic liquids have highlighted unusual behaviour which has been used to explain what has become known as the ‘ionic liquid effect’. The ‘ionic liquid effect’ is defined as the unique effects observed only in ionic liquids and is attributed to the fact that the liquids consist solely of charged ionic species.[30] Such effects are mediated by a chemical process based upon the interaction of the liquid’s ions with solutes dissolved within. Quantification of such effects has been carried out by Hallett *et al*[31] and Jones *et al*[32] using well understood S_N2 substitution reactions. Since such reactions require a specific interaction and corresponding leaving group, the solvation of the reagents will become critical to such processes. Hallett found that ionic liquids possessed the ability to overcome coulombic interactions traditionally observed in molecular solvents.[31] The result of this is that the liquids become ‘super-dissociating’ and restrict the formation of solute ion pairs and the reaction progressing by a very different process to that in molecular solvents. Similarly, Jones *et al* found that the differing rates of reaction could be explained by examining the reaction process from starting materials to its transition state.[32] It is found that the reactions in ionic liquids proceeded with minimal changes to the enthalpy of activation when compared to that of molecular solvents. Significant increases in the entropy of activations between ethanol and $[C_4mIm][NTf_2]$ of -250 $J.K^{-1}mol^{-1}$ and -229 $J.K^{-1}mol^{-1}$, respectively, led to the conclusion that ionic liquids can interact with the system with the ions ordering around the reaction intermediate as the reaction proceeds. It is for this reason that quantification of the ‘ionic liquid effect’ is of critical importance as the ability to predict the levels of chemical interaction an ionic liquid can possess will allow for the choice of liquids which exhibit maximum effects. Such interactions, observed both thermodynamically, kinetically and using molecular dynamics simulations present convincing evidence that the ‘ionic liquid effect’ not only exists but may rationalise the interesting chemical properties observed in ionic liquids. The unique physical properties found in ionic liquids, believed to be due to the ion-ion and ion-pair interactions has been defined as the ‘ionicity’ of the materials. The concept of ‘ionicity’ is based upon the physical or transport properties of ionic liquids which originate from the charged nature of the solvents.[33] While interactions between molecular solvent molecules are limited predominantly to van der Waals, electrostatic and hydrogen bonding, ionic liquids have the added ability to form ionic interactions due to the permanent charges associated with each molecule. Ionic liquids contain *two* components, oppositely charged ions, which can interact with themselves as well as surrounding solvent molecules.

Molecular solvents follow the traditional system whereby each molecule contains opposing charges within each molecule which results in a relatively neutral system. This differentiates from ionic systems where molecules are inherently charged and molecular solvents rely primarily on directional interactions such as hydrogen bonding to create solvent-solute interaction. The charged nature of ionic liquids is believed to promote increased inter-molecular interactions which in turn results in local structuring within the liquid itself. The ion-ion structure coupled with the charged nature of the system results in a highly conductive matrix whereby electron transfer is mediated. However, the strength of ion-ion interaction also mediates the bulk (viscosity) and nanoscale (ion pairing) properties of the liquid itself. It is then the strength of these physical properties, conductivity and viscosity, that defines its 'ionicity' and this in turn mediates the physicochemical properties observed within the liquid itself. Watanabe *et al*[34] and MacFarlane *et al*[33] discussed the use of Walden plots as an effective scale to measure ionicity based on the dissociative properties of the ions within the liquid. The strength of the ion interactions could then be related to thermodynamic parameters such as enthalpy of vaporisation to link the physicochemical properties of the liquids to the ionicity.

Both the 'ionic liquid effect' and 'ionicity' are believed critical to be the activities observed in ionic liquids but without accurate methods of characterisation the application of this novel class of liquids remains restricted. For this reason, the application of solvent probes to examine the nano-scale differences that are unique to ionic liquids may allow for the examination and quantification of the 'ionic liquid effect' (IL interaction with the probe) and 'ionicity' (disruption of the liquid structure by the probe) which in turn would be of great impact upon solvent characterisation.

1.2.3 Synthesis of ionic liquids

The synthesis of ionic liquids involves the reaction of the target cation and anion salts via metathesis reaction. The process is generally carried out in two stages; formation of the cation required and anion exchange to form the final liquid. Cation synthesis is commonly carried out using a phosphine or amine based systems such as 1-methylimidazole and the application of a quaternisation reaction to form the cation via scheme 1.1 below.

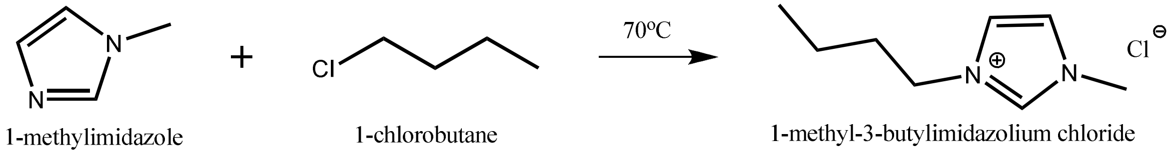

Scheme 1.1 Alkylation (S_N2) reaction of 1-methylimidazole to for cation halide salt.

Scheme 1.1 above shows the process of [C_4mIm][Cl] formation.[35] The alkylation (S_N2) reaction involves the use of relatively inexpensive haloalkanes which act as electrophillic alkylating agents and the resulting nucleophillic substitution reaction of the imidazole molecule results in the formation of the halide salt containing the cation with desired alkyl chain length. The formation of ionic liquids themselves involves the use of anion metathesis. The relevant cation and anion are dissolved in a suitable solvent and stirred for several hours. The reaction proceeds much as an acid-base elimination whereby the ions exchange their counter ions to form the ionic liquid and a salt by-product. Scheme 1.2 shows an example of the metathesis of [C_2mIm] [NTf_2] from its precursor salts.

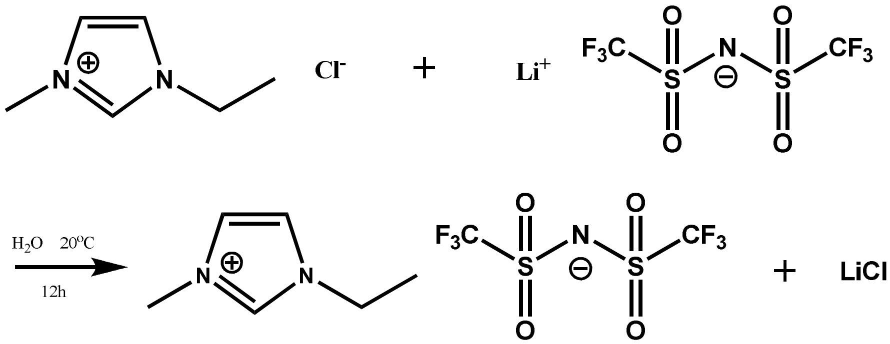

Scheme 1.2 Metathesis of [C_2mIm][NTf_2] from precursor salts.

Perfluorinated ionic liquids in particular have the simplest procedures as they produce hydrophobic ionic liquids. Upon formation, the ionic liquid phase separates from the water and water soluble by-products resulting in a high purity material. For ionic liquids which are water soluble or reactions carried out in organic solvents, the ionic liquids are removed by dissolving the liquids in non-polar solvents and washed with water to remove the hydrophilic by-products, commonly salts. Cations employed are the imidazolium, quaternary ammonium, pyrrolidinium, pyridinium and phosphonium ions while anion selection is bis(trifluoro)sulfonylimide ([NTf$_2$]$^-$), dicyanamide ([dca]), tosylate ([tos]$^-$) and dodecylbenzylsulfonic acid ([dbsa]$^-$). Figure 1.3 illustrates a selection of the most common ions employed to produce ionic liquids of what is only a small representative of the possible ions that can be used to create ionic liquids. Their IUPAC names and their abbreviations are also described.

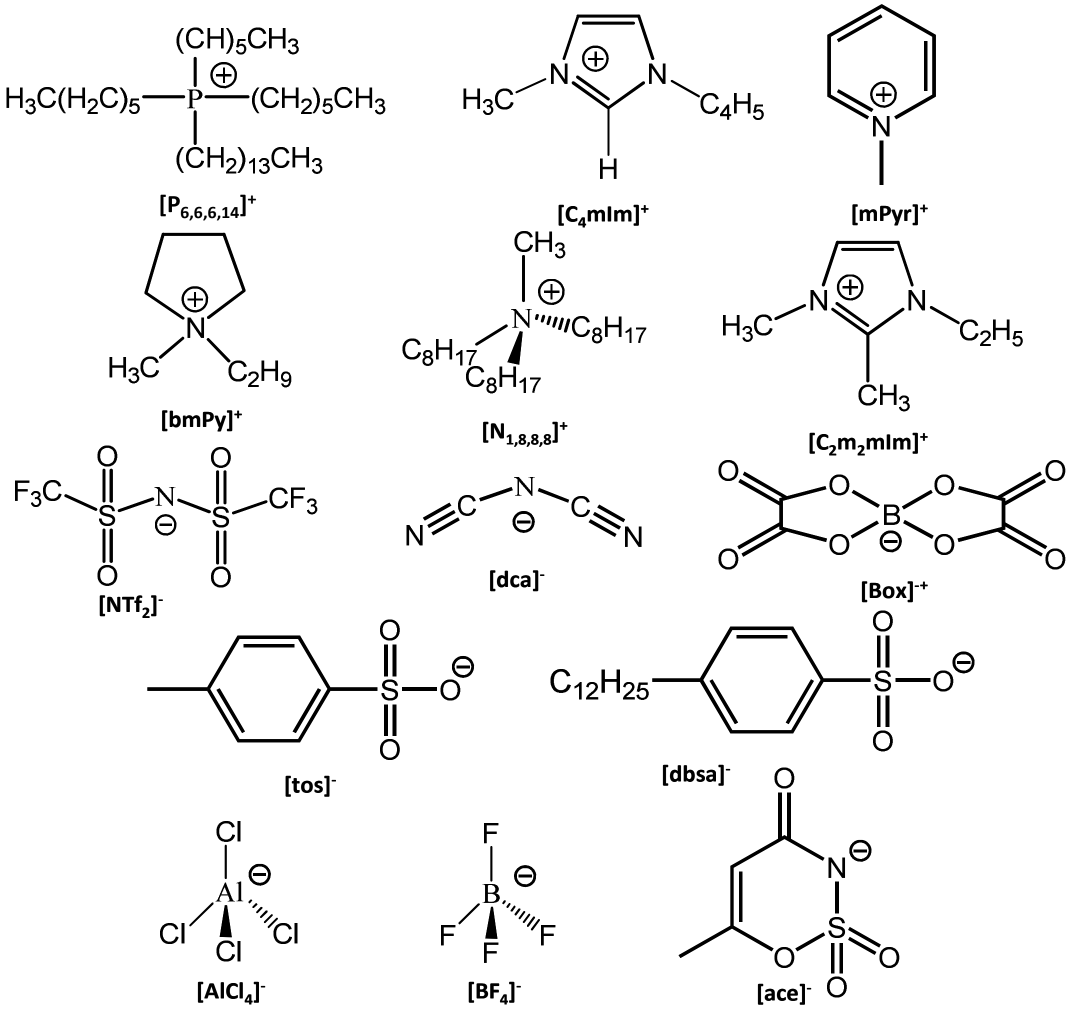

Fig 1.3 Examples of possible ions for synthesis of ionic liquids (from top; l-r):

Trihexyltetradecylphosphonium [P$_{6,6,6,14}$]$^+$, 1-ethyl-3-methylimidazolium [C$_2$mIm]$^+$, methylpyridinium [mPyr]$^+$, 1-butyl-3-methylpyrrolidinium [bmPy]$^+$, methyltrioctylammonium [N$_{1,8,8,8}$]$^+$, 1-ethyl-2,3-dimethylimidazolium [C$_2$m$_2$Im]$^+$, bis(trifluoro)sulfonyl imide [NTf$_2$]$^-$, dicyanamide [dca]$^-$, oxaloborate [Box]$^-$, tosylate [tos]$^-$, dodecylbenzylsulfonic acid [dbsa]$^-$, tetrachloroalminate [AlCl$_4$]$^-$, tetrafluoroborate [BF$_4$]$^-$, acesulfamate [ace]$^-$.

1.2.4 Characterisation of ionic liquids

Before ionic liquids can be utilised as standard solvents, detailed knowledge must first be gained into the processes that occur within the materials themselves. Increasing emphasis is being placed upon the characterisation of the chemical properties of these materials to gain a better understanding of their fundamental characteristics. These properties are then compared to conventional solvents to determine unique characteristics. Viscosity and density allow for an understanding of bulk properties of the system while several internal properties have also been investigated. [36-39] Ionic liquids are typically found to be more viscous than that of conventional molecular solvents. At 293K the viscosity of $[C_2mIm][NTf_2]$ was found to be 40 mPa s.[37] When compared to that of water, with viscosity of around 1mPa s at 293K the difference is found to be significant. In addition to this, it has been found that viscosity and density vary greatly depending upon the choice of ion constituents and follows the intuitive logic that the varying degree of ion : ion association and ion-pair : ion-pair associations will directly affect the physical nature of the liquids. Of particular interest is the van der Waals interactions which appear to be critical to these parameters. Tokuda *et al* found that increasing chain length of imidazolium based ionic liquids resulted in an increase in viscosity which is inversely related to the diffusion coefficient. It was concluded that this is due to the increasing cation-cation interactions based upon alkyl-chain van der Waals associations.[40]

Electrochemical analysis of ionic liquids has approximated the conductivity (and related impedance) and examination of diffusion coefficients has led to an increase in the understanding of the transport properties and solvent-solute interactions within ionic liquids. Examination of imidazolium based ILs found that they exhibited low electrical resistance values.[41] This would be expected due to the charged nature of the ions and the corresponding high concentration of such charges within a pure ionic liquid. Thermochemical analysis of ionic liquids such as phase equilibrium studies[42] have given great insight into the stability and solubility of ionic liquids and their interactions with their surroundings. Since ionic liquids consist of charged species and are ‘molten salts’ by definition, it would be expected that lattice formation or similar structuring would be present within the liquids and directly affect characteristics such as melting point. This is a critical parameter as the practical use of ionic liquids will depend on their liquidus range. Differential scanning calorimetry (DSC) has allowed for the determination of ionic liquid melting, crystallisation and glass transition (T_g) points and rationalise the relationship between ionic liquid structuring and physical characteristics. In general it is found that increasing ion size will significantly change the melting point of ionic liquids.[16] This is due to the increasing size producing weaker coulombic interactions in the crystal lattice. An example of this is $[C_2mIm]^+$ based ionic liquids where $[C_2mIm][Cl]$ was found to melt at 87 ºC and $[C_2mIm][NTf_2]$ was found to melt at -3 ºC.[16] Of particular importance is the fact that studies of ionic liquid melting points and crystal formation appears to show that with increasing side chain lengths, the resulting van der Waals interactions reduce the stronger hydrogen bonds present in favour of weaker interactions.[16] As such, it appears that alkyl chain length may play a more important role than the charge sites alone and may be integral to the characteristics of the liquids themselves.

Thermogravimetric analysis (TGA), coupled with DSC data, allows for decomposition temperatures to be examined and allow for the determination of limits of practical use and the overall stability of the liquids.[43, 44] Some studies have identified that certain perfluorination of the anions (with *stable* C-F bonds such as those in $[NTf_2]^-$) can also enhance the thermal stability of ionic liquids, a factor important in the implementation of ionic liquids as materials in batteries.[45] Spectroscopic methods of analysis have been employed to probe the structure of ionic liquids. Techniques such as infrared spectroscopy (IR) and Nuclear Magnetic Resonance (NMR) have allowed for analysis of diffusion[46] and structural analysis[47] of ionic liquids which further investigate the solvent-solvent interactions and their effects upon the transport properties of the liquids. Mass spectrometry has allowed for more detailed analysis of decomposition fragments and the pattern of such processes and determination of physical properties such as enthalpy of vapourisation[48], a property that is related to the thermal stability of the liquids. Integration into practical applications such as immobilisation in HPLC stationary phases has allowed for the investigation of the liquids ion exchange properties and more specific interactions such as those with aromatic compounds.[49]

From a toxicological perspective, ionic liquid characterisation has met with minimal focused studies of these novel solvents although the focus upon this area is increasing as the application of such materials becomes more commonplace.[50-52] Current studies typically conclude that ionic liquids are found to exhibit considerable levels of toxicity. Ionic liquids have been generally deemed to be toxic with phosphonium based ionic liquids being labelled corrosive in addition to irritating. Recent studies agree that the alkyl chain length of ionic liquids (particularly imidazolium cations) has a direct and substantial impact upon the toxicity of ionic liquids.[53, 54] Although current ionic liquids show considerable levels of toxicity, research into biologically compatible, inert ions have shown great promise. Tao *et al* reported the creation of amino acid based ionic liquids which could introduce a biodegradable characteristic to the solvents.[55] In addition to this, other bio-compatible molecules such as the sugar based anions, succinate and lactate, have also allowed for the formation of ionic liquids which have far lower toxicity levels.[56] Interestingly, while ionic liquids pose a threat to nature, the inherent cytotoxicity of the materials may have the potential for beneficial use. Current antifouling coatings typically contain organic derivatives of heavy metals such as tributyltin which over time are found to leech from these coatings into the environment. Ionic liquids have been successfully immobilised in polymers and found to be sufficiently trapped to avoid leaching. The toxic nature of ionic liquids inhibits growth as desired upon the polymer surface and so could potentially be used as durable thin film coatings for filters or equipment exposed to potential bio-fouling agents.

1.2.5 Structuring within ionic liquids

In recent years it has been observed that the unique properties of ionic liquids may be related to the ability of such materials to form pseudo-crystalline structures at nano-scale dimensions while retaining liquid properties at the macro-scale, similar to liquid crystal systems. Such properties are not present in common molecular solvents and are believed to result from the lattice-like anion-cation interactions and stacking/aggregation of cation head groups. Studies such as those by Miskolcky *et al*, [55] Luczak *et l* [56] and several others [57-59]examined the formation of micelle–like structures by addition of ionic liquids to water.[60, 61] The prevalence of such associations in aqueous solution provided insight into possible structural features that may exist throughout a bulk IL system, where extensive network of associated regions may exist. Dupont *et al* carried out X-ray studies upon the solid (crystal) structure, liquid and gas phase of ionic liquids. It was found that changing from solid to liquid that only solid to liquid that only a 10-20% expansion in the intermolecular interactions occurs.[62] As such the packing/organisation associated with crystal formation is retained with increased ion mobility allowing such structures to exist in liquid forms. The ability to form distinct structures intuitively leads to the hypothesis that such ordering creates multiple regions within the same liquid. This differs greatly from molecular solvents which present homogeneous environments throughout. Theoretical studies, particularly those by Lopes *et al*, have examined the configuration of ionic liquids and their separation into distinct regions based upon mutual interactions within the cation-anion system.[63-65] Mandal and Samanta investigated solution dynamics regions using steady-state fluorescence spectroscopy and the overlay and corresponding polarity values appear to imply the existence of multiple domains existing simultaneously within ionic liquids.[66] The prevalence of such structuring inherently adds significant complexity to the liquids and is believed to be a major contribution to the difficulty of effectively characterising the liquid properties and prediction of properties in these novel materials. However, since these structural features also appear to mediate the advantageous properties of the materials, the ability to quantify such parameters is imperative.

1.3 Solvation parameters: solvatochromic probe dyes

As previously discussed, the most common method of deducing solvent environment is to determine its polarity. This parameter has traditionally been quantified by determining the dielectric constant of the solvent in question. Extensive tables exist as such and this scale has become the default reference value in most cases. However, many solvents, specifically ionic liquids, due to their conductive nature, are not able to have their dielectric constants determined and as such this scale irrelevant. Alternative methods of polarity measurement have been examined in reviews by Reichardt[67] for solvatochromic dyes and Katritzky,[68] encompassing these and several other scales, to determine this parameter. The interaction of such dyes with the solvent system results in changes in the electronic distribution of the molecule and a resulting shift in spectra such as the vibrational and absorbance spectrum. This can then be easily determined using spectroscopic techniques such as UV-Vis spectroscopy.

However, both reviews incorporate large numbers of different scales/probes for interpreting this parameter. Katritzky examined 184 different scales[68] while Reichardt presented 78 dyes whose solvatochromic shifts were related to solvent polarity.[67] This large number of scales/probes clearly displays the inherent difficulty in effectively quantifying the parameter of ‘polarity’. This is due to the fact that the current understanding is that solvent polarity is the combination of a large number of individual interactions and processes working together simultaneously that define the solvent environment. While each scale is designed with the goal of being a definite method of forming a comparative scale, the fact is that there are too many processes at work to be determined by one single value. For this reason, each method is of importance as certain scales/molecules examine specific properties (H-bond acceptance/donation, electrostatics, etc) and a combination of scales can allow for a greater understanding of the overall properties of the solvent. Certain scales, namely Reichardt's $E_T(30)$ and Kamlet-Taft parameters, through their large range of compatible solvents and popular use, have become the most commonly used and are often referred to as the 'polarity' of the system. While this holds true for the parameters that the probe dyes can examine, it must be noted that this still only allows for the ordering of solvents by a limited number of interactions within the solvents and not the overall properties of the solvents. In the following study, to allow for reference to existing values of molecular solvents and ionic liquids, the $E_T(30)$ and Kamlet –Taft parameters were chosen for comparison.

The examination of the physicochemical properties of ionic liquids using spectroscopic probe dyes in conjunction with UV-Vis spectroscopy has become one of the most extensively used characterisation techniques.[12, 17, 69] To date, this technique has met with some success due to the ability of the dyes to quantify the coulombic interactions and hydrogen bond effects present within the liquid system. Considering that these are the primary ion-ion interactions which mediate the unique effects of ionic liquids, this field has begun to find increased importance in the understanding of subtle processes at work within the liquids.

Solvatochromic dyes, or more specifically halosolvatochromic dyes, are molecules that are sensitive to the environment within which they are placed by virtue of their chemical structure. The interactions between probe dye and solvents was observed as chemical shifts which often produce highly visible spectral changes which can be detected optically and more importantly by simple spectroscopic methods while the probe molecule itself remains unchanged. Large shifts can therefore be differentiated directly by the colour change observed, similar to that of a pH dye using UV-Vis spectroscopy and comparing the resulting λ_{max} for each solvent. When added to a solvent, specific and non-specific interactions between the solvent and the dye molecules occur[17]. The varying strength of these interactions, dependant on the solvent chosen, results in a shift in energy levels through intra-molecular interactions which stabilise the excitation band of the molecule resulting in a shift in the absorbance of the dye[17]. Reichardts dye 30 and Kamlet-Taft parameters are of particular interest as they have been used extensively to characterise ionic liquids.

1.3.1 Reichardts Dye

Reichardts Dye 30 (figure 1.4), based upon a betaine molecule is commonly employed to determine the polarity of a solvent. By observing the structure in figure 1.2 it can be seen that two distinct sites for interaction are available.

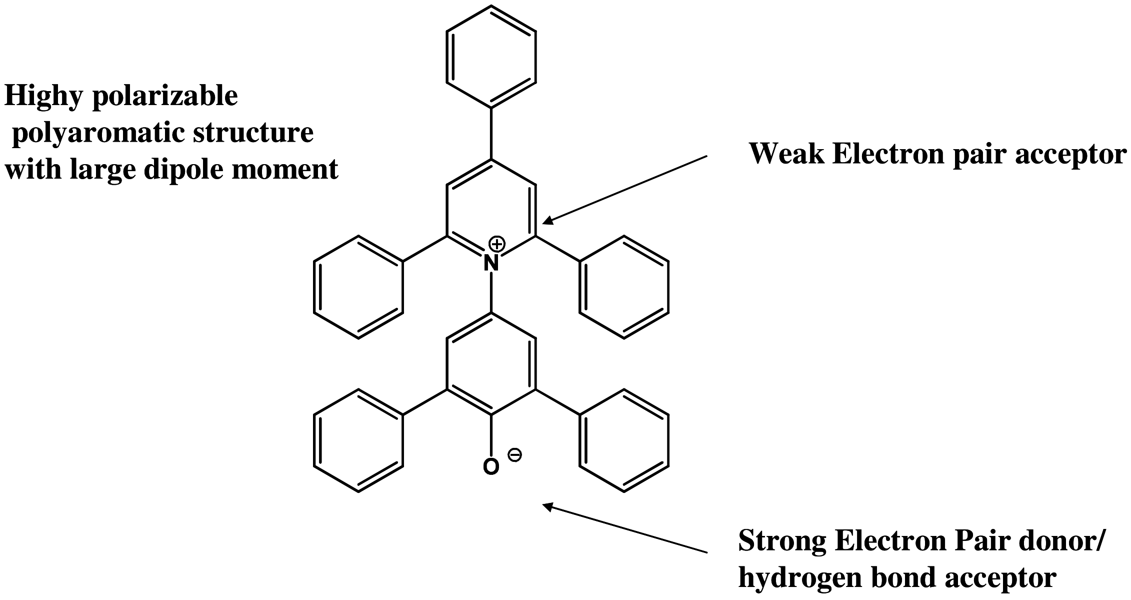

Figure 1.4 Reichardts dye 30 and its sites of interaction.[17]

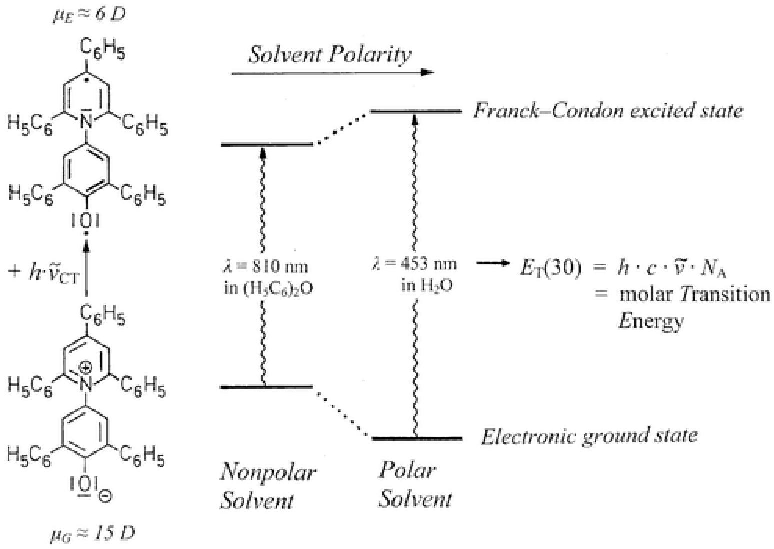

Figure 1.5 Peak shifts of solvatochromic dye based on solvent-solute interactions. [17]

The probe dye is sensitive to solvent interaction as the permanent dipole present in the molecule allows for registration of solvent-solute interactions (figure 1.4). The highly polarisable system, containing 44 π electrons allows for the effects of dispersion forces to be appreciated while the phenolate oxygen and positively charged nitrogen allow for specific interactions such as electron pair acceptance/donation and hydrogen bond formation stabilises the ground state of the molecule. Increased interaction at these sites, typically by polar solvents, results in stabilisation of the ground state of the dye with respect to its first excited state.[17] Figure 1.5 illustrates this process. The excited state is somewhat less stable as it contains the same electronic configuration as that of its ground state according to the Franck-Condon principle. This principle describes the changes in intensity of vibronic transitions. The principle states that when energy is absorbed by a molecule and electronic transition proceeds, the change from one vibrational energy level to another is more likely to occur if the two vibrational wave functions overlap. The excited state is also well less dipolar with a dipole moment of ~6D[70] versus 15D[70] for the ground state of the molecule. Stabilisation therefore increases the energy gap between the ground state and the excited state which results in a hypsochromic (blue) shift. The upper and lower limits of absorption shift are 453nm in water and 810nm in diphenyl ether which exhibits the large range of colours available to determine the polarity of a wide scope of solvents. The $E_T(30)$ scale is based on the λ_{max} shift of the Reichardt's dye and its direct relationship to the polarity of the solvent. $E_T(30)$ values are determined using equation **(1)**.[67]

$$E_T(30) = 28591/\lambda_{\max} \qquad \textbf{(1)}$$

Where;

λ_{max} is maximum wavelength absorbance of the solvatochromic dye.

The $E_T(30)$ scale was suitable for probing solvent polarity due to the conductive nature of ionic liquids which resulted in other scales such as dielectric constant becoming immeasurable. It has also been found that the dielectric constant is based on a theoretical model of the solvent and does not take interactions at the individual molecular level into consideration.[67] For this reason the $E_T(30)$ scale provided a far more reliable system for solvent investigation. The scale was based on solvent-solute interactions occurring at molecular level and avoided the over simplistic view used to derive the dielectric constant. However, the $E_T(30)$ scale also suffered from a degree of unreliability. In recent years, the popular usage of the $E_T(30)$ scale also resulted in the reformatting of the scale in line with S.I standards (Figure 1.6). However the use of the original kcal.mol^{-1} scale still persists as the most popular choice of reporting the parameter. Figueras [71] reported that 'solvent polarity scales based on shifts in λ_{max} of an indicator dye are of limited value where hydrogen bond interactions are possible' . For this reason a more detailed study of the solvent interactions was required. Multi-parameter studies were found to satisfy these criteria in addition to providing more information on individual processes within the solvent.

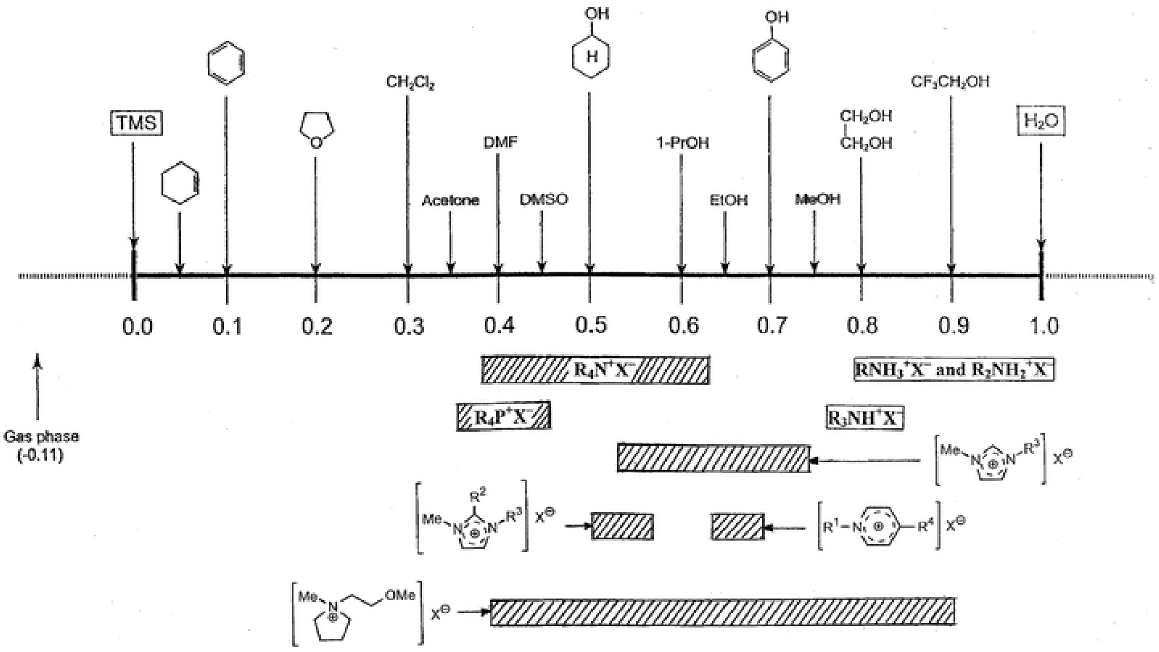

Figure 1.6 Normalised polarity scale, an S.I version of the $E_T(30)$ scale[17]

1.3.2 Kamlet-Taft Parameters

The application of aniline based dyes in conjunction with Reichardt's dye has allowed for the development of a more detailed probe scale known as Kamlet-Taft parameters. Although the subtle solvatochromic behaviours of the aniline based dyes do not allow for direct visual differentiation, the subtle shifts can be determined by spectroscopic methods and used empirically to examine the precise interactions between dye and solvent. Reichardts Dye 30, *n,n*-diethyl-4-nitroaniline and 4-nitroaniline are three probe dyes that are used as the basis of the Kamlet-Taft multi-parameter technique and used to investigate the solvent-solute interactions and were ideal for the analysis of ionic liquid and molecular solvent processes by probing specific properties with particular emphasis on the hydrogen bonding of the solvent (figure 1.7).

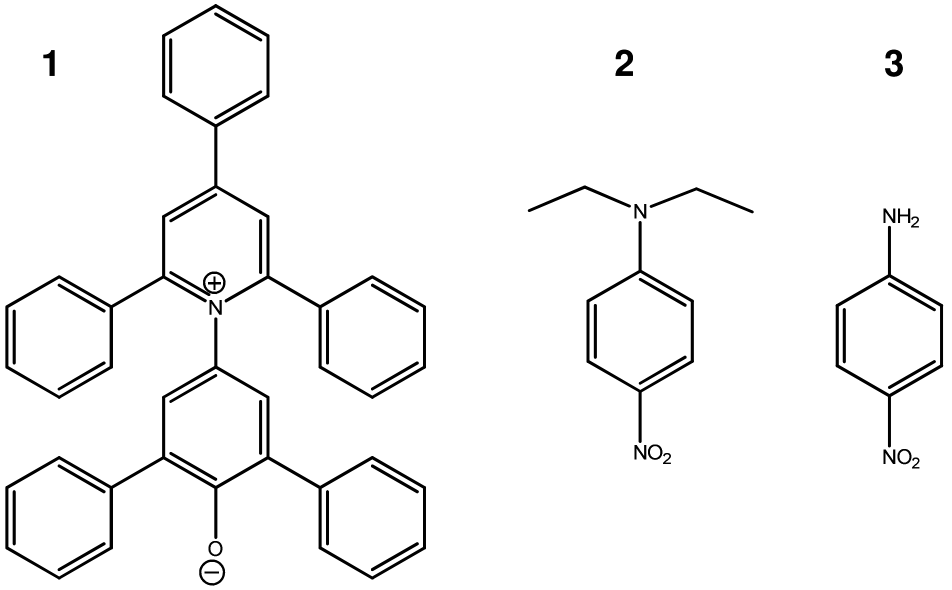

Figure 1.7 Kamlet-Taft dyes: Reichardt's Dye 30 (1), *n,n*-diethyl-4-nitroaniline (2) and 4-nitroaniline (3)

Kamlet and Taft[72-75] produced one such method of determining solvent properties by quantifying important intermolecular processes that occurred within solvents. This involved the use of three dyes with specific types of interaction available. Parameters were calculated based on a differential analysis whereby the shift of one dye is known to interact strongly with the process to be observed and is compared to another dye which is known to have limited interaction in the same process. Such comparisons were presented as three parameters known as hydrogen bond acidity (α), hydrogen bond basicity (β) and polarisabilty (π^*) scales and are explained below. To determine these parameters the following equations were used: [12]

$$\boldsymbol{\alpha} = -0.186 \times [10.91 - \upsilon_{RD30}] - 0.72\pi^{*} \qquad \textbf{(2)}$$

$$\boldsymbol{\beta} = [1.035\ \upsilon_{(max)\ nn} - \upsilon_{(max)\ na} + 2.64\ kK] / 2.80 \qquad \textbf{(3)}$$

$$\boldsymbol{\pi^{*}} = [27.52 - \upsilon_{(max)\ nn}]/3.182 \qquad \textbf{(4)}$$

Where $\upsilon = 10000/\lambda_{max}$ kK

α scale

The alpha scale is an empirical measure of the hydrogen bond acidity of the solvent system[74]. This is associated with the ability of solvent molecules to form hydrogen bonds with other species via hydrogen atoms which exhibit particularly strong interactions with small, strongly electronegative anions like oxygen, nitrogen or fluorine. Hydrogen bonding is a dominant force in molecular solvents and thus related directly to the polarity of the solvent. Previous studies have been carried out to investigate the relationship of these parameters to ionic liquids.[11, 69, 76, 77] It is found that the hydrogen bond ability is attributed to the particular cation species.[12]

β scale

The beta scale is the measurement of the hydrogen bond basicity or the solvents ability to accept a hydrogen bond.[75] This force is commonly observed for protic solvents or solvents where appreciable dipole moments occur within the solvent. Molecules containing electron withdrawing atoms such as oxygen typically exhibit this characteristic and this serves to enhance solvent solute interactions. In the case of ILs, basic hydrogen bond capability is usually related to both the cation and anion species with the anion having particular influence.[12]

π* scale

The π* scale measures the polarisability of the solvent molecule by examining π-π* transitions[72]. Polarisability is concerned with the distribution of the charge across the solvent molecule. This force is typically unimportant in small molecule systems such as the molecular solvents chosen for this study. However, in more complex systems and solvents containing delocalised charges or ring structures this feature becomes more important. In the case of ILs this factor is commonly observed to be enhanced compared to molecular solvents due to the inclusion of aromatic structures and the charged nature of the binary (anion/cation) system.[69]

1.4 Spirocyclic compounds: spiropyran and spirooxazine

A class of molecules known as spirocyclic compounds exhibit similar solvent dependent characteristics similar to that of established solvatochromic probe dyes. However, spirocyclic compounds also possess the ability to examine their surroundings through π interactions and aggregation effects which also affect the solvatochromic effect of the molecules and therefore may allow for more detailed analysis of solvent properties. Since the ‘ionicity’ of ionic liquids is said to be based upon specific interactions similar to these presented by spirocyclic compounds, it is proposed that the application of such molecules may prove to be a more effective method of determining such parameters than existing solvatochromic methods. The desired result is that such molecules may allow for the combination of simple spectroscopic techniques with detailed analysis of the solvent system which existing dyes (Reichardts, Kamlet-Taft) fail to fully appreciate.

1.4.1 Photochromism

Spirocyclic compounds have been subject to much interest due to the photo-induced switching properties inherent to these compounds. The phenomenon of photochromism was first discovered in 1867 by Fritzsche when he observed the photobleaching of tetracene.[78] The basic principle of a photochromic system follows the convention below:

$$\mathbf{A} \underset{h\nu_1,\ \Delta}{\overset{h\nu}{\rightleftharpoons}} \mathbf{B} \tag{5}$$

From its discovery, the interest in photochromic compounds was limited to only a few research groups. The subsequent naming of photochromism in 1950,[79] and the discovery of spiropyran in 1952 [80] created much interest in these systems and with advances in modern spectroscopy and synthetic processes allowed for new developments in this class of compounds. However, it was found that spiropyran exhibited degradation after repeated switching and thus limited the practical application of this compound. This lead to the development of compounds with similar structures but endowed with fatigue resistance. The most successful of these compounds was the group spirooxazine.

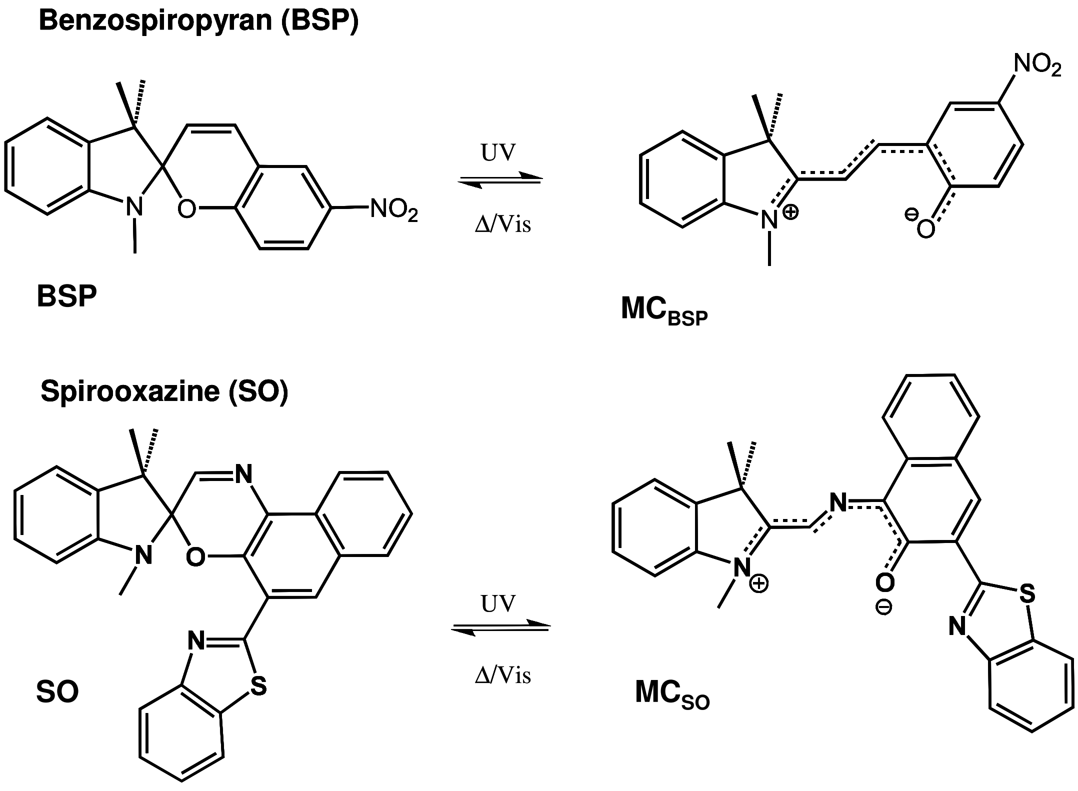

Figure 1.8 Spirocyclic compounds used in this study; λ_{max} **MC** in ACN: 560nm (**BSP**) and 642nm (**SO**)

This success was attributed to the retention of similar functionality as that found for spiropyrans but with combined durability. The discovery of spirooxazine lead to their integration into patented applications such as photosensitive lenses in eyewear by Transitions Optics Inc. More recently, it has been proposed that spirooxazines may be candidates as smart materials in production of molecular scale switches[81] and information storage[82] based on highly defined control of this switching based on irradiation of the molecule with ultraviolet and visible light (figure 1.8).

Figure 1.9 below shows the basic structure of spirocyclic compounds. The molecule can be divided into two halves for identification. Fragment A is known as the indoline fragment while fragment B is known as the pyran (when X = C) or oxazine (when X = N) fragment. The two fragments are connected via a carbon atom known as the C_{spiro}.

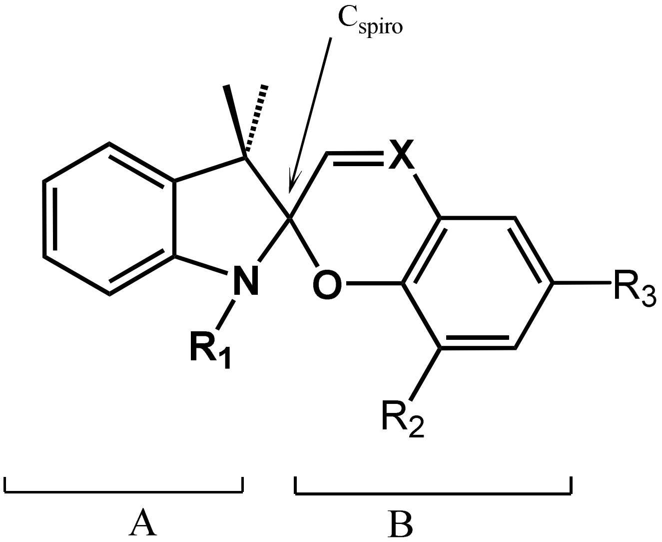

Figure 1.9 Major components of the spirocyclic compound. (A) indoline and (B) spiropyran (X=C) or spirooxazine (X=N) fragments.

The process of ring opening and closing in spirooxazine and spiropyran molecules occurs via a similar pathway. When in their respective closed forms, the molecules are in effect colourless. Any absorbance features observed for the compounds are due to local transitions on each respective part of the molecule. This is due to the fact that the two parts of the spirocyclic compounds are orthogonal to one another (figure 1.10).

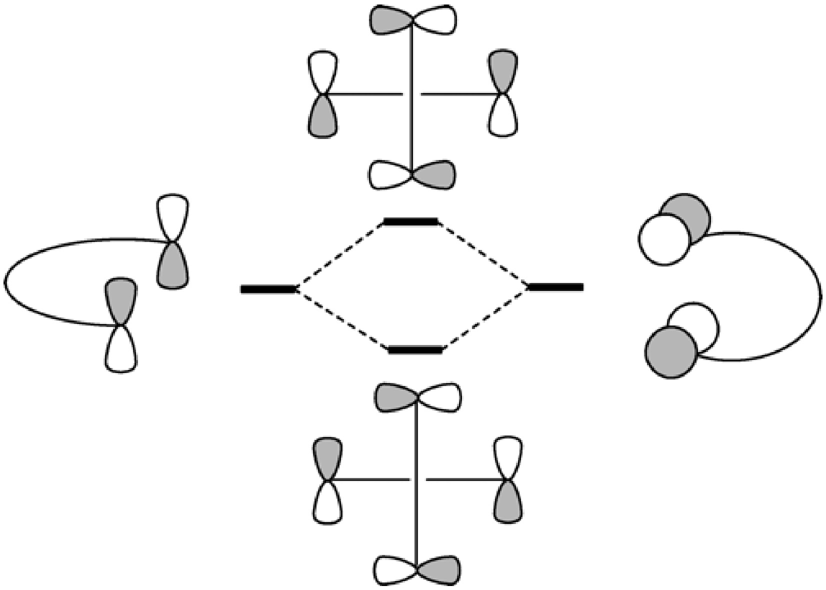

Figure 1.10 Atomic orbitals of centres located around C_{spiro} [83]

When the closed forms of the molecules are irradiated with ultraviolet light at 365nm a cleavage occurs at the C-O bond of the spiro (sp^3) carbon. Following this the molecule re-orientates to a planer configuration. The result is that the once orthogonal atomic orbitals now align and conjugation can occur. The result is that the entire molecular structure now absorbs in the visible region of the spectrum (figure 1.11). This is typically around 650nm in **SO** [83, 84] and 540nm in the case of **BSP**.[22]

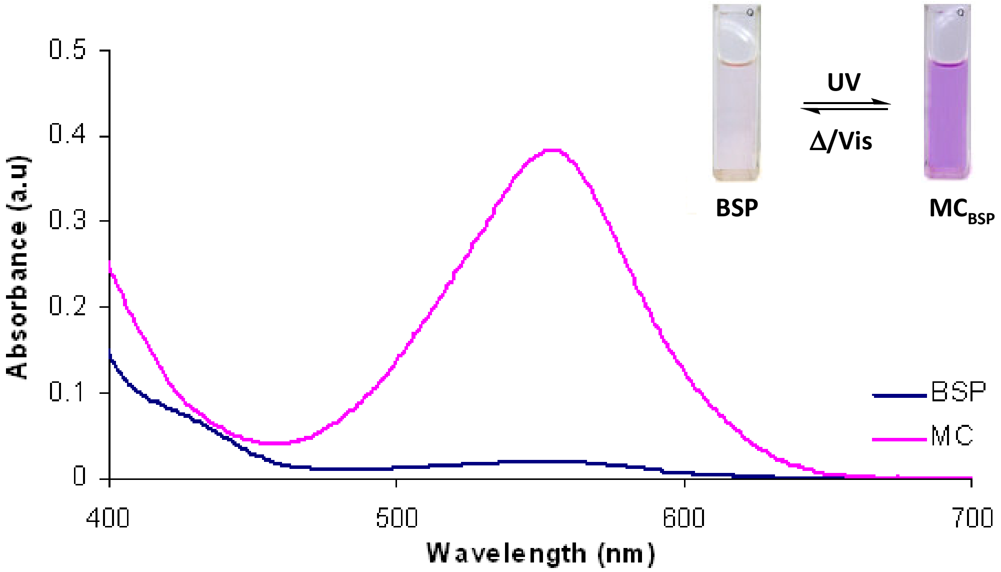

Fig 1.11 UV-Vis spectra of **BSP** in its closed (**SP**) and open (**MC$_{BSP}$**) forms. UV irradiation at (375nm) induces ring opening and formation of coloured compound from colourless closed state. Inset shows visible colour change between **SP** and **MC$_{BSP}$** forms.

Upon cleavage, a series of reorientations occur until the **MC** form is at its lowest energy, trans-trans-cis conformation, with the least amount of steric hindrance which becomes the longest lived form of **MC** and can be monitored spectroscopically. Possible conformations of **MC** are shown in figure 1.12.

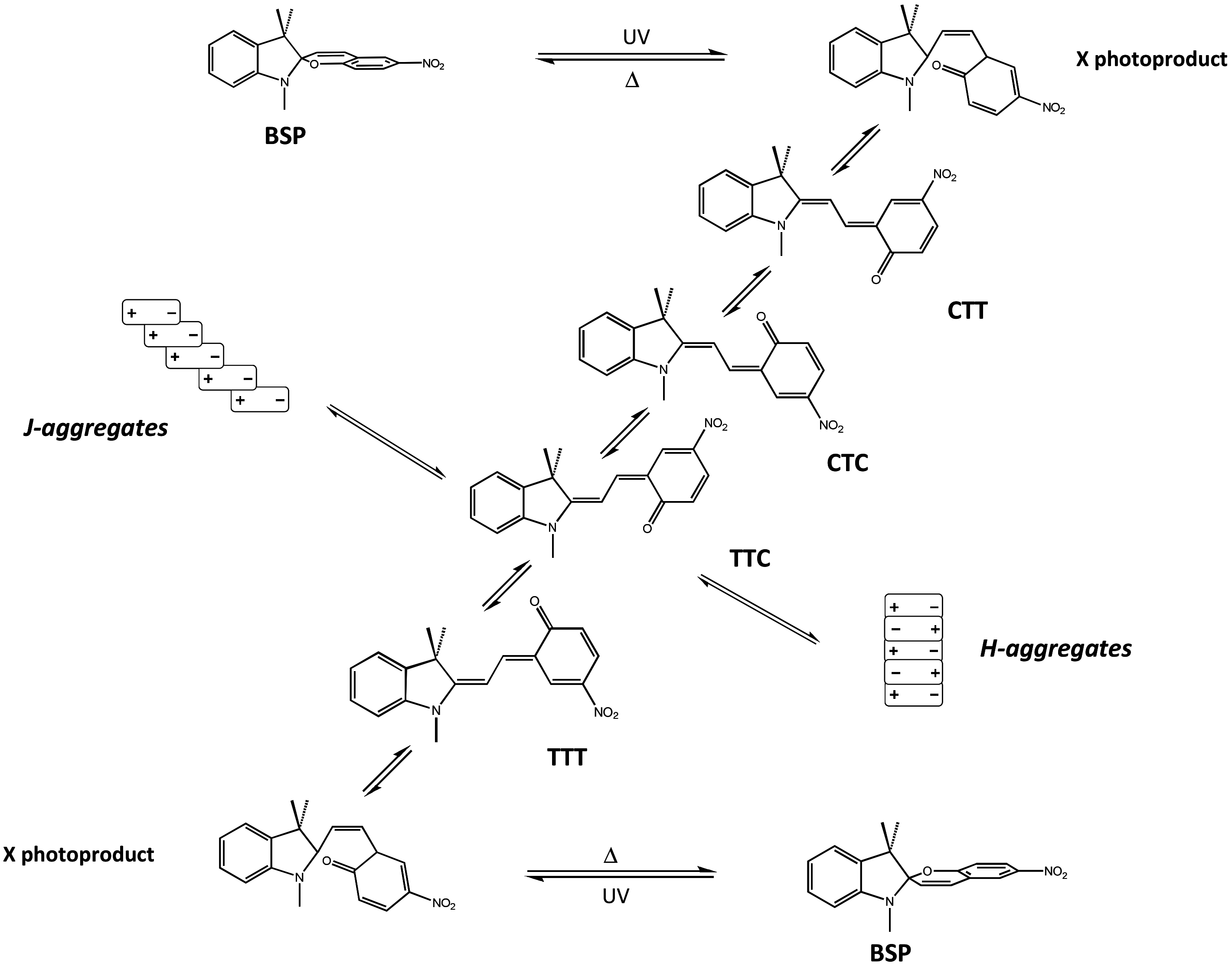

Figure 1.12 Ring opening/closing of spirocyclic compounds; spiropyran (**BSP**) is shown in this example[83]

The ring opening process to the stable **MC** form has been found to be an extremely fast process occurring within picoseconds and monitoring of such processes requires ultra-fast techniques[85, 86] and flash photolysis[87, 88] to observe the short lived species. Figure 1.12 illustrates some of the proposed transition states of spirocyclic compounds as they undergo reorientation to their most stable **MC** form. It has been found that spirocyclic compounds typically lead to a cis-cisoid conformer, also known as the **X** photoproduct, followed by rotation to the more stable trans form (figure 1.12). Upon reaching the most stable from of the merocyanine isomer (figure 1.13), spirocyclic compounds then undergo first order exponential decay to the closed spiro form. This involves the thermal back reaction of the major **MC** component and other minor components such as less favourable cis conformations of the open form. The major component, with the longest lifetime (second timescales) can be monitored by UV-Vis spectroscopy as the coloured **MC** form returns to is colourless closed form and from this the rate constant of thermal relaxation may be determined.

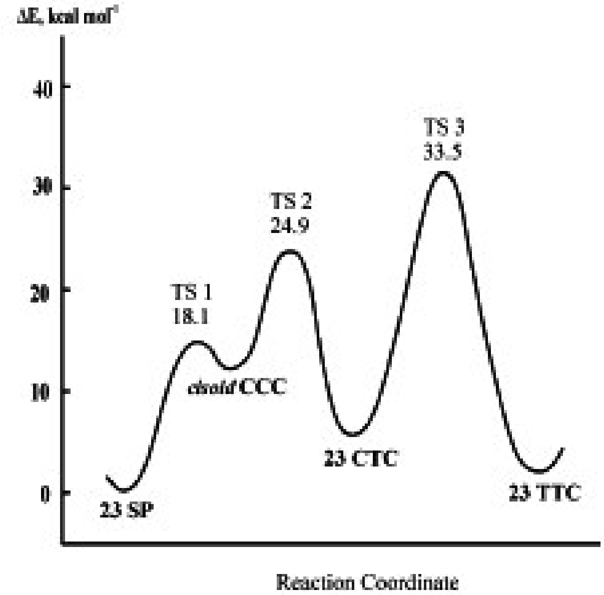

Figure 1.13 Reaction coordinates of energies of reorientation of merocyanine conformations.[83]

The rate at with the closing of the ring occurs after UV irradiation is directly affected by solvent polarity. In the case of spirooxazine (figure 1.8) the rate of closure has found to change from 50 seconds in ethanol to 5 seconds in hexane.[84] This is due to solvent-solute interactions such as hydrogen bonding, dipole-dipole forces, polarizability of the molecule and dipole moments which all contribute to the stabilisation of the merocyanine form.[84, 89] These intermolecular interactions play an important role in the kinetics of spirocyclic compounds based on their ability to stabilise the merocyanine form of the molecule. Upon irradiation with ultraviolet light, the open form of the spirocyclic compound becomes a zwitterion[83]. This produces two areas of distinct charge and so creates two distinct regions for interactions critical to stabilising the open form to occur. The most obvious are hydrogen bonding and dipole forces while other forces such as electron donation and acceptance also become important. With several phenyl rings and double bonding within the structure, it is possible that the π electrons play a role in the interactions within the solvent[89] and their distribution of the charges across the molecule. Certain environments prove destructive to spirocyclic compounds. When added to water, spirocyclic compounds are found to remain open by stabilisation of the merocyanine form. This is due to the permanent hydrogen bond interactions of water with the merocyanine form of the molecule and thus the deactivation of the thermal relaxation back to its spiro form.[90] To better explain the processes that can occur within this class of photochromic compounds, it was found that several effects were central to the features observed of spirocyclic compounds.

Spirooxazines are structurally similar to that of spiropyrans. The only difference between parent structures is the substitution of carbon for nitrogen (figure 1.9). Studies indicate that the resistance of spirooxazine to permanent photo-bleaching may be attributed to the indoline ring nitrogen group due to the fact that merocyanine form of spirooxazines is composed entirely of the singlet excited state and not of the triplet as observed for spiropyrans[83, 91]. This was also believed to be attributed to the nitro group.[91] This group is believed to improve the quantum yield of intersystem crossing and thus the formation of coloured forms by both the singlet and triplet manifold. This intersystem crossing is also believed to aid in the formation of singlet molecular oxygen.[83, 89] This reactive species has been proposed to lead to the degradation of spirocyclic compounds.[92, 93] Spiropyrans with no nitro group or spirooxazines are then believed to follow the singlet manifold exclusively and thus reduces the evolution of this destructive process.

1.4.2 Thermodynamic properties

To further examine the ring opening/closing process, the temperature sensitive kinetic effects can be used to determine the thermodynamic parameters which describe the reaction process in terms of solvent-solvent order and energy required for the opening/closing process to occur. The following section explains the thermodynamic parameters of thermal relaxation of *both* spirocyclic compounds but is illustrated using **SO** alone for clarity. The cleavage of the C-O bond and formation of the **MC$_{\mathbf{SO}}$** isomer, results in a system that is believed to lie at a higher energy than that of the closed (**SO**) form. The relatively unstable nature of the **MC$_{\mathbf{SO}}$** results in an overall thermal equilibrium **(6)** that lies predominantly on the side of **SO** as the molecule is found to spontaneously return to this conformation which affords the lowest energy.

$$\mathbf{SO} \underset{\Delta}{\overset{\Delta}{\rightleftharpoons}} \mathbf{MC_{SO}} \qquad \mathbf{(6)}$$

The relaxation process of spirocyclic compounds has been proposed to contain several isomers during thermal relaxation[85,87,88] illustrated in figures 1.10 and 1.11. For convention, equation **(7)** explains that the rate constant for thermal relaxation shall be known as the forward reaction, k_f and that the rate constant for ring opening shall be known as the reverse reaction, k_r. Most of the **MC** isomers close too fast (picosecond timescales) to be detected by conventional spectroscopic methods and so this study focuses on the most stable, ground state **MC_{SO}** form: the trans isomer (TTC configuration similar to that in figure 1.9).

$$MC_{SO} \underset{k_r}{\overset{k_f}{\rightleftharpoons}} SO \qquad \textbf{(7)}$$

Transition state theory can be employed to attempt to rationalise the above process with regards to the energy barrier of the relaxation process by proposing that a quasi-equilibrium exists at the peak of the energy barrier.[94] For **MC_{SO}** to return to **SO**, reorientation of the molecule must occur to allow the appropriate bonds to reform. This process involves rotation around the C-C bonds and results in a gradual reduction in the distance between the C_{spiro} carbon and phenolate oxygen. The process continues until such distances are reached that conditions become favourable for C-O bond formation. This distance and conformation has become known as the transition state of the process, denoted by **$MC^{\ddagger}_{SO}$**. Theoretical studies have attempted to rationalise these states[95] but the exact process and molecular conformations are still a matter of contention. Figure 1.14 illustrates the proposed molecular conformations of the process and equation **(8)** displaying the chemical process. For thermal relaxation, process I is the activation step where energy is required for the open **MC_{SO}** form to re-orientate to the transition state **MC$^{\ddagger}_{SO}$** and allow for process II, the spontaneous step, to take over and return the molecule to its closed **SO** form following C-O bond formation.

$$\underbrace{MC_{SO} \xrightleftharpoons{\Delta/\mathrm{vis}} MC^{\ddagger}_{SO}}_{\mathbf{I}}\ \underbrace{\xrightleftharpoons[\Delta/\mathrm{UV}]{} SO}_{\mathbf{II}} \qquad \mathbf{(8)}$$

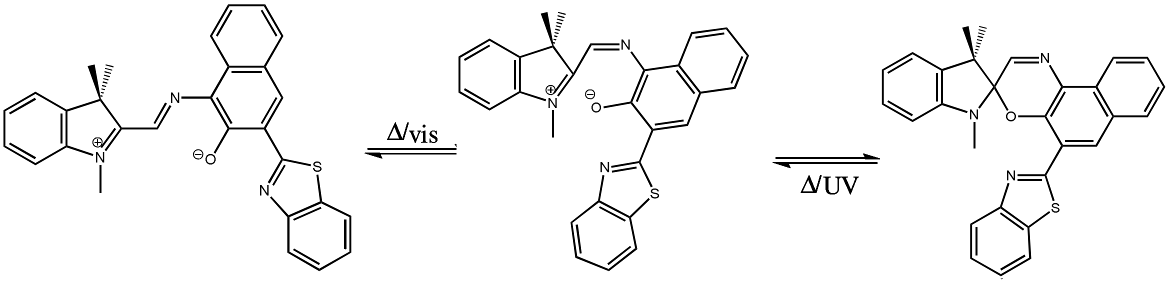

MC$_{SO}$ **MC$^{\ddagger}_{SO}$** **SO**

Figure 1.14 Thermal closing/opening of **SO** and illustration of possible transition state **MC$^{\ddagger}_{SO}$** conformation. The transition state is a short lived conformation during C-O bond forming and breaking.

Due to the strain placed on the system by the rotations and steric hindrances in formation of the transition state, energy is required to allow such states to exist, even if only for a short time. The relaxation process was carried out in darkness to ensure that the sole source of energy for relaxation is restricted to heat from the surrounding environment and not influenced by visible light. The requirement for such energy during the **MC$_{SO}$** reorientation process implies an energy barrier must exist. Figure 1.15 illustrates the reaction coordinates and relative energies of both the open and closed form of the molecules and the energy barrier which separates them. To the left of this barrier the **MC$_{SO}$** isomer exists while to the right **SO** is the dominant species with the transition state of the molecule, **MC‡$_{SO}$,** populating the energy maximum associated with steric hindrance and unfavourable conformations.

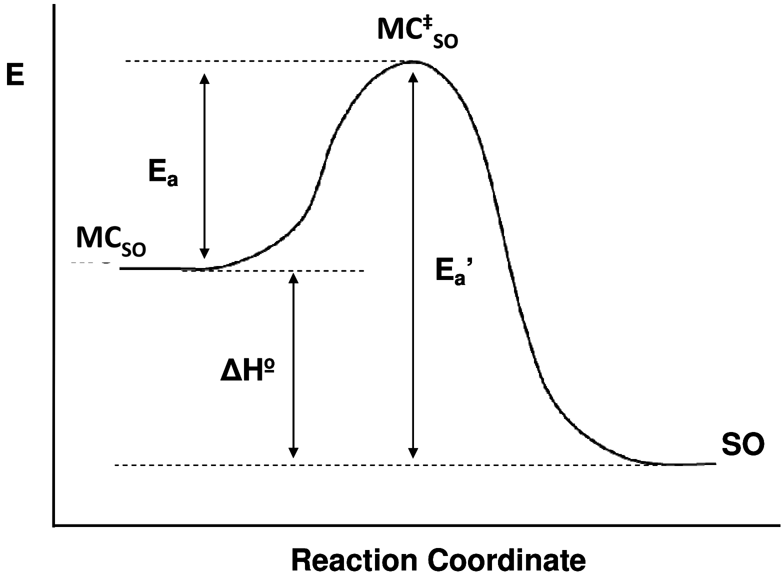

Figure 1.15 MC$_{SO}$→SO thermal relaxation and the thermodynamic barrier associated with the process.

The energy required to overcome the barrier related to **MC$_{SO}$** relaxation is known as the activation energy, E_a. Since the **MC$_{SO}$** form of the molecule is at a higher energy level than the final **SO** form, the thermal relaxation process overall is thermodynamically favourable ($\Delta G° < 0$). At the transition state the compound, when bond formation begins to occur and the subsequent return to the closed colourless form proceeds with no requirement for further energy input to the system, the molecule is at the highest energy coordinate on the **MC$_{SO}$→SO** conversion pathway (figure 1.15). This point is of particular interest as at the transition state, **MC‡$_{SO}$**, the interactions between the solvent and the spirocyclic molecules become critical as they mediate the entire relaxation process of the compound and therefore enables the system interactions to be determined thermodynamically. Transition state theory parameters were derived by analysis of the forward (closing) process, $k_f{}^{I}$ (equation **(9)**) of the molecule from its open $\mathbf{MC_{SO}}$ form to its transition state, $\mathbf{MC^{\ddagger}{}_{SO}}$ via process I (equation **(8)**). Variations in these rates are related to the energy barrier to the overall process (figure 1.14) which is solvent and temperature dependent. It must be noted however, that the forward reaction, k_f is the rate constant of the *overall* process i.e the rate of process I *and* process II, k_f^{I} and k_f^{II}. Transition state theory examines the activation process to transition state only, $\mathbf{MC_{SO}}\rightarrow\mathbf{MC^{\ddagger}{}_{SO}}$, and so this process influences the rate at which the activation step occurs, k_f^{I} (equation **(9)**)

$$\overbrace{\mathrm{MC_{SO}} \overset{k_f^{I}}{\rightleftharpoons} \mathrm{MC^{\ddagger}{}_{SO}} \overset{k_f^{II}}{\rightleftharpoons} \mathrm{SO}}^{k_f} \qquad \mathbf{(9)}$$

As $\mathbf{MC_{SO}}\rightarrow\mathbf{SO}$ relaxation proceeds, heat is absorbed as the energy required to overcome the activation energy barrier of relaxation (figure 1.15). Therefore, increasing heat from the systems surroundings would be expected to increase rates of relaxation. Linear relationships between this temperature increase and thermal relaxation results in an Arrhenius dependence from which important thermodynamic parameters may be derived. The Arrhenius equation **(10)**, is based upon the van't Hoff conclusion that the observed variation of the equilibrium constant with respect to temperature, a similar relaxation should be observed for the rate constant.[94] Arrhenius is however widely credited at applying this postulation and finding that the rate constant of reactions did have a linear response to temperature. For the **$MC_{SO} \rightarrow SO$** thermal relaxation process, this equation allows for the approximation of the activation energy of the process (E_a). Since the relaxation process is known to be an endothermic reaction, it is intuitive to believe that the subsequent solvent stabilisation, or lack of, will affect this energy barrier by stabilising the open **MC_{SO}** form and restricting the thermal relaxation process.

$$\ln k_f = -E_a/RT + \ln A \qquad \textbf{(10)}$$

where,
E_a = activation energy
R = gas constant
T = temperature (K)
A = pre-exponential factor

Equation **(10)** above is found to contain two factors which are believed to affect the rate of thermal relaxation of the compound. The first is the activation energy, which is the energy required for the molecule to overcome unfavourable conformations (**$MC^{\ddagger}_{SO}$**) to allow for the formation of the more stable closed **SO** form as seen by the negative sign associated with the activation energy with respect to k_f in equation **(9)**. For this process this energy is typically in the form of light (visible/white) or heat. The second factor, A, is known as the pre-exponential factor. This has been previously described as the collision frequency factor which is based on the approximation that atoms and molecules are presented as hard shells. For a reaction to proceed it is said that these spheres must collide and this factor encompasses this process. For the **$MC_{SO} \rightarrow SO$** thermal relaxation it is also believed that this factor may also account for solvent effects and processes during thermal relaxation that are not explained by the activation energy alone.

To examine the thermodynamic processes occurring the compound approaching transition state, $\mathbf{MC_{SO}} \rightarrow \mathbf{MC^{\ddagger}_{SO}}$, the Gibbs energy of activation ($\Delta G^{\ddagger}$) of the system is examined. Gibbs energy of activation is described as the overall capacity for work carried out by the system, which in this case, is the $\mathbf{MC_{SO}} \rightarrow \mathbf{MC^{\ddagger}_{SO}}$ molecular reorientation and solvent-solute interactions within a solvent into which it is dissolved. Equation **(12)** shows the relationship between enthalpy of activation ($\Delta H^{\ddagger}$) and entropy of activation ($\Delta S^{\ddagger}$) for the Gibbs energy of the system relating to the importance of temperature and solvent effects upon the overall thermal relaxation process.

$$\Delta G^{\ddagger} = \Delta H^{\ddagger} - T\Delta S^{\ddagger} \qquad \textbf{(11)}$$

Negative Gibbs energy of activation indicates that a reaction will proceed spontaneously, releasing energy (commonly heat), in the process while positive values imply that work has to be done upon the system for the reaction to proceed and thus a net input of energy. The process of **MC** closure has been extensively examined and found to require energy (light/heat) for the reaction to proceed. This implies that a positive Gibbs energy would be expected and figure 2.8 reflects this with an energy barrier which must be overcome to allow for relaxation to the closed **SO** form. However, since the reaction would be expected to proceed without the requirement of energy upon reaching the highest energy/transition state, Gibbs energy of activation is found to be equal to the magnitude of this barrier to the $\mathbf{MC_{SO}} \rightarrow \mathbf{MC^{\ddagger}_{SO}}$ process. $\Delta G^{\ddagger}$ can be determined for the process by first finding the enthalpy of activation, $\Delta H^{\ddagger}$ and entropy of activation, $\Delta S^{\ddagger}$ experimentally and using these values in equation **(13)**. This is achieved by using the linear relationship between temperature and the rate constant for the thermal relaxation process of **MC_{SO}→SO**. The Eyring equation **(12)**, uses this linear response to determine the enthalpic and entropic factors of activation.

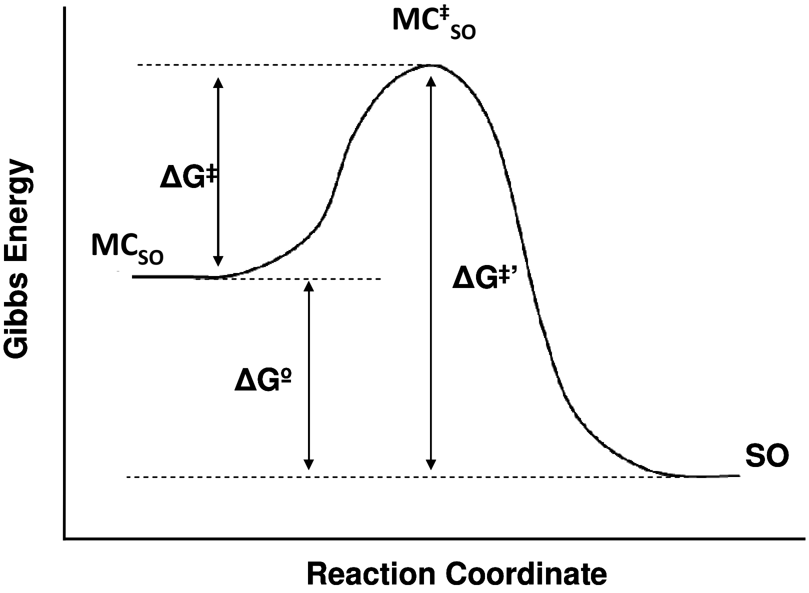

Figure 1.16 Gibbs energy diagram of **MC_{SO}→SO** opening/closing

$$\ln (k_f/T) = -\Delta H^{‡}/RT + \ln (k_B/h) + \Delta S^{‡}/R \qquad \textbf{(12)}$$

where,
k_f = rate constant of forward reaction
T = temperature (K)
$\Delta H^{‡}$ = enthalpy of activation
$\Delta S^{‡}$ = entropy of activation
R = gas constant
k_B = Boltzmann constant
h = Planck's constant

The enthalpy of activation, $\Delta H^{\ddagger}$, explains the energy that is used to do work by the system to reach the transition state. Enthalpy, under the definition of Gibbs energy, describes the ability of the process to do work on the system and transfer heat. Negative enthalpies describe an exothermic system whereby the work done by the system results in a net release of heat during the process. Conversely, positive enthalpies describe an endothermic process whereby the system absorbs heat during the systems process. For $\mathbf{MC_{SO}}\rightarrow\mathbf{MC^{\ddagger}_{SO}}$, a process which requires energy to proceed (figure 1.6), it is be expected that $\Delta H^{\ddagger}$ values will be positive. From equation **(12)** it can be seen that enthalpy of activation has an opposing effect upon the activation process. This implies that increasing the work carried out by the $\mathbf{MC_{SO}}$ molecule within the solvent system results in a reduction of the rate of the forward reaction.

The entropy of activation, $\Delta S^{\ddagger}$, is a parameter used to quantify the ordering within the system with respect to changes. These changes are typically heat transfer processes from hot to cold temperatures and resulting changes in internal energy as it reaches transition state. As such, in the case of $\mathbf{MC_{SO}}\rightarrow\mathbf{MC^{\ddagger}_{SO}}$, the input of energy (heat) during the process will result in a net increase in internal energy and therefore result in an increase in the entropy of the system. From a mechanical respect, entropy may also be viewed as a measure of molecular disorder within a system. $\Delta S^{\ddagger}$ for $\mathbf{MC_{SO}}\rightarrow\mathbf{MC^{\ddagger}_{SO}}$ examines the rigidity of a system based upon the reorganisation of the $\mathbf{MC_{SO}}$ molecules within the solvent system as they re-orientate to the transition state, $\mathbf{MC^{\ddagger}_{SO}}$. Conformational changes of the compound as it approaches its transition state result in changes in the ordering of the $\mathbf{MC_{SO}}$ - solvent system. Positive entropies imply that that transition state is more disordered than $\mathbf{MC_{SO}}$ while negative entropy describes a more rigid system whereby fewer interactions occur within the system. Comparison of equation **(11)** and **(12)** we see that the there is a direct relationship between the entropy of activation and the rate of the forward rate constant, k_f. Increasing the level of disorder within the system is therefore a positive influence upon the rate of thermal relaxation. Entropy change for the $\mathbf{MC_{SO} \rightarrow MC^{\ddagger}_{SO}}$ process can be affected by several factors. These are primarily believed to be the rigidity of the merocyanine molecule itself and $\mathbf{MC_{SO}}$-solvent interactions. $\mathbf{MC_{SO}}$ reorientation to $\mathbf{MC^{\ddagger}_{SO}}$ in inherently result in an increase in entropy as the conformation of the molecule changes. Such changes will then have a direct effect upon the solvent system, particularly when there are interactions between the solvent and the $\mathbf{MC_{SO}}$ molecules. However, movement and reorientation of the molecules that don't can also induce increased disorder through physical process such as 'pushing' the molecules out of the way as the conformation changes. It is this solvent-solute interaction that is deemed important for the analysis of ionic liquids as solvent structure will play a significant role in the entropic effects found and so allow for greater understanding of the physical properties of the liquids.

A derivative of the Eyring equation,[94] equation **(13)**, can be used to find the equilibrium of activation, $K^{\ddagger}$. This quasi-equilibrium can be used to describe which form of the **SO** molecules is favourable at transition state.

$$k_f = (k_B T/h)K^{\ddagger} \qquad \mathbf{(13)}$$

Figure 1.17 shows how this equilibrium process lies at the transition state and energetic factors such as heat or light can influence the direction the molecule will choose to follow and which side of equation **(8)** the process will prefer to lie.

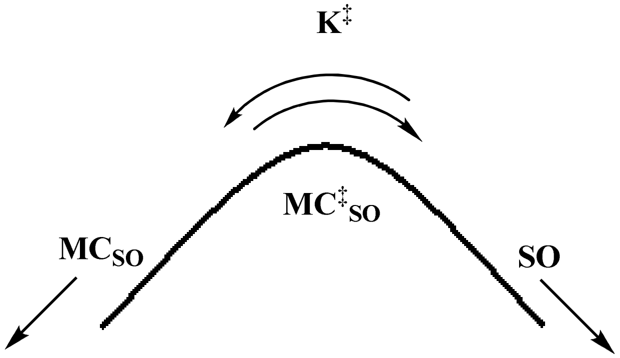

Figure 1.17 Equilibrium of activation, K‡ describing the direction the **MC_{SO}↔SO** process.

The larger the equilibrium of activation becomes the further to the right the equilibrium will lie and thus drive the forward (closing) process. Decreasing equilibrium implies that the equilibrium shifts towards the backwards (opening) process. Under this convention, the thermal relaxation of **MC_{SO}→SO** will result in a large K‡ since the process of thermal relaxation favours the formation of the lower energy **SO** form. However, during the relaxation process, factors such as solvent mediated stabilisation or steric interference may compete with the relaxation process (although never overcome it) and is reflected as a variation of the equilibrium constant. Thermodynamic parameters were determined by Microsoft Excel plots of rate constants as explained in appendix A-3.

1.4.3 Solvatochromism

Solvatochromism is the variation of the features (shape, intensity position) of the absorption band of spirocyclic compounds (figure 1.18). The effects of solvatochromism are believed to be due to two major mechanisms.[83] The first is due to shifts in the equilibrium of the molecule based on the polarity of the solvent into which it is placed. The observed shifts are found to occur due to the redistribution of the intensities of absorption bands in the solution which contains a mixture of isomers of the spirocyclic compound in equilibrium. In some cases this can be extended to the appearance of completely new bands if one particular isomer is favoured in the solvent. The second is the resulting specific interactions of the spirocyclic molecule with the solvent environment. The resulting shifts are based upon changes to the absorption band of the ring open **MC** form due to solvent interactions. Due to the charged nature of the structure, the result is solvent-solute interactions which vary with differing solvent polarities. The differing degree of charge associated with solvent molecules produced varying degrees of stabilisation to the **MC** form.

Studies have shown an increase in the dipole moment of spirocyclic compounds upon going from closed spiro form to the open merocyanine. An example of such results found spiropyran derivatives having dipole moments of 3.0-4.5D (10-15 C.m) in spiro form and 15-18D (50-60 C.m) in their merocyanine forms.[97] It has also been found that the **MC** structure is highly sensitive to the influence of substituents to both parts (A and B, figure 1.9 above) of the compound.[83] These substituents can alter the acceptor or donor properties of the compound and the polarisation of the π system of the **MC** form.

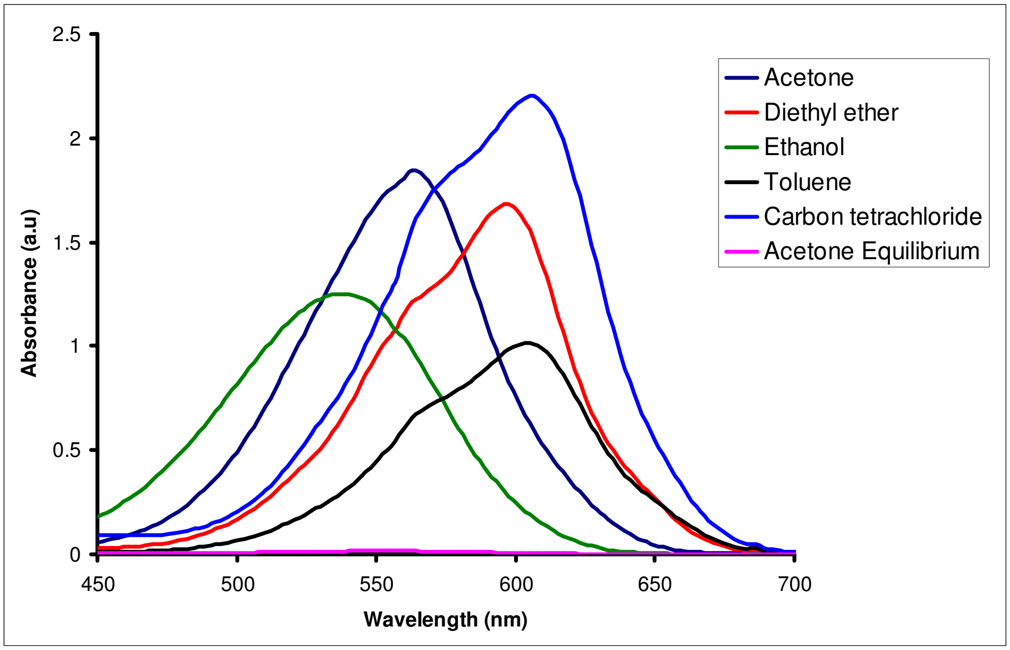

Fig 1.18 Solvatochromic effect of solvent-solute interactions upon UV-Vis spectra of **BSP** following irradiation with UV light (365nm).[96]

Negative solvatochromism has been induced in spirocyclic compounds by addition of electron withdrawing groups to the indoline fragment and electron donating groups to the naphthalene fragment resulting in a push-pull system.[98, 99] It has been found that nitro substituted compounds such as **BSP** (figure 1.8) display pronounced colour changes. The nitro group itself is a solvatochromic system and its interaction with the solvent results in visible shifts of the absorption bands of the merocyanine form. This is believed to be due to the redistribution of the electron density of the merocyanine.[100]

1.4.4 Thermochromism

Thermochromism is the ability of heat to induce a colour change in a molecule. Although many molecules have such properties including polythiophenes and liquid crystals, the most commonly known compounds are spirocyclic compounds.[101] The thermochromic effect of spirocyclic compounds is based on the thermal equilibrium between the open and closed form of the compounds. This equilibrium is influenced by solvent polarity and is observed visually for some spirocyclic compounds. In the case of **BSP** and **SO** (figure 1.8), solutions in non-polar solvents are found to be colourless due to the compounds being mostly in their closed forms. This is in contrast to polar solvents where the equilibrium shifts towards a mixture of open and closed form which results in faintly coloured solutions. Figure 1.8 shows the equilibrium between ring open and closed forms of spirocyclic compounds. Commonly the forward reaction is initiated using ultraviolet light (~365nm) while the back reaction to closed spiro form can occur in both visible light and darkness. Although the back reaction rate is enhanced with visible light, the fact that the process occurs in darkness shows the influence that heat has on the process. The influence on this thermal equilibrium can however be shifted by the introduction of substituents to the spirocyclic compounds. By introduction of electron withdrawing groups to the pyran/oxazine (B) fragment it has been found that the equilibrium can be shifted towards the open form. To maximise this effect, the substitution of nitro or arylazo groups at the ortho or para position relative to the phenolate oxygen can produce measurable levels of merocyanine in polar solvents.[83] Such a shift results in the ability to use heat to induce ring opening. Figure 1.19 demonstrates the effect of increasing temperature upon the equilibrium of **BSP**.[96]

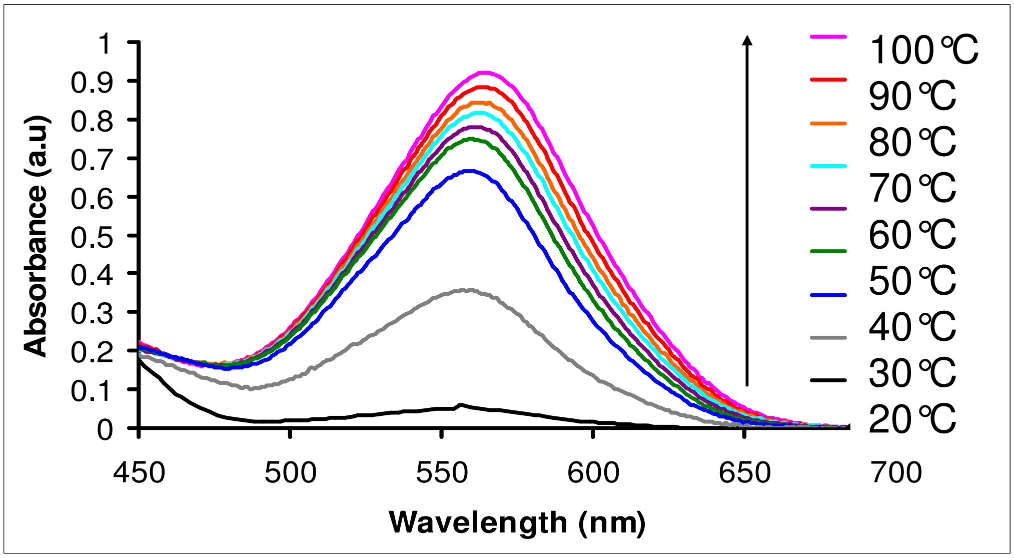

Figure 1.19 UV-Vis spectra overlay demonstrating thermal effects upon **BSP** after 10 minutes at designated temperature.[96]

1.4.5 Acidichromism

Acidichromism is the protonation of the merocyanine form due to the presence of excess protons (usually an acid) in solution (figure 1.20). When cleavage of the closed form is induced by ultra violet light, the resulting polar molecule exhibits a site characteristic of a Brønsted base (figure 1.8). The subsequent protonation results in a reduction of the merocyanine peak and the evolution of a characteristic peak for the protonated form (figure 1.21). Although bonding has occurred, the process can be reversed by the application of visible light to induce bond dissociation and reformation of the spiro form. However, unless the acidic solvent in which the spirocyclic compound is dissolved in is subsequently neutralised, the result is the formation of the protonated form once again upon cleavage of the C-O bond.

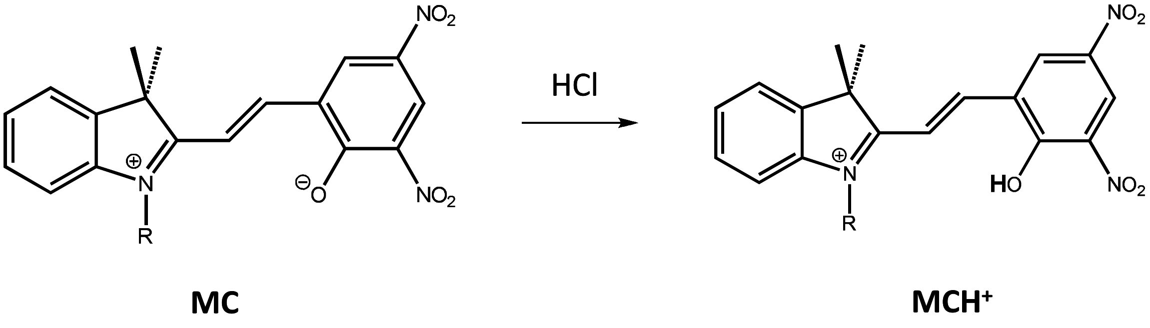

Fig 1.20 Protonation of **MC** derivative by addition of hydrochloric acid.[102]

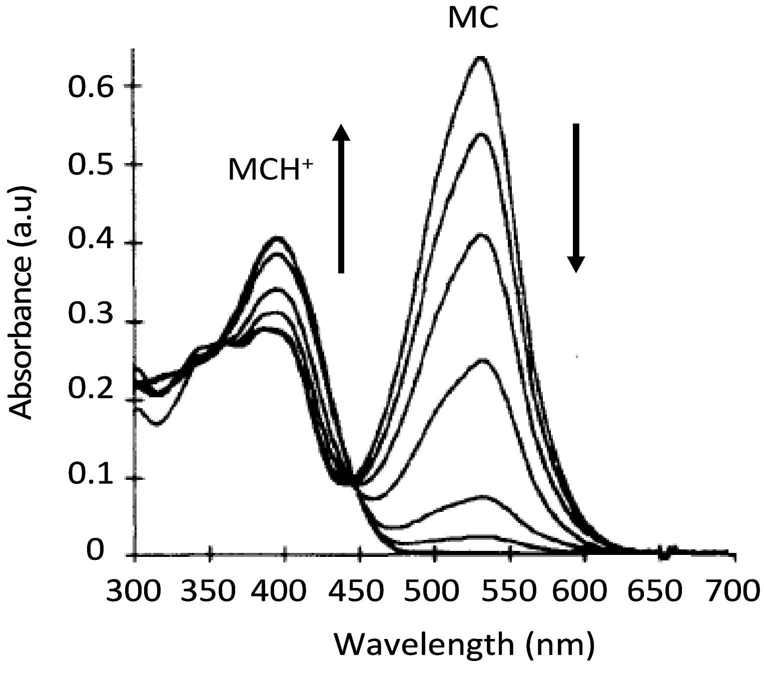

Fig 1.21 UV-Vis spectra illustrating the protonation of a spiropyran derivative.[102] Increasing concentrations of hydrochloric acid results in increased concentration of the protonated form of merocyanine; **MC-H** (395nm) and reduction in unprotonated **MC** (528nm) as reflected in increase/decrease in characteristic peaks for each form .

1.4.6 Application as ionic liquid probes

Environments provided by ionic liquids for spirocyclic compounds are found to be a very different system to that of molecular solvents. Ionic liquids consist solely of ions and so immediately present a highly charged environment. The solvent molecules themselves are large with each individual cation or anion comparable in size to the molecular solvent itself. Such variations can be assumed to have a significant role in the interactions possible between solvent and solute. The properties of spirooxazines in molecular solvents have been investigated and values found[84, 103] which act as a very reliable basis upon which results for similar studies carried out in ionic liquids may be compared.

The examination of spirocyclic compounds in ionic liquids allows the use of these compounds as probe molecules to examine solvent-solute interactions. Due to the solvent-kinetic relationship of spirocyclic compounds it has been proposed that this could be exploited to produce a suitable probe system.[67, 104] Comparison of the rates of thermal relaxation could in theory allow for the ordering of such solvents based on parameters similar to that of traditional solvatochromic dyes such as Nile red or Reichardts dye 30. Initial studies by Byrne *et al* examined a selection of $[NTf_2]^-$ based ionic liquids with a range of cation groups using **BSP**.[22] It was found that the **MC** form of the compound is somewhat sensitive to cation choice which as a result provided sufficient evidence that **MC** based solvatochromic effects could be extended to ionic liquids and as such provided a starting point for this thesis.

Ionic liquids are also of particular interest for application to spirocyclic compounds as the ability to tailor the solvent by ion selection may allow for more defined control of the processes central to photoswitching. Since spirocyclic compounds can be switched between their two forms, charged and uncharged, or from passive to active states, such switching has been successfully used for detection of metals based on the ability of merocyanine to bind metal ions with a solvatochromic response.[105] Protic ionic liquids could manipulate the acidichromic effects of spirocyclic compound while strategic choice of ions could allow for enhancement of the thermochromic effect, resulting in more defined states thru solvent mediated stabilisation of each form of the compounds with long lived/permanent isomers of the **SP/SO** and **MC$_X$** forms. Such control may allow for the potential for molecular electronics based upon photoswitchable molecules with defined on (1) and off (0) states, required for simple computational (binary) logic.

However, with probe dye characterisation of ionic liquids still in its infancy, further studies of their ability to effectively characterise this novel class of solvent must be carried out. The following study will attempt to further investigate current probe dye effectiveness and compare this to the use of spirocyclic compounds as dynamic probes based upon similar interactions. The resulting physicochemical data reported by the probe molecules will also be examined to aid in further characterisation of ionic liquids.

1.5 References

1. S. A. Forsyth, J. M. Pringle and D. R. MacFarlane, *Australian Journal of Chemistry*, 2004, **57**, 113-119.
2. N. O. Calloway, *Chemical Reviews*, 1935, **17**, 327-392.
3. P. Walden, *Bulletin de l'Academie Imperiale des Sciences de St.-Petersbourg*, 1914, 405.
4. J. S. Wilkes, J. A. Levisky, R. A. Wilson and C. L. Hussey, *Inorganic Chemistry*, 1982, **21**, 1263-1264.
5. C. L. Hussey, T. B. Scheffler, J. S. Wilkes and J. A. A. Fannin, *Journal of The Electrochemical Society*, 1986, **133**, 1389-1391.
6. X.-H. Xu and C. L. Hussey, *Journal of The Electrochemical Society*, 1992, **139**, 1295-1300.
7. F. H. Hurley and W. T. P., *Journal of the Electrochemical society*, 1951, **98**.
8. J. S. Wilkes and M. J. Zaworotko, *Journal of the Chemical Society, Chemical Communications*, 1992, **13**, 965-967.
9. C. M. Gordon, *Applied Catalysis A: General*, 2001, **222**, 101-117.
10. F. Rodrigues, G. M. do Nascimento and P. S. Santos, *Journal of Electron Spectroscopy and Related Phenomena*, 2007, **155**, 148-154.
11. L. Crowhurst, R. Falcone, N. L. Lancaster, V. Llopis-Mestre and T. Welton, *journal of organic chemistry*, 2006, **71**, 8847-8853.
12. C. P. Fredlake, M. J. Muldoon, S. N. V. K. Aki, T. Welton and J. F. Brennecke, *Physical Chemistry Chemical Physics*, 2004, **6**, 3280-3285.
13. S. Keskin, D. Kayrak-Talay, U. Akman and Ö. Hortaçsu, *The Journal of Supercritical Fluids*, 2007, **43**, 150-180.
14. Z. Duan, Y. Gu and Y. Deng, *Catalysis Communications*, 2006, **7**, 651-656.
15. J. D. Holbrey and R. D. Rogers, in *Ionic Liquids in Synthesis*, eds. P. Wasserscheid and T. Welton, VCH-Wiley, Weinheim, 2002.
16. *Ionic Liquids in Synthesis*, Second edn., WILEY-VCH, Weinheim, 2004.
17. C. Reichardt, *Green Chemistry*, 2005, **7**, 339-351.
18. I. Hemeon, N. W. Barnett, N. Gathergood, P. J. Scammells and R. D. Singer, *Australian Journal of Chemistry*, 2004, **57**, 125-128.
19. C. Chiappe and D. Pieraccini, *Journal of Physical Organic Chemistry*, 2005, **18**, 275-297.
20. I. Newington, J. M. Perez-Arlandis and T. Welton, *Organic Letters*, 2007, **9**, 5247-5250.
21. S. Carda-Broch, A. Berthod and D. W. Armstrong, *Analytical & Bioanalytical Chemistry*, 2003, **375**, 191-199.
22. R. Byrne, K. J. Fraser, E. Izgorodina, D. R. MacFarlane, M. Forsyth and D. Diamond, *Physical Chemistry Chemical Physics*, 2008, **10**, 5919-5924.
23. C. DeCastro, E. Sauvage, M. H. Valkenberg and W. F. Hölderich, *Journal of Catalysis*, 2000, **196**, 86-94.
24. K. Bica, C. Rijksen, M. Nieuwenhuyzen and R. D. Rogers, *Physical Chemistry Chemical Physics*, **12**, 2011-2017.
25. T. Ueki and M. Watanabe, *Macromolecules*, 2008, **41**, 3739-3749.
26. A. Lewandowski and A. Swiderska, *Solid State Ionics*, 2003, **161**, 243-249.
27. A. B. McEwen, H. L. Ngo, K. LeCompte and J. L. Goldman, *Journal of The Electrochemical Society*, 1999, **146**, 1687-1695.

28. A. J. Bard and L. R. Faulkner, *Electrochemical Methods: Fundamentals and Applications*, 2nd edition edn., John Wiley & sons, 2001.
29. H. L. Ngo, K. LeCompte, L. Hargens and A. B. McEwen, *Thermochimica Acta*, 2000, **357-358**, 97-102.
30. J. P. Hallett, C. L. Liotta, G. Ranieri and T. Welton, *ECS Transactions*, 2009, **16**, 81-87.
31. J. P. Hallett, C. L. Liotta, G. Ranieri and T. Welton, American Chemical Society, 2009.
32. S. G. Jones, H. M. Yau, E. Davies, J. M. Hook, T. G. A. Youngs, J. B. Harper and A. K. Croft, *Physical Chemistry Chemical Physics*, 2010, -.
33. D. R. MacFarlane, M. Forsyth, E. I. Izgorodina, A. P. Abbott, G. Annat and K. Fraser, *Physical Chemistry Chemical Physics*, 2009, **11**, 4962-4967.
34. K. Ueno, H. Tokuda and M. Watanabe, *Physical Chemistry Chemical Physics*, **12**, 1649-1658.
35. A. K. Burrell, R. E. D. Sesto, S. N. Baker, T. M. McCleskey and G. A. Baker, *Green Chemistry*, 2007, **9**, 449-454.
36. J. G. Huddleston, A. E. Visser, W. M. Reichert, H. D. Willauer, G. A. Broker and R. D. Rogers, *Green Chemistry*, 2001, **3**, 156-164.
37. J. Jacquemin, P. Husson, A. A. H. Padua and V. Majer, *Green Chemistry*, 2006, **8**, 172-180.
38. K. R. Harris, M. kanakubo and L. A. Woolf, *Journal of Chemical & Engineering Data*, 2006, **51**, 1161-1167.
39. O. O. Okoturo and T. J. VanderNoot, *Journal of Electroanalytical Chemistry*, 2004, **568**, 167-181.
40. H. Tokuda, K. Hayamizu, K. Ishii, M. A. B. H. Susan and M. Watanabe, *The Journal of Physical Chemistry B*, 2005, **109**, 6103-6110.
41. R. Fortunato, L. C. Branco, C. A. M. Afonso, J. Benavente and J. G. Crespo, *Journal of Membrane Science*, 2006, **270**, 42-49.
42. U. Domanska and A. Marciniak, *Fluid Phase Equilibria*, 2007, **260**, 9-18.
43. A. Fernandez, J. S. Torrecilla, J. Garcia and F. Rodriguez, *Journal of Chemical & Engineering Data*, 2007, **52**, 1979-1983.
44. V. Malatesta, C. Neri, M. L. Wis, L. Montanari and R. Millini, *J. Am. Chem. Soc.*, 1997, **119**, 3451-3455.
45. M. Hori, Y. Aoki, S. Maeda, R. Tatsumi and S. Hayakawa, *ECS Transactions*, **25**, 147-153.
46. T. Umecky, M. Kanakubo and Y. Ikushima, *Fluid Phase Equilibria*, 2005, **228-229**, 329-333.
47. L. Antonín, ccaron, R. D. ka, ccaron, P. S. V. M. ek, ccaron and ek, *Magnetic Resonance in Chemistry*, 2006, **44**, 521-523.
48. J. P. Armstrong, C. Hurst, R. G. Jones, P. Licence, K. R. J. Lovelock, C. J. Satterley and I. J. Villar-Garcia, *Physical Chemistry Chemical Physics*, 2007, **9**, 982-990.
49. Q. Wang, G. A. Baker, S. N. Baker and L. A. Colon, *The Analyst*, 2006, **131**, 1000-1005.
50. Y. L. Z. Z. Dongbin Zhao, *CLEAN - Soil, Air, Water*, 2007, **35**, 42-48.
51. M. Matsumoto, K. Mochiduki and K. Kondo, *Journal of Bioscience and Bioengineering*, 2004, **98**, 344-347.
52. S. Stolte, M. Matzke, J. Arning, A. Boschen, W.-R. Pitner, U. Welz-Biermann, B. Jastorff and J. Ranke, *Green Chemistry*, 2007, **9**, 1170-1179.

53. T. P. T. Pham, C.-W. Cho, J. Min and Y.-S. Yun, *The Society for Biotechnology, Japan*, 2008, **105**, 425-428.
54. K. M. Docherty, C. F. Kulpa and Jr, *Green Chemistry*, 2005, **7**, 185-189.
55. G.-h. Tao, L. He, N. Sun and Y. Kou, *Chemical Communications*, 2005, 3562-3564.
56. R. M. Vrikkis, K. J. Fraser, K. Fujita, D. R. MacFarlane and G. D. Elliott, *Journal of Biomechanical Engineering*, 2009, **131**, 074514-074514.
57. Q. Q. Baltazar, J. Chandawalla, K. Sawyer and J. L. Anderson, *Colloids and Surfaces A: Physicochemical and Engineering Aspects*, 2007, **302**, 150-156.
58. C. Jungnickel, J. Luczak, J. Ranke, J. F. Fernández, A. Müller and J. Thöming, *Colloids and Surfaces A: Physicochemical and Engineering Aspects*, 2008, **316**, 278-284.
59. B. L. Bhargava and M. L. Klein, *Molecular Physics: An International Journal at the Interface Between Chemistry and Physics*, 2009, **107**, 393 - 401.
60. Z. Miskolczy, K. Sebok-Nagy, L. Biczók and S. Göktürk, *Chemical Physics Letters*, 2004, **400**, 296-300.
61. J. Luczak, J. Hupka, J. Thöming and C. Jungnickel, *Colloids and Surfaces A: Physicochemical and Engineering Aspects*, 2008, **329**, 125-133.
62. J. Dupont, *Journal of the Brazilian Chemical Society*, 2004, **15**, 341-350.
63. J. N. C. Lopes, M. F. C. Gomes and A. A. H. Padua, *Journal of Physical Chemistry B*, 2006, **110**, 16816-16818.
64. J. N. C. Lopes and A. A. H. Padua, *Journal of Physical Chemistry B*, 2006, **110**, 3330-3335.
65. A. Seduraman, M. Klähn and P. Wu, *Calphad*, 2009, **33**, 605-613.
66. P. K. Mandal and A. Samanta, *The Journal of Physical Chemistry B*, 2005, **109**, 15172-15177.
67. C. Reichardt, *Chemical Reviews*, 1994, **94**, 2319-2358.
68. A. R. Katritzky, D. C. Fara, H. Yang, K. TÃ¤mm, T. Tamm and M. Karelson, *Chemical Reviews*, 2004, **104**, 175-198.
69. L. Crowhurst, P. R. Mawdsley, J. M. Perez-Arlandis, P. A. Salter and T. Welton, *Physical Chemistry Chemical Physics*, 2003, **5**, 2790-2794.
70. C. Reichardt, *Chemical Society Reviews*, 1992, **21**, 147-153.
71. J. Figueras, *Journal of the American Chemical Society*, 1971, **93**, 3255-3263.
72. M. J. Kamlet, J. L. Abboud and R. W. Taft, *journal of the American Chemical Society*, 1977, **99**, 6027-6038.
73. M. J. Kamlet, J. L. M. Abboud, M. H. Abraham and R. W. Taft, *Journal of organic chemistry*, 1983, **48**, 2877-2887.
74. R. W. Taft and M. J. Kamlet, *Journal of the American Chemical Society*, 1976, **98**, 2886-2894.
75. M. J. Kamlet and R. W. Taft, *Journal of the American Chemical Society*, 1976, **98**, 377-383.
76. B. R. Mellein, S. N. V. K. Aki, R. L. Ladewski and J. F. Brennecke, *J. Phys. Chem. B*, 2007, **111**, 131-138.
77. J. M. Lee, S. Ruckes and J. M. Prausnitz, *Journal of Physical Chemistry B*, 2008, **112**, 1473-1476.
78. J. Fritzsche, *Comptes rendus de l'Académie des sciences*, 1867, **69**, 1035.
79. Y. Hirshberg, *Comptes rendus de l'Académie des sciences*, 1950, **231**, 903.
80. E. Fischer and Y. Hirshberg, *Journal of the chemical society*, 1952, 4522.

81. G. Berkovic, V. Krongauz and V. Weiss, *Chemical Reviews*, 2000, **100**, 1741-1754.
82. D. A. Parthenopoulos and P. M. Rentzepis, *Science*, 1989, **245**, 843-845.
83. V. I. Minkin, *Chemical Reviews*, 2004, **104**, 2751-2776.
84. S. Minkovska, B. Jeliazkova, E. Borisova, L. Avramov and T. Deligeorgiev, *Journal of Photochemistry and Photobiology A: Chemistry*, 2004, **163**, 121-126.
85. J. Hobley, U. Pfeifer-Fukumura, M. Bletz, T. Asahi, H. Masuhara and H. Fukumura, *Journal of Physical Chemistry A*, 2002, **106**, 2265-2270.
86. F. Wilkinson, D. R. Worrall, J. Hobley, L. Jansen, S. L. Williams, A. J. Langley and P. Matousek, *Journal of the Chemical Society, Faraday Transactions*, 1996, **92**, 1331-1336.
87. A. K. Chibisov and H. Gorner, *Journal of Physical Chemistry A*, 1997, **101**, 4305-4312.
88. A. K. Chibisov and H. Gorner, *Journal of Physical Chemistry A*, 1999, **103**, 5211-5216.
89. R. Guglielmetti, *Photochromism: Molecules and Systems*, Elsevier, 1990.
90. Y. Liu, M. Fan, C. Zhang, W. Yang, L. Zhu, G. Zhang, Z. Shuai, J. Zhou, W. Yan, H. Fu and J. Yao, *Dyes and Pigments*, 2008, **76**, 264-269.
91. G. Such, R. A. Evans, L. H. Yee and T. P. Davis, *Polymer Reviews*, 2003, **43**, 547 - 579.
92. C. Salemi, G. Giusti and R. Guglielmetti, *Journal of Photochemistry and Photobiology A: Chemistry*, 1995, **86**, 247-252.
93. G. Bailllet, M. Campredon, R. Guglielmetti, G. Giusti and C. Aubert, *Journal of Photochemistry and Photobiology A: Chemistry*, 1994, **83**, 147-151.
94. K. J. Laidler and J. H. Meiser, *Physical Chemistry*, 3rd edition edn., Houghton Mifflin, Boston, 1999.
95. G. Cottone, R. Noto and G. La Manna, *Chemical Physics Letters*, 2004, **388**, 218-222.
96. R. Byrne, Dublin City University, 2008.
97. M. Bletz, U. Pfeifer-Fukumura, U. Kolb and W. Baumann, *The Journal of Physical Chemistry A*, 2002, **106**, 2232-2236.
98. N. A. Voloshin, A. V. Metelitsa, J. C. Micheau, E. N. Voloshina, S. O. Besugliy, N. E. Shelepin, V. I. Minkin, V. V. Tkachev, B. B. Safoklov and S. M. Aldoshind, *Russian Chemical Bulletin*, 2003, **52**, 2038-2047.
99. N. A. Voloshin, A. V. Metelitsa, J. C. Micheau, E. N. Voloshina, S. O. Besugliy, A. V. Vdovenko, N. E. Shelepin and V. I. Minkin, *Russian Chemical Bulletin*, 2003, **52**, 1172-1181.
100. A. S. Dvornikov, J. Malkin and P. M. Rentzepis, *The Journal of Physical Chemistry*, 1994, **98**, 6746-6752.
101. H. Durr and H. Bouas-Laurent, *Photochromism Molecules and systems*, Elsevier, Amsterdam, 2003.
102. J. Zhou, Y. Li, Y. Tang, F. Zhao, X. Song and E. Li, *Journal of Photochemistry and Photobiology A: Chemistry*, 1995, **90**, 117-123.
103. G. Favaro, F. Masetti, U. Mazzucato, P. Ottavi, P. Allegrini and V. Malatesta, *Journal of the Chemical Society, Faraday Transactions*, 1994, **90**, 333-338.
104. L. G. S. Brooker, A. C. Craig, D. W. Heseltine, P. W. Jenkins and L. L. Lincoln, *Journal of the American Chemical Society*, 1965, **87**, 2443-2450.

105. A. V. Chernyshev, N. A. Voloshin, I. M. Raskita, A. V. Metelitsa and V. I. Minkin, *Journal of Photochemistry and Photobiology A: Chemistry*, 2006, **184**, 289-297.

2

Novel Environments for Solution based Photochemistry: Thermodynamic and Kinetic Study of Spirocyclic Compounds in Ionic Liquids

2.1 Introduction

The following study represents a detailed study into the feasibility of spirocyclic compounds, spiropyran (**BSP**) and spirooxazine (**SO**), as probe molecules for investigating structuring within ionic liquids, by analysing their thermal relaxation rates in a number of bis(trifluoromethanesulfonyl)imide anion ($[NTf_2]^-$) based ILs (figure 1.3). The physiochemical properties of ionic liquids have been previously examined using picosecond time-resolved fluorescence[1] and solvatochromic probe dye studies using both single parameter studies based on pyridinium *N*-phenolate betaine dye,[2,3] nile red[4,5] and 2-nitrocycloexanone[6] and multiparameter studies using Kamlet-Taft parameters.[7-10] Solvatochromic methods are based on the principle that these dyes interact with the solvent into which they are added and the extent of these interactions is directly related to the rate of thermal relaxation of the compounds from their **MC** to **SP** forms. Both **BSP** and **SO** contain different functional groups which may allow for a more extensive analysis of the physicochemical properties of each liquid system based upon differing interactions occurring within the ionic liquids with each probe and the effect of changing the anion and cation component.

2.2 Experimental

Ionic liquids produced for this study were purified using previously reported techniques,[11] illustrated in Appendix A-1, and synthesised using precursor salts obtained from Sigma-Aldrich. Due to the hygroscopic nature of ionic liquids, all liquids synthesised were dried thoroughly by heating to 65ºC under high vacuum for 24 hours. The resulting dried liquids are then stored under nitrogen to exclude absorption of atmospheric water which could act as an interfering species to the ionic liquid itself or solute molecules within it. Absorbance measurements were carried out using a Perkin Elmer Lambda 900 spectrometer with a Perkin Elmer PTP-1 temperature controller. The ultraviolet irradiation source was a 3 UV LED array at 375 nm based on LEDs obtained from Roithner Lasertek (Germany) (Appendix A-2). The white light source was a Lumina obtained from Chiu Technical Corporation. Samples were irradiated at a distance of 1 cm for 30 seconds. Standard solutions of **BSP** and **SO** were made at 1 x 10^{-4}M concentrations in acetonitrile. 1 ml of this solution was placed in a vial and the solvent removed by N_2 stream. To this 1ml of the selected solvent is added to the vial and placed in a sonicator for 10 minutes at 40^{o}C. Samples were stored under argon in the dark at 20^{o}C for 15 hours before absorbance measurement was taken for equilibrium constant determination. The kinetic parameters of the **MC** thermal reversion to **BSP** and **SO** were determined at each temperature by monitoring the disappearance of the **MC** at the λ_{max} after removing the irradiating source. Reichardts dye 30 (sigma chemicals) , 4-nitroaniline (sigma chemicals) and n,n diethyl-4-nitroaniline (Fluorochem) were used as purchased. 1,3,3-trimethyl-5'-(2-benzothiazolyl)-spiroindoline-2,3'-naphtho(2,1-b)(1,4) oxazine (**SO**) was kindly supplied by Dr. Minkovska of the Bulgarian

Institute of Catalysis and used as supplied. 2,3-dihydro-1',3',3'-trimethyl-6-nitrospiro[1-benzopyran-2,2'-1H-indole] (**BSP**) was purchased from Sigma chemicals and used as supplied. HPLC grade acetonitrile was used without further purification. Tetradecyl(trihexyl)-phosphonium bis(trifluoromethylsulfonyl)imide ([$P_{6,6,6,14}$][NTf_2]), tetradecyl(trihexyl)-phosphonium dicyanamide ([$P_{6,6,6,14}$][dca]), tetradecyl(trihexyl)-phosphonium dodecylbenzenesulfonate ([$P_{6,6,6,14}$][dbsa]), triisobutyl(methyl)phosphonium tosylate ([$P_{1,4,4,4}$][tos]) were supplied by Cytec industries Tetradecyl(trihexyl)-phosphonium tris(pentafluoroethyl)trifluorophosphate ([$P_{6,6,6,14}$][FAP]) was supplied by Merck. Phosphonium based ILs were purified before use. Linear solvation energy relationship (LSER) analysis was carried out by Dr. Jason Hallett of Imperial College, London using our experimental data.

2.3 Results and Discussion

2.3.1 Solvent parameters

Solvent polarity

To allow for comparison of ionic liquids to molecular solvents and literature values, the commonly used $E_T(30)$ scale was chosen as the reference scale and initial means of organisation of the different ionic liquids. The polarities were determined by addition of 1x 10^{-3} M Reichardts dye 30 to a selection of molecular solvents and ionic liquids composed of a selection of popular cations. Immediate differences in polarities were apparent by distinct colouring of each solution as observed in figure 2.1a. Solvents in the figure were labelled **1**–**9** as follows: **1-**methanol, **2-**ethanol, **3-**acetonitrile, **4-**acetone, **5-**$[C_4mIm][NTf_2]$, **6-**$[C_2m_2Im][NTf_2]$, **7-**[bmPy]$[NTf_2]$, **8-**$[P_{6,6,6,14}][NTf_2]$, **9-**$[N_{1,8,8,8}][NTf_2]$.

Using equation **(1)** (chapter 1, section 1.3.1), the $E_T(30)$ values were found for selected solvents (table 2.1). $E_T(30)$ values were compared to the corresponding dielectric constants of the solvents where available and were found to disagree in their ordering of molecular solvents. This may have been due to the difficulty in approximating the polarity value of a solvent based on a generalised overview of the solvent system as stated by Reichardt where techniques for polarity approximations are "often inadequate since these theories regard solvents as a non-structured isotropic continuum, not composed of individual solvent molecules with their own solvent/solvent interactions, and they do not take into account specific solute/solvent interactions such as hydrogen-bonding and electron pair donation (EPD)/electron pair acceptance (EPA) interactions, which often play a dominant role in solute/solvent interactions.” [12]

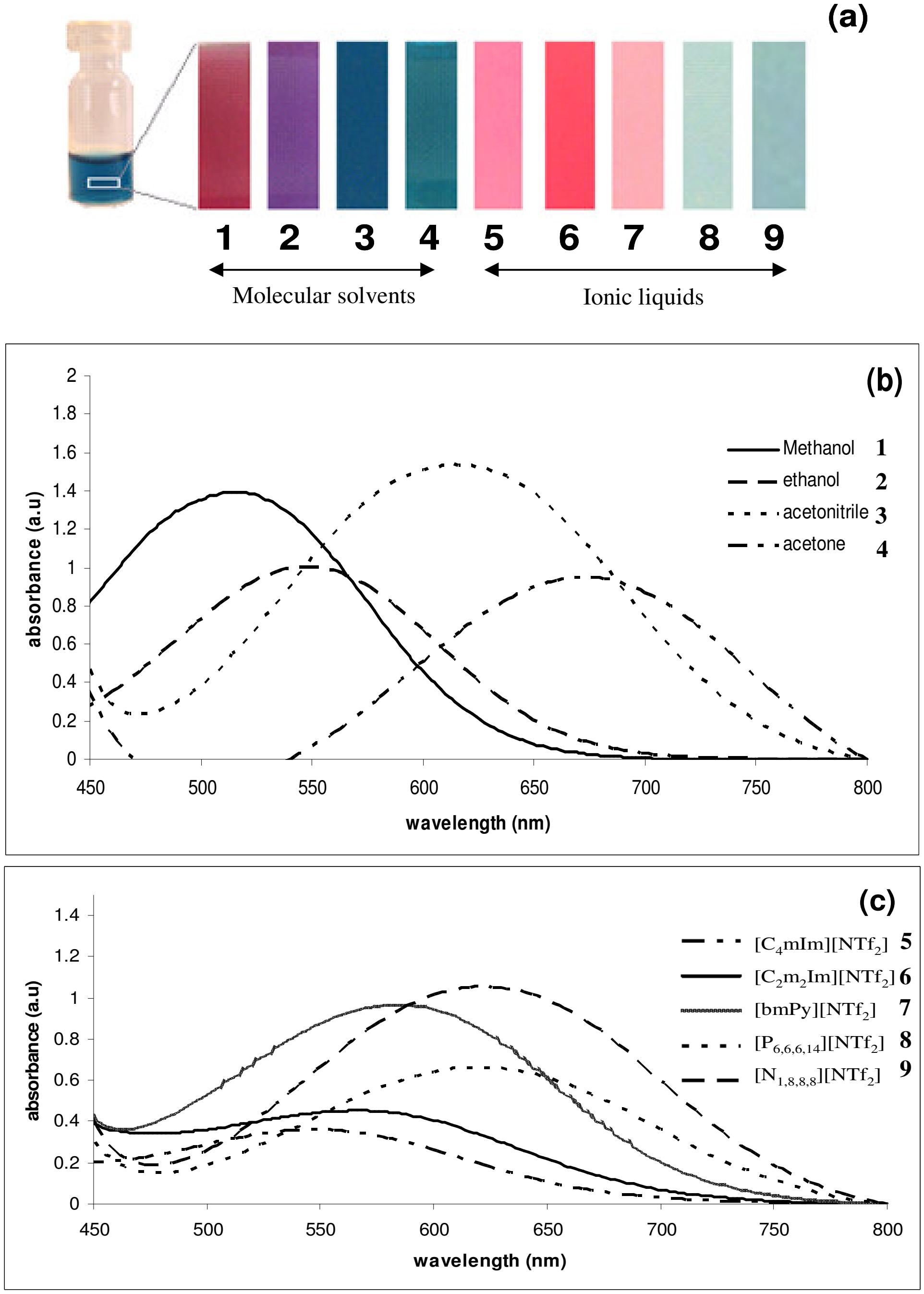

Figure 2.1 (a)Reichardts dye 30 in ILs and molecular solvents. Colours were enlarged from vials as shown. (b) UV-vis spectra of Reichardts dye 30 in molecular solvents. (c) UV-vis spectra of Reichardts dye 30 in ionic liquids.

In addition to this, reviews such as those by Katritzky's illustrate the availability of several hundred polarity scales and therefore the difficulty of quantifying polarity under one universal scale.[13]

Table 2.1 Experimental values for physicochemical properties (298K) of molecular solvents and ionic liquids. Reference values in parenthesis

Solvent	***Et(30) (kcal/mol)***	***α***	***β***	***π****
Triton X-100	69.7	1.98	0.653	0.733
methanol	55.4 (55.4)[2]	1.06 (1.05)[14]	0.62 (0.61)[14]	0.71 (0.73)[14]
ethanol	52.1 (51.9)[2]	0.90 (0.86)[15]	0.72 (0.77)[15]	0.63 (0.54)[15]
acetonitrile	46.4 (45.6)[2]	0.42 (0.35)[14]	0.37 (0.37)[14]	0.79 (0.79)[14]
acetone	42.5 (42.2)[2]	0.25 (0.20)[14]	0.57 (0.54)[14]	0.67 (0.70)[14]
hexane	(-31.0)[2]	0.04 (0.07)[8]	0.08 (0.04)[8]	-0.08 (-0.12)[8]
$[C_4mIm][\,NTf_2]$	52.4 (51.5)[16]	0.72(0.69)[14]	0.24 (0.25)[14]	0.90 (0.97)[14]
$[C_2m_2Im][\,NTf_2]$	50	0.42	0.1	1.02
$[\,bmPy][\,NTf_2]$	49.6 (50.2)[9]	0.57 (0.43)[8]	0.23 (0.25)[8]	0.87 (0.95)[8]
$[P_{6,6,6,14}][\,NTf_2]$	46.1	0.37	0.27	0.83
$[N_{1,8,8,8}][\,NTf_2]$	45.9	0.33	0.23	0.87

The highly conductive nature of ionic liquids restricts the measurement of their dielectric constant and so ionic liquid polarity are commonly reported using the E$_T$(30) scale. These values are compared to E$_T$(30) values found in molecular solvents, whose dielectrics are known, to obtain information of their approximate polarity. Values found in table 2.1 imply that ionic liquids exhibit generally polar characteristics. Imidazolium and pyrrolidinium based ILs appear similar to that of short chain alcohols while phosphonium and tetra-alkyl ammonium ILs have polarities comparable to polar aprotic solvents such as acetonitrile. Ring based ILs (imidazolium and pyrrolidinium) were found to have the highest E$_T$(30) values followed by the alky-chained cations. Separation of $E_T(30)$ values, based upon cation structure, into ring based and alkyl chained cation provided a similar trend to that observed with aprotic and protic solvents. The ring based cation $[C_4mIm]^+$ has a strong C2 hydrogen bonding sites and exhibits the most polar characteristics. This is followed by dimethyl imidazolium and pyrrolidinium cations which have moderate hydrogen bonding. This appears to indicate that hydrogen bond ability placed a 'protic' characteristic upon ionic liquid systems. The remaining alkyl chain based ILs have less hydrogen bond ability due to extensive non-polar influences of the alkyl chain side groups and presented more aprotic characteristics.

Kamlet-Taft parameters

Due to the limitations of single parameter studies[17], Kamlet-Taft multiparameter studies were carried out to explicitly examine molecular interactions due to hydrogen bonding and charge distribution in each solvent system. To investigate this, three solvatochromic dyes, Reichardts dye (1×10^{-4} M), 4-nitroaniline (5×10^{-5} M) and *n,n*-diethyl-4-nitroaniline (5×10^{-5} M), were added to each of the ionic liquids and the resulting peak shifts were recorded using UV-Vis spectrometry. These shifts were examined empirically to quantify each parameter using equations **(2), (3)** and **(4)** (chapter 1, section 1.2.2) which are summarised in table 2.1. In molecular solvents, α values are typically found to increase with increasing polarity with a corresponding decrease in β values. π^* values vary depending on the ability of the solvent molecule to polarize the system.

2.3.2 Effects of cation change on the properties of spirocyclic compounds in ionic liquids based on the $[NTf_2]^-$ anion

Kinetic parameters

The kinetics of thermal relaxation of $\mathbf{MC_{SO}}$→**SO** and $\mathbf{MC_{BSP}}$→**BSP** were investigated at the corresponding λ_{max} of each respective **MC** found in each solvent system and compared to Kamlet-Taft parameters (table 2.1) to examine polarity-kinetic relationships. The thermal relaxation of each compound is found to follow a first order exponential decay curve from which the first order rate constant in each solvent is found by plotting $\ln(A/A_0)$ vs. time and the rate determined from the slope of the curve using equation **(14)** below and summarised in tables 2.2 and 2.3. Analysis of first order decay curves to determine rate constants is discussed in appendix A-5

$$Ln\frac{[A]}{[A_0]} = -kt \qquad \textbf{(14)}$$

Where,
[A] = absorption at time t
$[A_0]$ = absorption at 0 seconds
k = rate constant
t = time (s)

Analysis of **SO** in non-viscous, simple molecular solvents retained a polarity-kinetic relationship characteristic of spirocyclic compounds (figure 2.2). Table 2.1 shows a linear relationship between $E_T(30)$, α and β values and rates of relaxation. It is found that α values in molecular solvents are relatively high (1.05 kcal/mol in methanol), due to hydrogen bonding dominating the solvent-solvent and solvent-solute interactions in molecular solvents. Similar trends are not observed for β values with varied response observed across the molecular solvents examined. For polar protic solvents, both hydrogen bond donation and acceptance are high which implies that the solvents could interact with the charge sites of the merocyanine and thus increase the lifetime of this form.

Table 2.2 Rate constants for $\mathbf{MC_{SO}} \rightarrow$ **SO** (298K) in molecular solvents and ionic liquids. Reference values in parenthesis

Solvent	***Et(30) (kcal/mol)***	***MC λ_{max}***	***SO k (10^{-2} s^{-1})***
methanol	55.4 (55.4)[2]	640	3.2
ethanol	52.1 (51.9)[2]	642	3.8 (2.0)[18]
acetonitrile	46.4 (45.6)[2]	642	5.0 (5.2)[18]
acetone	42.5 (42.2)[2]	642	5.1 (5.4)[18]
Triton X-100	69.7	648	3.5
$[C_4mIm][NTf_2]$	52.4 (51.5)[16]	642	2
$[C_2m_2Im][NTf_2]$	50	640	2.3
[bmPy][NTf$_2$*]*	49.6 (50.2)[9]	642	2.2
$[P_{6,6,6,14}][NTf_2]$	46.1	648	1.1
$[N_{1,8,8,8}][NTf_2]$	45.9	646	1.5

Thermal relaxation rates of $\mathbf{MC_{SO}}$ in molecular solvents are slower in alcohols (polar protic) with rates of 3.2 x 10^{-2} s^{-1} and 3.8 x 10^{-2} s^{-1} in methanol and ethanol respectively. Polar aprotic solvents have an approximate 1.5 fold increase in relaxation rates to 5.2 x 10^{-2} s^{-1} and 5.5 x 10^{-2} s^{-1} in acetonitrile and acetone respectively which is believed to be due to the lack of the hydrogen bonding in these solvents (as found by Kamlet-Taft parameters) which decreases the relative stability of **SO**.

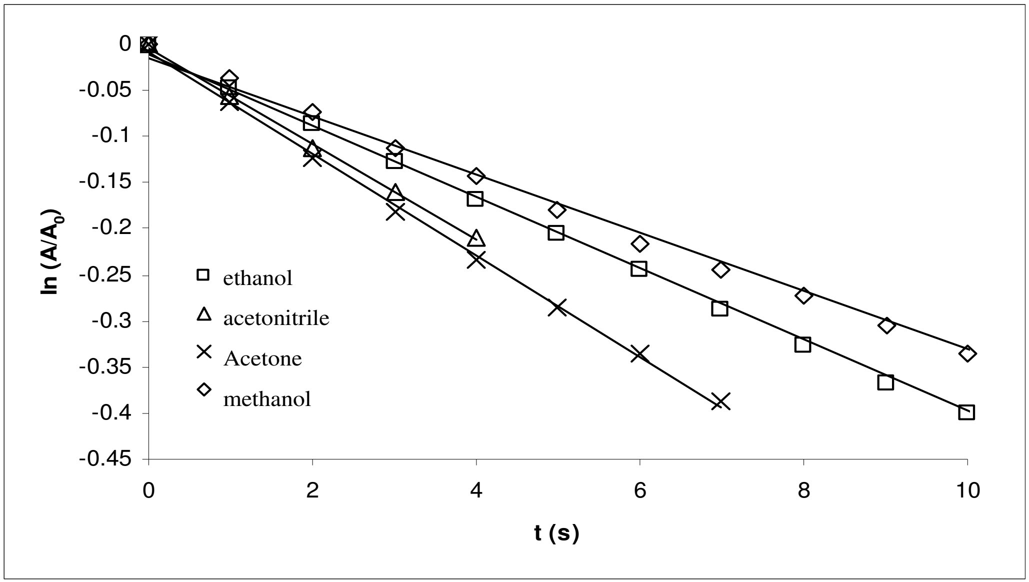

Figure 2.2 First order thermal relaxation of **SO** in molecular solvents.

To examine the possibility of viscosity effects and increasing the complexity of the solvent system, **SO** was added to Triton X-100 which appeared to have similar viscosity to that of ionic liquids, particularly phosphonium and alkyl ammonium based ILs. In addition to this, Triton X-100 molecules are known to contain both polar and non-polar segments in each molecule, each of which would interact with the spirocyclic compound differently. $E_T(30)$ values reported highly polar environments at 69.7kcal.mol^{-1} while Kamlet-Taft parameters described a high α value of 1.98 which implies significant H-bond donation. Examination of the thermal relaxation rate in Triton X-100 appeared to be similar to that of **MC$_{SO}$** relaxation in alcohols. This value is unexpected since the $E_T(30)$ polarity, strength of H-bond interactions and the higher viscosity of the system would be expected to enhance stability and increase the lifetime of the **MC$_{SO}$**. However, thermal relaxation is found to be equal to the average relaxation rate within polar protic solvents of 3.5x10^{-2} s^{-1}. This similarity implies that **SO** may be somewhat immune to physical (viscosity) properties of molecular solvents and exhibit general rates of relaxation depending on solvent-solute interactions (H-bond/electrostatic)

Photoswitching of **SO** in ionic liquids (figure 2.3) appears to result in a general increase the **MC$_{SO}$** lifetime, with thermal relaxation rates corresponding to that of highly polar molecular solvents. When the thermal relaxation rates are compared to the Kamlet-Taft parameters it is found that ionic liquids did not show the same correlation as observed in molecular solvents. α values appeared significantly lower for alkyl chain based ILs ($[N_{1,8,8,8}]^+$ and $[P_{6,6,6,14}]^+$) relative to ring based ILs. Comparison of these values to thermal relaxation rates fail to rationalise the kinetics observed based upon hydrogen bonding since the effects appear reversed when compared to those established molecular solvents. β values are relatively constant across all the selected ionic liquids and generally smaller than those found in molecular solvents. Since β values are believed to correspond to the influence of the anion, which is common to each ionic liquid, and implies that the $[NTf_2]^-$ anion is somewhat benign and had minimal interactions with the **MC$_{SO}$** which correspond well to previous studies[19]. A common anion results in any variations in the relaxation kinetics most likely arising primarily from cation interactions. Since the rate constants observed are all relatively constant, when divided into ring based and alkyl chain based IL subclasses, this suggests that variations in hydrogen bonding behaviour has limited influence on the mechanism and that cation structure may be more influential than previously thought. The relatively high π* values suggest that coulombic interactions may also be influential for ionic liquid interactions. High values are expected due to the charged nature of ionic liquids but the relatively constant π* values also correlate well against the equivalent rate constants. Ion based electrostatic interactions tend to be much stronger than hydrogen bonds and these appear to dominate the relaxation kinetics and possibly the polarity scales. This may result in $E_T(30)$ values of limited use for interpreting kinetics of thermal relaxation of **SO** in ionic liquids.

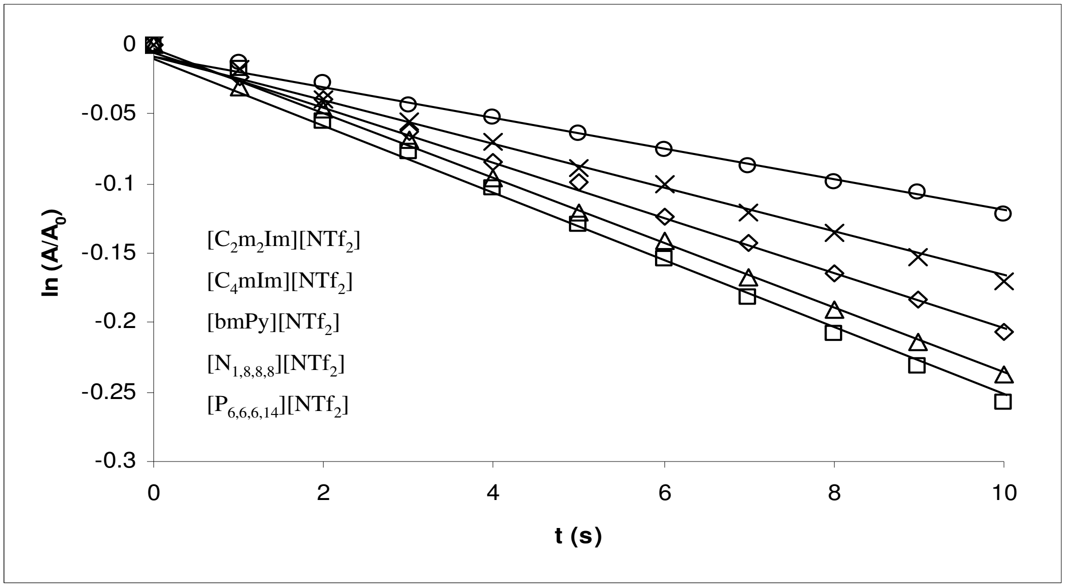

Figure 2.3 First order thermal relaxation of **SO** in selected ionic liquids.

Comparison of **MC$_{SO}$→SO** thermal relaxation in molecular solvents and ionic liquids of similar polarity highlight the discrepancies in the approximation of solvent parameters. Figure 2.4 shows that the rate of relaxation of **MC$_{SO}$→SO** decreases in two ionic liquids compared to molecular solvents with comparable $E_T(30)$ values. The thermal relaxation curves of [C$_4$mIm][NTf$_2$] and ethanol and [P$_{6,6,6,14}$][NTf$_2$] and acetonitrile clearly illustrates that ionic liquids extend the lifetimes of **MC$_{SO}$** while the molecular solvents exhibit faster relaxation rates.

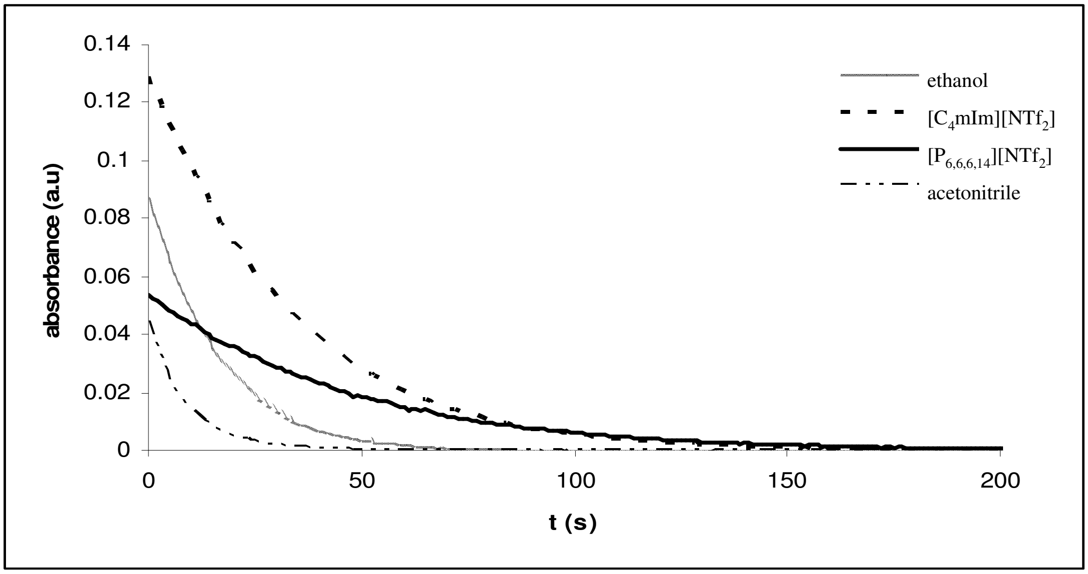

Figure 2.4 Baseline corrected first order decay curves for the thermal relaxation of **SO** in molecular solvents and ionic liquids of similar $E_t(30)$ polarity but differing rates of decay:

- ethanol (52.1 kcal/mol) and $[C_4mIm][NTf_2]$ (52.4 kcal/mol)
- acetonitrile (46.4 kcal/mol) and $[P_{6,6,6,14}][NTf_2]$ (46.1 kcal/mol)

The rate constants for **MC_{BSP}→BSP** were determined in a similar manner to that of **SO**[19] with $1x10^{-4}$ M solutions of **BSP** irradiated with UV light. The first order exponential decay of **MC_{BSP}→BSP** in ionic liquids was used to determine the rates of thermal relaxation using equation **(14)**. The resulting rates are summarised in table 2.3 and compared to $E_T(30)$ and, where applicable, Kamlet-Taft parameters.

Table 2.3 Physicochemical study of **BSP** in molecular solvents and ionic liquids.[19] Reference values in parenthesis.

Solvent	$E_T(30)$ (kcal/mol)	BSP λ_{max} MC (nm)	BSP k ($x10^{-4}$ s^{-1})
Ethanol	51.8 (51.9)[2]	539	3
Acetonitrile	45.5 (45.6)[2]	554	3.8
Dichloromethane	40.6 (40.7)[2]	578	95
Hexane	(-31.0)[2]	578	566
Triton X-100	69.7	565	14.5
$[C_2mIm][NTf_2]$	53.3 (53.1)[3]	544	0.7
$[C_2m_2Im][NTf_2]$	51.79	548	5
$[pmPy][NTf_2]$	48.9	549	12.1
$[bmPy][NTf_2]$	48.1(48.3)[8]	551	11.4
$[P_{6,6,6,14}][NTf_2]$	47.97	574	0.3

Thermal relaxation of **MC$_{BSP}$** in non-viscous simple molecular solvents was found to obey a linear response of increasing rates of relaxation with decreasing polarity. However, the addition of **BSP** to a viscous, complex molecular solvent; Triton X-100, was found to deviate from such relationships. Triton X-100 is found to be highly polar and exhibit a strong H-bond donor property (table 2.1) under $E_T(30)$ and Kamlet-Taft parameters respectively. Rates of **MC$_{BSP}$** thermal relaxation are found to be $14.5x10^{-4}s^{-1}$. Such values would be associated with a solvent of polar aprotic or mild non-polar properties. This appeared counterintuitive since polarity values would appear to imply a highly stabilising environment. The viscosity of the solvent is also observed to be much higher than that of the other molecular solvents chosen in this study. Previous studies have shown that viscosity can have a significant effect upon the rates of thermal relaxation of spirocyclic compounds. For Triton X-100 it appears that viscosity does not affect the thermal relaxation of $\mathbf{MC_{BSP}}$ as expected. Triton X-100, containing both a hydrophilic *and* hydrophobic component, may possibly have interactions between the solvent's non-polar groups which increase the rate of thermal relaxation regardless of the viscous nature of the liquid (which could possibly related to the association of polar and/or non-polar groups to one another).

$\mathbf{MC_{BSP}}$ thermal relaxation rates in ionic liquids also appear to not yield correlations based upon solvent $E_T(30)$ polarity values and rates of $\mathbf{MC_{BSP}}$ thermal relaxation, showing no linear relationship as established in molecular solvents (figure 2.5). This lack of correlation is believed to arise from the complex nature of the ionic liquids due to solvent-solvent interactions leading to the possibility of structuring present within the liquid itself. These effects seem similar to those of Triton X-100, where polarity and viscosity are not complimented by the rate of thermal relaxation. **BSP**, like **SO**, appears immune to viscosity effects as observed in molecular solvents but the fact that an extensive network of alkyl chains are present within $[P_{6,6,6,14}][NTf_2]$ and $[N_{1,8,8,8}][NTf_2]$ systems, it is proposed that the interactions of such chains from an extended network of cations which present themselves as steric hindrance to the relaxing $\mathbf{MC_{SO}}$ molecules. Comparison of $\mathbf{MC_{BSP}}$ thermal relaxation rates to Kamlet-Taft parameters for $[P_{6,6,6,14}][NTf_2]$, $[C_2m_2Im][NTf_2]$ and $[bmPy][NTf_2]$ did not correlate as was concluded from $\mathbf{MC_{SO}}$ studies.

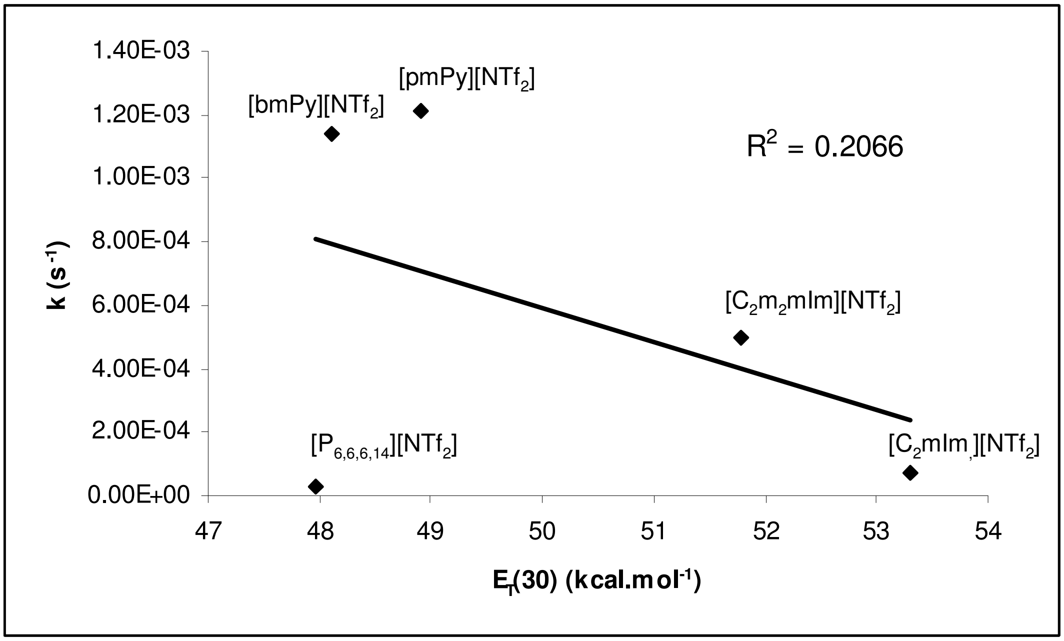

Figure 2.5 Inconsistencies between solvent polarity and **BSP** kinetics in ionic liquids.

BSP is found to be somewhat more sensitive than **SO** with respect to solvatochromic effects. Detectable changes in **MC$_{BSP}$** λ_{max} and appreciable changes in rates of thermal relaxation for each ionic liquid was also observed which were not as apparent for **SO**. Interestingly, separation into, imidazolium, pyrrolidinium and phosphonium ILs was found to group thermal relaxation rates into linear responses as observed in molecular solvents. Comparison of both structures in figure 1.8 highlights the structural differences which may be critical to this sensitivity. The increased availability of phenolate oxygens and the presence of a nitro group on the pyran fragment of **MC$_{BSP}$** molecules appear to endow the desirable solvatochromic and kinetic properties upon the compound. Replacement of the nitro group with a benzene ring and the restrictive nature of the benzothiophene group in close proximity to the phenolate oxygen on **MC$_{SO}$**

appears to remove the important interactions and charge distributions which allow for the effective implementation of such compounds and solvent probes. For this reason, **BSP** may be sensitive enough to detect a change of cation species but augmentations such as functionalisation within of the cation appears difficult to quantify as reflected by similar rates of relaxation in each cation class.

Thermodynamic Parameters

The requirement to separate ionic liquids based upon cation base structure (ring or alkyl chain based) to somewhat correlate the polarity-kinetic relationship of spirocyclic compounds strengthens the proposed influence of solvent structure upon physicochemical effects. To further examine the structural influence of ionic liquids, the thermodynamic parameters of spirocyclic compounds were observed within ionic liquids. Using the Arrhenius (equation (**10**)**;** chapter 1, section.1.4.2) and Eyring (equation (**12**) and (**13**); chapter 1, section 1.4.2) equations the thermodynamic parameters were determined for **SO** in a range of ionic liquids with differing cation groups and summarised in table 2.4 below. The reaction process for thermal relaxation of spirocyclic compounds was deemed to be similar throughout the range of ionic liquids and allowed for comparison of results found (See appendix A-4)

Table 2.4 Thermodynamic Parameters of activation for $\mathbf{MC_{SO}} \rightarrow \mathbf{MC^{\ddagger}_{SO}}$ thermal relaxation.

Solvent	***Activation energy(E_a) (kJ.mol^{-1})***	***$\Delta H^{\ddagger}$ (kJ.mol^{-1})***	***$\Delta G^{\ddagger\,298}$ (kJ.mol^{-1})***	***$\Delta S^{\ddagger}$ (J.K^{-1}.mol^{-1})***	***$K^{\ddagger\,298}$ (x10^{-15})***	***$E_T(30)$ (kcal.mol^{-1})***
Triton X-100	91.73	89.3	81.37	26.6	5.56	69.7
methanol	86.15	83.72	81.41	7.76	5.09	55.4
ethanol	84.16	81.72	81.21	1.7	6.06	52.1
acetonitrile	66.24	63.81	80.43	-55.78	8.05	46.4
acetone	68.47	66.04	80.45	-48.37	8.26	42.5
$[C_4mIm][NTf_2]$	95.08	92.64	82.77	33.13	3.2	52.4
$[N_{1,8,8,8}][NTf_2]$	89.31	86.88	83.49	11.36	2.48	45.9
$[bmPy][NTf_2]$	88.3	85.87	82.55	11.13	3.49	49.6
$[C_2m_2Im[NTf_2]$	87.56	85.12	82.41	9.11	3.77	50
$[P_{6,6,6,14}][NTf_2]$	81.88	79.45	84.2	-15.95	1.77	46.1

1 calorie = 4.184 Joules

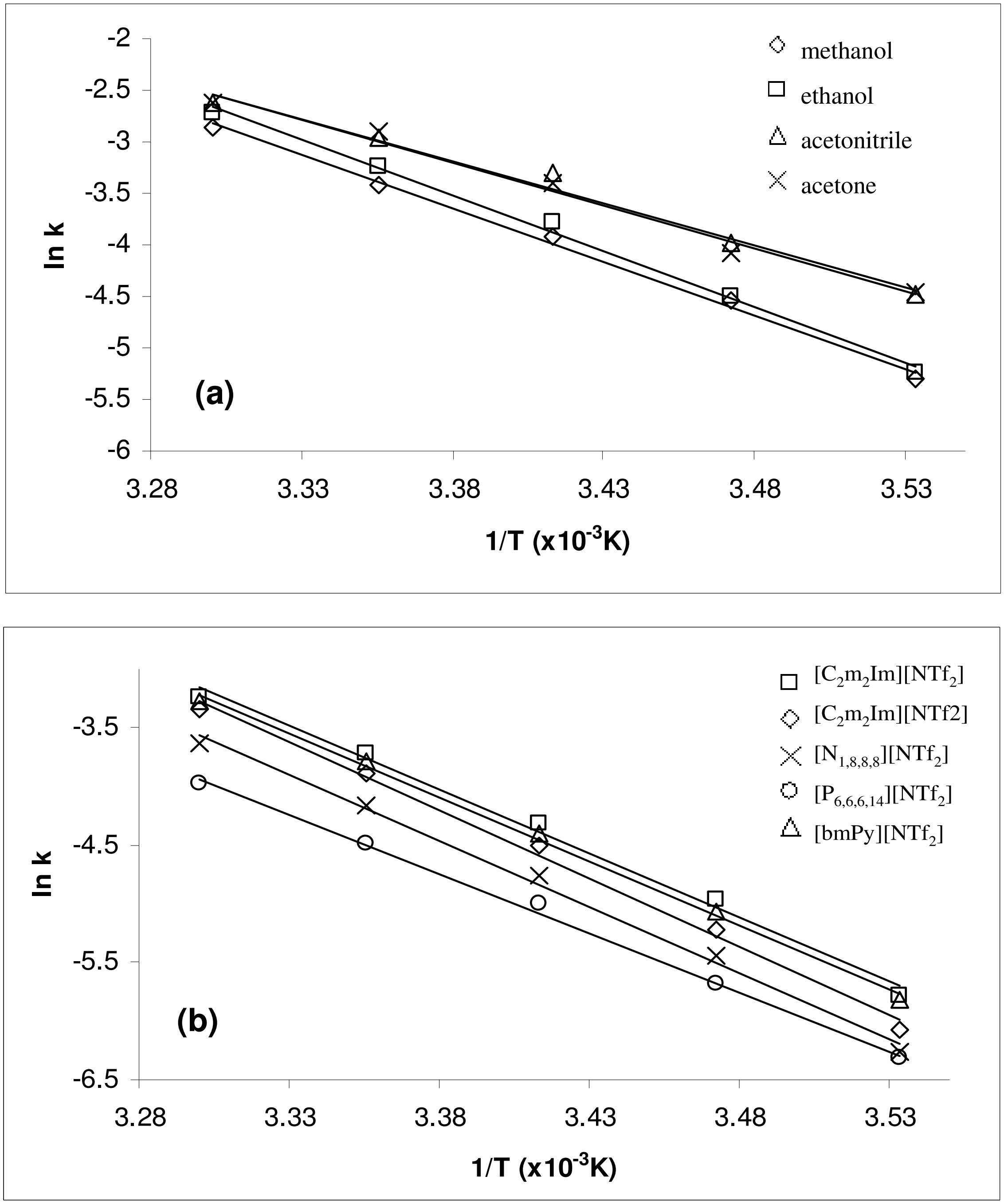

Figure 2.10 Arrhenius plots for **MC$_{SO}$→SO** in (a) molecular solvents and (b) ionic liquids.

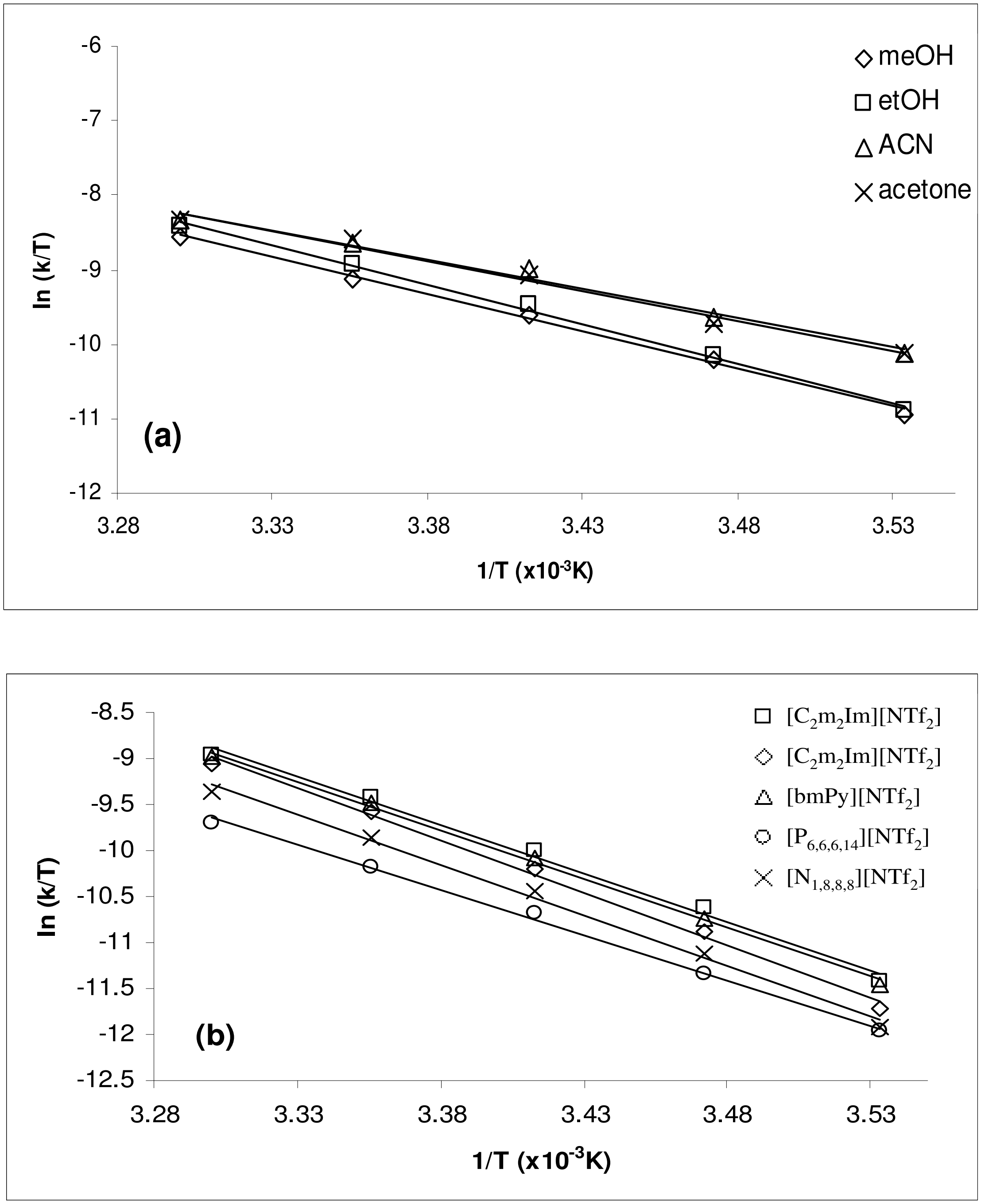

Figure 2.11 Eyring plots for **MC_{SO}→SO** thermal relaxation in (a) molecular solvents and (b) ionic liquids.

Activation energies (E_a) varied between 66.24 and 91.73 kJ.mol^{-1} in molecular solvents and 81.88 and 95.08 kJmol^{-1} in ionic liquids (table 2.4). Since **MC_{SO}** is a zwitterion, it is intuitive to expect that these polar molecules would have increasing interactions with solvent molecules of increasing polarity and hence this isomer would be stabilised relative to the **SO** isomer. The charged nature of the ionic liquids ions would therefore be expected to enhance this stability and this is reflected in the increased values observed in ionic liquids. $\Delta G^{\ddagger}$ values for the **MC_{SO}→$MC^{\ddagger}_{SO}$** process were estimated using equation **(11)**. Values are found to be positive and approximately +82 kJ.mol^{-1} in all solvents, as observed in polar molecular solvents (table 2.4). The lack of significant differences for $\Delta G^{\ddagger}$ values appear to arise from compensation effects between $\Delta H^{\ddagger}$ and $\Delta S^{\ddagger}$ factors within the system.[20] A general reduction in $\Delta H^{\ddagger}$ values is typically met with a reduction in $\Delta S^{\ddagger}$ values which in turn buffered the negative effects upon the $\Delta G^{\ddagger}$ values. However, since enthalpic processes dominate the molecular reorientation process, it is found that the changes in these values had the greatest effect upon the Gibbs energies of activation of the process. Enthalpies of activation, $\Delta H^{\ddagger}$, are also found to share similarities to the activation energy of the system since $\Delta H^{\ddagger}$ calculates the amount of energy required to allow for the molecular reorientation to occur, which in the case of **MC_{SO}→$MC^{\ddagger}_{SO}$**, is an endothermic process. The positive $\Delta H^{\ddagger}$ values between +79.45 and +92.64 kJ.mol^{-1} indicate that thermal relaxation is an activated process and the system's absorbance of heat from its surroundings allow for the relaxation to proceed. The variations imply that the differing structures of the IL cation has an important role in the stabilisation of the compound. Analysis of [C_4mIm][NTf_2] and

$[P_{6,6,6,14}][NTf_2]$ with values of +92.64kJ.mol^{-1} and +79.45kJ.mol^{-1} respectively appears to show that access to the charge centre and thus electrostatic effects/molecular orbitals directly mediates the ability for the **MC_{SO}** to for the **$MC^{‡}_{SO}$** transition state.

$\Delta S^{‡}$ observed for **SO** ranged from -55.78 to +26.60 J.K^{-1}.mol^{-1} in molecular solvents and -15.95 to +33.13 J.K^{-1}.mol^{-1} in ionic liquids (table 2.4). Positive values indicate that the **$MC_{SO} \rightarrow MC^{‡}_{SO}$** process is more disordered compared to the ground state form. Since solvent-solute interactions would be expected to occur between the charged **MC_{SO}** and polar regions of the solvent molecules it is believed that this would promote the association of **MC_{SO}** in these regions of the solvents. Positive entropies also imply a less constrained molecule and may be related to the movement associated with the transition state being less solvated than the completely open, planar **MC_{SO}** form. Since the solvent molecules are interacting with the charge centres and possibly somewhat ordered around the **MC_{SO}**, the resulting reorientation to **$MC^{‡}_{SO}$** results in increasing disorder within the solvent system. Negative entropy of activation values indicate a more ordered, rigid system is present in solution. This would suggest that the solvent-solute interactions are minimal compared to that of polar solvents and so the stabilisation of the system was far less than that of polar solvents. The result is that **$MC_{SO} \rightarrow MC^{‡}_{SO}$** process occurs with minimal solvent interaction and as such the **MC_{SO}** molecules do not move to/from charge sites due to the distinct lack of them within the solvents. As such the system order is not particularly affected and remains ordered.

$\Delta S^{\ddagger}$ values were found to increase sharply with the addition of **SO** to Triton X-100. A large increase in entropic value ($18.84 J.K^{-1}.mol^{-1}$ higher than methanol) is observed and is expected to result in greater stabilisation of the **MC$_{SO}$** form. However, kinetics faster than that in methanol is observed (table 2.2). It is believed that such deviations may be due the occurrence of both polar and non-polar regions within the same molecule may be taken as an example of a molecular solvent which appears to approach ionic liquid characteristics. Such effects further support the proposal that the formation of a complex, heterogeneous system results in difficulty effectively correlating various system parameters using spirocyclic compounds.

All ionic liquid entropies of activation were found to be positive with the exception of $[P_{6,6,6,14}][NTf_2]$. Although a negative entropy was observed for this ionic liquid, the value was still considerably more positive than that of acetonitrile which had an $E_T(30)$ value similar to the ionic liquid. It is possible that the long alkyl chains of the phosphonium cation were interacting with one another via van der Waals interactions, resulting in the formation of an extensive cation network which in turn restricted the reorientation of the **MC$_{SO}$**. Negative values of entropy of activation could be interpreted as the solvents rigidity resulting in a more stable system which requires much more energy to be supplied to induce molecular disorientation. Since $[P_{6,6,6,14}][NTf_2]$ is found to be more viscous than the other ionic liquids chosen, it is intuitive to believe that this physical property would significantly influence the relaxation process of the **MC$_{SO}$** form.

The **MC_{SO}**$\rightarrow$**$MC^{\ddagger}_{SO}$** process, which results in the reduction of charge on the molecule as the molecule relaxes to its closed form, means the entire system becomes less charged and more disordered (less solvent-solute interactions). For this reason, $\Delta S^{\ddagger}$ are of particular interest in the investigation of ionic liquids as such values could possibly give valuable insight into the ordering of the liquids which may quantify the complexity of such systems. This ordering and the subsequent solvent mediated stabilisation of the **MC_{SO}** form is believed to be related to the observed rates of thermal relaxation and the entropy of activation could possibly be used to determine the level of structuring that is present within the ionic liquid which the spirocyclic compounds are dissolved in.

Analysis of thermodynamic parameters was also found to be difficult to correlate with observed rates of thermal relaxation. Previous attempts to rationalise properties of spirooxazines has also yielded similar conclusions.[21] Chibsov and Gorner stated that variations in activation energy was found for spirooxazines they studied in different solvents and varying functional groups but that trends in polarity may be ruled out. A relationship between thermal relaxation rates and activation energies is observed for **SO** in molecular solvents. It was found that upon going from protic to aprotic solvents that E_a reduced by around 20 $kJ.mol^{-1}$ with a 1.5 fold increase in the rate constant. This was expected since lower activation energy typically results in increased rate constants according to the Arrhenius equation relaxation processes. Examination of the **MC_{SO}**$\rightarrow$**SO** rate constants and their activation energies fails to yield a linear relationship with one another in ionic liquids. This may be due to physical factors within the ionic liquids themselves such as steric hindrances and physical properties such as solvent viscosity. More complex interactions resulting from the much larger dimensions of the ionic components and the prevalence of permanent charges may also facilitate unexpected interactions and so deviations from expected values. Chiappe *et al* have also stated that large E_a and pre-exponential factors may also be a significant contributing factor to diffusional kinetics which may be similar to processes occurring during thermal relaxation.[22] A lack of correlation between $\Delta H^{\ddagger}$ and the rates constants for **SO** in ionic liquids is also observed. This is expected since a relationship between $\Delta H^{\ddagger}$ and E_a exists, whereby both parameters examine the energy required for the transition state to be reached resulted. $\Delta G^{\ddagger}$ showed subtle but linear response to kinetics. Since decreasing Gibbs energy of activation would indicate the system becoming more thermodynamically favourable this could account for a shift in the equilibrium of activation resulting in increasing rates of relaxation. $\Delta G^{\ddagger}$ is observed to be more positive in ionic liquids compared to molecular solvents. This correlates well with observed kinetics since the thermal relaxation rates in ionic liquids were noticeably slower than that of molecular solvents.

2.3.3 Effects of anion change on the properties of spiropyran in phosphonium based ionic liquids

The effects of anion change was examined using **BSP** since kinetic and solvatochromic studies found it to be more sensitive than **SO**. The inconclusive thermodynamic parameters found for cation change are believed to be due to the complex structuring within ionic liquids but **BSP** was selected to ensure that probe sensitive was not a factor. Phosphonium cation based ILs were chosen due to their stability and the fact that this class of ionic liquid failed to correlate with established trends in molecular solvents.

Kinetic parameters

The rates of thermal relaxation were determined as before to investigate any relationship with polarity or solvatochromic shifts and comparison to thermodynamic parameters. Reichardt's dye 30 and its empirically derived $E_T(30)$ scale were used to quantify the parameters in table 2.6.[2] Ground state equilibrium constants (K_e) between **BSP** and **$\mathrm{MC_{BSP}}$** in the ionic liquids was examined at equilibrium using Beer's law (**15**) to determine if the liquid environments had any effects upon **BSP** upon addition to the ionic liquids.

$$\mathrm{BSP} \rightleftharpoons \mathrm{MC_{BSP}} \qquad K_e = \frac{[MC_{BSP}]}{[BSP]} = \frac{A}{\varepsilon_{mc} \times C - A} \qquad \mathbf{(15)}$$

Where
A = equilibrium absorbance at the absorption maximum
C is the total concentration of BSP initially dissolved
$\varepsilon_{MC} = 3.5 \times 10^4\ M^{-1}cm^{-1}$ for the MC form of BSP according to Flannery[23]
(Extinction coefficient is known to be solvent dependent, but the effect is relatively small compared to the effects seen in this study.)

The ground state thermal equilibrium between the **BSP** and **MC$_{\mathbf{BSP}}$** is affected by changes in solvent polarity. Polar solvents promote the formation of the coloured (**MC$_{\mathbf{BSP}}$**) form and non-polar solvents promote the formation of the colourless (**BSP**) form. This relationship has been confirmed by plotting the K_e value vs. $E_T(30)$ values in the corresponding molecular solvents.[24] The correlation between the π-π* transition energies of the **MC$_{\mathbf{BSP}}$** isomer and $E_T(30)$ implies the contributions of different solute-solvent interactions, as measured by Reichardt's dye 30, are comparable with **MC$_{\mathbf{BSP}}$** values. Therefore, transition energies of the **MC$_{\mathbf{BSP}}$** isomer can be used to probe micro-polarity of a solvent at the molecular level.[19]

Table 2.6 Kinetic and polarity parameters of **BSP** in molecular solvents and ionic liquids. Reference values in parenthesis.

	$E_T(30)$	*BSP*		
Solvent	*(kcal/mol)*	*λ_{max} MC_{BSP} (nm)*	*k_f^{293} ($x10^{-4}s^{-1}$)*	*K_e ($x10^{-2}$)*
Ethanol	51.8 (51.9)[2]	539	1.9	4.57
Acetonitrile	45.5 (45.6)[2]	554	8.4	3.85
Dichloromethane	40.6 (40.7)[2]	578	70.	0.51
Triton X-100	69.7	565	15.4	0.37
$[P_{1,4,4,4}]$[tos]	48.2	560	5.19	1.74
$[P_{6,6,6,14}]$[FAP]	48.0	564	7.31	1.16
$[P_{6,6,6,14}][NTf_2]$	47.9	570	6.51	1.16
$[P_{6,6,6,14}]$[dbsa]	46.6	574	8.12	1.45
$[P_{6,6,6,14}]$[dca]	46.1	578	25.03	0.57

The experimental K_e values obtained (Table 2.6) for the phosphonium based ionic liquids are similar to aprotic molecular solvents, ranging from 1.16 – 1.74 x 10^{-2}. [$P_{6,6,6,14}$][dca] however the ionic liquid has a much smaller equilibrium constant (5.7 x 10^{-3}) in comparison to the rest of the ionic liquids and this value is similar to that of the non-polar solvent dichloromethane. As stated above when plotting K_e vs. $E_T(30)$ values in the corresponding non-viscous, simple molecular solvents, good linearity is achieved.[24] $E_T(30)$ values of the phosphonium based ILs studied appear to have similar values to acetonitrile (45.5 kcal/mol), though these results deviate from the expected linear relationship for K_e vs. $E_T(30)$ (figure 2.13). This can be clearly seen when comparing the K_e and $E_T(30)$ values of [$P_{6,6,6,14}$][dbsa] and [$P_{6,6,6,14}$][FAP]. [$P_{6,6,6,14}$][dbsa] has a larger equilibrium constant but smaller $E_T(30)$ value, although [$P_{6,6,6,14}$][dca] has the smallest equilibrium constant coupled with the smallest $E_T(30)$ value (46.1 kcal/mol) of the ionic liquids studied. This would suggest that the molecular probes (**BSP** and Reichardt's dye 30) exhibit different modes of interactions within the phosphonium ionic liquids studied herein. In general, phosphonium based ILs fit into the same category as aprotic molecular solvents, compared with the K_e values obtained for molecular solvents.

Experimental results (table 2.6) show that a direct relationship between the equilibrium constant K_e and the solvatochromic absorption shift of $\mathbf{MC_{BSP}}$ exists. As K_e decreases, the λ_{max} is found to shift towards longer wavelengths. This trend is also seen in the ionic liquids studied, with [$P_{6,6,6,14}$][dca]-MC λ_{max}= 578 nm and K_e = 5.7 x 10^{-3} while [$P_{1,4,4,4}$][tos]-$\mathbf{MC_{BSP}}$ exhibits a λ_{max}= 560 nm and K_e = 1.74 x10^{-2}. Comparison of

MC_{BSP} λ_{max} in dichloromethane is found to display similar shifts to those in $[P_{6,6,6,14}]$[dca], but the $E_T(30)$ value is significantly lower. However the sharp increase in thermal relaxation relative to the other ionic liquids is similar to the increase observed for dichloromethane relative to the other molecular solvents.

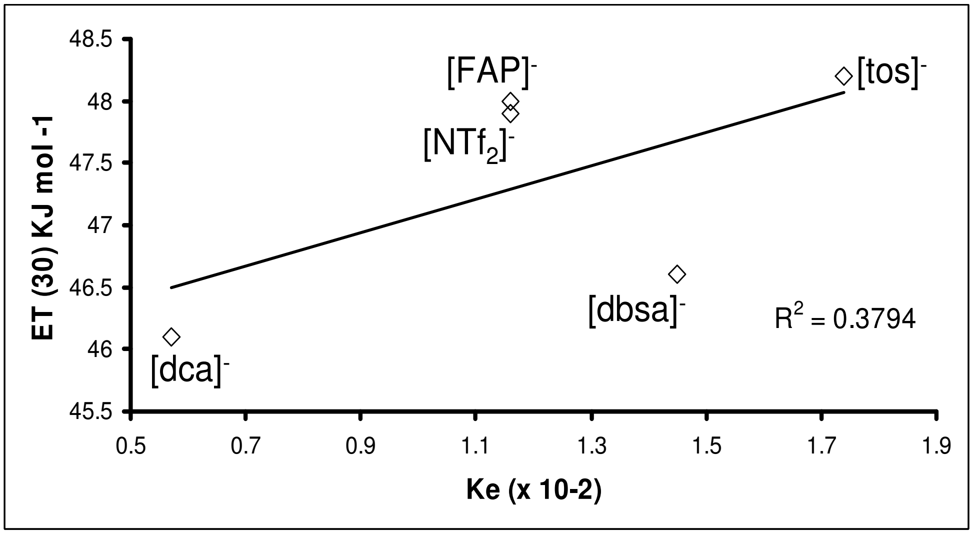

Figure 2.13 $E_T(30)$ vs. K_e of **BSP** in ionic liquids

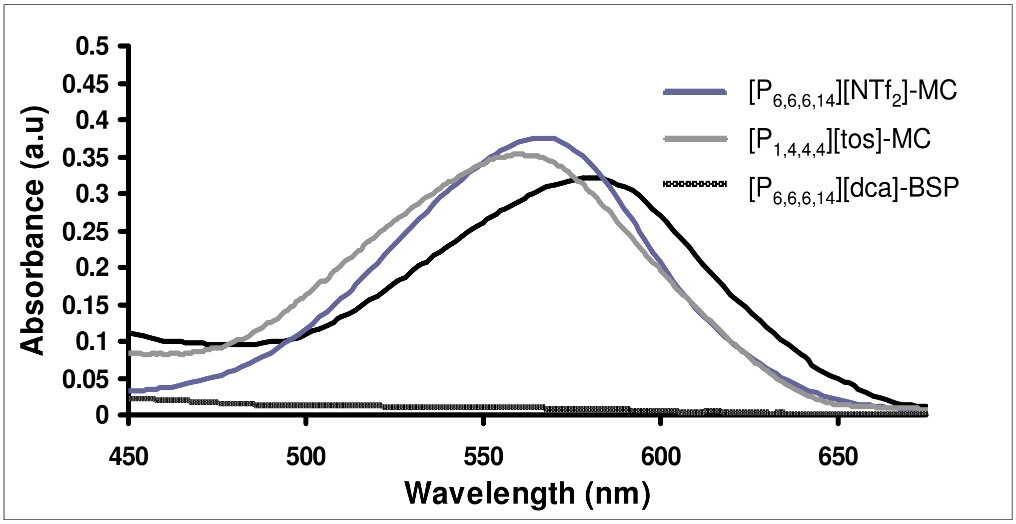

Figure 2.14 UV-vis spectra for solutions of 10^{-4}M **BSP**. λ_{max} of $[P_{6,6,6,14}][NTf_2]$-**MC**, $[P_{6,6,6,14}]$[dca]-**MC** and $[P_{1,4,4,4}]$[tos]-**MC** with $[P_{6,6,6,14}][NTf_2]$-**BSP** for reference.

Figure 2.14 displays the resulting spectra of selected **BSP**-IL solutions after 60 seconds of UV irradiation and λ_{max} shifts associated with solvent-solute interaction. First-order decay curves for the thermal relaxation of **MC$_{BSP}$** were plotted and examples are shown for $[P_{6,6,6,14}][NTf_2]$, $[P_{6,6,6,14}]$[dca], $[P_{1,4,4,4}]$[tos] and acetonitrile in figure 2.15. The rate constants for **MC$_{BSP}$** thermal relaxation in the selected ionic liquids are summarised in table 2.6. It can be seen from that all but one of the ionic liquids studied exhibit similar rate constants to acetonitrile at their respective **MC$_{BSP}$** λ_{max}, whereas $[P_{6,6,6,14}]$[dca] exhibits a much faster thermal reversion to **BSP** with a rate constant of 25.03 x 10^{-4} s^{-1}. From the K_e values and λ_{max} positions in table 2.6, it would be expected that the $[P_{1,4,4,4}]$[tos] should exhibit the longest **MC$_{BSP}$** lifetime and this hypothesis proved to be correct with the rate constant of 5.19 x 10^{-4} s^{-1}.

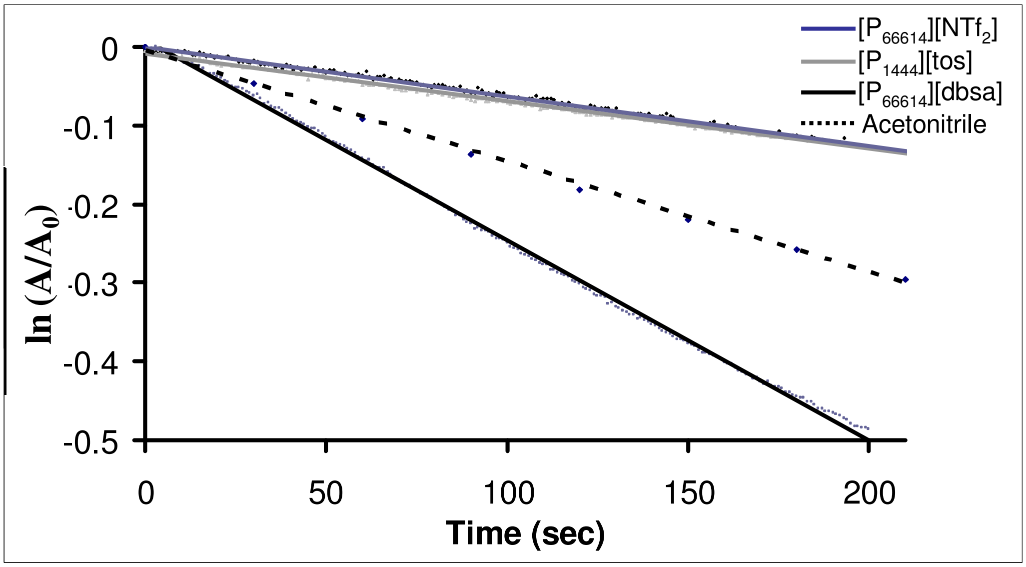

Figure 2.15 Thermal relaxation of MC$_{BSP}$ in $[P_{6,6,6,14}][NTf_2]$, $[P_{6,6,6,14}]$[dca] and $[P_{1,4,4,4}]$[tos] at 293K

The thermal relaxation of MC in $[P_{6,6,6,14}]$[dca] is 5 times faster than that of $[P_{1,4,4,4}]$[tos]. However, comparing $[P_{6,6,6,14}]$[dca] with dichloromethane, whose λ_{max} position is identical, their rate constants differ by approximately a factor of three.

Thermodynamic parameters

Table 2.7 summarises the thermodynamic properties of **BSP** for the thermal relaxation of **MC$_{BSP}$** in ionic liquids. As previously observed for **SO** in molecular solvents and in literature, E_a values are found to be higher in polar solvents indicating solvent based **MC** stabilisations, ranging from 75 to 105 kJ.mol^{-1}.[25, 26]

Table 2.7 Thermodynamic parameters for thermal relaxation of **MC$_{BSP}$** to **BSP**.

Solvent	***E_a* *(kJ.mol^{-1})***	***$\Delta H^{\ddagger}$* *(kJ.mol^{-1})***	***$\Delta S^{\ddagger}$* *(JK^{-1}mol^{-1})***	***$\Delta G^{\ddagger}$* *(kJ.mol^{-1})***
$[P_{1,4,4,4}]$[tos]	71.0	69.0	-72.8	90.7
$[P_{6,6,6,14}]$[FAP]	76.0	74.0	-54.6	90.3
$[P_{6,6,6,14}]$[NTf2]	90.0	87.0	-8.2	89.4
$[P_{6,6,6,14}]$[dbsa]	88.0	85.0	-12.3	88.7
$[P_{6,6,6,14}]$[dca]	75.0	73.0	-46.1	86.7

It can be seen that E_a values for phosphonium based ILs lie within the region of non-polar solvents such as benzene and chloroform, 70.6 and 95.9 kJ.mol^{-1} respectively.[26] The activation energy of **MC$_{BSP}$** thermal relaxation in $[P_{6,6,6,14}][NTf_2]$ and

$[P_{6,6,6,14}]$[dbsa] is quite high compared to the rest of the ionic liquids studied and is very similar to the molecular solvent DMF literature value of +90 kJ.mol^{-1}.[25] This could indicate that the **MC$_{\mathbf{BSP}}$** thermal relaxation process is strongly dependant on temperature. Albeit, it was observed that $[P_{1,4,4,4}]$[tos] had the smallest thermal relaxation E_a and $\Delta H^\ddagger$ values of +71 kJ.mol^{-1} and +69 kJ.mol^{-1}, respectively.

Small pre-exponential factors (10^9-10^{10} s^{-1}) are associated with negative activation energies with respect to photochromic dyes.[27] Such values are related to the molecular collisions and various other minor contributions to the thermal relaxation process that are not explained by the activation process and activation energy barrier. It has been suggested that the **BSP-MC$_{\mathbf{BSP}}$** equilibrium is almost isoentropic due to the balance between two opposite contributions to ΔS^0, a positive contribution related to the increased torsional freedom in the **MC$_{\mathbf{BSP}}$** isomer and a negative contribution due to solvent reorientation around the more polar **MC** form.[27] As reported previously for the thermal relaxation of photomerocyanines, $\Delta S^\ddagger$ values for the ionic liquids examined show a strong linear correlation with E_a (figure 2.17).[28,29] As expected, the experimental activation entropies ($\Delta S^\ddagger$) found for **MC$_{\mathbf{BSP}}$** in the majority of ionic liquids studied were significantly negative (e.g. $[P_{1,4,4,4}]$[tos] $\Delta S^\ddagger$ = -72.8 J K^{-1} mol^{-1}), indicating a more ordered system. This could be due to electrostatic interactions with the charged **MC$_{\mathbf{BSP}}$** form or the result of extensive alkyl chain interactions (expected due to higher viscosity of the phosphonium based ILs). This correlates well with the small **MC$_{\mathbf{BSP}}$** thermal relaxation rate constants observed for ionic liquids such as $[P_{1,4,4,4}]$[tos] when compared to $[P_{6,6,6,14}][NTf_2]$ and $[P_{6,6,6,14}]$[dbsa] which have more positive values of $\Delta S^\ddagger$ (-8.2 and

-12.3 J K^{-1} mol^{-1} respectively) and larger rate constants for the **MC_{BSP}** thermal relaxation.

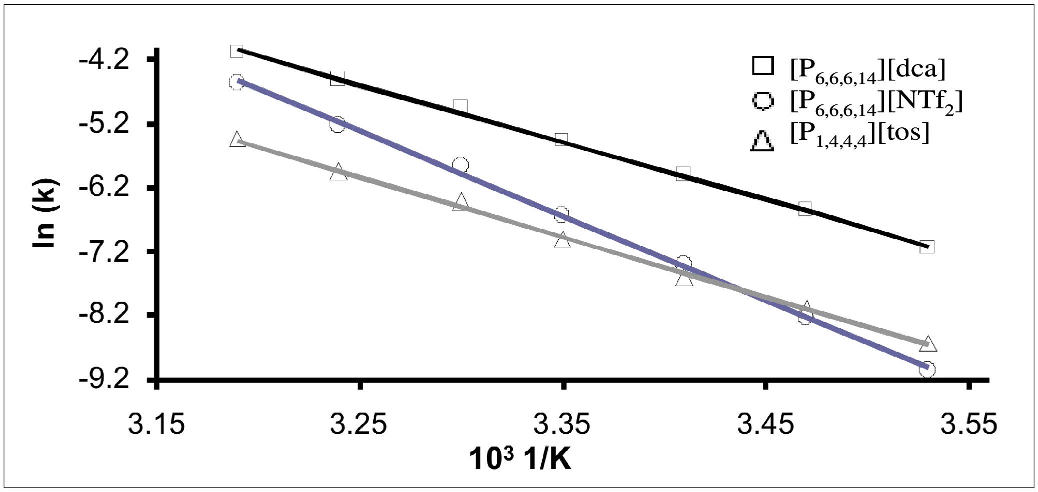

Figure 2.16 Arrhenius plot for the thermal relaxation of **MC_{BSP}**.

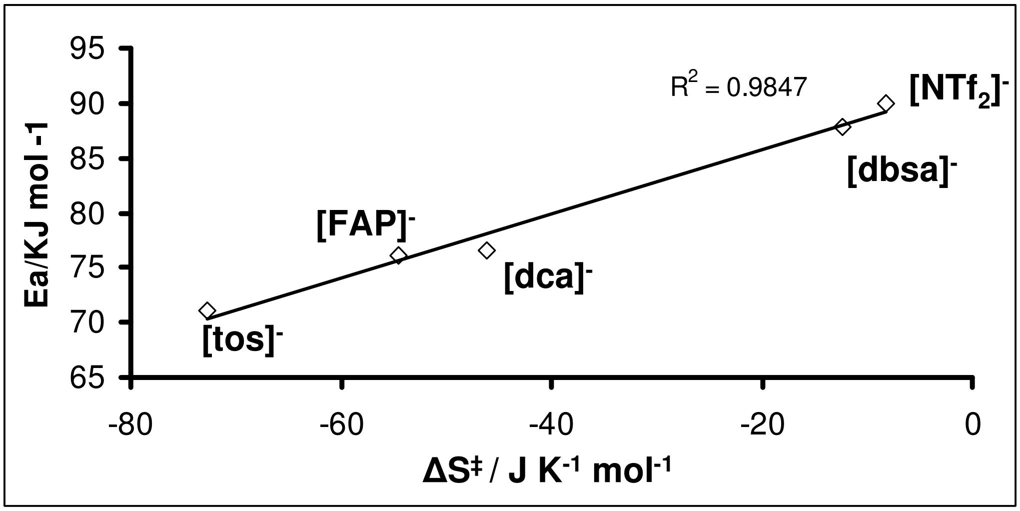

Figure 2.17 Plot of E_a vs. $\Delta S^{\ddagger}$ for **MC_{BSP}** thermal relaxation process in phosphonium based ILs (anions labelled).

2.3.4 Linear solvation energy relationship (LSER) analysis of solvent-solute interactions of spirocyclic compounds and ionic liquids

Kamlet-Taft values in ionic liquids were examined in more detail using linear solvation energy relationships (LSERs) and comparison to thermodynamic and kinetic parameters of spirocyclic compounds. The use of LSERs allows for relationships to be established between chemical properties such as polarity and properties of solutions such as solubility, free energy and enthalpy and wavelengths of light absorbance.[15] The multiparameter dependancy upon the values described by LSERs has resulted in very successful application of Kamlet-Taft parameters to such relationships.[30] Equation **(16)** below describes the general formula for determination of LSERs based upon Kamlet-Taft Parameters.[15]

$$XYZ = XYZ_0 + a\alpha + b\beta + s\pi^{*}... \qquad \textbf{(16)}$$

XYZ represents the property being examined which in this case is the solvatochromic shift of the λ_{max} of the merocyanine form of each spirocyclic compound. α, β and π* represent the Kamlet-Taft parameters described previously while XYZ_0, a, b and s are solvent dependant coefficients which indicate the sensitivity of each parameter to the property being examined. Using λ_{max} values obtained for $\mathbf{MC_{BSP}}$ and $\mathbf{MC_{SO}}$ in previous sections, the relationship of solvation effects based upon Kamlet-Taft parameters to solvatotochromic shifts of the spirocyclic compounds. Linear regression analysis of the components of the solvation process was compared to experimentally derived shifts to determine the parameters which influenced the overall process. Figure 2.18 illustrates the resulting plots of such analysis.

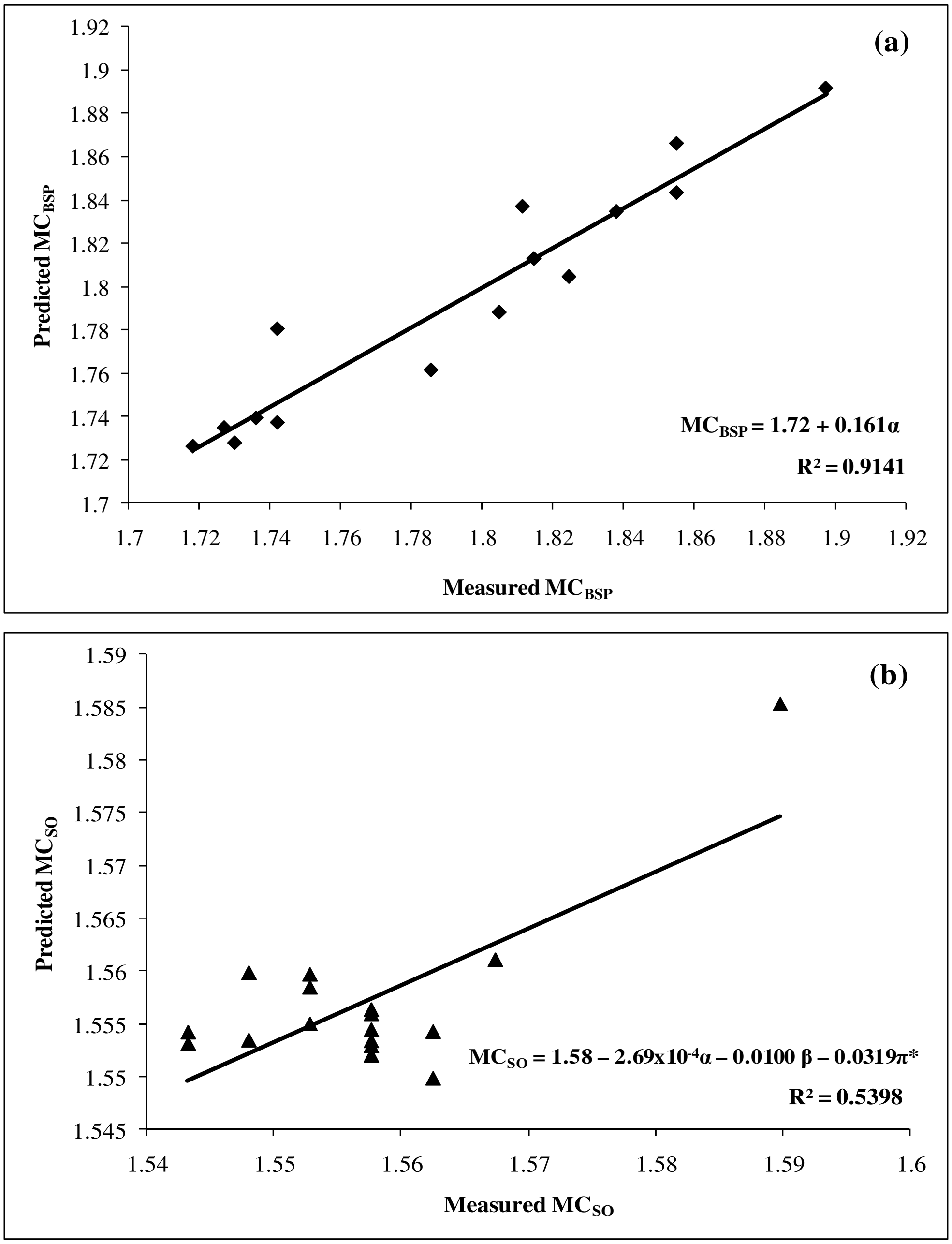

Figure 2.18 Plots illustrating (a) the alpha relationship to $\mathbf{MC_{BSP}}$ λ_{max} and (b) the lack of linear correlation and mild π^* relationship to $\mathbf{MC_{SO}}$ λ_{max}.

It is found that **MC_{BSP}** is strongly dependent upon α values and therefore heavily influenced by the hydrogen bond of the solvent. Analysis of the regression output resulted in a linear relationship with an R^2 value of 0.9141 reinforcing the direct relationship of α to solvatochromic shift. The resulting LSER equation was expressed as **MC_{BSP}** $= 1.72 + 0.161\alpha$ and omitted the β and π* values as they were deemed to be outside statistical significance due to high P-values, particularly compared to the very low α P-value of 2.65×10^{-8}. Such a value implies that hydrogen bond donation of the solvent dominates the interaction process of **MC_{BSP}**. This agrees well with previous findings whereby through space interactions with the phenolate oxygen were proposed to be important for **MC_{BSP}** stabilisation and thus increased lifetimes.[19] It must be noted that the values for Triton X-100 were omitted as and outlier due to extremely anomalous values. This may be due to acid impurities within the solvent which was not cleaned, nor its purity accurately obtainable prior to use.

For **MC_{SO}**, examination of the LSER equation; **MC_{SO}** $= 1.58 - 2.69 \times 10^{-4}\alpha - 0.0100\beta - 0.0319\pi^*$ illustrates a slight π* influence upon the solvatochromic effects. However the R_2 value of 0.5398 can be deemed to be too low to find linear correlation in the data. Examination of the P-values for α and β are found to be 0.95 and 0.26 respectively and too high to be statistically significant. Removal of these parameters from the LSER equation resulted in the equation; **MC_{SO}** $= 1.58 - 0.0319\pi^*$. However a further reduction in the R_2 value to 0.4694 slope results in this equation being generally rejected (figure 2.19).

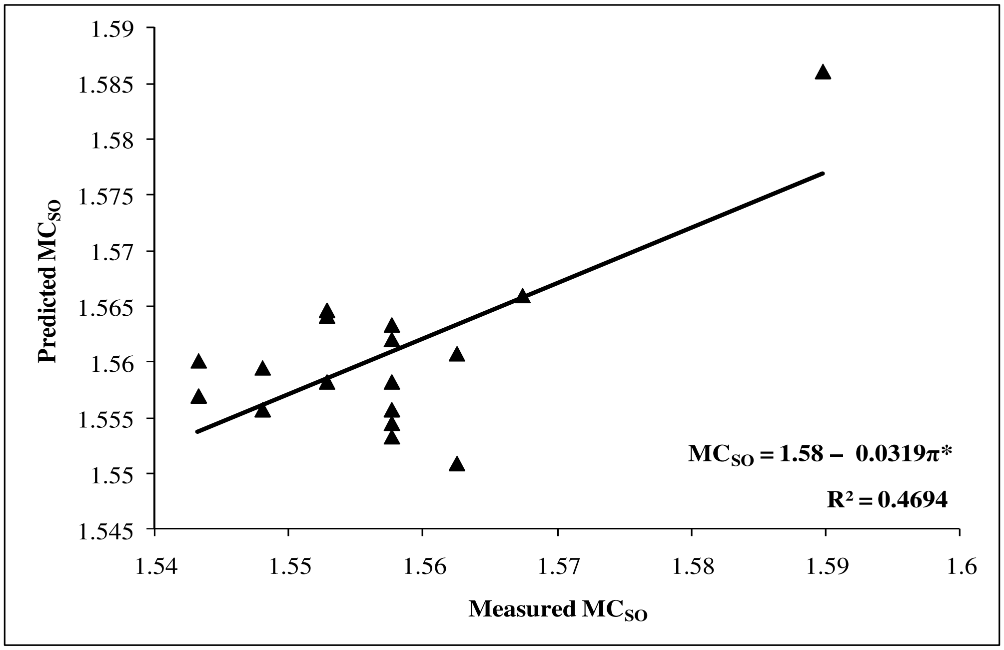

Figure 2.19 Plot of sole π^* dependence to $\mathbf{MC_{SO}}$ λ_{max}

It must be noted that although the π^* values are believed to have a minor influence upon $\mathbf{MC_{SO}}$, the values observed were within the limits of error and so may not be taken as very significant. This also agrees with a general proposal put forward earlier in the chapter that $\mathbf{MC_{SO}}$ may be somewhat solvent independent or at most influenced primarily by electrostatic interactions which explains its lack of sensitivity when employed as a solvent probe. The lack of a nitro group and functionalisation of the compound with a benzothiophene group in close proximity to the phenolate oxygen is believed to result in no visible solvatochromic effects. Figure 2.18b shows a clustering of points indicating little change in λ_{max} and the restriction of access of solvent molecules to the important charge site at the phenolate oxygen effectively removes the ability for significant H-bonding to occur and so the removal of the influence α and β values upon the solvatochromic process of the compound.

2.4 Conclusions

Initial studies using spirocyclic compounds as solvent probes yielded promising results and insight into the choice of spirocyclic derivative. Comparison of rates of thermal relaxation of **SO** and **BSP** in ionic liquids found little correlation with polarity (E_T(30) and Kamlet-Taft), as established in molecular solvents, strengthening the belief that ionic liquid environments are more complex than those presented by molecular solvents. However, detectable changes in **BSP** λ_{max} and rates of thermal relaxation, which were not visible in ionic liquids containing **SO,** implies that more significant solvent-solute interactions occur for **BSP** in ionic liquids and is therefore a more sensitive probe. It is proposed that the through space interactions of the ionic liquids and spirocyclic compounds occur through different processes for each compound. While both $\mathbf{MC_{BSP}}$ and $\mathbf{MC_{SO}}$ contain similar charge sites, the lack or restriction of the phenolate oxygen and presence of a nitro group on the pyran fragment of $\mathbf{MC_{BSP}}$ appears important for the effectiveness of this probe of solvent analysis. LSER analysis appears to confirm such effects by illustrating the strong relationship of $\mathbf{MC_{BSP}}$ to the hydrogen bond donation strength (α values) of the solvent and a complete lack of correlation and possible independence of $\mathbf{MC_{SO}}$ solvatochromic effects to Kamlet-Taft solvation parameters

The structures of **MC$_{BSP}$** and **MC$_{SO}$** are believed to exhibit a more complex delocalisation of charge and the resulting sensitivity to a larger number of environmental parameters which may be overlooked by existing probes. However, the increased sensitivity of **BSP** compared to **SO** may be due to ionic liquid ions being able to interact closer with the charged sites to allow effects such as hydrogen bonding to occur and more effectively approximate the polarity/solvation properties of the ionic liquids. Functionalisation of the **SO** molecule close to the phenolate oxygen may restrict access to this site and thus reduce its ability to stabilise its **MC$_{SO}$** form.

Increased viscosity is known to decrease the rate of thermal relaxation of spirocyclic compounds. However, such effects appear to be reduced when the complexity of the liquid system is increased. A viscous molecular solvent, Triton X-100 was probed using both spirocyclic compounds and found to produce conflicting kinetic results. Once again, the effects were more visible in **BSP** reinforcing the belief that both probes interact through differing processes and strengths. Thermal relaxation rates were faster than simple molecular solvents such as methanol for **SO** and much faster than polar aprotic solvents for **BSP**. Polarity and H-bond parameters exhibited values which would be expected to produce much slower rates of relaxation while **BSP** solvatochromic shifts predicted that the local environment of the liquid was somewhat non-polar. Viscosity appeared to have no influence upon the kinetics of either spirocyclic compound. It was concluded that established relationships between physical properties (viscosity) and polarity were only upheld in simple, small molecule systems typically encountered in molecular solvents. Triton X-100 molecules contain both polar and non-polar components and could be described as a molecular solvent analogue to ionic liquids. The results observed within Triton X-100 serve to rationalise the conflicting results are observed within ionic liquids, most notably phosphonium and alkyl ammonium based ILs. Although the influence of viscosity cannot be completely ruled out as a contributing factor, the formation of distinct regions and the partial influence of each particular region appears to mediate the kinetic effects of the spirocyclic compounds. For molecular solvents, **MC$_{SO}$** is observed to have its highest activation energy barrier in Triton X-100 yet examination of the $K^{\ddagger}$ value would imply that this value should be lower. It is proposed that the high activation energy value is influenced by the polar components of the liquid while the overall efficiency (and direction of equilibrium) of relaxation is influenced by the non-polar regions.

The implied correlation of kinetic values of spirocyclic compounds when first subdivided based upon cation species and structure (ring or alkyl chain based) results in the hypothesis that effective comparison using these probes requires similar solvent environments. The use of spirocyclic probes in ionic liquids with similar base structure possibly creates systems with essentially the same structuring and the changes in values (most effectively observed by **BSP**) result from the changes to the cation functionalisation and/or anion. The fact that probe dyes exhibit conflicting results illustrates that fact that the complex nature of solvation may be too complex to examine using individual probe dye studies which focus on a single property. The effect of changing a component of the ionic liquid (particularly the cation) appears to result in extensive reorganisation and changes in solvent-solute interactions to the extent that solvatochromic probe dyes fail to quantify in values that can be compared. This is particularly prevalent for alkyl chain based cations, such as phosphonium and quaternary ammonium ions, which exhibit higher viscosities, believed to be related to extensive van der Waals interactions between aliphatic chains which is proposed to form a continuous cationic ‘mesh’. Such features appear too great for spirocyclic probes to compare. Future comparative studies of ionic liquids using spirocyclic compounds will be carried out using ionic liquids of similar base structure and examining changes to this through functionalisation or counter ion choice.

2.5 References

1. K. Iwata, M. Kakita and H. Hamaguchi, *Journal of Physical Chemistry B*, 2007, **111**, 4914-4919.
2. C. Reichardt, *Chemical Reviews*, 1994, **94**, 2319-2358.
3. C. Reichardt, *Green Chemistry*, 2005, **7**, 339-351.
4. S. V. Dzyuba and R. A. Bartsch, *Tetrahedron Letters*, 2002, **43**, 4657-4659.
5. H. Jin, B. O'Hare, J. Dong, S. Arzhantsev, G. A. Baker, J. F. Wishart, A. J. Benesi and M. Maroncelli, *Journal of Physical Chemistry B*, 2008, **112**, 81-92.
6. G. Angelini, C. Chiappe, P. DeMaria, A. Fontana, F. Gasparrini, D. Pieraccini, M. Pierini and G. Siani, *Journal of organic chemistry*, 2005, **70**, 8193-8196.
7. L. Crowhurst, R. Falcone, N. L. Lancaster, V. Llopis-Mestre and T. Welton, *Journal of organic chemistry*, 2006, **71**, 8847-8853.
8. L. Crowhurst, P. R. Mawdsley, J. M. Perez-Arlandis, P. A. Salter and T. Welton, *Physical Chemistry Chemical Physics*, 2003, **5**, 2790-2794.
9. B. R. Mellein, S. N. V. K. Aki, R. L. Ladewski and J. F. Brennecke, *Journal of Physical Chemistry B*, 2007, **111**, 131-138.
10. J. M. Lee, S. Ruckes and J. M. Prausnitz, *Journal of Physical Chemistry B*, 2008, **112**, 1473-1476.
11. A. K. Burrell, R. E. D. Sesto, S. N. Baker, T. M. McCleskey and G. A. Baker, *Green Chemistry*, 2007, **9**, 449-454.
12. C. Reichardt, *Solvents and Solvent Effects in Organic Chemistry*, 3rd edn., WILEY-VCH Verlag GmbH & Co. KGaA, Weinheim, 2004.
13. A. R. Katritzky, D. C. Fara, H. Yang, K. TÃ¤mm, T. Tamm and M. Karelson, *Chemical Reviews*, 2004, **104**, 175-198.
14. C. P. Fredlake, M. J. Muldoon, S. N. V. K. Aki, T. Welton and J. F. Brennecke, *Physical Chemistry Chemical Physics*, 2004, **6**, 3280-3285.
15. Y. Marcus, *Chemical Society Review*, 1993, **22**, 409-416.
16. M. J. Muldoon, C. M. Gordon and I. R. Dunkin, *Journal of the Chemical Society, Perkin Transactions 2*, 2001, 433-435.
17. J. Figueras, *Journal of the American Chemical Society*, 1971, **93**, 3255-3263.
18. S. Minkovska, B. Jeliazkova, E. Borisova, L. Avramov and T. Deligeorgiev, *Journal of Photochemistry and Photobiology A: Chemistry*, 2004, **163**, 121-126.
19. R. Byrne, K. J. Fraser, E. Izgorodina, D. R. MacFarlane, M. Forsyth and D. Diamond, *Physical Chemistry Chemical Physics*, 2008, **10**, 5919-5924.
20. G. Favaro, F. Masetti, U. Mazzucato, P. Ottavi, P. Allegrini and V. Malatesta, *Journal of the chemical society, Faraday Transactions*, 1994, **90**, 333-338.
21. A. K. Chibisov and H. Gorner, *Journal of Physical Chemistry A*, 1999, **103**, 5211-5216.
22. C. Chiappe and D. Pieraccini, *Journal of Physical Organic Chemistry*, 2005, **18**, 275-297.
23. J. B. Flannery, *Journal of the American Chemical Society*, 1968, **90**, 5660-5671.
24. X. Song, J. Zhou, Y. Li and Y. Tang, *Journal of Photochemistry and Photobiology A: Chemistry*, 1995, **92**, 99-103.
25. H. Gorner, *Physical Chemistry Chemical Physics*, 2001, **3**, 416-423.

26. Y. Sueishi, M. Ohcho and N. Nishimura, *Bulletin of the Chemical Society of Japan*, 1985, **58**, 2608-2613.
27. di Nunzio Maria R., G. P. L., Romani Aldo and F. Gianna, *ChemPhysChem*, 2008, **9**, 768-775.
28. D. E. Wetzler, P. F. Aramendia, J. M. Laura and R. Fernández-Prini, *Physical Chemistry Chemical Physics*, 1999, 4955-4959.
29. G. Sciaini, D. E. Wetzler, J. Alvarez, R. Fernandez-Prini and M. Laura Japas, *Journal of Photochemistry and Photobiology, A: Chemistry*, 2002, **153**, 25-31.
30. M. J. Kamlet, J. L. M. Abboud, M. H. Abraham and R. W. Taft, *The Journal of Organic Chemistry*, 1983, **48**, 2877-2887.

3

Investigation of Structuring in Ionic Liquids Based On The $[NTf_2]^-$ Anion

3.1 Introduction

Chapter 2 described investigations into the physical properties of ionic liquids using the photoactive compounds **SO** and **BSP** as molecular probes to examine solvent-solute interactions and compare their kinetic and thermodynamic parameters to existing probe dyes. However, deviations in the properties of thermal relaxation for both compounds were observed and appear to support the belief that ionic liquids present far more complex environments than the homogeneous systems exhibited by molecular solvents coupled with physical parameters such as higher viscosities.

Recent studies have proposed that imidazolium based ionic liquids may form ordered liquid systems resembling crystalline environments based on stacking of mutual charges (aggregation) or ordered association of cation to surrounding anions and vice versa.[1,2] Lopes *et al* examined the formation of nanostructured domains in ionic liquids containing the imidazolium cation using computational analysis and found that the cations could be divided into two specific regions: a polar head group where the ion charge resides and a non-polar region where side groups extend into space (figure 3.1).[3] These polar head groups appear to interact preferentially with one another to form aggregates by three dimensional π-stacking and mutual association of the charged imidazolium rings with anion species to form polar regions. Alkyl side-chains extend away from these regions and through side-chain/van der Waals interactions form a complex network of non-polar regions. John D. Holbrey and Robin D. Rogers state that ionic liquid order is based upon short range ordering and long range disorder.[4] In the case of imidazolium based ILs the short range π-π stacking of polar regions and the long range van der Waals interactions of the alkyl chains compete for influence of the ionic liquid properties. As the chain lengths increase it would be expected that such interactions will dominate the ordering process and so become the influential factor in the overall structure of the liquid system. As the size of the non-polar regions increases, this may result in a dispersal and reduction in the size of the polar regions within the liquids which further alter the physicochemical properties of the materials based upon the relative populations of each region.

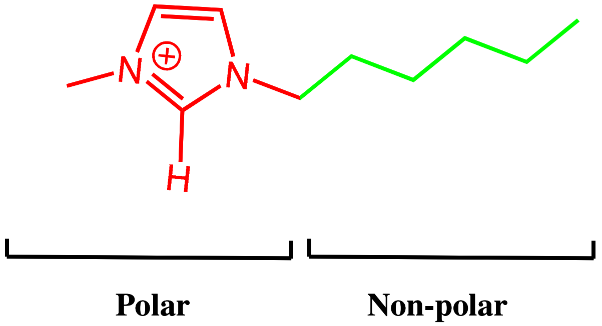

Figure 3.1 Imidazolium cation C_6mIm showing polar (red) and non-polar (green) regions of the molecule based on findings and convention of identification by Lopes et al.[5]

Conventional polarity probes, such as Reichardts dye 30, provide information about the polarity of a solvent due to the absorption shift which accompanies the interaction of solvent molecules with the charge sites of the dye and the resulting effect on the excitation band gap. Single parameter techniques were proposed to be too vague to interpret individual interactions and so to compliment such studies, the combination of three dyes by Kamlet and Taft enabled hydrogen bonding behaviour of solvents to be examined and thus break down the overall polarity parameter into three specific effects.[6-8] Both single and multiparameter probe studies have seen considerable use in evaluating ionic liquids in an attempt to understand trends in their physico-chemical properties but evidence suggests the more complex solvent systems of ionic liquids fail to be appreciated by the probes dyes to the same extent that they are in molecular solvents (where such interpretation of probe dyes was developed). Differences such as ionic liquid ions being far larger than molecular solvent molecules and the complex distribution of charge results in liquids whose ability to interact with probe molecules will differ greatly than that observed in molecular solvents and used to derive physicochemical parameters. If ionic liquids possess defined regions of distinct polarity, unlike molecular solvents which are accepted as uniform throughout, then such divisions could present problems for parameter determination as the solvent parameters are likely to be dramatically different in each of these regions. Conventional probe dyes typically contain static charge sites associated with a specific interaction mechanism. For this reason, the probe molecules would be expected to interact preferentially with one region type in an ionic liquid and ignore the rest of the liquid system. This results in parameters appearing similar for each ionic liquid in contrast to the range in kinetic parameters observed upon monitoring the behaviour of the dynamic probe dye **BSP**. The inability of such probe dyes to appreciate the overall ionic liquid system stems from the fact that solvent polarity is assumed to be of macroscopic proportions and that the entire solvent system acts as a homogeneous medium with similar regions throughout. The result is that such approximations fail to realise the possibility of nano-structured regions each with dramatically different characteristics existing.[9,10] Characterisation of ionic liquids with a single 'polarity' term also fails to describe the type and magnitude of individual interactions that make each ionic liquid unique.[11-14]

The **MC** isomer is sensitive to its immediate molecular environment and corresponding specific and non-specific interactions that occur mediate the compound's equilibrium between both isomers.[15-18] In Section 2.3.2, the conclusion was that the kinetics and thermodynamics of the **BSP**-**MC$_{\mathbf{BSP}}$** equilibrium was sensitive to the nature of both the cation and anion, through the formation of through-space orbital interactions with the **MC** isomer, and the cation mediating the **MC$_{\mathbf{BSP}}$** thermal relaxation rates back to **BSP**. Similar processes were expected for **SO** but polarity-kinetic trends were not apparent, possibly due to differing levels of interaction between the spirocyclic compound derivatives. It is believed that the functionalisation of the **MC$_{\mathbf{SO}}$** and its substituents restrict interactions with the ionic liquid ions to electrostatic/non-specific interactions.

SO is therefore proposed to act as a reference compound when investigating solvent structure as the relatively weak interactions means that the process of thermal relaxation would be somewhat independent of the solvent system used. The more specific interactions of **BSP** within the ionic liquids could therefore quantify the level of liquid structuring through the degree of such interactions. The ability for photochromic spirocyclic compounds to switch between two forms allows for the interactions associated with each region within the ionic liquids to be examined. The closed forms, being non-polar would be expected to preferentially interact with non-polar domains, while the open, zwitterionic **MC** forms would be able to interact with the polar or charged regions of the ions. As thermal relaxation occurs, the probe molecules would be expected to migrate based upon their dynamic interactions between polar and non-polar regions as the charged **MC** isomer reverts to the uncharged **SP** form and solvent reorganisation occurs. Previous spectroscopic studies of spiropyran in (molecular) solutions containing lipid bi-layers have exhibited diffusional properties believed to be due to the differing associations of each form of the compound.[19] The similarity between bi-layer formation and the proposed ordering of ionic liquids infers the possibility that similar mechanisms may allow for the ordering of ionic liquids to be probed by photochromic compounds with the capability to interact within each of the regions and thus report the extent of structuring present.

The spirocyclic compounds themselves are large molecules of similar size to individual ionic liquid molecules. Approximations of molecular size using Chem3D visualisation software is illustrated in figure 3.2. $[C_6mIm]^+$ is found to me approximately 12Å in length with similar dimensions observed for **BSP** at approximately 11Å and **MC$_{\mathbf{BSP}}$** at approximately 14Å. The introduction of such molecules would therefore be expected to somewhat disrupt the ordering of the ionic liquid structure. Such reorganisation around the probe and the resulting thermodynamic parameters of the system will therefore provide insight into solvent structure and intra-molecular interactions that occur. Increasing the length of the non-polar side-chain of the imidazolium ion (figure 3.3) should affect the ordering of the ionic liquid at the molecular level due to increased volume of non-polar regions, and related increased dispersion and corresponding expansion of polar regions arising from dissociation of imidazolium head groups from one another. Since the **MC** isomer preferentially resides in polar/charged regions, it is anticipated that increasing the surrounding non-polar regions could possibly influence the **MC**↔**SP** equilibrium by favouring the **SP** form of the molecule. If structured polar domains exist, then their stabilising influence on **MC** should reduce the effect of these non-polar regions and subsequently provide rates of thermal relaxation much slower than that expected for the cations containing side-chains which would endow non-polar properties upon the liquids. If nano-structuring of these domains exists in ionic liquids it should be possible to observe a non-linear relationship between K_e and thermal relaxation of the **MC** form, due to the different molecular environments observed as a result of the liquid structure and their differing influences that occur at different stages during the relaxation of the compound. Thermodynamic and kinetic studies were carried out to examine the extent of structuring in imidazolium based ILs based on equilibrium effects, rates of thermal relaxation and the effect upon solvent ordering due to the introduction of a dynamic probe molecule.

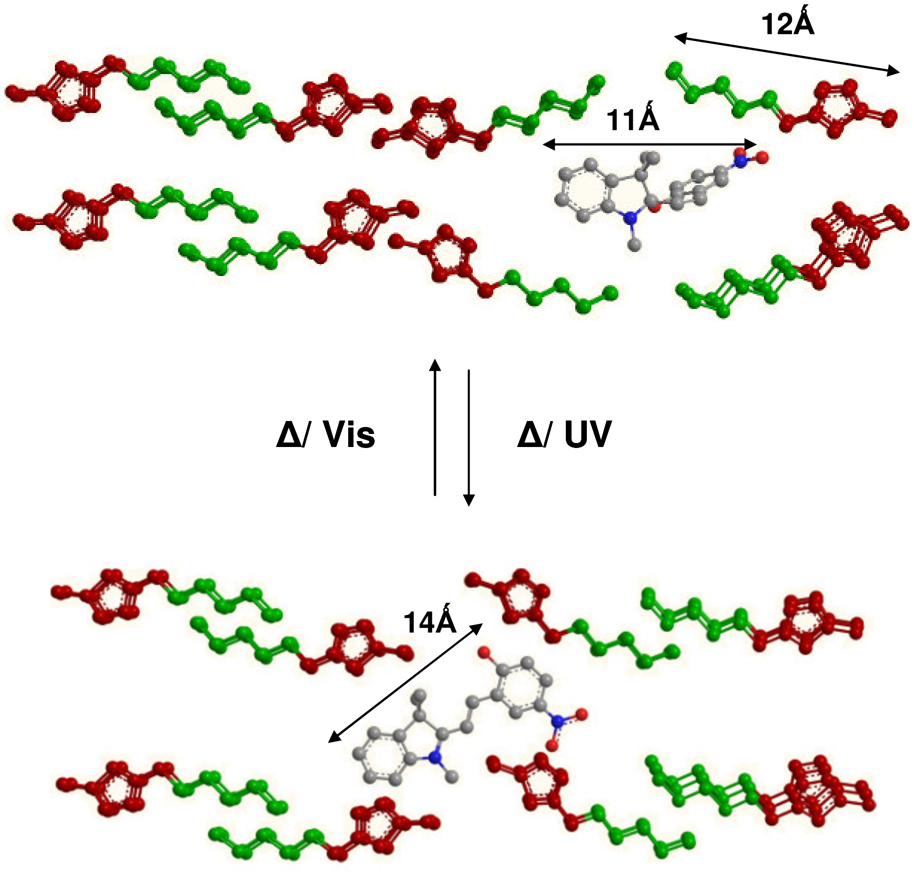

Figure 3.2 Schematic of proposed 3D ordering of imidazolium cations with **BSP** probe in [C_6mIm][NTf_2] showing preferred residence of the **MC$_{BSP}$** (lower) and **BSP** (upper) forms of the probe in polar and non-polar regions, respectively. Anions are located within the polar domains associated with the imidazolium ring but are omitted for clarity. A review by Dupont illustrates the structure of such anion-cation associations.[20]

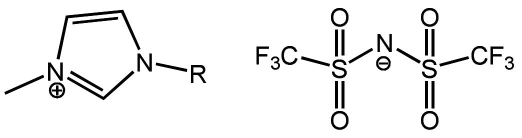

[C_nmIm]$^+$ **[NTf_2]$^-$**

R = ethyl: [C_2mIm][NTf_2]
butyl: [C_4mIm][NTf_2]
hexyl: [C_6mIm][NTf_2]
octyl: [C_8mIm][NTf_2]
decyl: [C_{10}mIm][NTf_2]
dodecyl: [C_{12}mIm][NTf_2]

Figure 3.3 Cations and anion used in this study. 1-alkyl-3-methylimidazolium [C_nmIm]$^+$ and bis(trifluoromethanesulfonyl)amide [NTf_2]$^-$.

3.2 Experimental

Ionic liquids were synthesised and purified in-house with salts obtained from Sigma-Aldrich using previously reported techniques (Appendix A-1).[21] Ionic liquids produced are stored under nitrogen to minimise uptake of water. Spectrometric studies were carried out using a Perkin Elmer Lambda 900 spectrometer (Foss Ireland) with Perkin Elmer PTP-1 temperature controller. Samples were irradiated with UV light at 375nm using an in-house fabricated array based on 375nm UV LEDs (Roithner Lasertechnik, Vienna, Austria). Reichardts dye 30 (Sigma-Aldrich chemicals) and 6-Nitro-1',3',3'-trimethylspiro[2H-1-benzopyran-2,2'-indolin] 1',3'-Dihdro-1',3',3'-trimethyl-6-nitrospiro (**BSP**) (Sigma-Aldrich chemicals) were used as purchased with no further purification. 1,3,3-trimethyl-5'-(2-benzothiazolyl)-spiroindoline-2,3'-naphtho(2,1-b)(1,4) oxazine (**SO**) was previously synthesized and supplied by Dr. Minkovska of the Bulgarian Academy of Sciences.

3.3 Results and Discussion

3.3.1 Polarity and solvatochromic effects

Ionic liquid polarities were previously determined using the ET_{30} scale as described previously[22] and summarised in table 3.1. The resulting spectroscopic shifts relating to solvent-dye interactions of Reichardt's dye 30 are found to be linearly related to increasing side-chain length, as this decreases the overall ionic liquid polarity by reduction of polar region density and increasing non-polar characteristics. However, the decreases in polarity according to the $E_T(30)$ scale* are relatively minor when compared to that of molecular solvents of similar chain lengths. $E_T(30)$ values of 52.6 kcal.mol^{-1} for [C_2mIm][NTf_2] and 53.2 kcal.mol^{-1} for [C_6mIm][NTf_2] were observed while similar chain lengths in molecular solvents with a polar region and extending non-polar side chain (e.g. alcohols) had $E_T(30)$ values of 51.9 kcal.mol^{-1} and 48.8 kcal.mol^{-1} for ethanol (C_2) and 1-hexanol (C_6) respectively.[9] This would imply that the probe dye was observing similar regions within the ionic liquids but increasing side chain length still had an effect due to their proximity to such regions (figure 3.4). Comparison of thermal relaxation of **MC$_{BSP}$** to these $E_T(30)$ values presented linear correlations which implies a similar influence of alkyl chain length upon thermal relaxation of spirocyclic compounds (figure 3.5) and therefore sensitivity to ionic liquid physical properties. Solvatochromic effects are not observed for **MC$_{SO}$** as this molecule due to its lack of a nitro group, present in **MC$_{BSP}$**, and believed to mediate solvatochromic effects in spirocyclic compounds.

---

* 1 calorie = 4.186 Joules to allow conversion of ET(30) values (calories) to thermodynamic units (Joules)

The lack of large solvatochromic shifts for **MC$_{BSP}$** in ionic liquids is believed to be due to **MC$_{BSP}$** residing in similar polar regions within each liquid. This may be due to the **MC** molecules being surrounded by polar head groups, they are then somewhat shielded from the effects of increasing chain lengths thus reducing the overall impact alkyl chain length. Minor effects are still observed however, possibly due to increasing side-chain lengths corresponding to an increasing separation of polar groups within non-polar domains of increasing dominance. This leads to a liquid system that appears more non-polar throughout to spirocyclic compounds and thus generate solvatochromic shifts corresponding to such environments for **MC$_{BSP}$** (figure 3.6).

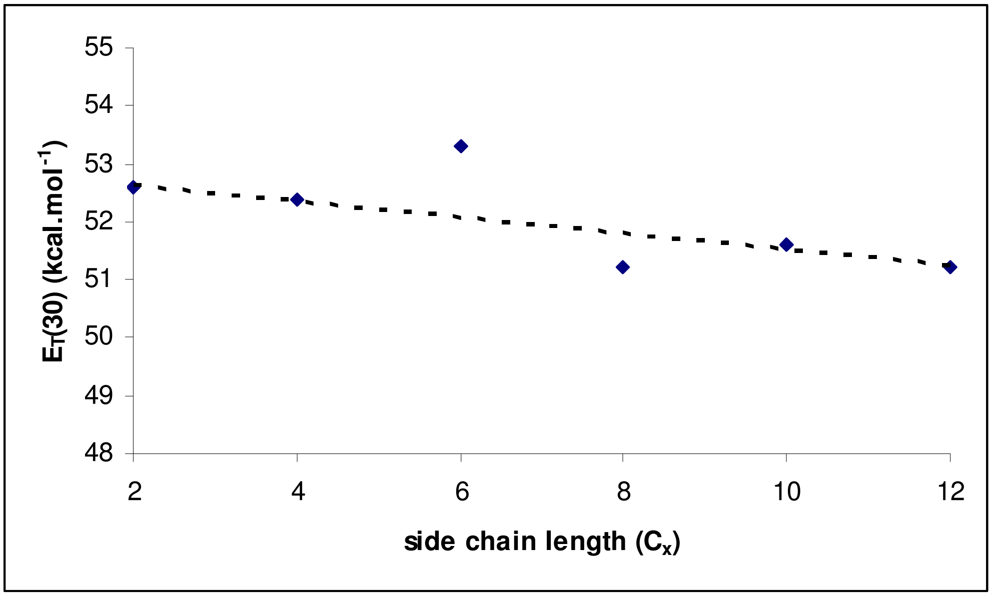

Figure 3.4 $E_T(30)$ values of imidazolium based ILs with increasing cation side-chain length.

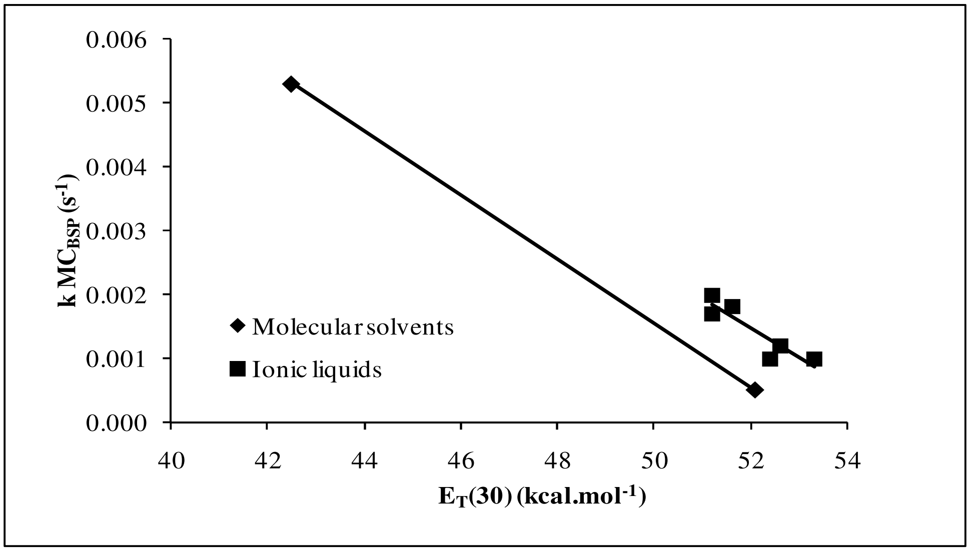

Figure 3.5 **MC$_{BSP}$** solvatochromic shift versus E$_T$(30) polarity.

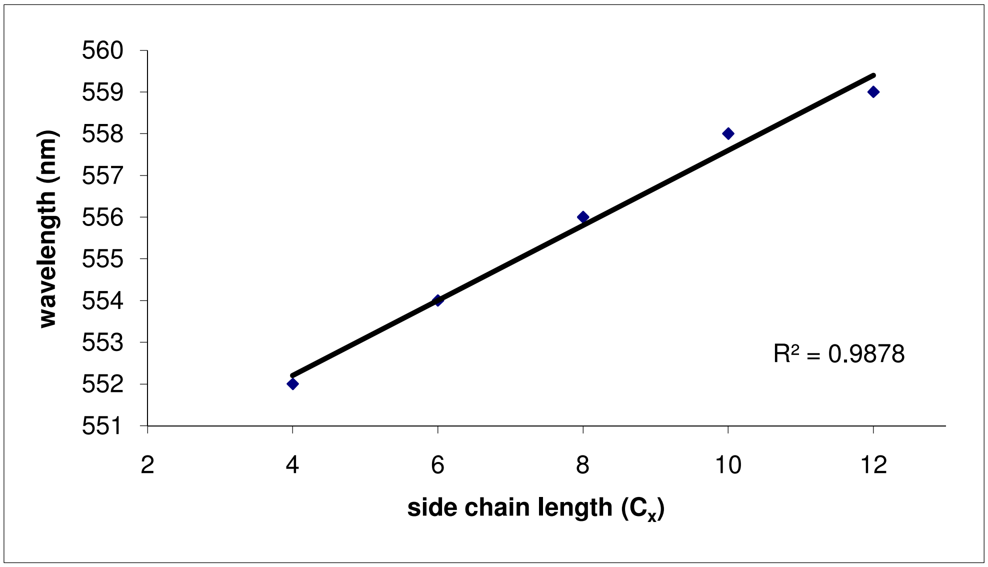

Figure 3.6 **MC$_{BSP}$** solvatochromic shift versus imidazolium cation side-chain length.

Table 3.1. Physicochemical properties of spirocyclic compounds in molecular solvents and ionic liquids. Reference values in parenthesis

SO

					Arrhenius (MC_{SO}-SO)		*Eyring (MC_{SO}-$MC^{‡}_{SO}$)*			
IL	λ*max* MC_{SO}	k_{25}	ET_{30}	K_e	E_a	*A*	$\Delta S^{‡}$	$\Delta H^{‡}$	$\Delta G^{‡}_{25}$	$K^{‡}$
	(nm)	($x10^{-2}\ s^{-1}$)	(kcal.mol^{-1})	($x10^{-3}$)	($kJ.mol^{-1}$)		($J.K^{-1}.mol^{-1}$)	($kJ.mol^{-1}$)	($kJ.mol^{-1}$)	($x10^{-15}$)
ethanol[22]	642	(3.8)	(52.1)	-	(89.89)	(2.037x10^{13})	(6.4)	(87.45)	(81.05)	(5.23)
acetone[22]	642	(5.1)	(42.5)	-	(69.51)	(4.929x10^{10})	(-44.73)	(67.08)	(80.41)	(8.83)
$[C_2mIm][NTf_2]$	642	2.3	52.6(52.6)[23]	6.62	95.23	1.11x10^{15}	34.92	92.8	82.39	3.68
$[C_4mIm][NTf_2]$	642	2.5	52.4(50.0)[24]	4.38	95.18	1.14x10^{15}	35.20	92.75	82.26	3.95
$[C_6mIm][NTf_2]$	644	2.2	53.3(51.9)[23]	3.84	92.35	3.16Ex10^{14}	24.52	89.91	82.61	3.51
$[C_8mIm][NTf_2]$	646	2.5	51.2(51.1)[14]	4.97	90.79	1.91x10^{14}	20.31	88.35	82.3	3.82
$[C_{10}mIm][NTf_2]$	644	2.3	51.6(51.0)[24]	3.77	92.87	4.39x10^{14}	27.23	90.44	82.33	3.68
$[C_{12}mIm][NTf_2]$	646	2.6	51.2	5.03	95.32	1.34x10^{15}	36.48	92.89	82.02	4.2

BSP

					Arrhenius(MC_{BSP}-BSP)		*Eyring (MC_{BSP}-$MC^{‡}_{BSP}$)*			
IL	λ*max* MC_{BSP}	k_{25}	ET_{30}	K_e	E_a	*A*	$\Delta S^{‡}$	$\Delta H^{‡}$	$\Delta G^{‡}_{25}$	$K^{‡}$
	(nm)	($x10^{-3}\ s^{-1}$)	(kcal.mol^{-1})	($x10^{-3}$)	($kJ.mol^{-1}$)		($J.K^{-1}.mol^{-1}$)	($kJ.mol^{-1}$)	($kJ.mol^{-1}$)	($x10^{-16}$)
Ethanol	539	0.5	(52.1)[22]	-	109.78	9.26x10^{15}	52.51	107.32	91.68	8.55
Acetone	560	5.3	(42.5)[22]	-	104.50	1.26x10^{16}	55.18	102.07	85.63	8.62
$[C_2mIm][NTf_2]$	552	1.2	52.6(52.6)[23]	8.66	106.69	6.43x10^{15}	49.55	104.26	89.49	2.02
$[C_4mIm][NTf_2]$	552	1	52.4(51.6)[24]	7.02	96.93	8.71x10^{13}	13.79	94.49	90.38	1.65
$[C_6mIm][NTf_2]$	554	1	53.3(51.9) [23]	11.6	98.84	2.67x10^{14}	21.48	96.41	90.01	1.65
$[C_8mIm][NTf_2]$	556	1.7	51.2(51.1)[14]	5.31	103.34	2.18x10^{15}	40.55	100.9	88.82	2.71
$[C_{10}mIm][NTf_2]$	558	1.8	51.6(51.0)[24]	7.94	106.68	1.02x10^{16}	52.42	104.24	88.62	2.96
$[C_{12}mIm][NTf_2]$	559	2	51.2	7.63	105.27	5.73x10^{15}	46.15	102.14	88.39	3.22

3.3.2 Kinetic parameters

Samples were placed in thermostatically controlled UV-Vis spectrometer and were irradiated in -situ using a 375nm LED array (appendix A-2) to induce **MC** formation. Upon removal of the UV light source**,** the first order thermal relaxation decay curves were then examined using equation **(14)** (chapter 2, section 2.3.2). Rates of thermal relaxation were recorded at 298K and summarised in table 3.1. Slight increases in rates of relaxation were observed with increasing chain length upon addition of **BSP** to the ionic liquids. Increasing chain length resulted in rates of thermal relaxation doubling from $1.0\text{x}10^{-3}\text{s}^{-1}$ in $[C_4mIm][NTf_2]$ to $2.0\text{x}10^{-3}\text{s}^{-1}$ in $[C_{12}mIm][NTf_2]$ (figure 3.7). Since lengthening of the side-chains would be expected to promote more inter-chain interactions it is believed that such interactions place a strain upon the mutual interactions of the polar head groups. This strain in turn may cause the polar head groups to separate further from each other, dispersing the polar region and reducing the overall charge density within the region that stabilise the solute molecules.[20] Early investigations into ionic liquid structuring reported deviations from traditional correlations between viscosity and diffusion for the diffusion coefficients of solutes within ‘wet’ or hydrated ionic liquids.[25] Further studies concluded that this could be explained through the ionic liquid system swelling to accommodate the solvent molecules, as had been observed previously in studies involving IL/molecular solvent binary mixtures, such as $[C_4mIm][PF_6]$ and naphthalene.[26]

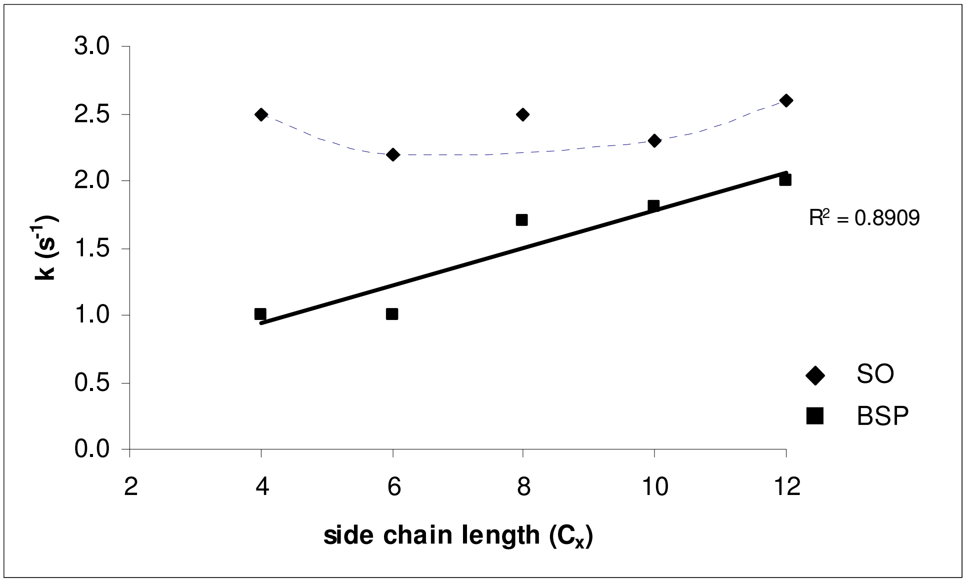

Figure 3.7 Rate of thermal relaxation of MC isomer to **BSP / SO** versus cation side-chain length.

SO was found to have similar relaxation rates of approximately $2.3x10^{-2}s^{-1}$ within all ionic liquids (figure 3.7),with increasing chain length having no apparent effect. This agreed with our previous findings and is believed to be due to the solvent-solute interactions being predominantly electrostatic, and its influence is therefore of similar strength in each ionic liquid.[22] Further support for this hypothesis comes from the rates of thermal relaxation, which were ten times faster for $\mathbf{MC_{SO}}$→**SO** relaxation than those observed for $\mathbf{MC_{BSP}}$→**BSP**. This would be expected, due to considerably weaker electrostatic forces stabilising the $\mathbf{MC_{SO}}$. These relatively weak electrostatic forces also means that **SO/** $\mathbf{MC_{SO}}$ molecules are relatively free to move within the ionic liquid due to the absence of any strong direct interactions in polar or non-polar nano-regions in the ionic liquid and as such the alkyl chain length effects are negligible. **SO** molecules may therefore spontaneously migrate to an intermediate region between the two regions and where variations in side chain length and head group interaction would have less impact.

3.3.3 Thermodynamic parameters

The dependence of the rate of **MC↔BSP/SO** thermal relaxation with temperature was investigated using equations (**10**)-(**12**) (chapter 1, section 1.4.2) to estimate the activation energy (E_a), entropy of activation ($\Delta S^{\ddagger}$), enthalpy of activation ($\Delta H^{\ddagger}$) and Gibbs energy of activation ($\Delta G^{\ddagger}$). The alternative Eyring **(13)** (chapter 1, section 1.4.2) was used to derive the equilibrium of activation, $K^{\ddagger}$ based upon the transition state theory for the process i.e $\mathbf{MC_{BSP/SO}} \leftrightarrow \mathbf{MC^{\ddagger}_{BSP/SO}} \leftrightarrow$ **BSP/SO**.[27] The results are summarised in table 3.1 above. The reaction process for thermal relaxation of spirocyclic compounds was deemed to be similar throughout the range of ionic liquids and allowed for comparison of results found (See appendix A-4). $\Delta S^{\ddagger}$ values for $\mathbf{MC_{BSP/SO}} \rightarrow \mathbf{MC^{\ddagger}_{BSP/SO}}$ were positive and increased with chain length (figure 3.8, table 3.1). $\Delta S^{\ddagger}$ is employed as a measure of the amount of reorientation of the system during the thermal relaxation from $\mathbf{MC_{BSP}} \rightarrow \mathbf{MC^{\ddagger}_{BSP}}$ within the ionic liquid, and it is related to the rigidity of the solvent and the overall thermal stability of the system as it approaches its transition state. Changes in this parameter were obvious for $\mathbf{MC_{BSP}} \rightarrow \mathbf{MC^{\ddagger}_{BSP}}$ with entropies from +13.79 $J.K^{-1}.mol^{-1}$ in $[C_4mIm][NTf_2]$ rising to +46.15 $J.K^{-1}.mol^{-1}$ in $[C_{12}mIm][NTf_2]$. Positive values imply that the IL-solute system undergoes significant reorientation during the activation step of the thermal relaxation process. The observed increase in entropic values may be due to evolution of structured domains within the ionic liquids as increasing chain length will strengthen side chain interactions in the non-polar regions. Upon formation of the polar $\mathbf{MC_{BSP}}$ molecules, these molecules will situate themselves within the polar domains of the ionic liquids. Re-orientation of $\mathbf{MC_{BSP}}$ to its transition state, $\mathbf{MC^{\ddagger}_{BSP}}$

results in a reduction in molecular charge and so migration towards the non-polar regions of the ionic liquids. As alkyl chain lengths are increased the $\mathbf{MC_{BSP}}$ molecules are driven more efficiently into the polar domains and so the relative populations of $\mathbf{MC_{BSP}}$ in polar domains increases with chain length. As the compound migrates to non-polar domains the disorder of the system is increased through solvent (non-polar side chain structuring) disruption and is observed as positive entropies of activation. As populations of $\mathbf{MC_{BSP}}$ increase, the disorder is also found to increase due to more $\mathbf{MC_{BSP}}$ molecules being available to disrupt the system upon re-orientation to the transition state. In addition to this, steric effects from solvent-solvent and solvent-$\mathbf{MC_{BSP}}$ interactions could result in expansion of polar regions, allowing an easier transfer of the probe molecule during $\mathbf{MC_{BSP}}$**-BSP** and easier disruption of nano-domains due to reduced cohesive interactions between cation head groups. At short chain lengths ($[C_2mIm]^+$), it would be expected that little ordering exists and the ionic liquid ions are in random motion much like molecular solvents.

Since disorder of the system is increased as chain lengths increases, the ionic liquid may be adopting a more structured initial form at the nano-scale, with defined polar and non-polar regions between which the $\mathbf{MC_{BSP/SO}}$ and **BSP/SO** molecules can move dynamically as the equilibrium shifts. The physical size of the probe molecule itself is expected to significantly disrupt the established ionic liquid structure with reorientation of ions close to the spirocyclic compounds to accommodate the guest molecules. The subsequent switching and proposed movement during the transition of **$MC_{BSP/SO}$** (charged) to **BSP/SO** (uncharged) means that examination of the **$MC_{BSP/SO} \rightarrow MC^{\ddagger}_{BSP/SO}$** process should involve molecular reorientation to accommodate the probe molecules and thus a change in the entropy of the system related to this reorganisation.

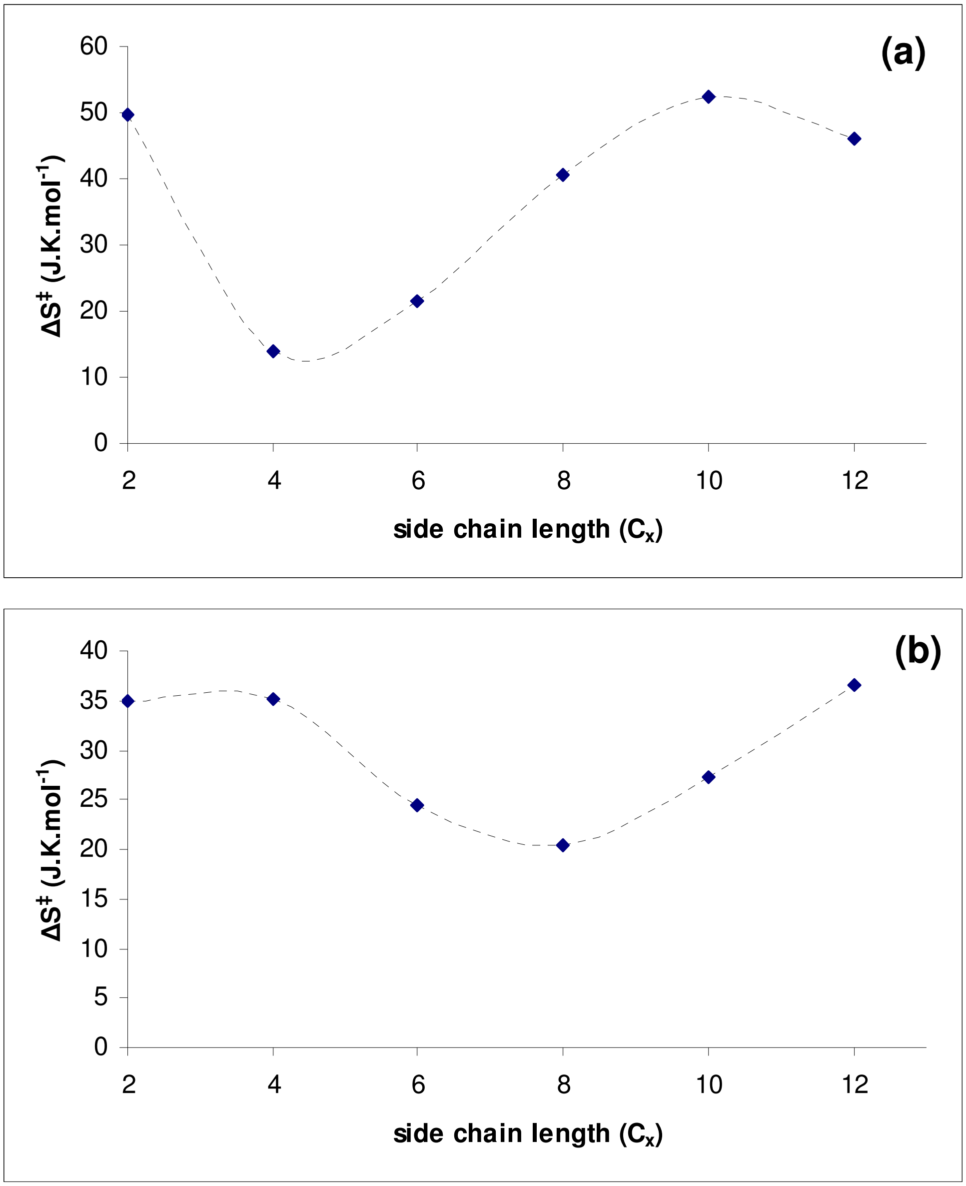

Figure 3.8 Entropies of activation of **BSP** (a) and **SO** (b) versus cation side-chain length.

Positive entropies imply that the interactions between the ionic liquid ions are weak enough for the spirocyclic compound to disrupt the system. This means the ionic liquid structure itself may be able to facilitate dynamic movement of the probe molecules between the ionic liquid polar/non-polar regions. **SO** thermodynamic parameters showed no clear correlation between the entropies of activation and chain length. This suggests that for the **MC_{SO}-$MC^{\ddagger}_{SO}$** thermal relaxation in the various ionic liquids is relatively independent of the nano-structure of the ionic liquid.

Activation energies (E_a) are initially found to be comparable to molecular solvents in $[C_2mIm][NTf_2]$ at 102.07 $kJ.mol^{-1}$ which is believed to have minimal structuring present. A 10 $kJ.mol^{-1}$ decrease in activation energy to 96.93 $kJ.mol^{-1}$ is observed when **BSP** is added to $[C_4mIm][NTf_2]$ which could indicate the formation of nano-domains in the liquid system. A gradual increase back to initial activation energies (105.27 $kJ.mol^{-1}$ in $[C_{12}mIm][NTf_2]$) is subsequently observed with increasing chain length (figure 3.9), similar to that of entropies of activation (figure 3.8). Similar effects are also present in ionic liquids where **SO** was added but the effects are found to be less apparent. Activation energies of **SO** also follow similar patterns as those observed for entropies of activation (figure 3.7). These values also appear to strengthen the reasoning why similar rates of thermal relaxation for **MC_{SO}** are observed in all ionic liquids.

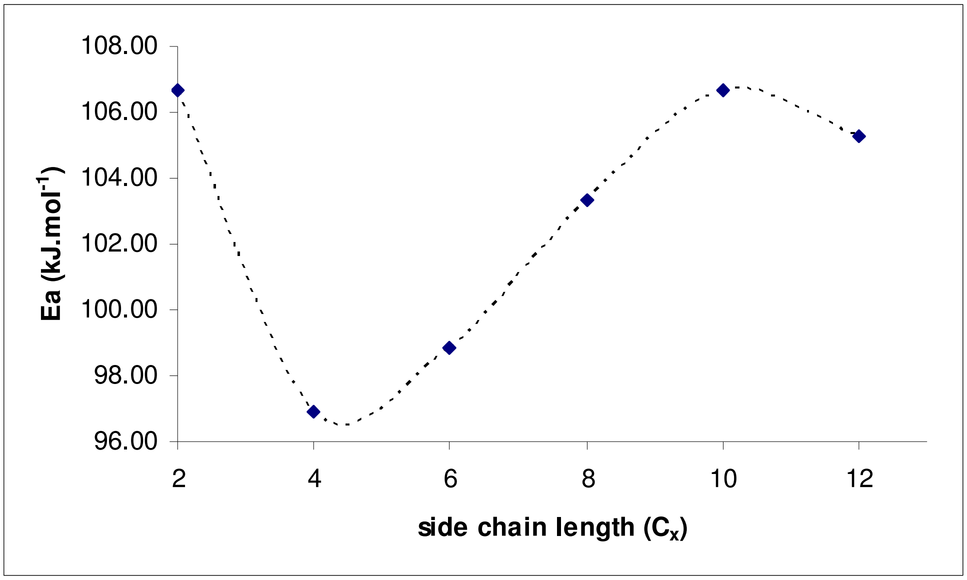

Figure 3.9 Activation energy of **MC$_{\mathbf{BSP}}$-BSP** thermal relaxation versus cation side-chain length.

Activation energies for **MC$_{\mathbf{BSP}}$** appear contradictory as increasing energy barriers would be expected to yield slower rates of relaxation. However, this could arise due to compensation for the increased separation of charged sites and increase in the size and frequency of non-polar regions as side chain length is increased. **MC$_{\mathbf{BSP}}$**, being a polar molecule will seek to associate in polar domains and as such attempt to resist interaction with non-polar domains as they less favourable to merocyanine stability. Although the activation barriers increase, it appears that once the compound reaches its transition state the increasing size of the non-polar domains facilitates increasing efficiency of **$\mathbf{MC^{\ddagger}_{BSP}\rightarrow BSP}$** thermal relaxation and is reflected increasing rates of thermal relaxation. Since activation energies only explain the **$\mathbf{MC_{BSP}\rightarrow MC^{\ddagger}_{BSP}}$** process and thermal relaxation explains the overall **$\mathbf{MC_{BSP}\rightarrow BSP}$** process, which may be the source of such contradictory results which at first appeared counterintuitive.

The thermodynamic parameters of **SO** showed little or no variance with increasing chain length. Since **SO** is believed to interact with the ionic liquids primarily through electrostatic interactions, it is proposed that the process of thermal relaxation is also somewhat independent of the nature of the ionic liquid, provided the charged centre remains unchanged, as is the case in this study. The functionalisation of the **SO** substituent may provide sufficient steric hindrance to prevent hydrogen bonding which would influence the relaxation process. The ability of the **SO** and $\mathbf{MC_{SO}}$ molecules to move somewhat freely between the ionic liquid nanostructured regions also means that the $\mathbf{MC_{SO}} \Rightarrow \mathbf{SO}$ conversion could occur with relatively little interaction with the ionic liquid ions. As a result, the process for thermal relaxation is similar in all ionic liquids tested, and is independent of chain length.

The ground state equilibrium, K_e, and transition state equilibrium, $K^{\ddagger}$, were also examined to determine the effects of chain length and ionic liquid nanostructure on the $\mathbf{MC_{SO}}$-**SO** and $\mathbf{MC_{BSP}}$-**BSP** equilibria (table 3.1). Ground state equilibria were determined using equation **(15)** (chapter 2, section 2.3.3). Ground state equilibrium constants were found to be consistent in relation to increasing ionic liquid cation side-chain length for both **BSP** and **SO** (figure 3.10a, figure 3.11a). K_e values of approximately $7x10^{-3}$ for **BSP** and $5x10^{-3}$ for **SO** were observed in each of the ionic liquids. This implies that the spirocyclic compounds remained in their closed (**BSP/SO**) form in preference to the respective $\mathbf{MC_{BSP/SO}}$ form in each of the ionic liquids (<1% **MC** form exists). Since the closed, **BSP/SO** forms of the compounds are believed to be generally at lower energy level than that of the respective merocyanine form in each ionic liquid, it would be expected that they would be primarily in the closed form at equilibrium. However, the size and prevalence polar regions and length of alkyl side chains within the ionic liquids may aid in shifting the equilibrium of the spirocyclic compounds. Examination of the shorter chain (more polar) ionic liquids showed little change in equilibrium constants compared to that of the longer chain cations. This would appear to reinforce the existence of domains within the solvent system, as increasing the chain length of the ionic liquid cation should favour the formation of the spiro form. If the spirocyclic compounds are residing in the non-polar regions in their closed form then it would appear that changing the size of such regions has little effect upon the equilibrium. Since spirocyclic compounds thermodynamically favour residing in such regions due to the uncharged nature of their closed form (and its lower thermodynamic energy level), intuitively it would be expected that the contribution of the non-polar regions of each ionic liquid to the equilibrium constant would be similar or equivalent in each of the ionic liquids.

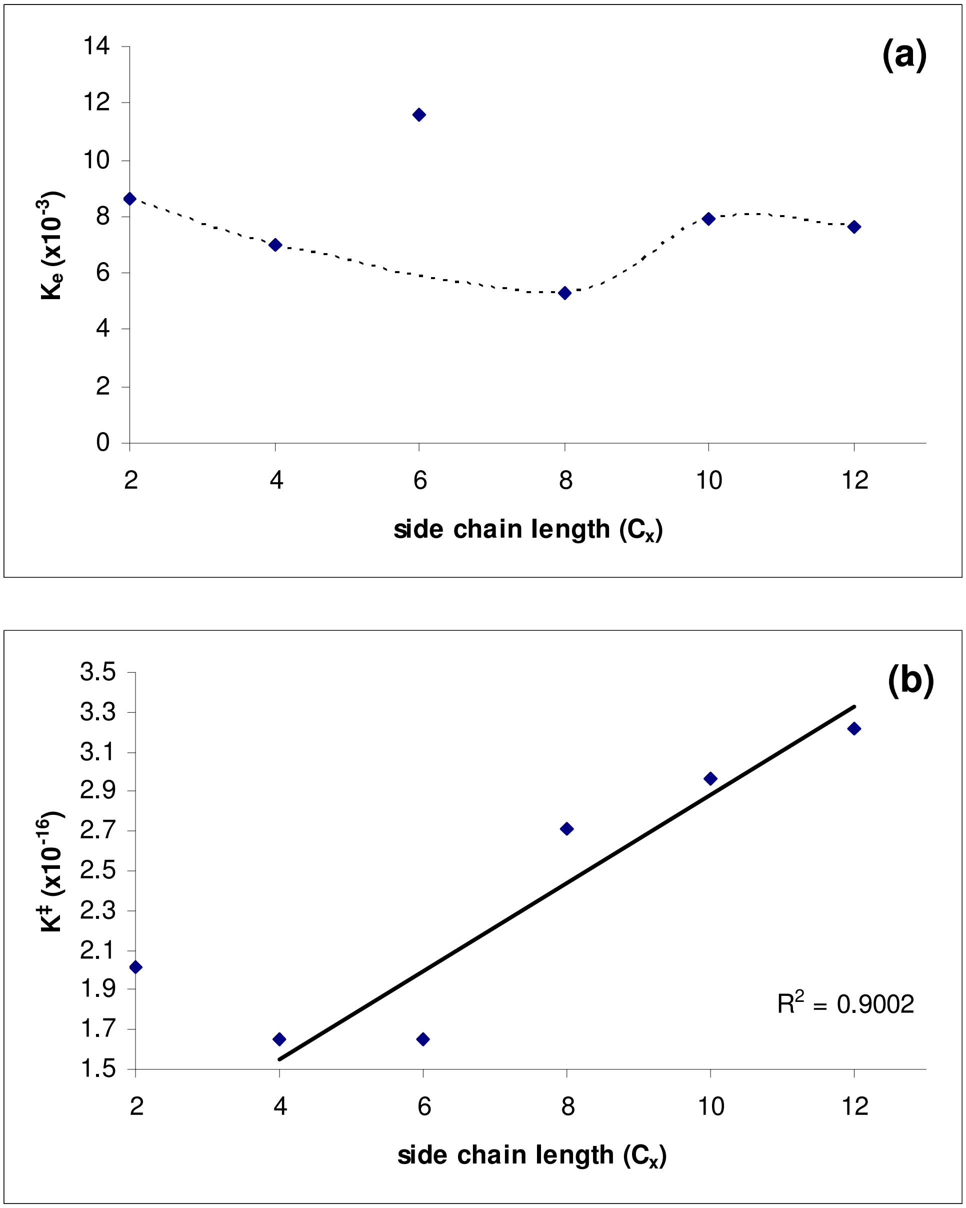

Figure 3.10 (a) Ground state equilibria (K_e) of $\mathbf{MC_{BSP}\leftrightarrow BSP}$ and (b) Equilibria of activation ($K^‡$) for $\mathbf{MC_{BSP}\leftrightarrow MC^{‡}_{BSP}\leftrightarrow BSP}$ versus cation side chain length.

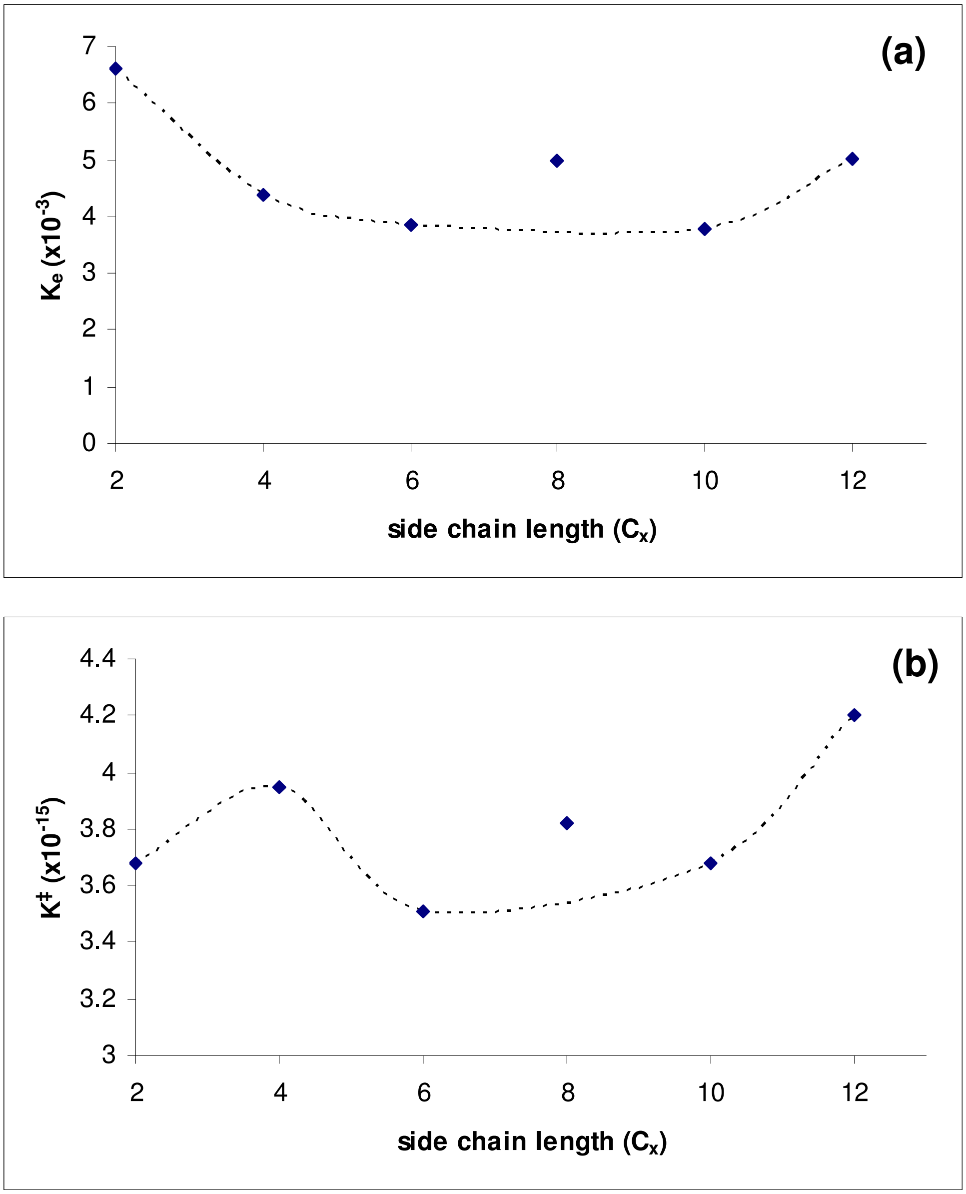

Figure 3.11 (a) Ground state equilibria (K_e) of **MC_{SO}↔SO** and (b) Equilibria of activation ($K^‡$) for **MC_{SO}↔$MC^‡_{SO}$↔SO** versus cation side chain length.

To examine the effect of polar regions of the ionic liquids, the equilibrium of activation, $K^{\ddagger}$, is examined. The equilibrium is based on the thermodynamic interconversion between $\mathbf{MC_{BSP/SO}}$ and the respective **BSP/SO** forms, and the process of relaxation is based upon which is the preferred state of the molecule. This equilibrium constant is determined using equation **(14)** (chapter 1, section 1.4.2) The transition state equilibrium determines whether the process of relaxation preferentially occurs. At this transition state ($\mathbf{MC^{\ddagger}}$) the compound is in the process of relaxation to **BSP/SO.** However, sufficient interaction with the ionic liquid system will increase the stability of the merocyanine form which competes with the forward ($\mathbf{MC_{BSP/SO}}$→**BSP/SO**) process. Unlike the ground state equilibrium constants, where the compound is predominantly in its most stable, ground state (closed) form , the transition state of compounds, $\mathbf{MC^{\ddagger}_{BSP/SO}}$**,** is at peak energy during the thermodynamic process and as such less stable than either the **BSP/SO** or $\mathbf{MC_{BSP/SO}}$ form. By established convention for thermal relaxation of spirocyclic compounds, the reaction predominantly lies to the **BSP/SO** but examination of the relaxation process at their transition states acts as a measure of the ‘resistance’ present through solvent stabilisation which in turn affects the overall relaxation process (activation barriers and rates of relaxation). For imidazolium based ILs this could possibly be interpreted as the competing influence of the non-polar domains for the **BSP/SO** forms and polar regions for the $\mathbf{MC_{BSP/SO}}$. The result is that any changes in the equilibrium is therefore sensitive on changes to the system which can only be observed when the spirocyclic compounds are in the process of thermal relaxation and migrating within the ionic liquid. Since the ground state (closed) form of the probe molecules require energy to form their respective merocyanine isomers, the ground state equilibrium K_e, is somewhat biased towards the closed form and so the compound resides consistently in the non-polar regions of the ionic liquids. This may explain why there is little relationship between the rate constants and the ground state equilibrium constants. In the case of merocyanine thermal relaxation and the transition state equilibrium, the opposite occurs as the compound must now relax to its **BSP/SO** form from its higher $\mathbf{MC^{\ddagger}_{BSP/SO}}$ transition state.

With increasing chain length, structuring within the solvent is proposed to disperse and weaken the relative interactions of the polar regions. Theoretical models by Lopes agreed with this convention with $[C_{12}mIm]^+$ based ILs showing a majority of non-polar regions compared to that of $[C_4mIm]^+$ ILs. Reduction in the strength of **MC**-IL interactions results in reduced stability of the merocyanine form and further enhance the formation of the closed form which shifts the equilibrium toward the closed form of the compound. This is observed as increasing and linear $K^{\ddagger}$ values from $1.65x10^{-16}$ in $[C_4mIm]^+$ to $3.22x10^{-16}$ in $[C_{12}mIm]^+$ (figure 3.10b) and is in line with the linear response found for the rate constant. For **SO** the response in $K^{\ddagger}$ values due to chain length was not as clear as that observed for **BSP** (figure 3.11b). This is believed to be due to the passive nature of $\mathbf{MC_{SO}}$ -IL interactions and the relatively independent nature of the relaxation process resulting from this.

The above results appear to illustrate effects which may be related to the proposed physical disruption of the nano-structured regions within ionic liquids upon the addition of spirocyclic compounds. Photoswitching of these compounds may also result in migration of the compounds between each of the regions within the ionic liquids and/or the re-organisation of the ions around the compound depending upon the charges/form of the spirocyclic compound present. If separation of head groups occurs upon increased alkyl chain length, then the distance between the imidazolium ring charge/C2 proton and the **MC** isomer may be increased by competing interactions (alkyl chain van der Waals versus C2 hydrogen-**MC$_{\mathbf{BSP}}$** hydrogen bonding) and would imply a reduction in the ability of the **MC** molecules to stabilise polar guests. Rates of thermal relaxation of **MC$_{\mathbf{BSP}}$** were found to increase with increasing chain length which is believed to be due to the reduction in the effectiveness of stabilisation interactions within polar regions with concurrent increase in the impact of non-polar regions that favour **MC$_{\mathbf{BSP}}$** conversion to **BSP**.

Deviations from expected results that are observed for the thermodynamic parameters examined under the Arrhenius and Eyring equations way originate from assumption that solvent thermal equilibrium is maintained throughout the entire process and reorganisation of the solvent is sufficiently fast. Chiappe *et al*[28] concluded that dynamic contributions to the transition state may be present in ionic liquids which result in slower solvent relaxation which competes for influence over the entire process. This would appear to agree with our findings where activation parameters may be influenced by the solvent structure in the polar domain as the charged **MC$_{\mathbf{BSP}}$** begins its relaxation process. However, once the compound passes its transition state and becomes more non-polar, the corresponding non-polar domains begin to influence the remaining relaxation process. The occurrence of two separate processes may contribute to the loss of solvent equilibrium and the formation of a complex multi-stage solvent system which is not accounted for by traditional transition state theory which was created using homogeneous, single phased molecular solvents.

Under thermodynamic processes, the entropic factor, $\Delta S^{\ddagger}$ appears to have the largest variation and so dominates the overall effects of the ionic liquid system. The ordering, and subsequent evolution of disorder through $\mathbf{MC_{BSP}}\rightarrow\mathbf{MC^{\ddagger}_{BSP}}$ formation, greatly influences the rate constant which is in turn believed to be related to the presence of structuring within the liquids. Similarly, it would appear that under Arrhenius dependencies that the rate of thermal relaxation was influenced by the pre-exponential factor, A as opposed to the activation energy barrier. However, pre-exponential factors appear to encompass all other processes occurring that the activation energy, E_a, does not quantify and so it is difficult to explain exactly factor explicitly mediates such effects. Figure 3.8b also shows interesting characteristics whereby the entropy of activation for $\mathbf{MC_{SO}}\rightarrow\mathbf{MC^{\ddagger}_{SO}}$ is observed to reach a local minimum for C6-C8 side-chain lengths before returning to similar entropy values for C12 as seen for C2 chain length cations. A possible explanation for this is the competing forces of hydrogen bonding and van der Waals interactions. Previous studies into gellation characteristics and 2D self assembly of monolayers has found the process is mediated by the relative strengths of such interactions.[29-31] At shorter chain lengths, hydrogen bonding would be expected to dominate structuring of the ionic liquid structure.

With increasing side chain lengths, van der waals interactions would be expected to become more influential and thus contribute in parallel to hydrogen bonding to the overall stability of the ionic liquid. The effect of two complimentary forces is enhanced stability of the cation structure and therefore a more rigid structure as observed by decreased entropies of activation. As the side chains continue to increase, the van der waals interactions would begin to dominate the process of organisation within the ionic liquid. As a result the effect of hydrogen bonding becomes less apparent with the formation of more extensive side-chain interactions. It is believed that loss of these head group interactions and proposed dissolution of the polar regions results in only one interactive force (van der Waals) contributing to the stabilisation of the liquid structure. This loss of hydrogen bonding may result in more head group freedom and so a corresponding increase in entropy (solvent freedom) is observed. The effects were only observed when **SO** was added to the ionic liquids and may be due to its bulky nature. The inability of the probe to interact closely with the cation possibly allows the solvent system to remain relatively unperturbed by the probe and so exhibit these properties. The ability for **BSP** to interact with the imidazolium cation may aid in the retention of a similar level of hydrogen bond influence in each ionic liquid. This as such removes its influence upon the system and the linear nature of entropy of activation values with increasing side chain lengths in figure 3.9 relates to increasing van der Waals forces solely.

3.4 Conclusions

Following on from discrepancies found by traditional physicochemical parameters the hypothesis of nano-structuring into polar and non-polar domains within ionic liquids was examined. Examination of imidazolium based ILs with increasing alkyl chain lengths provided a clear trend based upon cation functionalisation, which appears to dominate the physical properties within this class of ionic liquids. However, the ability to clearly quantify differences in $E_T(30)$ values and rates of thermal relaxation showed that such structuring produces regions which differ greatly in their chemical properties and may only be sufficiently examined using dynamic probes such as spiropyran. Addition of the spirocyclic compounds results in moderate changes to thermodynamic parameters which are believed to be mediated by increasing nano-structuring with increasing alkyl chain lengths and thus van der Waals associations. **BSP** was found to be sensitive enough to quantify thermodynamic and kinetic parameters due to its intimate interaction with the imidazolium cation when in its zwitterionic **MC**$_{\mathbf{BSP}}$ form. **SO** failed to achieve the same effect and this was believed to be due to its inability to form hydrogen bonds and its restriction to electrostatic interactions with the ionic liquids. Similar steric effects were found in Chapter 2 with a range of cation species and this implies that access to the phenolate oxygen of the **MC** form is critical to interaction and thus characterisation of the ionic liquids by spirocyclic compounds. Probing of ionic liquids with **BSP** suggests that the molecule may dynamically transfer between the polar and non-polar nano-structured domains in the ionic liquid. Ground state equilibria values were similar regardless of the ionic liquid cation chain length, which suggests that stabilisation effects are similar for each form of the probe molecule in each ionic liquid. This implies that the ratio of the probes, in their equilibrium state, resided in similar presumably non-polar domains (since **BSP/SO** dominate in the ground state) in each ionic liquid.

Trends observed trends in thermodynamic parameters and particularly similarities in the behaviour of activation energies and entropies of activation reinforces the concept of proposed structuring within imidazolium based ILs and a possible insight into competing interaction between electrostatic headgroup and akyl chain van der Waals forces in the formation of nano-domains. The similar reduction in activation energies and entropies of activation, $\Delta S^{\ddagger}$, in both **BSP** and **SO** imply that a universal process, somewhat independent of the probe, is occurring within the ionic liquids and appears to be mediated by alkyl chain length. Positive $\Delta S^{\ddagger}$ values indicate that the system may undergo considerable reorganisation during thermal relaxation of the spirocyclic compounds. It is proposed that the spirocyclic probe is therefore disrupting the ionic liquid nano-structure when photoswitching occurs. Possible migration of the compounds between the nano-structured regions may cause of such entropic changes but it is also possible that the reorganisation of the system is around the spirocyclic compound. In this case, the spirocyclic compound stays relatively stationary and ionic liquid constituents may rearrange around the compound depending upon its form. As such, the compounds would, in essence, probe each nano-domain as the cation structure that surrounds the molecules will be determined by the form (**SP/MC**) of the molecule and therefore its reduced/enhanced interactions with cation charge sites. Following this hypothesis, such interactions with the ionic liquids may help rationalise why rates of relaxation are found to be slower in ionic liquids when compared to molecular solvents. In reality, it is most probable that the effects determined by the thermal relaxation process are a combination of a migratory process as well as a solvent buffering effect through its own reordering. To determine the importance of each process it would be intuitive to attempt to anchor the probe molecules within each domain and examine the effectiveness of thermal relaxation to determine the physicochemical properties of the liquids.

Interestingly, the reduction in entropy of activation values for **SO** to show the important forces which mediate the formation of the nano-structuring observed within ionic liquids. The expansion/dissolution of polar regions is believed to be central to the dispersion of the charged regions and disruption of the worm like conductive channels as proposed by Lopes *et al.*[5] The lack of specific interactions of **SO** which was deemed negative for probing specific regions within ionic liquids may therefore be beneficial for examining an interfacial process occurring between *both* polar and non polar domains. The compounds ability to ‘observe’ rather than interact with ion-ion interactions allows for a unique perspective of possible processes occurring within ionic liquid which experimentally confirm the mainly theoretical approximations of the changes in structuring based upon nano-domain self organisation.

3.5 References

1. C. S. Consorti, P. A. Z. Suarez, R. F. de Souza, R. A. Burrow, D. H. Farrar, A. J. Lough, W. Loh, L. H. M. da Silva and J. Dupont, *The Journal of Physical Chemistry B*, 2005, **109**, 4341-4349.
2. K. Iwata, H. Okajima, S. Saha and H.-o. Hamaguchi, *Accounts of Chemical Research*, 2007, **40**, 1174-1181.
3. J. N. A. Canongia Lopes and A. A. H. Padua, *The Journal of Physical Chemistry B*, 2006, **110**, 3330-3335.
4. *Ionic Liquids in Synthesis*, Second edn., WILEY-VCH, Weinheim, 2004.
5. J. N. C. Lopes and A. A. H. Padua, *Journal of Physical Chemistry B*, 2006, **110**, 3330-3335.
6. R. W. Taft and M. J. Kamlet, *Journal of the American Chemical Society*, 1976, **98**, 2886-2894.
7. M. J. Kamlet and R. W. Taft, *Journal of the American Chemical Society*, 1976, **98**, 377-383.
8. M. J. Kamlet, J. L. Abboud and R. W. Taft, *Journal of the American Chemical Society*, 1977, **99**, 6027-6038.
9. C. Reichardt, *Chemical Reviews*, 1994, **94**, 2319-2358.
10. J. Figueras, *Journal of the American Chemical Society*, 1971, **93**, 3255-3263.
11. L. Crowhurst, R. Falcone, N. L. Lancaster, V. Llopis-Mestre and T. Welton, *Journal of organic chemistry*, 2006, **71**, 8847-8853.
12. C. P. Fredlake, M. J. Muldoon, S. N. V. K. Aki, T. Welton and J. F. Brennecke, *Physical Chemistry Chemical Physics*, 2004, **6**, 3280-3285.
13. K. A. Fletcher, I. A. Storey, A. E. Hendricks, S. Pandey and S. Pandey, *Green Chemistry*, 2001, **3**, 210-215.
14. M. J. Muldoon, C. M. Gordon and I. R. Dunkin, *Journal of the Chemical Society, Perkin Transactions 2*, 2001, 433-435.
15. B. G. Jeliazkova, S. Minkovska and T. Deligeorgiev, *Journal of Photochemistry and Photobiology A: Chemistry*, 2005, **171**, 153-160.
16. B. I. Ipe, S. Mahima and K. G. Thomas, *Journal of the American Chemical Society*, 2003, **125**, 7174-7175.
17. L. S. Atabekyan, *High Energy Chemistry*, 2002, **36**, 397-404.
18. A. K. Chibisov and H. Görner, *Chemical Physics*, 1998, **237**, 425-442.
19. C. J. Wohl and D. Kuciauskas, *Journal of Physical Chemistry B*, 2005, **109**, 21893-21849.
20. J. Dupont, *Journal of the Brazilian Chemical Society*, 2004, **15**, 341-350.
21. A. K. Burrell, R. E. D. Sesto, S. N. Baker, T. M. McCleskey and G. A. Baker, *Green Chemistry*, 2007, **9**, 449-454.
22. S. P. Coleman, R. Byrne, S. Minkovska and D. Diamond, *Physical Chemistry Chemical Physics*, 2009, **11**, 5608-5614.
23. C. Reichardt, *Green Chemistry*, 2005, **7**, 339-351.
24. S. V. Dzyuba and R. A. Bartsch, *Tetrahedron Letters*, 2002, **43**, 4657-4659.
25. U. Schroder, J. D. Wadhawan, R. G. Compton, F. Marken, P. A. Z. Suarez, C. S. Consorti, R. F. d. Souza and J. Dupont, *New Journal of Chemistry*, 2000, **24**, 1009-1015.

26. M. G. Del PoÌpolo, C. L. Mullan, J. D. Holbrey, C. Hardacre and P. Ballone, *Journal of the American Chemical Society*, 2008, **130**, 7032-7041.
27. K. J. Laidler and J. H. Meiser, *Physical Chemistry*, 3rd edition edn., Houghton Mifflin, Boston, 1999.
28. C. Chiappe, M. Malvaldi and C. S. Pomelli, *Pure and Applied Chemistry*, 2009, **81**, 767-776.
29. T. R. Minna, M. Florian, F. Santeri, R. Bernhard, Z. Ulrich, L. Markku and R. Timo, *European Journal of Inorganic Chemistry*, 2007, **2007**, 4028-4034.
30. N. Zweep, A. Hopkinson, A. Meetsma, W. R. Browne, B. L. Feringa and J. H. van Esch, *Langmuir*, 2009, **25**, 8802-8809.
31. S. Khanna, M. K. Khan and P. Sundararajan, *Langmuir*, 2009, **25**, 13183-13193.

4

Specific Probing of Ionic Liquid Domains Using Functionalised Spiropyran Derivatives

4.1 Introduction

Chapter 3 provided insight into the existence of structured regions within ionic liquids based upon the imidazolium cation and the effect such structuring had upon the photochemical properties of spirocyclic compounds. However, the formation of such structuring can not be restricted to only this class of ionic liquid. Indeed, recent studies such as those by Pott *et al* postulate the formation of discrete domains within quaternary ammonium based ILs, similar in structure to that of phosphonium based ILs.[1] Given the relatively larger sizes of this class of cation ~12 Å for $[C_6mIm]^+$ vs ~25Å for $[P_{6,6,6,14}]^+$) and the increase in side-chain interactions since quaternary cations contain four alkyl chains, it is believed that such liquids may produce a much more extensive structured network. In Chapter 3 it was found that the form of the spirocyclic compound (**BSP/SO↔MC$_{\mathbf{BSP/SO}}$**) mediated the interactions with the ionic liquid, and the functionalisation of the spirocyclic compound could significantly alter this interaction. In the case of **SO** it was found that the interactions with the ionic liquids was limited to weak and relatively uniform electrostatic interactions in each ionic liquid. This was believed to be due to the restrictive nature of the benzothiophene derivative of the compound which may have reduced the access and subsequent stabilisation of **MC$_{\mathbf{SO}}$** at the phenolate oxygen site. As thermal relaxation occurred it is believed that the spirocyclic molecules may migrate to some degree between the nanostructured domains in response to the formation/removal of charged sites and disrupting the ordering of the ionic liquids in the process. Although the process yielded very interesting insight into the structure of the liquid system, taking into account the complex structuring and individual effects on each domain it is believed that this spontaneous migration was predominantly restricted to regions adjacent to the interfaces between the domains and not penetrating significantly into the bulk of each nano-structured domain. To address this, the spiropyran probe was tailored to be more compatible with selected regions within the liquids by covalent attachment of functional groups that preferentially interact with these domains. By ‘locking’ the compound within these regions, the thermodynamic properties of the spirocyclic compound could be used to give detailed information on this region alone, by removing the ability for the probe to migrate between domains.

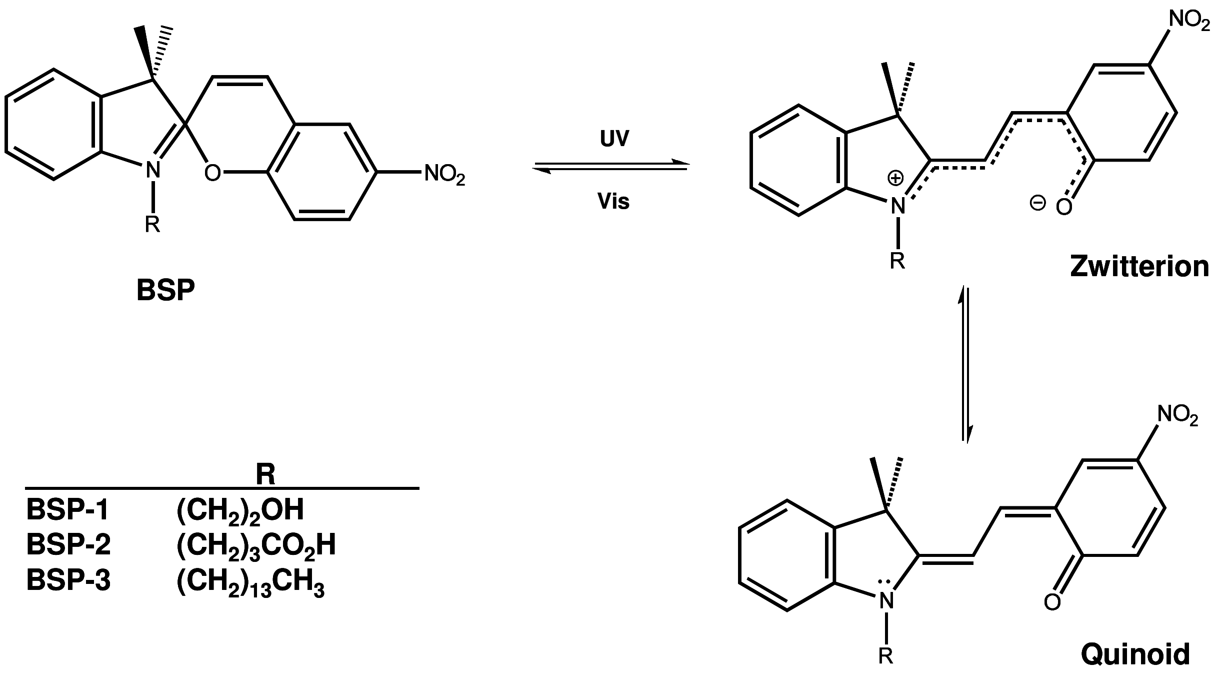

	R
BSP-1	$(CH_2)_2OH$
BSP-2	$(CH_2)_3CO_2H$
BSP-3	$(CH_2)_{13}CH_3$

Figure 4.1 Spiropyran derivatives employed for specific probing of ionic liquids and their photoswitching

Three spiropyran derivatives containing hydroxyl (**BSP-1**), carboxylic acid (**BSP-2**) and aliphatic chain ($C_{14}H_{29}$) (**BSP-3**) functional groups were added to phosphonium based ILs and examined using spectroscopic techniques to determine the physicochemical properties and structural effects in each of the different regions within the ionic liquids (figure 4.1). The thermal relaxation behaviour of the **MC** isomer is employed to report on each environment within which it resides and as such, the structuring would be expected to yield thermodynamic, kinetic and solvatochromic parameters that are not quantifiable based on classical solvent models and probe techniques. In previous chapters it has been argued that the solvent properties of ionic liquids may not be well accounted for by conventional macroscopic parameters like polarity and dielectric constant, which have been extensively used to classify molecular solvents. As observed in chapter 2, the use of conventional solvatochromic probe dyes (Nile Red and Reichardts dye)[2] proved ineffective as it was found that all ionic liquids studied appeared to have the same or similar properties to moderately polar solvents with little variation across a range of cation and anions. This was in stark contrast to their behaviour as reaction solvents since different ionic liquids exhibited very different properties (e.g reaction rates). Such contradictory results do not invalidate the use of solvatochromic dyes for ionic liquid characterisation, but rather imply that more sophisticated models are required to understand solute/solvent interactions within ionic liquids. Since classical molecular solvents present relatively homogeneous systems, these solvatochromic dyes can accurately classify the bulk environment through localised solvation-type interactions. However, the possible existence of nano-structured polar/non-polar regions as discussed in Chapter 3 meant this more complex behaviour could be explained via the polar solvatochromic dyes preferentially locating in specific regions and thus only be used to probe the state of one particular region while ignoring the rest of the solvent environment. Similarly, it was concluded that solvatochromic probes such as those used in Kamlet-Taft and Reichardt's studies were limited to a specific region within the liquids and thus could not report on regions beyond their immediate environments. This behaviour may explain the often highly contradictory results obtained when solvatochromic probes are used to classify ionic liquids.

As discussed previously, more sophisticated approaches are needed to help characterize the solvation properties of ionic liquids that can account for the multiple solvent–solute interactions that are possible throughout the liquid. Current attempts to examine these interactions have yielded interesting findings but are still generally only reporting upon one region or interaction at a time. In sensor science, one develops a molecule to monitor a single parameter in its local environment. In the literature there has been considerable interest in the probing of ionic liquid nano-structure. For example, time resolved fluorescence spectroscopy based on Prodan[3] and other probe molecules have been used to study the solvation dynamics in ionic liquids,[4,5] and it has been proposed that coumarin 153 is preferentially solvated by the cation via dipole relaxation.[6] Iwata investigated the behaviour of 2-aminoquinoline in several ionic liquids using similar techniques and found that certain imidazolium ionic liquids form complexes with 2-aminoaquinoline.[7] Linear and Nonlinear Raman spectroscopy showed evidence that imidazolium ionic liquids were homogeneous macroscopically, but heterogeneous in the nanometre scale.[8] Molecular dynamics simulations support this view.[9,10] Recently, more complex molecular sensors have been synthesised to respond to multiple parameters, each by a different analytical technique. de Silva *et al* has pioneered this area of sensor science with his 'multiplexing sensor molecules', which can be regarded as nano-sized robots (nano-bots) that migrate to pre-selected locations (e.g. on the basis of polarity), monitor its local environment (through host-guest complexation chemistry) and send information back via fluorescence emission signalling.[11] The **MC** isomer possesses similar abilities to these molecules whereby several specific probes are added to the solvent and using thermal relaxation properties (as opposed to fluorescence) the properties of each distinct ionic liquid region may be reported.

Chapter 2 found that the photochromic properties of **BSP** in phosphonium based ILs exhibits a non-linear relationship between the equilibrium constant (K_e) and the rate of thermal isomerisation (k) of **MC** to **BSP** which contradicts what is expected for **BSP** in molecular solvents and suggests the isomers experience different localised molecular/solvation environments.[12] Similar observations have been also found with respect to the photochromic behaviour of spirooxazines in ionic liquids.[13] Wohl and Kuciauskas previously demonstrated the ability to control the position of **BSP** in a phospholipid bilayer by substituting various functional groups at the indoline moiety of the **BSP**. They reported that the position of the **BSP** in the phospholipid bilayer was reflected in the thermal ring closing kinetics of the **MC**. It is anticipated that the three functionalised **BSP** molecules can be used for similar purposes and describe a new type of multiplexing molecular probe that can be positioned in specific molecular environments to explore the interactions and structure of ionic liquids.

Controlling the location of a molecular probe through molecular interactions in a complex system such as a micelle or phospholipid bilayer through modification of its chemical structure is very appealing, as one can monitor specific molecular environments on demand.[11,14] Pison *et al* investigated the solubility of fluorinated gases in trihexyltetradecylphosphonium bis(trifluoromethylsulfonyl)amide with supporting molecular simulation calculations.[15] and found that unexpected solubility profiles of certain sized fluorinated gases could be explained by their location with respect to the ionic liquid ions. For example **BSP-1** and **BSP-2** (figure 4.1) have polar appendages located at the indoline nitrogen. It is hoped that these **BSP** derivatives embed themselves within polar domains and report their locations via solvatochromic shift of the **MC** isomer λ_{max}. Furthermore, such photochromic probes have the potential to report on specific and non-specific interactions via kinetic and thermodynamic parameters associated with the $\mathbf{MC_{BSP}}\rightarrow\mathbf{BSP}$ thermal relaxation process (Chapter 1). By this convention, it is anticipated that **BSP-3** would locate within non-polar regions and report on this differing molecular environment. Integration of each derivative into specific domains within the ionic liquids can be examined to determine the specific properties of each domain and compared to the processes observed in traditional molecular solvents. The resulting environments detected can then be compared to the solvatochromic probe Reichardt's dye 30 as a solvent-dependent reference probe to compare the apparent solvent polarity ($E_T(30)$ scale) to determine if differing interactions result in different regions within the ionic liquids being examined. First-order rate constants for the thermal relaxation of $\mathbf{MC_{BSP\text{-}x}}$ were determined using equation **(14)** (chapter 2, section 2.3.2). Thermodynamic parameters were determined using equations (**10**) - (**13**) previously described (Chapter 1, section 1.4.2) to probe each environment that each derivative was positioned within.

4.2 Experimental

1-(2-hydroxyethyl)-3,3-dimethylindoline-6'-nitrobenzospiropyran **(BSP-1)** was purchased from TCI chemicals and used as received. **BSP-2** and **BSP-3** were synthesised as reported previously.[16,17] Anhydrous acetonitrile, ethanol and dichloromethane was purchased from Sigma Aldrich and used without further purification. Tetradecyl(trihexyl)-phosphonium bis(trifluoromethylsulfonyl)imide ($[P_{6,6,6,14}][NTf_2]$), Tetradecyl(trihexyl)-phosphonium dicyanamide ($[P_{6,6,6,14}]$[dca]), Tetradecyl(trihexyl)-phosphonium dodecylbenzenesulfonate ($[P_{6,6,6,14}]$[dbsa]), triisobutyl(methyl) phosphonium tosylate ($[P_{1,4,4,4}]$[tos]) were supplied by Cytec industries. Tetradecyl(trihexyl)-phosphonium tris(pentafluoroethyl)trifluorophosphate ($[P_{6,6,6,14}]$[FAP]) was supplied by Merck. Commercially available phosphonium based ionic liquids contain traces of phosphines, HCl and water and recognizing the sensitivity of molecular probe studies by spectroscopic methods to these contaminants, detailed purification developed by Ramnial *et al* was followed.[18] All ionic liquids were stored under reduced pressure until further use. All spectra were recorded with a UV-Vis-NIR Perkin-Elmer Lambda 900 spectrometer. The ultraviolet irradiation source was a 3 UV LED system at 375 nm produced for LEDs purchased from Roithner Lasertechnik. The white light source was a Lumina obtained from Chiu Technical Corporation. Standard solutions of **BSP** derivatives were made up to 1 x 10^{-4}M in acetonitrile as described in Chapter 2. Samples were stored under argon in the dark at 20°C for 15 hours before absorbance measurements were taken. The kinetic parameters of the thermal reversion of **MC** to **BSP** were determined at each temperature by monitoring the decreasing absorbance at the λ_{max} of the **MC** isomer after removal of the irradiating source.

4.3 Results and discussion

4.3.1 BSP-1: Hydroxyl derivative

The physical, kinetic and thermodynamic properties of the **BSP-1** are tabulated in table 4.1. The UV-Vis absorption spectrum of **BSP-1** at room temperature in molecular solvents is found to exhibit a major absorption band in the visible region 550 nm (table 4.1) due to an increase of absorbance in the visible region due to the formation of the $\mathbf{MC_{BSP\text{-}1}}$ isomer as previously established for spirocyclic photochromic compounds. UV-vis absorption spectra of the $\mathbf{MC_{BSP\text{-}1}}$ isomer in ethanol (λ_{max} = 538 nm), $[P_{6,6,6,14}]$[dbsa] (λ_{max} = 560 nm), and $[P_{6,6,6,14}]$[dca] (λ_{max} = 576 nm) can be seen in figure 4.4a. Once again, as found in Chapter 2, comparison of $\mathbf{MC_{BSP\text{-}1}}$ λ_{max} to ET(30) values for the ionic liquids failed to produce a linear relationship (correlation coefficient, R^2 =0.4827) which is commonly found in molecular solvents (Figure 4.2).

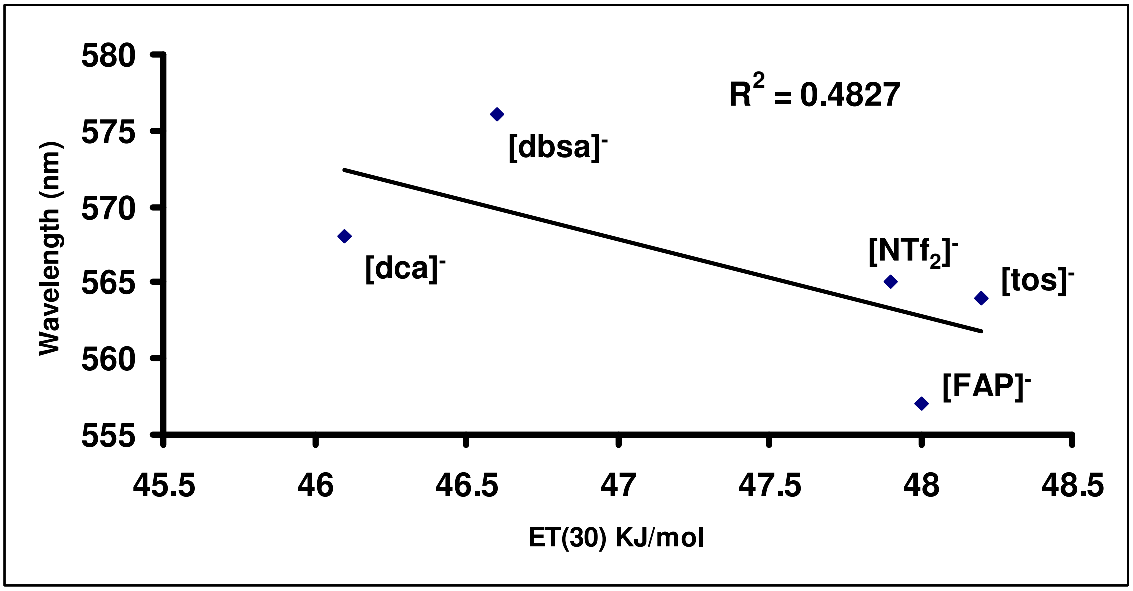

Figure 4.2 Correlation between **MC**(λ_{max}) and $E_T(30)$ values for ionic liquids

First-order rate constants and thermodynamic parameters for the thermal relaxation of $\mathbf{MC_{BSP\text{-}1}}$ were illustrated in figure 4.4b. Surprisingly, the longest $\mathbf{MC_{BSP\text{-}1}}$ time constant is found to be in [$P_{6,6,6,14}$][FAP] (over 3300s) which is unexpected as according to the $E_T(30)$ scale, it should be the least polar of the ionic liquids studied. This result further indicates that the $E_T(30)$ scale cannot be used with confidence to characterise polarity in ionic liquids. Furthermore, it would appear that the $\mathbf{MC_{BSP\text{-}1}}$ isomer in general has shorter lifetimes in comparison to the $\mathbf{MC_{BSP}}$ (where R = CH_3) isomer studied previously with $\mathbf{MC_{BSP\text{-}1}}$ isomer lifetime of in [$P_{1,4,4,4}$][tos] is reduced by over 60%.[12] This result is also not expected as longer lifetimes should occur due to the more polar hydroxyl group preferentially interacting with polar regions. A linear correlation between $\mathbf{MC_{BSP\text{-}1}}$ λ_{max} and its thermal relaxation rate constant (k) was found for in the ionic liquids (Figure 4.3) and suggests that the **BSP-1** molecule observes different solvation environments compared to the reported behaviour of **BSP** in phosphonium ionic liquids.[12]

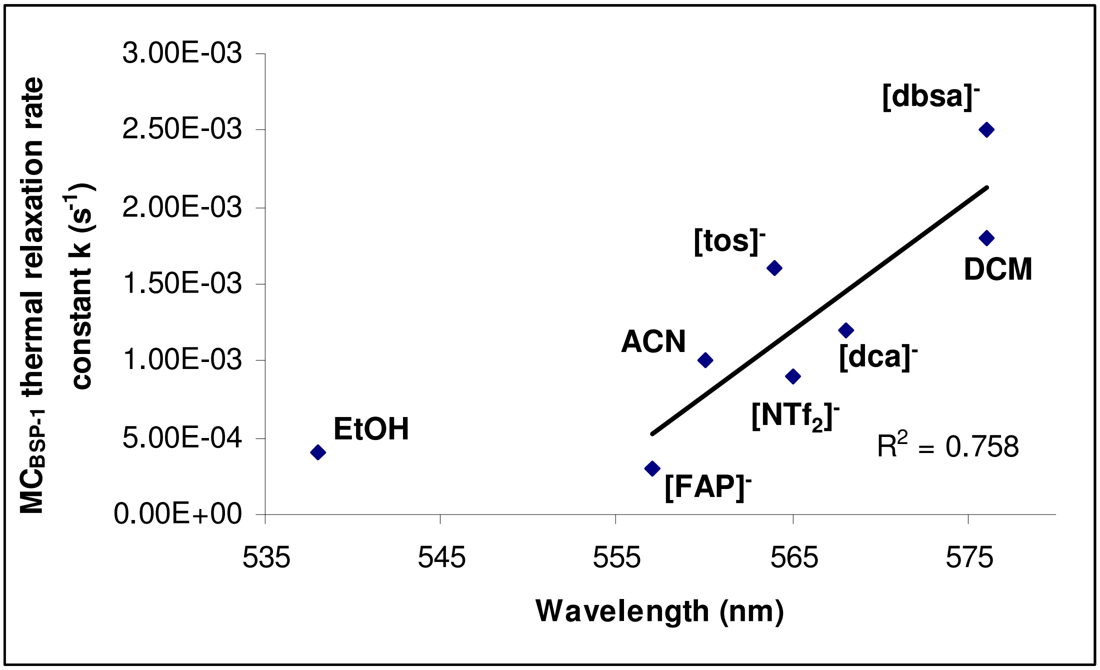

Figure 4.3 Correlation between MC (λ_{max}) and its thermal relaxation rate constant (k) for **BSP-1.**

Table 4.1 Photo-physical constants of BSP-1 and E_T(30) values of various phosphonium based ionic liquids and organic solvents. (BSP and Reichardt's dye 30 concentration 10^{-4} M). All measurements carried out at 293 K.

					Arrhenius		Eyring			
Solvent	E_T30(kcal.mol^{-1})[a]	λ_{max} MC (nm)[b]	k(s^{-1})[c]	1/k (s)	E_a (kj.mol^{-1})	A (s^{-1})	$\Delta H^{\ddagger}$ kj.mol^{-1}	$\Delta S^{\ddagger}$ J.K^{-1}.mol^{-1}	$\Delta G^{\ddagger}$ kj.mol^{-1}	$\Delta K^{\ddagger}$
[P_{1444}][tos]	48.2	564	1.60E-03	625	62.71	2.37E+08	60.11	-93.31	87.45	2.3E-16
[P_{66614}][dbsa]	46.6	576	2.50E-03	400	72.15	1.83E+10	69.64	-56.90	86.31	4.1E-16
[P_{66614}][NTf_2]	47.9	565	9.00E-04	1111	92.02	1.30E+13	89.42	-2.54	90.17	3.3E-17
[P_{66614}][dca]	46.1	568	1.20E-03	833	75.59	3.79E+10	73.00	-51.09	87.97	1.6E-16
[P_{66614}][FAP]	48	557	3.00E-04	3333	92.43	9.82E+12	89.84	-4.90	91.27	4.9E-17
Ethanol	51.8	538	4.00E-04	2500	65.27	2.04E+09	62.84	-92.55	89.96	6.6E-17
Acetonitrile	45.5	560	1.00E-03	1000	94.23	6.74E+13	91.80	11.66	88.38	1.6E-16
Dichloromethane	40.6	576	1.80E-03	556	97.28	4.44E+14	94.84	28.00	86.64	2.9E-16

[a] ET(30) values are from the literature.
[b] Merocyanine λ_{max} measured after 1 min UV light.
[c] Thermal relaxation rate constant calculated from plotting ln(At/A0) vs. time where k = slope.

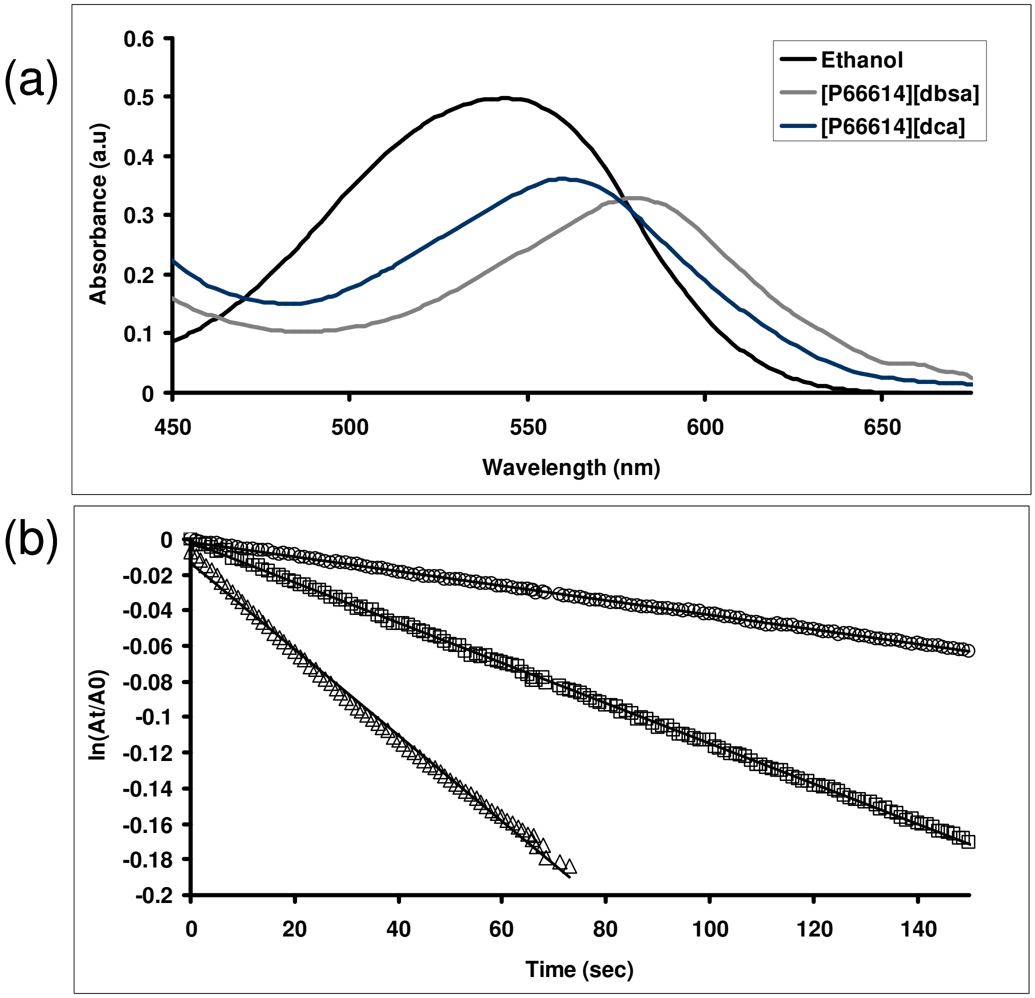

Figure 4.4 **(a)** Absorption spectra of 10^{-4}M solutions of **BSP-1** in ethanol (λ_{max}= 538 nm), $[P_{6,6,6,14}]$[dbsa] (λ_{max}= 576 nm), and $[P_{6,6,6,14}]$[dca] (λ_{max}= 568 nm) when irradiated with UV light (365 nm) for 60 seconds. **(b)** Thermal relaxation of MC isomer in ethanol (○, $k^{-1} = 4 \times 10^{-4}$), $[P_{6,6,6,14}]$[dca] (□, $k^{-1} = 1.2 \times 10^{-3}$) and $[P_{6,6,6,14}]$[dbsa] (Δ, $k^{-1} = 2.5 \times 10^{-3}$). All measurements at 293 K.

From the linear Arrhenius dependences in all cases, the values of activation energy (E_a) and the pre-exponential factor are derived (figure 4.4b). It has been noted from the literature for molecular solvents that **MC** thermal relaxation E_a values range from 75 to

105 kJ mol^{-1} with a tendency to be higher in polar solvents,[19,20] From the results above (table 4.1) it can be clearly seen that for **BSP-1,** the activation energy for ethanol is very low at 65.27 kJ mol^{-1}. This could be due to the hydroxyl group preferentially interacting with the intermolecular hydrogen bonding/charged sites of the solvent system and so resulting in less solvent-solute interactions with the **MC$_{\mathbf{BSP-1}}$** charge sites, particularly the phenolate oxygen. Activation energies for acetonitrile and dichloromethane produced values of 94.23 and 97.28 kJ mol^{-1} respectively which were within the expected range. For interactions within ionic liquids, [P$_{1,4,4,4}$][tos] is found to have the lowest activation energy at 62.71 kJ mol^{-1} with [P$_{6,6,6,14}$][NTf$_2$] and [P$_{6,6,6,14}$][FAP] having similar E$_a$ values of 92.02 and 92.43 kJ mol^{-1}, respectively. This would indicate that the **MC$_{\mathbf{BSP-1}}$** thermal relaxation process as in [P$_{6,6,6,14}$][NTf$_2$] and [P$_{6,6,6,14}$][FAP] are strongly dependent on temperature.

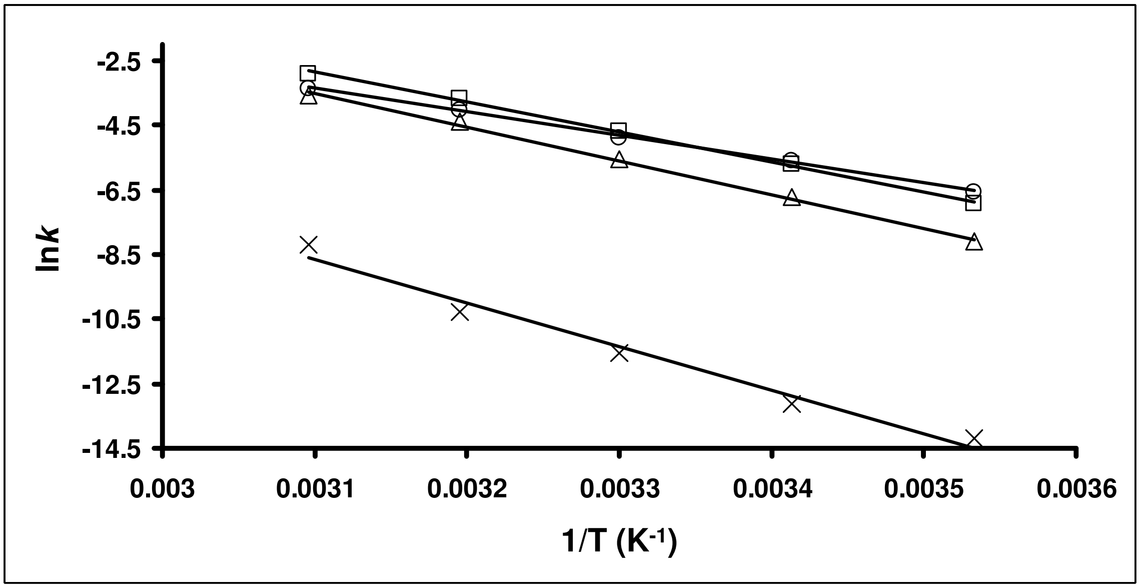

Figure 4.5 Arrhenius plot for the thermal relaxation of MC (BSP-1) in [P$_{6,6,6,14}$][NTf2] (X), [P$_{6,6,6,14}$][dca] (□), [P$_{6,6,6,14}$][FAP] (Δ) and [P$_{1,4,4,4}$][tos] (□) after 60 seconds UV irradiation. BSP concentration 1 x 10^{-4}M (correlation coefficients >0.98).

Thermodynamic parameters of **MC$_{\mathbf{BSP-1}}$**, were derived and are presented in table 4.1. Plots of ln k vs. 1/T are shown in figure 4.5 for thermal relaxation of **MC$_{\mathbf{BSP-1}}$** in [P$_{6,6,6,14}$][NTf2], [P$_{6,6,6,14}$][dca], [P$_{6,6,6,14}$][FAP] and [P$_{1,4,4,4}$][tos]. As expected, the experimental activation entropies ($\Delta S^{\ddagger}$) found for **MC$_{\mathbf{BSP-1}}$** in the ionic liquids studied are significantly negative (e.g. [P$_{1,4,4,4}$][tos] $\Delta S^{\ddagger}$ = -93.31 JK^{-1}mol^{-1} and [P$_{6,6,6,14}$][dca] $\Delta S^{\ddagger}$ = -51.09 JK^{-1}mol^{-1}), indicating that the transition state is more ordered than that of the completely open **MC$_{\mathbf{BSP-1}}$** form. It is observed that [P$_{1,4,4,4}$][tos] had the smallest activation energy and enthalpy of activation values of 62 kJ mol^{-1} and 66 kJ mol^{-1}, respectively, and similar results are also found for **MC$_{\mathbf{BSP-1}}$** in [P$_{1,4,4,4}$][tos].[12] Small pre-exponential factors (10^{8}–10^{10} s^{-1}) are commonly associated with negative activation energies with respect to photochromic dyes.[21] In [P$_{6,6,6,14}$][NTf2] and [P$_{6,6,6,14}$][FAP], it would appear that relatively longer **MC$_{\mathbf{BSP-1}}$** lifetimes at 293 K implies that it is more solvated, but from the thermodynamic data it would seem that the **MC$_{\mathbf{BSP-1}}$** thermal relaxation process is strongly dependent on temperature. This indicates that the energetic (enthalpic) factor dominates over the entropic contribution at lower temperatures, as reflected by the near zero $\Delta S^{\ddagger}$ values found (table 4.1). At the outset, it was anticipated that the more polar **BSP-1** derivative would associate itself with polar domains, resulting in a higher degree of solvation for the photo-induced **MC$_{\mathbf{BSP-1}}$** isomer (figure 4.6). The thermodynamic parameters calculated in [P$_{1,4,4,4}$][tos], [P$_{6,6,6,14}$][dca] and [P$_{6,6,6,14}$][dbsa], show the MC$_{BSP-1}$ isomer is involved in additional molecular interactions compared to the **BSP-1** isomer (negative entropic contribution).

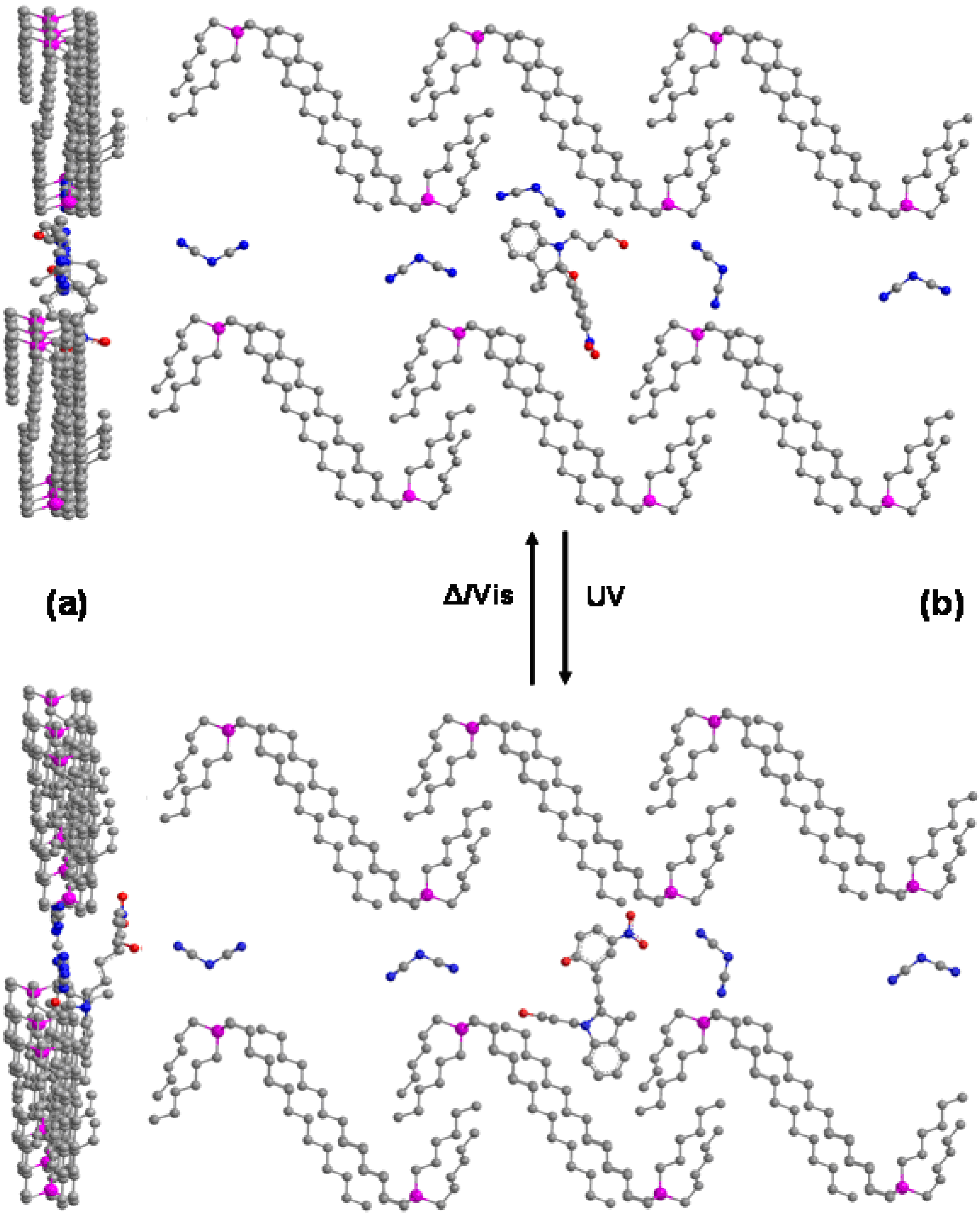

Figure 4.6 Proposed schematic (ChemBioDraw Ultra 11.0) representation of BSP-1 photoinduced isomerisation to MC isomer in $[P_{6,6,6,14}][dca]$. Isomerisation of BSP-1 to MC does not have a significant effect on surrounding polar environment as seen in experimental results. (a) displays cross section of segment of ionic liquid containing BSP-1. (b) top down view of same segment.

4.3.2 BSP-2: Carboxylic acid derivative

The physical, kinetic and thermodynamic properties of the carboxylic acid derivative, **BSP-2**, in phosphonium ionic liquids and molecular solvents were determined and tabulated in table 4.2, below. The covalent attachment of a carboxylic acid group is believed to create a more polar molecular probe, similar to that of **BSP-1**, which is expected to enhance intermolecular interactions such as hydrogen bonding, albeit with slightly differing processes than that of the more simple hydroxyl group. Kinetic and thermodynamic parameters in molecular solvents provided results which agreed with established trends for photochromic spirocyclic compounds whereby enhanced kinetics is expected as solvent polarity decreases.[22] The UV-Vis absorption spectrum of the $\mathbf{MC_{BSP\text{-}2}}$ isomer in ethanol (λ_{max} = 546 nm), $[P_{66614}]$[dbsa] (λ_{max} = 579 nm), and $[P_{66614}]$[dca] (λ_{max} = 569 nm) in figure 44a are found to exhibit positive solvatochromism. Once again it was observed that λ_{max} $\mathbf{MC_{BSP\text{-}2}}$ vs. $E_T(30)$ values did not observe a linear relationship in ionic liquids. For **BSP-2,** it was found that the $\mathbf{MC_{BSP\text{-}2}}$→**BSP-2** thermal relaxation rate constant was highest in dichloromethane (8 x $10^{-4}s^{-1}$). This value was double that of acetonitrile (4 x $10^{-4}s^{-1}$) and four times faster than ethanol (2 x $10^{-4}s^{-1}$). First-order plots for the thermal relaxation of $\mathbf{MC_{BSP\text{-}2}}$ are shown for ethanol, $[P_{6,6,6,14}]$[dca], and $[P_{66614}]$[dbsa] in figure 4.7b.

Table 4.2 Photo-physical constants of BSP-2 and $E_T(30)$ values of various phosphonium based Ionic liquids and organic solvents. (BSP and Reichardt's dye 30 concentration 10^{-4} M). All measurements carried out at 293 K.

					Arrhenius		Eyring			
Solvent	ET$_{30}$(kcal.mol^{-1})	λ_{max} *MC (nm)*	k(s^{-1})	1/k (s)	E$_a$ (kj.mol^{-1})	A (s^{-1})	ΔH‡ kj.mol^{-1}	ΔS‡ J.K^{-1}.mol^{-1}	ΔG‡ kj.mol^{-1}	ΔK‡
[P$_{1444}$][tos]	48.2	565	1.20E-03	833	98.58	4.57E+14	95.98	27.03	88.06	1.63E-16
[P$_{66614}$][dbsa]	46.6	579	3.00E-04	3333	84.28	1.36E+10	73.91	-59.50	91.34	4.91E-17
[P$_{66614}$][NTf$_2$]	47.9	560	2.30E-03	435	94.32	1.77E+14	88.25	9.24	85.54	3.76E-16
[P$_{66614}$][dca]	46.1	569	6.00E-04	1667	80.28	5.65E+10	84.28	-26.79	92.13	8.18E-17
[P$_{66614}$][FAP]	48	555	1.00E-04	10000	79.33	1.49E+10	76.73	-59.24	94.09	1.63E-17
Ethanol	51.8	546	2.00E-04	5000	105.35	1.33E+15	102.92	36.42	92.24	3.28E-17
Acetonitrile	45.5	548	4.00E-04	2500	112.27	1.17E+17	109.83	73.73	88.23	1.66E-17
Dichloromethane	40.6	552	8.00E-04	1250	105.50	5.50E+15	103.06	48.24	88.93	1.310E-16

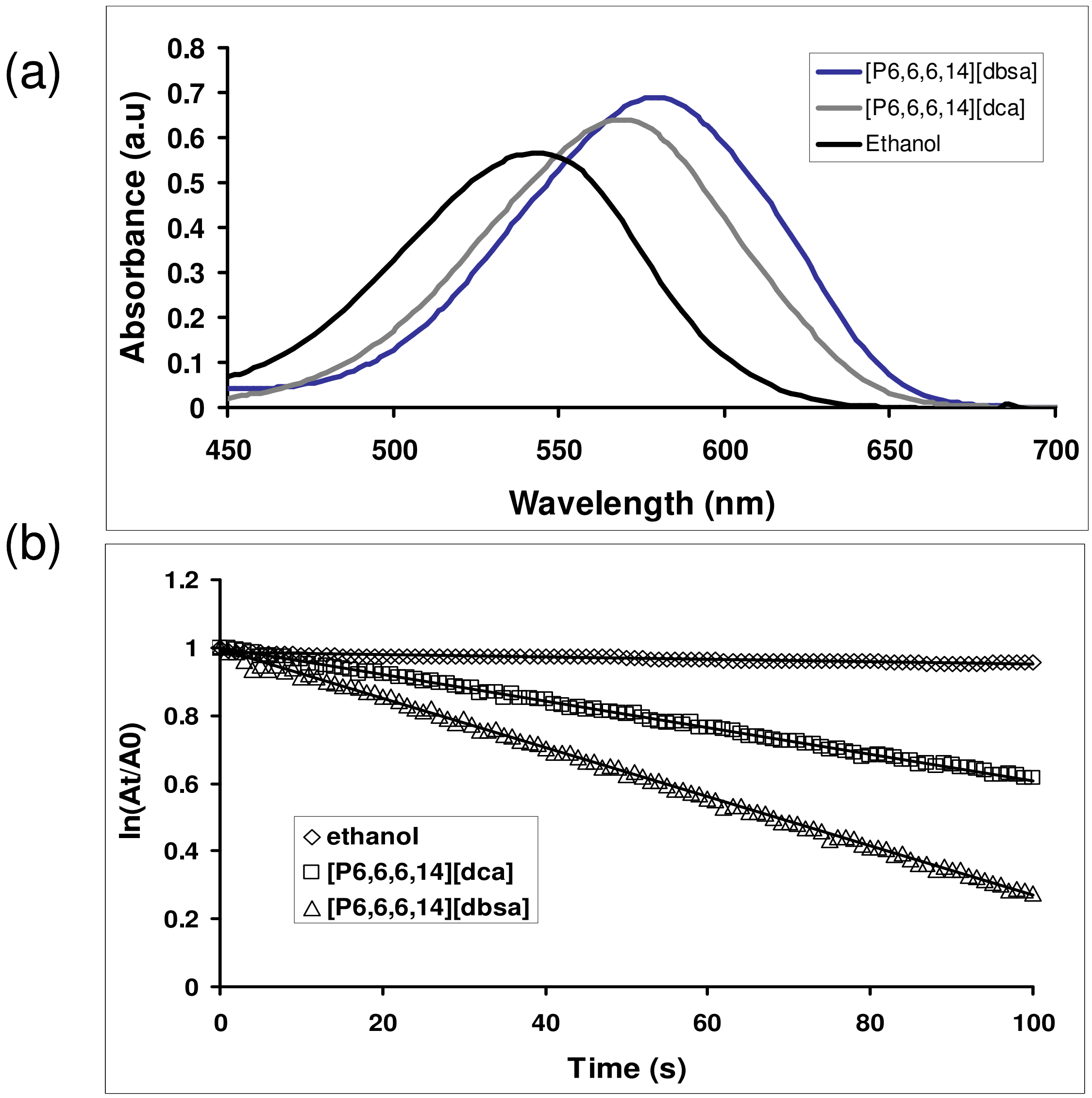

Figure 4.7 (a) Absorption spectra of 10^{-4}M solutions of BSP-2 in ethanol (λ_{max} = 546 nm), [P_{66614}][dbsa] (λ_{max} = 579 nm), and [P_{66614}][dca] (λ_{max} = 569 nm) when irradiated with UV light (365 nm) for 60 seconds. (b) Thermal relaxation of MC isomer in ethanol (◊, k^{-1} = 2 x 10^{-4}), [P_{66614}][dca] (□, k^{-1} = 6 x 10^{-4}) and [P_{66614}][dbsa] (Δ, k^{-1} = 3 x 10^{-4}). All measurements at 293 K.

The linear temperature dependence of the rate of thermal relaxation of **MC_{BSP-2}** in the ionic liquids studied were plotted in figure 4.8 which allowed Arrhenius dependences to determine the activation energies (E_a) and the pre-exponential factors (table 4.2). Molecular solvents exhibit **MC_{BSP-2}→BSP-2** thermal relaxation E_a values in the range 105-112 kJ mol^{-1}. Which is good agreement with literature values.[19, 20] In ionic liquids, **BSP-2** was found to have the highest activation energy of 98.58 kJ mol^{-1} in $[P_{1,4,4,4}]$[tos]. This is in contrast to **BSP-1** which has its lowest E_a 62.71 kJ mol^{-1} in this ionic liquid. In this case, $[P_{6,6,6,14}]$[dca] was found to be similar to $[P_{6,6,6,14}]$[FAP] with E_a values of 80.28 and 79.33 kJ mol^{-1}, respectively. This differs from **BSP-1** where $[P_{6,6,6,14}][NTf_2]$ was found to be similar to $[P_{6,6,6,14}]$[FAP] and $[P_{6,6,6,14}]$[FAP] having activation energy around 23 kJ.mol^{-1} lower in **BSP-2**.

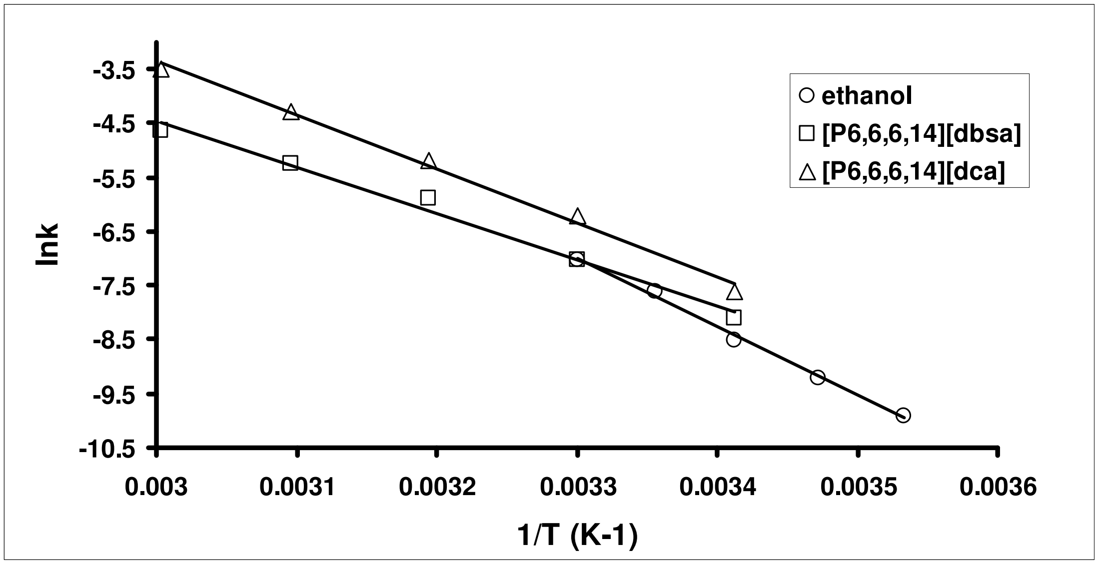

Figure 4.8 Arrhenius plot for the thermal relaxation of MC (BSP-2) in ethanol (○), [P6,6,6,14][dbsa] (□), and [P6,6,6,14][dca] (Δ) after 60 seconds UV irradiation. BSP concentration 1 x 10^{-4}M (correlation coefficients >0.98).

Interestingly, $[P_{6,6,6,14}]$[dbsa], which is generally assumed to be a non-polar liquid due to the prevalence of multiple long alkyl chains, was found to exhibit rates of $\mathbf{MC_{BSP\text{-}2}}$**→BSP-2** thermal relaxation between those of acetonitrile and ethanol (k = 3 x $10^{-4}s^{-1}$). This rate would imply that the solvent system is somewhat polar, and this impression is reinforced by the significantly negative value of $\Delta S^{\ddagger}$ (-59.50 $JK^{-1}mol^{-1}$) as seen for **BSP-1**, which suggests the transition state $\mathbf{MC^{\ddagger}_{BSP\text{-}2}}$ is in a relatively polar environment whereby probe reorganisation and thermal relaxation is restricted due to solvent stabilisation. This negative value implies that the solvent-solute system is ordered and as such a more structured system.

Similar effects were observed for $[P_{6,6,6,14}]$[dca] with an increase in the $\Delta S^{\ddagger}$ values being the only feature of significance. $[P_{6,6,6,14}]$[dca] was found to be -26.79 $JK^{-1}mol^{-1}$ which is less negative than that of $[P_{6,6,6,14}]$[dbsa] at -59.50 $JK^{-1}mol^{-1}$ which implies increased torsional C=C rotation. In this case, rates of thermal relaxation were more in line with values found with non-polar solvents. This may be due to the fact that the $[dca]^-$ anion is smaller than $[dbsa]^-$, which has a long alkyl chain attached. If the $[dbsa]^-$ alkyl chains enhance particular domain structure/size, then the reduced anion size should allow for less steric hindrance arising from anion interaction, resulting in faster thermal relaxation rate constants. Examination of **BSP-2** in $[P_{1,4,4,4}]$[tos] may confirm the above hypothesis of structuring, as the cation contains isobutyl side chains, in contrast to from the other phosphonium cations which contained long alkyl chains, and this should reduce Van der Waals interaction effects. The $[tos]^-$ anion also has a shorter methyl group attached to the phenyl ring than that of the related $[dbsa]^-$ anion. The reduced size of the anions and lack of intermolecular interactions could result in a more homogeneous liquid system similar to that of molecular solvents. This interpretation appears to be supported by the $\Delta S^{\ddagger}$ value which is found to be positive at 27.03 $JK^{-1}mol^{-1}$ (such as values observed in molecular solvents) and close to that of ethanol (36.42 $JK^{-1}mol^{-1}$). Furthermore, rates of **MC_{BSP-2}→BSP-2** thermal relaxation are found to be far larger than any other ionic liquid. This may be due to the fact that the ions are still generally non-polar in nature but the removal of steric hindrance effect allows the MC to revert to the BSP isomer in a less restricted manner.

4.3.3 BSP-3: Tetradecane derivative

A non-polar tetradecane **BSP** derivative (**BSP-3**) was added to the ionic liquids to examine whether interactions with the non-polar domains within the ionic liquid would be enhanced. Following the contention that the non-polar side chain would interact with the alkyl chains of the phosphonium cations through Van der Waals forces it is anticipated that this would result in preferential migration of the **BSP-3** molecule into alkyl-chain rich regions of the ionic liquid. However, it is also documented that **BSP** derivatives with long aliphatic chains are known to form *J*- and *H*- aggregates when irradiated with UV light due to strong intermolecular forces,[17,22] with nitro containing **BSP** derivatives preferentially forming *J*-aggregates.[23,24] It is therefore required to investigate whether **BSP-3** spontaneously forms aggregates when irradiated with UV light, as this would have an important consequence on the interpretation of thermodynamic and kinetic parameters. It is known that **MC** λ_{max} gives an indication of the presence of *H*- (shorter wavelength shifts) and *J*- (longer wavelength shifts) aggregates. Therefore we initially investigated the photochromic behaviour of (1 x 10^{-4}M) **BSP-3** in ethanol, diethyl ether and hexane, figures 4.9 and 4.10a. It can be clearly seen that **BSP-3** forms the non-aggregated **MC$_{\mathbf{BSP-3}}$** isomer in ethanol, but the presence of *J*-aggregates are quite clearly observed in diethyl ether and hexane. We have also investigated the effect of increasing concentration of **BSP-3** on aggregation in molecular solvents while no *J*-aggregation behaviour was observed for **BSP-3** in polar solvents at concentration levels up to 1 x 10^{-3}M (figure 4.9)

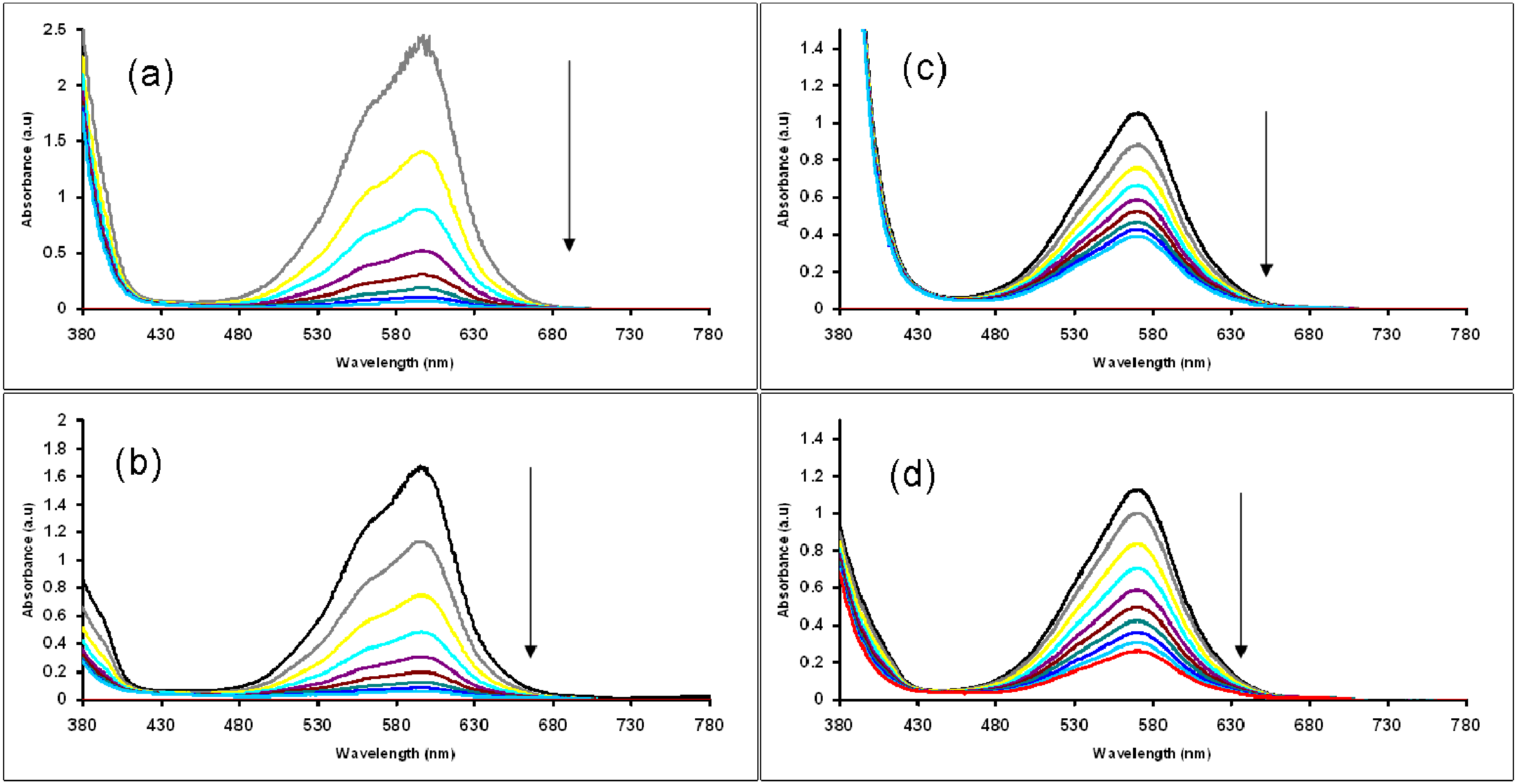

Figure 4.9 Continuous UV-vis spectra of (a) BSP-3 (1 x 10-3M) in diethyl ether,(b) BSP-3 (1 x 10-4M) in diethyl ether, (c) BSP-3 (1 x 10-3M) in acetone, and (d) BSP-3 (1 x 10-4M) in acetone, after 60 seconds of UV light 365 nm

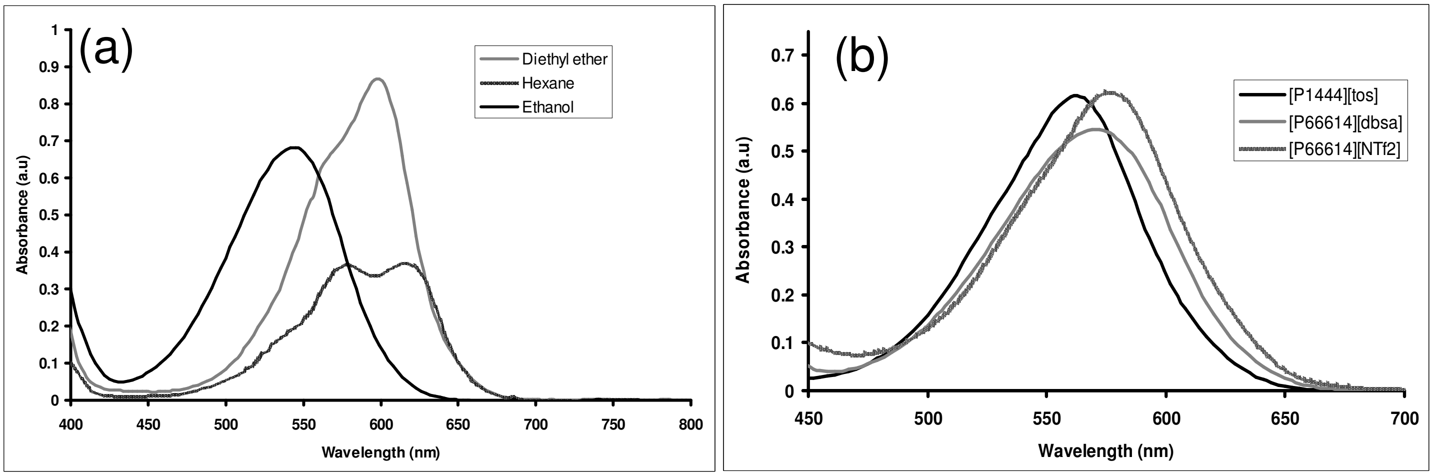

Figure 4.10 UV-vis spectra of BSP-3 (1 x 10^{-4}M) after 60 seconds of UV (365 nm) light in molecular solvents (a) and phosphonium based ionic liquids (b).

The physical, kinetic and thermodynamic properties of the **BSP-3** are tabulated in table 4.3 and UV-Vis absorption spectra of **BSP-3** in $[P_{1,4,4,4}]$[tos] (λ_{max} = 565 nm), $[P_{6,6,6,14}]$[dbsa] (λ_{max} = 572 nm) and $[P_{6,6,6,14}][NTf_2]$ (λ_{max} = 575 nm) are shown in figures 4.10b and 4.11. Examination of the solvatochromic shifts suggests that the **MC$_{\mathbf{BSP\text{-}3}}$** isomer in ionic liquids is located in non-polar regions with positive solvatochromic shifts of λ_{max} to values in the region of 570nm. It must also be noted that no evidence of *H*- or *J*-aggregation is observed from the UV-Vis spectrum, which in fact shows a very symmetrical spectrum indicating the presence the non-aggregated **MC$_{\mathbf{BSP\text{-}3}}$** isomer.[21]

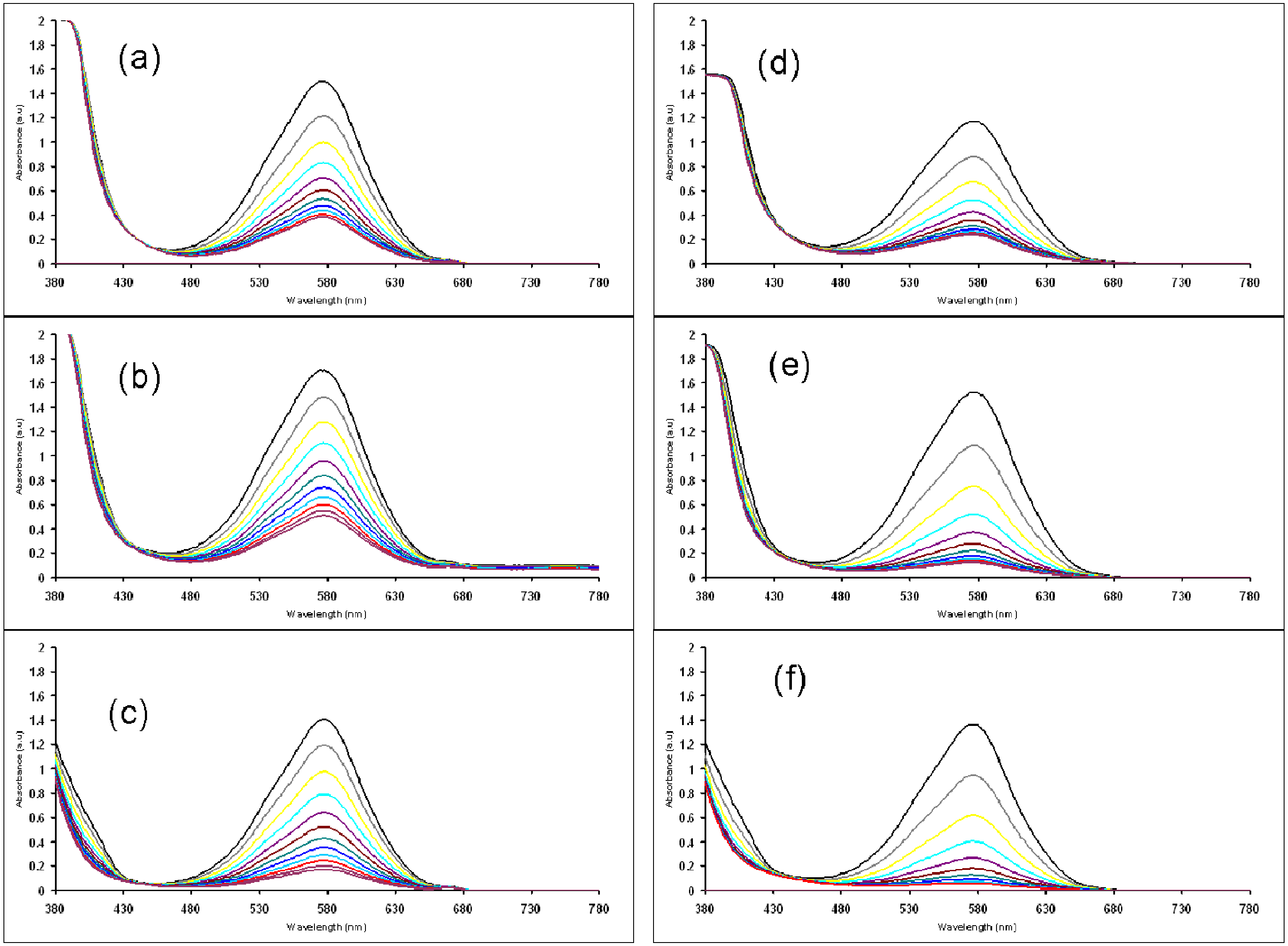

Figure 4.11 Continuous UV-vis spectra of (a) BSP-3 (1 x 10-3M) in [P6,6,6,14][dca],(b) BSP-3 (5 x 10-4M) in [P6,6,6,14][dca], (c) BSP-3 (1 x 10-4M) in [P6,6,6,14][dca], (d)BSP-3 (1 x 10-3M) in [P6,6,6,14][NTf2], (e) BSP-3 (5 x 10-4M) in [P6,6,6,14][NTf2], and (f) BSP-3 (1 x 10-4M) in [P6,6,6,14][NTf2] after 60 seconds of UV light 365 nm.

No evidence of aggregation was found with samples at 1 x 10^{-3}M. The $\mathbf{MC_{BSP\text{-}3}}$ λ_{max} values were similar to that of dichloromethane which is non-polar in nature. Again, there appeared to be no consistent relationship between the $\mathbf{MC_{BSP\text{-}3}}$ λ_{max} and $E_T(30)$ values for **BSP-3** in the selected ionic liquids indicating that the structural complexity extends to every region (polar *and* non-polar) of liquid.

Examination of the rate constants appeared to conflict with the initial assumptions that the ionic liquid domains probed were primarily non-polar in nature due to positive solvatochromism. In fact, rates of thermal relaxation were found to be slower in ionic liquids than that in molecular solvents. For example $[P_{6,6,6,14}]$[dbsa] had a rate of 5 x 10^{-4} s^{-1} compared to that of acetonitrile at 1.3 x 10^{-3} s^{-1}. Such inconsistencies may be due to steric effects arising from intermolecular structuring, such as alkyl chain interactions, between the ionic liquid cations. As the **BSP-3** molecule contains the tetradecane carbon chain, it would be expected to associate itself with the alkyl chains of the phosphonium cation, and such associations would locate the spiropyran fragment into particular non-polar nano-domains created by the aliphatic carbon chains. With the spiropyran moiety surrounded by non-polar alkyl chains, the solvate-sensitive nitro group would 'sense' a non-polar domain, which in turn generates the positive shifts observed in the $\mathbf{MC_{BSP\text{-}3}}$ isomer UV-vis λ_{max}. The physical size of the $\mathbf{MC_{BSP\text{-}3}}$ and its constriction within this nano-domain would however result in reduced mobility of the spirocyclic compounds and in turn decrease relaxation kinetics (Figure 4.12).

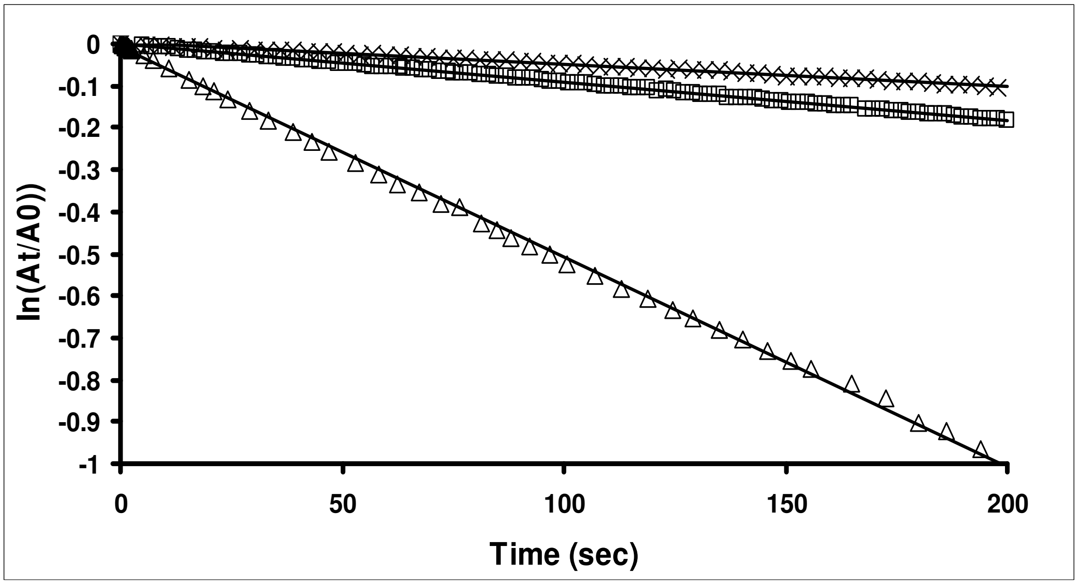

Figure 4.12 Thermal relaxation of **MC** isomer in [P_{66614}][dbsa] (X, $k^{-1} = 5 \times 10^{-4}$), [$P_{66614}$][dca] (□, $k^{-1} = 9 \times 10^{-4}$) and dichloromethane (Δ, $k^{-1} = 4.7 \times 10^{-3}$). All measurements at 293 K.

If this hypothesis is correct, very different thermodynamic contributions towards the thermal relaxation process should be observed compared to the more polar derivatives **BSP-1** and **BSP-2**. Thermodynamic parameters appear to compliment this hypothesis with positive entropies of activation $\Delta S^{\ddagger}$ between 30 $JK^{-1}.mol^{-1}$ and 66 $JK^{-1}.mol^{-1}$ found in all ionic liquids. Comparison of **BSP-3** to **BSP-1** and **BSP-2** thermodynamic parameters also showeda general increase in $\Delta H^{\ddagger}$ values which may indicate that as the **MC**$_{\textbf{BSP-3}}$ isomer relaxes back to its **BSP-3** isomer, the polar cavity into which the spirocyclic moiety has been orientated by tetradecane van der Waals interaction with the cation alkyl chains, induces disorder around the re-orientating isomer and increasing the entropy of the system. Similarly, orientation of the spirocyclic moiety of **MC**$_{\textbf{BSP-3}}$ into the polar cavity will provide an environment more suited to interact with the polar

MC$_{\mathbf{BSP\text{-}3}}$ form and is reflected in higher enthalpies of activation, relate to the increased stabilization effects. See figure 4.13 for a schematic illustration of this hypothesis. Activation energies were also found to be high exhibiting values close to 100 kJ.mol^{-1} suggesting a reduced degree of torsional rotation. If this is so, it would create a greater energy barrier for relaxation of the **MC$_{\mathbf{BSP\text{-}3}}$** isomer to its closed form (**BSP-3**) and inhibit the process.

Table 4.3 Photo-physical constants of **BSP-3** and $E_T(30)$ values of various phosphonium based Ionic liquids and organic solvents. (**BSP-3** and Reichardt's dye 30 concentration 10^{-4} M). All measurements caried out at 293 K.

					Arrhenius		Eyring			
Solvent	ET_{30}(kcal.mol^{-1})	λ_{max} *MC (nm)*	k(s^{-1})	1/k (s)	E_a (kj.mol^{-1})	A (s^{-1})	$\Delta H^{\ddagger}$ kj.mol^{-1}	$\Delta S^{\ddagger}$ J.K^{-1}.mol^{-1}	$\Delta G^{\ddagger}$ kj.mol^{-1}	$\Delta K^{\ddagger}$
$[P_{1444}]$[tos]	48.2	565	6.00E-04	1667	101.40	7.34E+14	98.39	30.98	89.31	1.64E-16
$[P_{66614}]$[dbsa]	46.6	572	5.00E-04	2000	111.91	5.38E+16	109.32	66.67	89.78	8.19E-17
$[P_{66614}][NTf_2]$	47.9	575	8.00E-04	1250	96.69	1.37E+14	94.10	17.03	89.11	1.31E-16
$[P_{66614}]$[dca]	46.1	573	9.00E-04	1111	97.52	2.21E+14	94.93	20.98	88.78	1.47E-16
$[P_{66614}]$[FAP]	48	572	7.00E-04	1429	94.79	6.56E+13	92.20	10.89	89.01	1.15E-16
Ethanol	51.8	542	2.00E-04	5000	105.74	2.18E+15	103.30	41.03	91.28	6.55E-17
Acetonitrile	45.5	561	1.30E-03	769	87.38	1.52E+13	87.38	-1.10	87.70	2.13E-16
Dichloromethane	40.6	579	4.70E-03	213	88.50	3.13E+13	86.06	5.27	84.52	7.7E-16

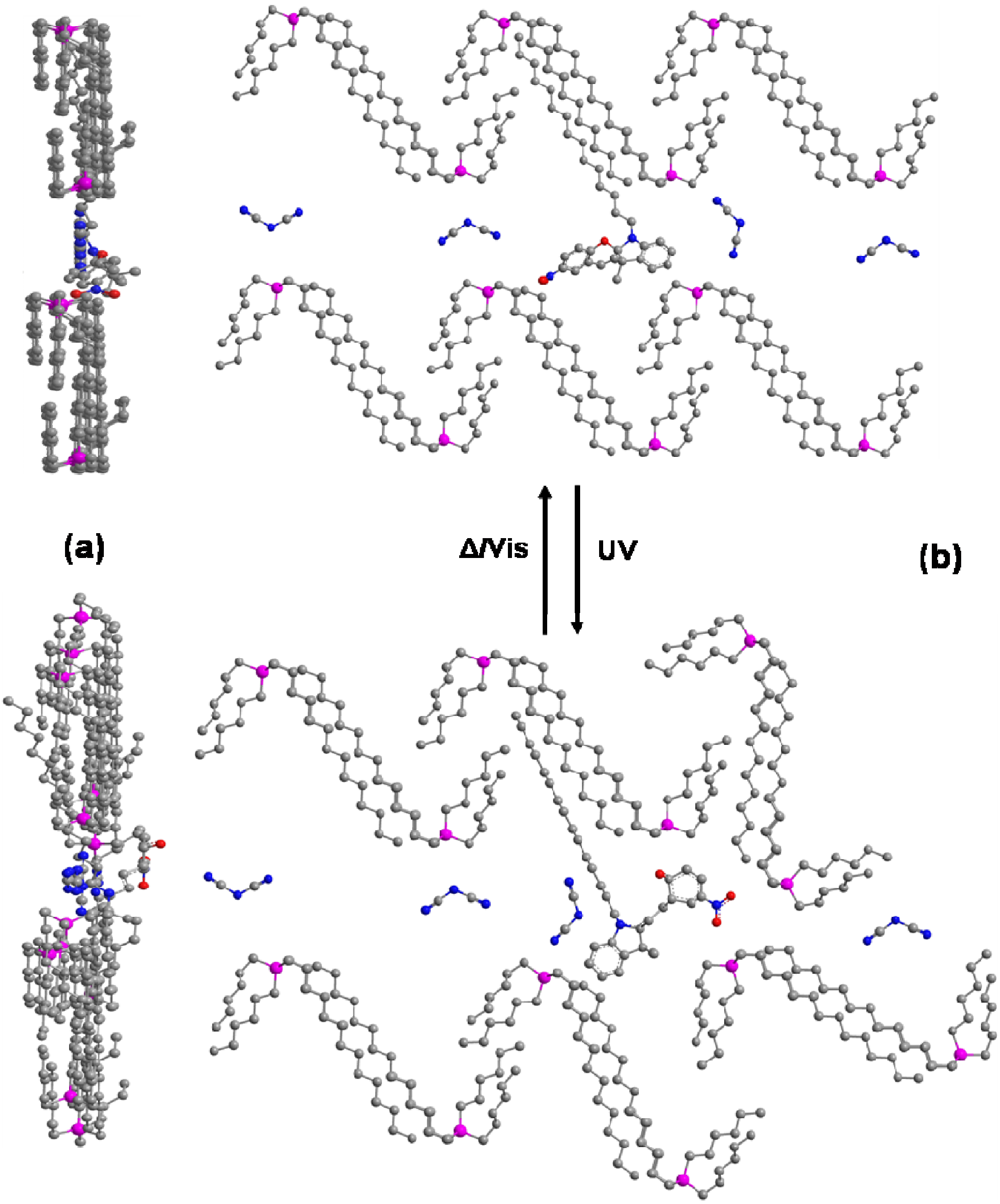

Figure 4.13 Proposed schematic (ChemBioDraw Ultra 11.0) of BSP-3 photoinduced isomerisation to MC isomer in $[P_{6,6,6,14}][dca]$. Photo-isomerisation of BSP-3 to MC appears to have significant effect on surrounding environment, increasing the entropic contribution to the thermal relaxation process, as seen in experimental results. (a) displays cross section of segment of ionic liquid containing BSP-3. (b) top down view of same segment.

4.4 Conclusions

BSP-1 and **BSP-2** exhibit generally negative entropies of activation ranging from -50JK^{-1}mol^{-1} to -90JK^{-1}mol^{-1} implying relatively low solvent-solute interactions and possible anion interactions with ionic liquid polar functional groups. Higher than expected activation energies of 60kJ.mol^{-1} to 100kJ.mol^{-1} obtained for polar probes maybe be due to ionic liquid functional groups competing with the charged sites of the merocyanine (**MC**) isomer thus reducing **MC** stabilisation effects. Differences in thermal relaxation rate constants (2.5x10^{-3}s^{-1} in BSP-1 and 3x10^{-4}s^{-1} in **BSP-2** in [$P_{6,6,6,14}$][dbsa]) imply that while the polar probe systems are primarily located in polar/charged regions, each probe experiences slightly differing polar domains. **BSP-3** entropies of activation are positive and between 30 JK^{-1}mol^{-1} to 66 JK^{-1}mol^{-1}. The association of the non-polar functional group is believed to locate the spiropyran moiety in the interfacial polar and non-polar regions. The thermal relaxation of the **MC** form causes solvent reorientation to accommodate the molecule as it reverts to its closed form. Slow thermal relaxation rate constants were observed in contrast to high activation energies (5 x 10^{-4}s^{-1} and 111.91 kJ.mol^{-1} respectively, for **BSP-3** in [$P_{6,6,6,14}$][dbsa]) may have been due to steric effects due to proposed nano-cavity formation by the alkyl chains in phosphonium based IL structuring.

The application of photochromic compounds as tailored molecular probes proves effective for the investigation of the proposed domains/regions within ionic liquids and the subtle differences between polar, non-polar and the interface. The integration of functional groups with predetermined polar/non-polar properties allows for the probes to be selectively located in a particular region within the ionic liquids based on a mutual attraction of the attached functional group. Once pre-located in the desired location within the liquid, the application of ultraviolet light and subsequent formation of the **MC** form of the photoactive compounds results in analysis of the region based upon the probes thermodynamic and kinetic parameters, related to the extent of interaction with the solvent molecules in the particular domain. Polar functionalised derivatives **BSP-1** and **BSP-2** were believed to interact with the polar domains and possibly the anions also believed to be located within the cavities formed by the phosphonium cations. The extent of the functional group interaction was also observed through the entropies of activation which were found to be generally negative for the polar derivatives. This was due to the fact that the functional groups already associated with polar regions within the ionic liquids and thus the effect of the ring opening/closing of the compound and introduction of a zwitterion had minimal disruption. The opposite was observed for non-polar derivative **BSP-3** which had positive entropies of activation. The tetradecane chain is believed to locate the compound in such a way that its ring opening/closing is the primary source of charge-charge interactions and therefore produces system reorganisation upon **MC** formation and subsequent relaxation. The ability to predetermine the location of a probe molecule within an ionic liquid now opens up the ability to further study the physico-chemical interactions of certain domains with user specific characteristics but also lead to the development of more advanced materials.

4.5 References

1. T. Pott and P. Meleard, *Physical Chemistry Chemical Physics*, 2009, **11**, 5469-5475.
2. K. A. Fletcher, I. A. Storey, A. E. Hendricks, S. Pandey and S. Pandey, *Green Chemistry*, 2001, **3**, 210-215.
3. S. N. Baker, G. A. Baker, C. A. Munson, F. Chen, E. J. Bukowski, A. N. Cartwright and F. V. Bright, *Industrial & Engineering Chemistry Research*, 2003, **42**, 6457-6463.
4. P. K. Mandal, A. Paul and A. Samanta, *Journal of Photochemistry and Photobiology, A: Chemistry*, 2006, **182**, 113-120.
5. R. Karmakar and A. Samanta, *Chemical Physics Letters*, 2003, **376**, 638-645.
6. R. Karmakar and A. Samanta, *The Journal of Physical Chemistry A*, 2002, **106**, 6670-6675.
7. K. Iwata, M. Kakita and H.-O. Hamaguchi, *Journal of Physical Chemistry B*, 2007, **111**, 4914-4919.
8. K. Iwata, H. Okajima, S. Saha and H.-O. Hamaguchi, *Accounts of Chemical Research*, 2007, **40**, 1174-1181.
9. J. N. C. Lopes, M. F. C. Gomes and A. A. H. Padua, *Journal of Physical Chemistry B*, 2006, **110**, 16816-16818.
10. J. N. C. Lopes and A. A. H. Padua, *Journal of Physical Chemistry B*, 2006, **110**, 3330-3335.
11. U. Seiichi, I. Kaoru and A. P. de Silva, *Angewandte Chemie International Edition*, 2008, **47**, 4667-4669.
12. R. Byrne, S. Coleman, K. J. Fraser, A. Raduta, D. R. MacFarlane and D. Diamond, *Phys. Chem. Chem. Phys.*, 2009, **11**, 7286-7291.
13. S. Coleman, R. Byrne, S. Minkovska and D. Diamond, *Physical Chemistry Chemical Physics*, 2009, **11**, 5608-5614.
14. C. J. Wohl and D. Kuciauskas, *Journal of Physical Chemistry B*, 2005, **109**, 21893-21899.
15. L. Pison, J. N. Canongia Lopes, L. P. N. Rebelo, A. A. H. Padua and M. F. Costa Gomes, *The Journal of Physical Chemistry B*, 2008, **112**, 12394-12400.
16. R. Rosario, D. Gust, M. Hayes, F. Jahnke, J. Springer and A. A. Garcia, *Langmuir*, 2002, **18**, 8062-8069.
17. C. P. McCoy, L. Donnelly, D. S. Jones and S. P. Gorman, *Tetrahedron Letters*, 2007, **48**, 657-661.
18. T. Ramnial, S. A. Taylor, M. L. Bender, B. Gorodetsky, P. T. K. Lee, D. A. Dickie, B. M. McCollum, C. C. Pye, C. J. Walsby and J. A. C. Clyburne, *The Journal of Organic Chemistry*, 2008, **73**, 801-812.
19. H. Gorner, *Phys. Chem. Chem. Phys.*, 2001, **3**, 416-423.
20. Y. Sueishi, M. Ohcho and N. Nishimura, *Bulletin of the Chemical Society of Japan*, 1985, **58**, 2608-2613.
21. M. R. di Nunzio, P. L. Gentili, A. Romani and G. Favaro, *ChemPhysChem*, 2008, **9**, 768-775.
22. V. I. Minkin, *Chemical Reviews*, 2004, **104**, 2751-2776.
23. P. Uznanski, *Synthetic Metals*, 2000, **109**, 281-285.

24. P. Uznanski, *Langmuir*, 2003, **19**, 1919-1922.

5

Physicochemical and Theoretical Study of ‘Ionicity’ Based Upon Liquid Ion Pair Formation in Ionic Liquids Using Spiropyran

5.1 Introduction

While previous chapters focused on nano-scale features mediating ionic liquid bulk properties, final investigations of this thesis focused upon the atom level and its influence on the formation these critical nano-scale features. The complementary nature of opposing charges within the liquids intuitively results in ion-ion associations and the formation of Liquid Ion Pairs (LIPs). Ion pairs can be defined as two member aggregates which, if they exist for sufficient time scales, appear as electrically neutral species.[1] The formation of such LIPs is believed to influence the viscosity and transport properties of the materials by the formation of persistent, nano-structured domains, which mediates their unique properties and endows favourable properties upon ionic liquids that make them more suitable than molecular solvents for many applications. Nano-structured domains are dynamic and composed of large numbers of ionic components forming complex structures at macromolecular scales. However, more discrete structuring, at the level of individual of each cation and anion pair, and their level of mutual interaction may be critical to the formation of these larger, property defining structures. These fundamental properties originate from nano-scale structural features mentioned above and studied in Chapters 3 and 4, which are not easily characterised by experiment alone, but provide the basis for the understanding of the unique macroscopic effects, known as the "ionic liquid effect" and "ionicity", that seem to be observed solely in ionic liquids.[2] To determine the extent to which these "ionicity" effects exist within ionic liquids, the physico-chemical properties must be measured, as before, allowing for systematic isolation of the unique and critical properties that govern these effects. Recent studies of ionic liquids have concluded that evaluation under the assumption that they behave similarly to molecular solvents is inaccurate and does not encompass the majority of the liquid properties.[3,4] Ionic liquids are now described as complex media which contain distinct regions which each have specific properties and combine to form the bulk properties of the liquid system. Chapter 2 elaborated upon such findings by examining the property of solvent polarity within ionic liquids. The fact that traditional polarity probes such as Reichardt's dye 30 can provide information about the polarity of organic solvents but fails in ionic liquids illustrates the increased complexities of liquids.

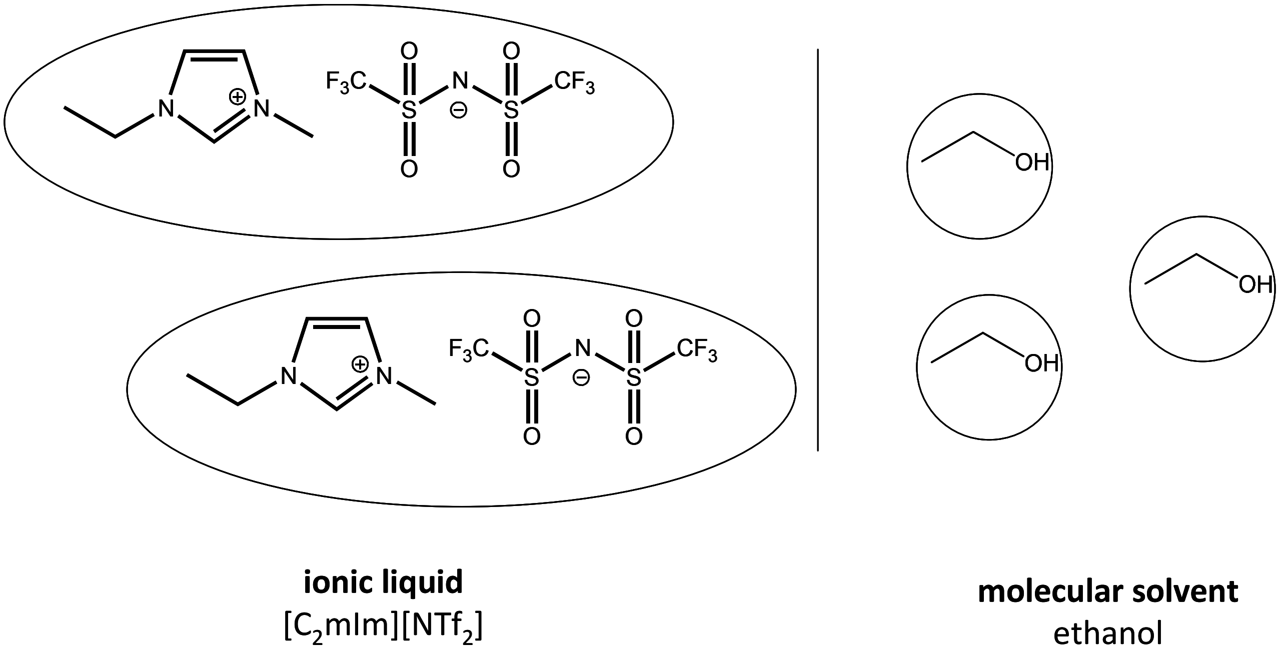

Figure 5.1 Comparison of molecular composition of ionic liquids versus molecular solvents. Spheres represent each solvent component. Ionic liquids are seen to contain two molecules which adds complexity to the system. Molecular solvent components, being single molecules, present a homogeneous system.

Molecular solvents consist of solvent molecules, of a single type, ranging from polar solvents containing molecules with dipoles, to non-polar solvents consisting of essentially neutral molecules. In contrast, in ionic liquids, each solvent component (figure 5.1) consists of two ionic components, each of which has a distinct and opposing charge. The result is that the liquid system is far more complex with a combination of attractive and repulsive forces within the ion pair and between individual ion in the bulk system. Since each molecule is essentially identical within molecular solvents, solvent-solvent interactions are similar throughout and a homogeneous medium results. In contrast, evidence is emerging than in ionic liquids the differing interactions result in ordered regions within the liquid system with nano-scaled dimension. Probe dyes with permanent dipoles will therefore preferentially locate in localised polar or highly charged nano-domains within ionic liquids and thus report similar findings despite the wide variations in the characteristics of the surrounding non-polar domains. More sophisticated spirocyclic solvatochromic probes that can be switched photonically between polar and non-polar states, enabling the probe molecule to migrate spontaneously between polar/non-polar IL nano-structured domains confirming the complexities of the systems.[3,4]

Chapter 2 investigated the photo- and solvatochromic properties of **BSP** in ionic liquids containing the $[NTf_2]^-$ anion and showed that the kinetics and thermodynamics of the **BSP**- **MC$_{BSP}$** equilibrium was sensitive to the nature of the cation[5]. Cation-based interactions inhibit the **MC$_{BSP}$** conversion back to the **BSP** isomer, and may include through-space orbital interactions, that may be specific to the $[C_2mIm]^+$ cation,[16] as well as more general electrostatic interactions. Contemporaneous studies suggest that ionic liquids may form ordered systems resembling pseudo-crystalline systems based on stacking of mutual charges (aggregation) or ordered association of cation species and related cation-anion interactions and vice versa.[6-8] models proposed by Lopes *et al* suggest that this dynamic nano-domained structure arises from a head group wherein the ion charge resides, and a non-polar tail groups where alkyl side-chains extend into space.[9] Chapter 3 examined the effect of non-polar side-chain length and it was found that increasing this chain length appeared to reduce the influence of the polar regions and their stabilisation effects upon $\mathbf{MC_{BSP/SO}}$. A possible explanation for this effect is that the increasing strength of van der Waals interactions causes expansion of polar regions and so reduces their charge density. As such the expansion would be expected to increase the distance between both the cation-cation and cation-anion interactions and dispersion of the charges associated with this. It is now proposed that the strength of these atom-scale interactions may be more central to the physical properties of ionic liquids than previously expected. As a result, the ability to establish trends between the interaction strengths and the effect upon the transport effects (ionicity) of ionic liquids may allow the influence of such interactions to be fully understood. Since spiropyran is a charged species in its $\mathbf{MC_{BSP}}$ form, it is intuitive to assume that solvent-solute interactions will occur during the thermal relaxation process that are related to solvent structure. Although thermal relaxation has provided insight into the proposed nano-structuring of the liquids, minor inconsistencies have been observed which could not be explained by conventional solvent-solute interactions. For example, ion interactions at each charge site in the molecule would be expected to stabilise the zwitterionic $\mathbf{MC_{BSP}}$

form. However, the formation of ion-pairs in the liquid itself may offset probe stabilisation, resulting in a competition, or “tug of war”, between inter (**MC$_{BSP}$** **-**ion) and intra (ion**-**ion) interactions. The ability of the ionic liquids to form tightly-bound liquid ion pairs may therefore reduce the ability of the liquid to interact with solutes and thus mediate the ionicity and overall effects observed. Since **MC$_{BSP}$** is sensitive to such interactions, the thermodynamic and kinetic parameters can identify trends in liquid properties and assist in gaining an understanding of the processes at work. The following chapter exploits this link between the atomic, nano and macro scales for the investigation of ionic liquid transport properties by examining the ability of **MC$_{BSP}$** to disrupt ion-pair formation and compare this to physicochemical properties derived from the rate of thermal relaxation of **BSP.**

To further understand the effects observed between **BSP** and the IL ions, electronic structure calculations were used to quantify the competitive probe-ion and ion-ion interactions. The calculated interaction strengths, ΔE, for each individual ion’s interaction with both **MC$_{BSP}$** and its solvent counterion provide a quantitative indication of the level of interaction occurring in each case. This allows the extent of the competition between probe-ion and ion-ion interactions ΔΔE to be quantified and compared to the observed physicochemical properties. Since theoretical models are comprised of gas phase structures at 0K and the resulting outputs are used as approximations (visual and energetic) of proposed interactions that occur in the liquid phase. Based upon findings of previous studies,[1,10] two phosphonium based ILs were chosen based on their Walden plot values to determine the effects of ion-pair formation upon the properties of the ILs. Trihexyltertadecylphosphonium Chloride; $[P_{6,6,6,14}][Cl]$ and trihexyltertadecylphosphonium bistrifluoro(sulfonyl)imide; $[P_{6,6,6,14}][NTf_2]$ were chosen due to the anticipated large differences in effects due to the more localised charge on $[Cl]^-$, meaning $[P_{6,6,6,14}][NTf_2]$ is expected to be more weakly bound and therefore have more ion mobility. The theoretical models can be used to determine if the formation of the charged $\mathbf{MC_{BSP}}$ form can, through zwitterionic interactions with the cation and anion, compete with the inherent IL ion-pairing and other native ionic liquid interactions. Preservation of the IL nano-structure, with liquid ion pair formation predominating over solute stabilisation, is essential to maintain the transport properties within the liquids and avoid significant local fluctuations; on the other hand, solvent-mediated biasing of photo-switchable equilibria could be a useful sensor design feature and possible application in photochemical control of physical properties such as viscosity.

5.2 Experimental

5.2.1 Electronic structure calculations

All calculations presentend in this thesis were carried out by Dr. Damien Thompson (Tyndall National Institute, Cork). IL and ion-probe electronic structures were obtained for the systems listed in Table 1 using the Gaussian03 program[11] with the B3LYP hybrid HF-DFT functional[12] and 6-311++G** basis sets. Stable geometries were obtained via nuclear relaxation to root mean square (RMS) atomic forces and displacements below 0.0003 and 0.0012 a.u. respectively, followed by electronic structure determination using the gfoldprint and POP=FULL keywords to generate output files formatted for molecular electrostatic potential (MEP) visualisation using MOLEKEL UNIX version 4.3.[13] All atomic charges were computed using a natural population analysis (NPA).[14] The basis set used is larger than in previous studies of IL structures and also uses the complete $[P_{6,6,6,14}]^+$ side-chains which were previously truncated to four carbon length chains to reduce calculation costs.[10] Some calculations were repeated using the MP2 method to include electron correlation effects.[15] The MP2 method is at least one order of magnitude more expensive than B3LYP and so we restricted its use to the two smallest complexes, namely $\mathbf{MC_{BSP}}$:$[Cl]^-$ and $\mathbf{MC_{BSP}}$:$[NTf2]^-$. As shown in Supporting Information, while the more detailed MP2 method provides as expected closer van der Waals's contacts via the more explicit, and possibly overestimated treatment of dispersion forces and so stronger ΔE values, the general features of the probe-ion complex geometries are preserved and the anion-dependent complexation energy difference ΔΔE is similar for both methods.[16]

5.2.2 Physicochemical experiments

Trihexyl,tetradecyl phosphonium chloride (Cytec industries, Niagara, Canada) and trihexyl,tetradecyl phosphonium bistrifluoro(sulfonyl)imide (Sigma Aldrich) were purified using previously reported techniques[17] and were stored under argon to exclude uptake of water. Spectrometric studies were carried out using a Cary 50 UV-Vis spectrometer (JVA Analytical, Dublin, Ireland) with temperature controller and fibre optic reflectance probe accessory. Samples were irradiated with UV light at 375nm using an in-house fabricated array of UV LEDs (Roithner Lasertechnik, Vienna, Austria) (see Appendix **A-2**). Reichardts dye 30 (Sigma-Aldrich chemicals) and 6-nitro-1’,3’,3’-trimethylspiro[2H-1-benzopyran-2,2’-indolin] 1’,3’-dihdro-1’,3’,3’-trimethyl-6-nitrospiro (**BSP**) (Sigma-Aldrich chemicals) were used as purchased with no further purification.

5.3 Results and Discussion

Computed properties for the range of ionic liquid and ion-probe complexes considered in the present study are given in table 5.1 below. Comparison of the inter-ion distances in each ionic liquid pair with the ion-probe distances, together with the computed complexation energies, provides a quantitative analysis of the strength of ion pairing for intra-IL interactions and the competitive arrangement of the ionic liquid ions around the zwitterionic $\mathbf{MC_{BSP}}$ probe molecule.

5.3.1 Ionic liquid ion-ion complexation

Computed structures of the anion:$[P_{6,6,6,14}]^+$ ion pairs indicate that $[Cl]^-$ forms a tighter pair, lying 0.3Å closer to the phosphorus centre than is the case for the nitrogen centre of $[NTf_2]^-$ (Table 5.1). For $[P_{6,6,6,14}][Cl]$ the tetrahedral orientation of the P-C carbons allows for a clean approach of $[Cl]^-$ to the positive phosphorus centre. As $[Cl]^-$ approaches the P^+ centre it interacts also with CH_2 hydrogens, resulting in a cradle-like structure with the chloride sitting in the centre (Figure 5.2). The complex is characterised by moderate hydrogen bond type interactions between $[Cl]^-$ and CH_2 hydrogens and longer-range interactions between $[Cl]^-$ and the P^+ centre.[18] The chloride-phosphorus interaction, while longer range, is not believed to be of lesser importance than the chloride-side-chain interactions. The computed dipole moment of 12 D along the Cl---P axis illustrates how the Cl---P electrostatic interaction drives complexation; the computed separation of 3.8 Å at the upper limit of dipole-dipole interactions.

Replacing $[Cl]^-$ with the alternative $[NTf_2]^-$ anion gives significantly weaker ion pairing, the IL complexation strength decreases from -3.5 to -2.9 eV (Table 1), giving an anion-dependent liquid ion pairing energy difference ΔΔE of approximately -0.6 eV. The negative charge on $[NTf_2]^-$ is more delocalised resulting in an overall reduction in the strength and therefore effectiveness of the charge-charge interaction, compared with the single-atom $[Cl]^-$ anion (Figure 5.2). The significant net negative charge on the oxygens in particular allows $[NTf_2]^-$ to form more, but weaker, intermolecular interactions with the phosphonium, principally via the alkyl side-chains (Figure 5.2).

Table 5.1 Computed IL and ion-probe electronic structures.

Complex	Close contact distances (Å)	ΔE (eV)	Δq (a.u)
$[P_{6,6,6,14}]$ [Cl]	2.4, 2.4, 2.7 ($H_{CH2} : Cl$); 3.8 ($P : Cl$)	-3.54	-0.09
$[P_{6,6,6,14}]$ $[NTf_2]$	2.2 ($H_{CH2} : N$); 2.3, 2.4 ($H_{CH2} : O_{=S}$); 2.6 ($H_{CH2} : F$); 4.1 ($P : N$)	-2.89	-0.04
$[C_2mIm]$ [Cl]	2.6 ($H_{CN2} : Cl$); 2.7 $C_{CN2} : Cl$); 2.9 ($H_{CH3} : Cl$); 2.9 ($H_{CH2} : Cl$)	-3.93	-0.18
$[C_2mIm]$ $[NTf_2]$	2.0 ($H_{CN2} : O$); 2.4 ($H_{CH2} : O$); 2.5 ($H_{CH3} : O$); 3.0 ($C_{CN2} : O$); 3.0 ($H_{CN2} : N$); 3.5 ($C_{CN2} : N$)	-3.33	-0.05
$[Cl]^-$: $\mathbf{MC_{BSP}}$	2.5 ($Cl : H_{N\text{-}CH3}$); 2.8 ($Cl : H_{CH3}$); 3.3 ($Cl : N$)	-0.98	-0.05
$[NTf_2]^-$: $\mathbf{MC_{BSP}}$	2.4 ($O_{=S} : H_{CH3}$); 2.6 ($O_{=S} : H_{Ph}$); 2.9 ($N : H_{N\text{-}CH3}$); 3.6 ($N_{NTf2} : N_{\mathrm{MC}}$)	-0.73	-0.03
$[P_{6,6,6,14}]^+$: $\mathbf{MC_{BSP}}$	2.4, 2.4, 2.7 ($H_{CH2} : O_{Ph}$); 3.6 ($P : O_{Ph}$)	-0.48	+0.01
$[C_2mIm]^+$: $\mathbf{MC_{BSP}}$	1.8 ($H_{CN2} : O_{Ph}$); 2.8 ($H_{CH2} : O_{Ph}$); 3.2 ($C_{CN2} : H_{Ph}$); 3.2 ($H_{CH3} : O_{Ph}$)	-0.76	+0.05
$[P_{6,6,6,14}]^+$: $\mathbf{MC_{BSP}}$: $[Cl]^-$	2.5, 2.5, 2.9 ($H_{CH2} : Cl$); 4.0 ($P : Cl$) 2.4 ($Cl : H_{N\text{-}CH3}$); N/A ($Cl : H_{CH3}$); 4.3 ($Cl : N_{MC}$); 2.4, 2.7 ($H_{CH2} : O_{Ph}$); 3.9 ($P : O_{Ph}$)	-0.58	-0.02
$[C_2mIm]^+$: $\mathbf{MC_{BSP}}$: $[Cl]^-$	2.2 ($H_{CN2} : O_{Ph}$); 2.3 ($H_{CH3} :O_{Ph}$); 2.4 ($H_{N\text{-}CH3}: Cl$); 2.7 ($H_{CH2} : Cl$); 2.9 $C_{CN2} : Cl$); 2.9 ($H_{CN2} : Cl$)	-0.64	-0.02
$[C_2mIm]^+$: $\mathbf{MC_{BSP}}$: $[NTf_2]^-$	2.1 ($H_{CN2}:O_{Ph}$); 2.3 ($H_{CH3}:O_{Ph}$); 2.3 ($H_{N\text{-}CH3}: O_{NTf2}$); 2.3 ($H_{CH2} : O_{NTf2}$); 2.5 ($H_{CN2} : O_{NTf2}$); 2.7 ($H_{CH3\text{-}EMIM} : O_{NTf2}$); 3.0 ($H_{CH3\text{-}MC} : O_{NTf2}$)	-0.65	+0.01

Geometries and electronic structures calculated with B3LYP/6-311++G** model chemistry. ΔE for the two-species systems is the binding energy of the complex, as computed from the self-consistent field (SCF) energies of the complex relative to the isolated species. For the final three entries, the three-species full IL-probe complexes, ΔE is the energy of the three-species complex minus the energies of the IL complex and the isolated $\mathbf{MC_{BSP}}$. More negative values indicate more favourable binding. Δq is the degree of charge transfer between species, as measured from the total charge of each species in the complex and isolated systems. Negative Δq values generally indicate net transfer of electron density from the anion to the cation or probe, except in the 7th/8th entries, where the positive Δq indicates transfer of electron density from the probe to the cation, the 9th/10th entries where the negative Δq is the net electron transfer to $\mathbf{MC_{BSP}}$ and the 11th (final) entry where the positive Δq is the net electron transfer from $\mathbf{MC_{BSP}}$. These small net **MC**-centered Δq values in the three-species complexes are coupled in each case with larger inter-IL transfers: -0.09 a.u from $[Cl]^-$ to $[P_{6,6,6,14}]^+$, the same as for the IL in the absence of the probe (first entry); -0.09 a.u. from Cl^- to $[C_2mIm]^+$, half that in the neat IL reflecting the broken valence orbital interaction discussed in the text; -0.04 a.u from NTf_2^- to $[C_2mIm]^+$, close to the -0.05 a.u. in the neat IL. A stable electronic structure was not obtained for the 158-atom, 2210-basis function $[P_{6,6,6,14}]^+$:$\mathbf{MC_{BSP}}$:$[NTf_2]^-$ complex within a reasonable computational time, despite multiple attempts starting from a variety of different initial geometries and basis sets.

Similar to the $[P_{6,6,6,14}][Cl]$ IL described above, moderate contacts of approximately 2.4 Å are computed for the $[P_{6,6,6,14}][NTf_2]$ complex. The similarity in intermolecular distances may therefore be attributed to the cation, with the alkyl side-chains of the cation regulating the complexation distance in both ion pairs. The increased size of the $[NTf_2]^-$ anion restricts the approach to the phosphorus charge centre of the cation with a calculated $N^-:P^+$ distance of 4.1Å. At this distance, little or no electronic interaction can occur as reflected in the relatively low binding energy and negligible degree of electron transfer (Table 5.1). In common with $[P_{6,6,6,14}][Cl]$, longer-range electrostatic interactions drive complexation, as reflected in the computed dipole moment of 17 D parallel to the P---N axis of $[P_{6,6,6,14}][NTf_2]$, with shorter-range polar interactions between the anion and the phosphonium alkyl chains mediating the interaction.

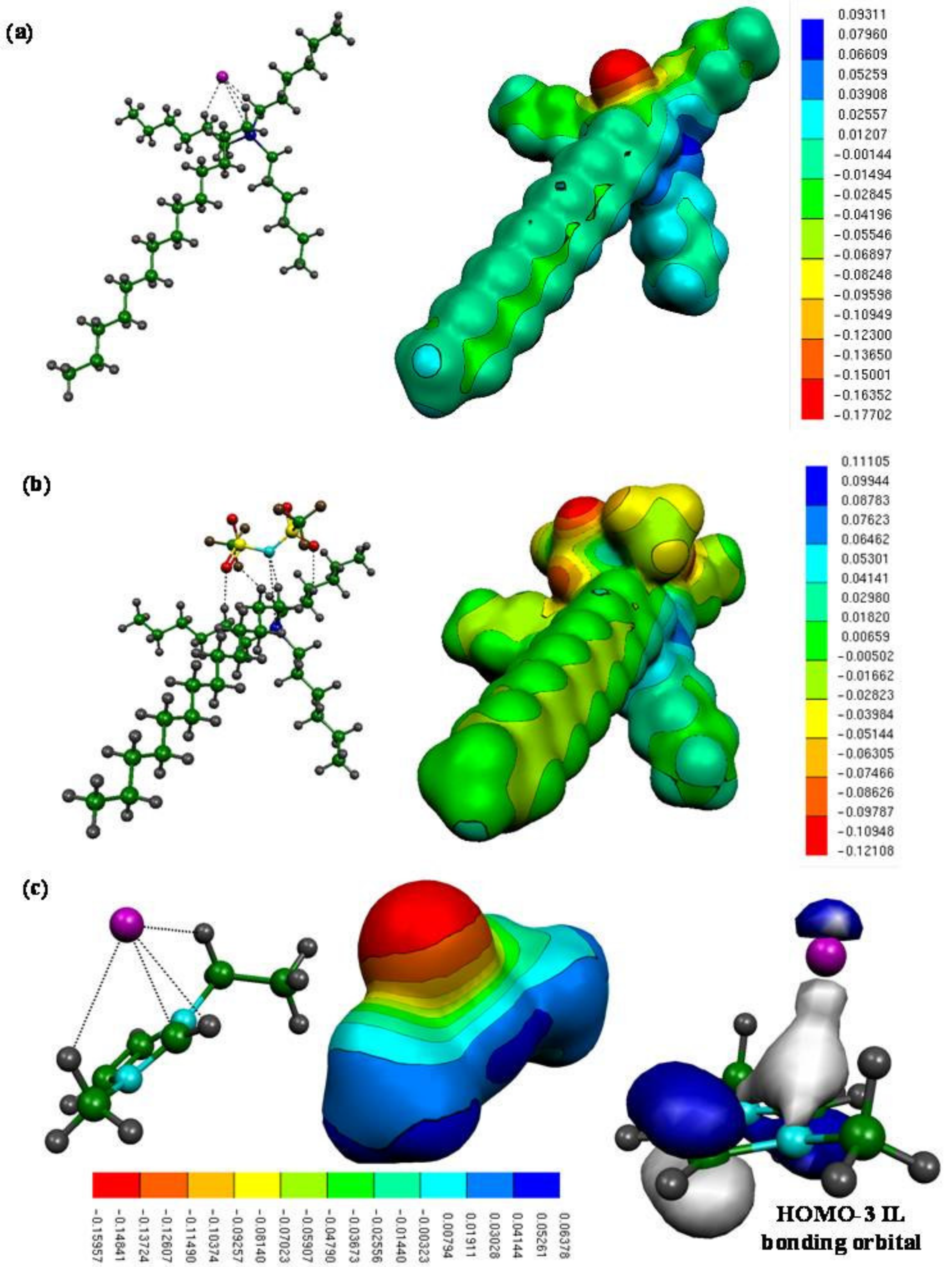

Figure 5.2 Complexation geometries with close contacts (corresponding distances are given in Table 5.1) marked by dashed lines for net neutral phosphonium-based ILs, **(a)** with Cl^- and **(b)** with NTf_2^-; carbon atoms are green, hydrogens grey, phosphorus atoms are blue, chlorines magenta, nitrogens cyan, oxygens red, sulphurs yellow and fluorine atoms are brown. Also shown are computed Molecular Electrostatic Potential (MEP) surfaces generated as described in the text and with surfaces coloured according to regions of net charge as marked in the scale bars, with the scale set in each case according to the largest net negative and net positive sites in each complex. The computed structure for C_2mIm chloride is given in panel **(c)** along with, on the far righthand side in a slightly different orientation, the valence HOMO-3 IL bonding orbital that enhances liquid ion pairing[45]; the [C_2mIm][NTf_2] complex is described in Appendix A-4.

These calculations give a greater understanding as to why $[P_{6,6,6,14}][Cl]$ has a lower thermal decomposition temperature of 330 ^{o}C compared to 420 ^{o}C for $[P_{6,6,6,14}][NTf_2]$.[19-21] Considering the structure of $[P_{6,6,6,14}][Cl]$ in Figure 5.2a) the Cl^- ion is located in a favourable position (2.4 Å) to extract a hydrogen atom from one of the alkyl chains thus promoting a Hoffman like elimination mechanism for thermal decomposition at lower temperatures than that of the sterically-constrained (Figure 5.2b) $[P_{6,6,6,14}][NTf_2]$.[22]

In the reference, short-tail, imidazolium-based ILs, the computed ion pairing energies are -3.9 and -3.3 eV respectively for the $[Cl]^-$ and $[NTf_2]^-$ anions, with the $[C_2mIm][NTf_2]$ structure given in Appendix A-4. These pairing energies are consistent with those calculated for similar pairs in earlier studies.[15] In general, the electrostatic potentials are reduced slightly upon switching from $[P_{6,6,6,14}]^+$ to the more delocalised $[C_2mIm]^+$, the ring atoms of $[C_2mIm]^+$ more nucleophilic than the methylene groups bound to phosphorus in $[P_{6,6,6,14}]^+$. There is also a more significant reduction in the maximum net *negative* charge upon switching from the highly-localised $[Cl]^-$ anion to the more delocalised $[NTf_2]^-$. $[C_2mIm][Cl]$ is the strongest bound of the four IL pairs and includes also a through-space orbital interaction as shown in Figure 5.2c. This HOMO-3 orbital lies 2.5 eV below the HOMO and is the most high-lying through-space orbital observed in the present study, contributing to the relatively large degree of electron transfer of -0.18 a.u. in the $[C_2mIm][Cl]$ pair. The contribution of this orbital to inter-ion bonding has been previously described in an earlier study of imidazolium chloride ILs.[23] Furthermore, the calculated electronic structure of the $[C_2mIm][NTf_2]$ pair is consistent with the measured valence band spectrum[24,25] with a moderate HOMO-LUMO gap of -6 eV and near-valence occupied orbitals composed of both anion- and cation-centered orbitals; the calculated MO diagram and surfaces are given in Supporting Information. The most interesting, and potentially most useful, features of the IL pairs may be summarised as follows:

(1) The LIP energies range from -3.5 and -3.9 eV for Cl-based ILs, with imidazolium 0.4 eV more stabilising than phosphonium

(2) For NTf_2-based ILs the LIP energies are lower, -2.9 and -3.3 eV, with imidazolium *vs.* phosphonium having the same incremental effect on binding of 0.4 eV

(3) In terms of anion strength, Cl-based ILs are 0.6 eV more stable than the corresponding NTF_2-based ILs (-3.5 *vs.* -2.9 for $[P_{6,6,6,14}][Cl]$ *vs.* $[P_{6,6,6,14}][NTf_2]$ and -3.9 *vs.* -3.3 eV for $[C_2mIm][Cl]$ *vs.* $[C_2mIm][NTf_2]$). This is a consequence of the primary charge delocalisation and secondary steric accessibility effects described above - similar effects, though with reversed priority, make $[C_2mIm]^+$ a better cation than $[P_{6,6,6,14}]^+$

(4) The 0.6 *vs.* 0.4 eV incremental effect of changing anion *vs.* changing cation points to charge delocalisation as a stronger predicator than steric accessibility

> for headgroup-mediated interactions, suggesting that one may re-design the regions around the given charge center (for example, to change the hydrophobic interactions) without significantly changing the intrinsic strength of the hydrophilic headgroup interactions.

Having characterised the ion pair interaction within the ionic liquids, interactions with the open, charged **MC_{BSP}** form of **BSP** were calculated, to probe whether the zwitterionic **MC_{BSP}** isomer can compete for ionic liquid IL pair interaction sites and possibly disrupt the ionic liquid structure upon **$BSP \rightarrow MC_{BSP}$** photoswitching.

5.3.2 Probe-anion complexation

In common with ion pairing in the ionic liquid, Cl^- interacts more strongly than $[NTf_2]^-$, in this case $[Cl]^-$ sits 0.2Å closer than $[NTf_2]^-$ to the N^+-CH_3 site on **MC_{BSP}** (Table 5.1), and the anions coordinate in a similar way to that observed for the interaction of the anions with the phosphonium cation in the ionic liquid pairs. The methyl hydrogens on the indoline ring play a significant role in the coordination of the anions, with contacts at ~2.4 Å as the ion associates with the positive N^+-CH_3 centre. The coordination of the anion with the methyl groups mediates the overall interaction and stabilisation of the **MC_{BSP}** -anion couple (Figure 5.3). Natural population analysis (NPA)[14] of atomic charges gives a net charge of +0.28 on the methyl group of N^+-CH_3 compared with an average of +0.07 on the other two methyl groups, and so it is the ability of the more compact $[Cl]^-$ anion to make a strong contact with the N^+-CH_3 centre that provides the enhanced probe stabilisation with

$[Cl]^-$ compared to $[NTf_2]^-$. Reference MP2 calculations given in Appendix A-4 confirm the general features of the probe-anion complexes and the enhanced probe stabilisation with $[Cl]^-$. Compared with the findings of liquid ion pairing above, the degree of electron transfer is lower and the charge surface around the anion is more negative, due to the inferior stabilisation by the neutral **MC** zwitterion.

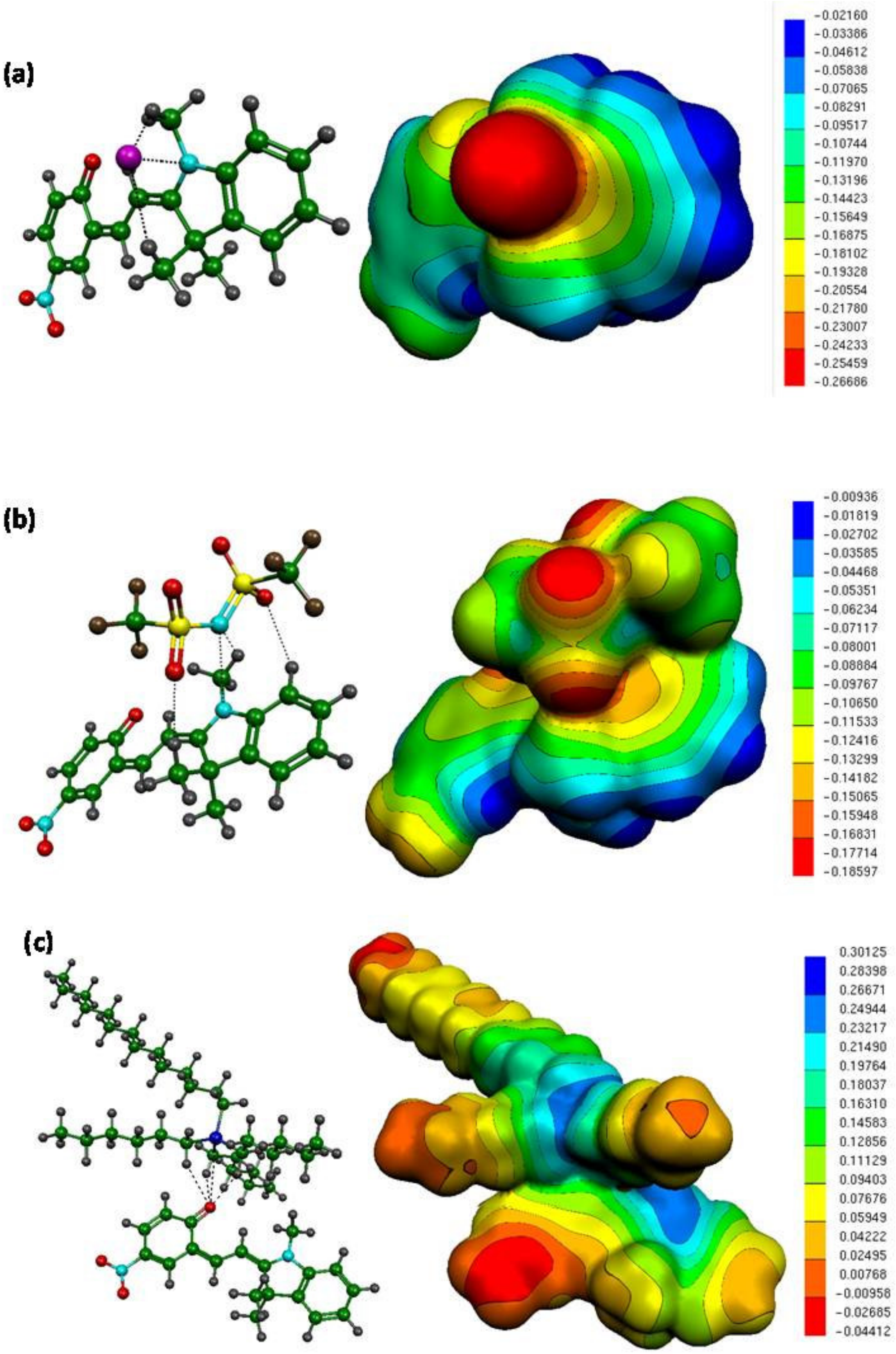

Figure 5.3 Complexation geometries with close contacts (Table 5.1) marked by dashed lines for charged ion- **MC$_{\mathbf{BSP}}$** complexes, panel **(a)** the anionic complex with [Cl]$^-$ and **(b)** the anionic complex with [NTf$_2$]$^-$ and **(c)** the cationic complex with [P$_{6,6,6,14}$]$^+$; carbon atoms are green, hydrogens grey, phosphorus atoms are blue, chlorines magenta, nitrogens cyan, oxygens red, sulphurs yellow and fluorine atoms are brown. Also shown are computed Molecular Electrostatic Potential (MEP) surfaces generated as described in the text and with surfaces coloured according to regions of net charge as marked in the scale bars, with the scale set in each case according to the largest net negative and net positive sites in each complex.

5.3.3 Probe-cation complexation

The **MC$_{BSP}$**:[$P_{6,6,6,14}$]$^+$ complex features contact distances similar to those in [Cl]$^-$:[$P_{6,6,6,14}$]$^+$ (Table 5.1), with the $O_{(Ph)}$ bound to the **MC$_{BSP}$** phenyl ring acting as the negatively-charged centre. The strength of the interaction is weaker than for [Cl]$^-$:[$P_{6,6,6,14}$]$^+$, with negligible electron transfer (Table 5.1) and relatively weak stabilisation due to the decreased nucleophilicity compared with [Cl]$^-$, and negative charge (-0.34 ± 0.02 a.u. averaging over all systems) of the **MC$_{BSP}$** O_{Ph} site; the phosphonium methyl H contacts to the **MC$_{BSP}$** O_{Ph} centre of 2.4 to 2.7 Å are significantly weaker than the intramolecular stabilisation due to the O---H contact of 2.2 Å within **MC$_{BSP}$**. **MC$_{BSP}$**:cation interactions are also generally weaker than **MC$_{BSP}$**:anion, due to the decreased localisation of net charge at the **MC$_{BSP}$** positive centre.

Replacing phosphonium with [C_2mIm]$^+$ strengthens probe stabilisation by 0.3 eV, with closer contacts and enhanced electron transfer (Table 5.1, Figure 5.3c and Appendix A-4) in agreement with earlier calculations of tightly-bound [C_2mIm]$^+$:**MC$_{BSP}$** complexes.[5] As for the LIPs in section 1, [C_2mIm]$^+$ has a more delocalised positive charge than the phosphonium cation as reflected in the maximum net positive charge in the electrostatic surfaces in Figure 5.3c and Appendix A-4. The most salient features of single ion probe stabilisation may be summarised as follows:

(1) $[Cl]^-$ gives an increased stabilisation of 0.3 eV of **MC** compared with $[NTf_2]^-$

(2) $[C_2mIm]^+$ interacts 0.3 eV more strongly than $[P_{6,6,6,14}]^+$ with **MC**. The differences in probe stabilisation caused by changing anion and cation are due to charge localisation and steric accessibility effects, similar to the liquid ion pairs described above

(3) The phenolic oxygen anion site in $\mathbf{MC_{BSP}}$ is stronger than the indoline nitrogen cation site (Figure 5.1), making the net effect of a small shift in charge localisation (imidazolium *vs.* phosphonium) at a very nucleophilic site similar to the net effect of a large shift in charge localisation (chloride *vs.* NTf_2^-) at a mildly electrophilic site. The consistency in the computed energy differences is encouraging, as is the general trend that $\mathbf{MC_{BSP}}$ feels the effect of changing ion strength less acutely than does the counterion in the IL pair, 0.3 *vs.* 0.4-0.6 eV.

5.3.4 Probe-anion-cation complexation

The final, and computationally most demanding, system calculated in this study is the three-species system $[P_{6,6,6,14}]^+$: **MC$_{BSP}$**:$[Cl]^-$ with the probe **MC$_{BSP}$** molecule complexed simultaneously by both IL ions. The computed structure of the complex is shown in figure 5.4 and summarised table 5.1; in general all inter-molecular contacts are weakened in the three-species complex compared with the corresponding two-species systems, particularly for ion- **MC$_{BSP}$** contacts and to a lesser extent for ion-ion contacts, giving an effective complexation energy for the full IL-probe system of -0.58 eV (Table 5.1), computed from the electronic energies of the three-species complex relative to the IL ion pair and the isolated probe molecule.

The moderate binding energy, negligible electron transfer to **MC$_{BSP}$** and weakened intermolecular contacts all indicate that, while the zwitterionic probe is electrostatically stabilised by the presence of the ionic liquid pair, **MC$_{BSP}$** is not sufficiently polar to break the ionic liquid pair. This is supported by reference calculations that replaced the large phosphonium with the computationally more amenable imidazolium cation emim$^+$ and allowed computation of the influence of the *cation* on the full ionic liquid stabilisation of **MC$_{BSP}$**. While the detailed electronic structures will be reported as part of a larger study of $[C_2mIm]^+$-based ILs, the computed $[C_2mIm]^+$: **MC$_{BSP}$**:$[Cl]^-$ complexation energy of -0.64 eV is very similar to the phosphonium value of -0.58 eV.

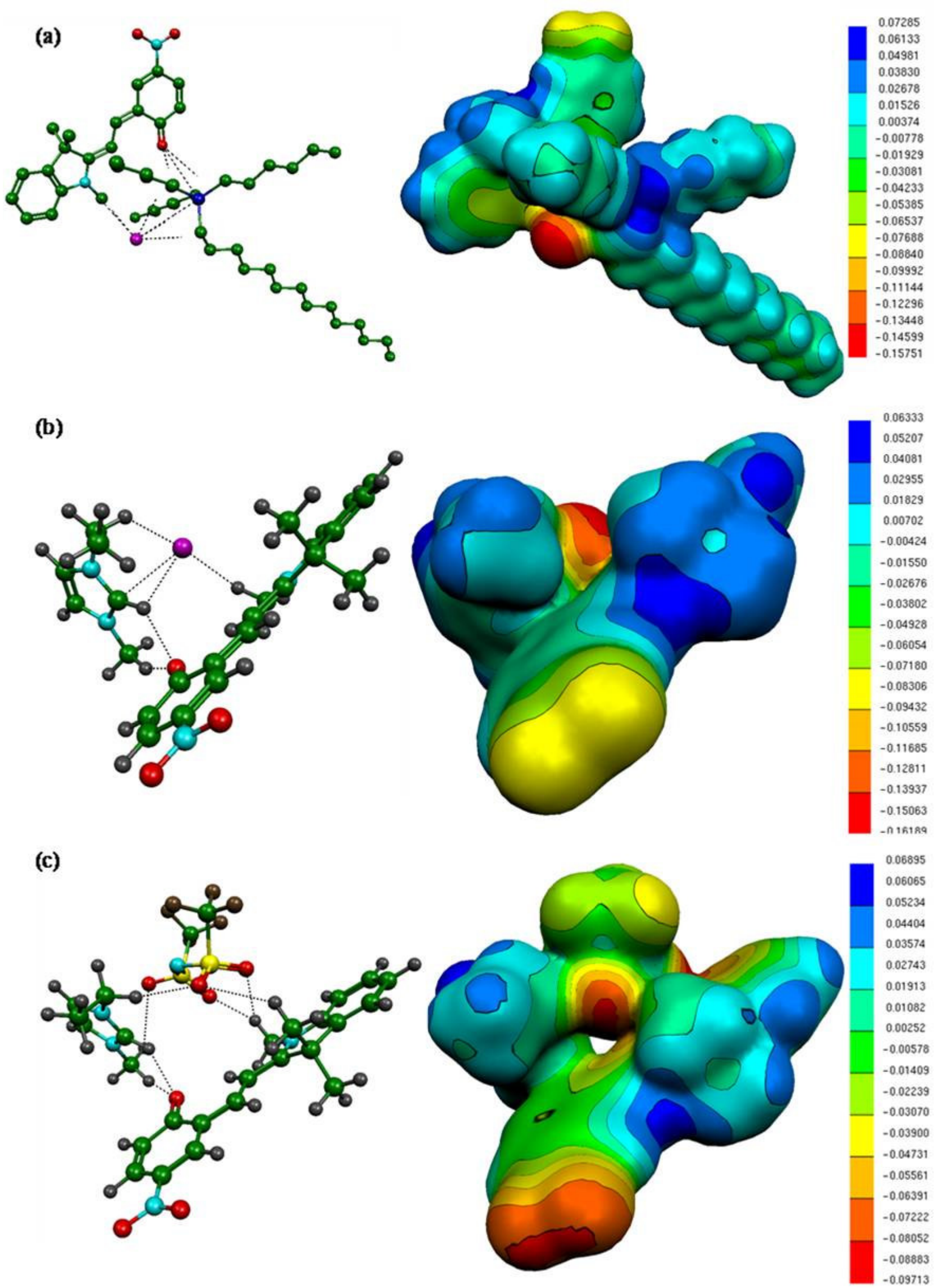

Figure 5.4 Complexation geometries with close contacts (Table 5.1) marked by dashed lines for the net neutral complex of **MC$_{\mathbf{BSP}}$** coordinated by **(a)** both ions of the phosphonium-chloride IL; hydrogens are omitted for clarity (and so some contact lines appear truncated), carbon atoms are green, phosphorus atoms are blue, chlorines magenta, nitrogens cyan and oxygens red. Also shown is the computed Molecular Electrostatic Potential (MEP) surface generated as described in the text and with the surface coloured according to regions of net charge as marked in the scale bar. Panels **(b)** and **(c)** show the corresponding structures calculated for **MC$_{\mathbf{BSP}}$** coordinated by [C_2mIm][Cl] and [C_2mIm][NTf_2] ILs; carbon atoms are green, hydrogens grey, chlorines magenta, nitrogens cyan, oxygens red, sulphurs yellow and fluorine atoms are brown.

This suggests that, while the nature of both the cation and the anion can have a dramatic effect on inter-ion IL binding energies and to a lesser extent individual ion-**MC$_{BSP}$** interactions (Table 5.1), the net electrostatic stabilisation available to **MC$_{BSP}$** may not strongly depend on the nature of the ionic liquid polar headgroups. That is, a similar small amount of charge-stabilisation will be available to **MC$_{BSP}$** following inter-ion IL stabilisation, and it is the size of the non-polar region that dictates the amount of stabilisation that actually occurs.

This is supported by reference calculations that replaced the large phosphonium with the computationally more amenable imidazolium cation $[C_2mIm]^+$ (Table 5.1). The computed $[C_2mIm]^+$:**MC$_{BSP}$**:Cl^- net three-site complexation energy of -0.64 eV is very similar to the phosphonium value of -0.58 eV. Indeed the valence IL bonding orbital observed in $[C_2mIm][Cl]$ is removed by the probe, zwitterion stabilisation stretching the H---Cl contact to 2.9 Å and precluding significant covalent bonding. Replacing Cl^- with NTf_2^- to form $[C_2mIm]^{++}$:**MC$_{BSP}$**:NTf_2^- gives a net complexation energy of -0.65 eV. The similar, up to 0.02 a.u. lower, maxium net charges in all of the IL:probe, compared with LIP, electrostatic potential surfaces illustrate how LIP formation "soaks up" the majority of the ionic liquid charge resulting in only mild zwitterion stabilisation. The similar net residual complexation energies in all the cation:**MC$_{BSP}$**:anion systems in Table 5.1 suggests that, while the nature of both the cation and the anion can have a dramatic effect on inter-ion IL binding energies and to a lesser extent individual ion-**MC$_{BSP}$** interactions (Table 5.1), the net electrostatic stabilisation available to **MC$_{BSP}$** may not strongly depend on the nature of the IL polar headgroups. That is, a similar small amount of charge-stabilisation will be available to **MC$_{BSP}$** following inter-ion IL stabilisation, and it is in fact the size of the non-polar region that dictates the amount of stabilisation that actually occurs (as described in more detail in the next section). The most salient features of probe stabilisation by IL pairs may be summarised as follows:

(1) $[C_2mIm]^+$ gives a stronger complex than the phosphonium cation, by 0.5 eV, so the net incremental stabilisation involves a complex sum of 0.4 (IL pairing) + 0.3 (cation:**MC$_{BSP}$** stabilisation) - 0.2 eV (this inferred value arises from the weaker contacts overall for the 3-site *vs.* the two isolated LIP and single-ion:probe 2-site complexes)

(2) $[Cl]^-$ gives a stronger complex than $[NTf_2]^-$, by 0.6 eV, and so the net stabilsation can be attributed to 0.6 (IL pairing) + 0.3 (anion:**MC$_{BSP}$** stabilisation) - 0.3 eV (weaker contacts overall for the 3-site *vs.* the two 2-site complexes)

(3) Subtracting the IL pairing energies from the cation:probe:anion binding energies gives 0.6, 0.6 and 0.7 eV for $[P_{6,6,6,14}]^+$:**MC$_{BSP}$**:Cl^-, $[C_2mIm]^+$:**MC$_{BSP}$**:Cl^- and $[C_2mIm]^+$:**MC$_{BSP}$**:NTf_2^- respectively as given in Table 1. Thus, approximately the same net headgroup stabilisation of the probe is potentially available for each system. Not only then does the “tug of war” between intra-IL and IL-probe interactions tend to cancel differences between ion reactivities (including both

non-covalent and also $[C_2mIm]^+$-based covalent interactions), the three-site complexation energies for $P_{6,6,6,14}^+$:**MC$_{BSP}$**:Cl^- and $[C_2mIm]^+$:**MC$_{BSP}$**:NTf_2^- are almost the same (-4.1 and -4.0 eV), so the poorer cation reactivity of $P_{6,6,14}^+$ compared to $[C_2mIm]^+$ has the same effect as the poorer anion reactivity of $[NTf_2]^-$ compared to $[Cl]^-$.

5.3.5 Headgroup stabilisation vs Tail disordering

Comparison of probe stabilisation energies with known barriers to alkyl chain diffusion is instructive and indicates that the electrostatic stabilisation of the probe by the polar IL headgroups is severely penalised by the long non-polar tails of the quaternary phosphonium ion, the (putative) electrostatic interaction being too weak to overcome the chain diffusion activation barrier. From previous experimental and simulation studies we may estimate the barrier to alkyl chain diffusion as 0.2 kcal/mol per CH_2 group.[26, 27] For $[P_{6,6,6,14}]^+$, this corresponds to a diffusion barrier of 6.4 kcal/mol per cation, which is just less than half the electrostatic interaction (-0.58 eV, or -13.4 kcal/mol). Phosphonium-based ILs form a tightly-woven hydrophobic “gel”, as described below, and so the tight electrostatic coupling at the probe shown in figure 5.4 would require significant disruption of the mesh and movement/reorientation of a large number of alkyl chains. The required relaxation would propagate radially in three dimensions, and so we may anticipate that, for systems with such large non-polar regions, the IL nano-structuring will preclude significant **MC$_{BSP}$** stabilisation. The hydrophobic "gel" hypothesis above is supported by crystallographic studies based upon a similar structure

($[P_{10,10,10,10}][Br]$) that show significant structuring based upon side-chain interaction[28] while structural analysis of imidazolium based IL structures found that the differences between solid and liquid structure results in only a small 10-15% expansion in the volume of the system.[29] Since nano-scale structuring appears to be a common characteristic of all ionic liquids, small expansions may be expected within phosphonium based ILs, preserving pseudo-crystalline ordering and thus rigidity within the liquids.

To summarise the insights obtained from the electronic structure calculations, the intra-IL ion-ion binding energy (ΔE) and extent of charge transfer (Δq) were both found to be stronger for $[P_{6,6,6,14}][Cl]$ than for $[P_{6,6,6,14}][NTf_2]$. Computed binding energies are approximately 0.5 eV higher for the chloride based IL. This value implies that the chloride based IL ion pairing interaction is much stronger, as indicated by the Walden plots in previous studies.[1, 10] Similarly, increased Δq values show a greater interaction for $[P_{6,6,6,14}][Cl]$ than for $[P_{6,6,6,14}][NTf_2]$, though both Δq values are < 0.1 a.u. (Table 5.1), indicating that non-covalent interactions dominate the ion-ion pairing in phosphonium based ILs. Computed binding energies are significantly lower for $\mathbf{MC_{BSP}}$ -ion interactions compared to that of ionic liquid ion-ion interactions. $[Cl]^-$ again provides better stabilisation compared with $[NTf_2]^-$, with a ΔE value of -0.98eV for $\mathbf{MC_{BSP}}$:$[Cl]^-$ compared with -0.73 eV for $\mathbf{MC_{BSP}}$ -$[NTf_2]^-$. Both $\mathbf{MC_{BSP}}$ -anion interactions are approximately three to four times weaker than the phosphonium-anion pairing. In addition, the differences in the energies $\Delta\Delta E$ for $\mathbf{MC_{BSP}}$ as a function of the anion are approximately half that calculated for the ionic liquids. The zwitterionic $\mathbf{MC_{BSP}}$ probe is thus less sensitive than the ionic liquid cation to the nature of the anion. Most importantly, from the range of ΔE values, -0.7 to -1.0 eV for $\mathbf{MC_{BSP}}$ -anion compared with -2.9 to -3.5 eV for the ionic liquid pair, it is clear that while $\mathbf{MC_{BSP}}$ coordinates the ionic liquid anion, it is unable to break the ionic liquid pair. Similarly for the $\mathbf{MC_{BSP}}$ -cation interaction, with $\mathbf{MC_{BSP}}$ -$[P_{6,6,6,14}]^+$ complexation is less than one sixth the strength of the anion$^-$-$[P_{6,6,6,14}]^+$ IL pairing. While IL- $\mathbf{MC_{BSP}}$ through-space interactions can stabilise $\mathbf{MC_{BSP}}$ in $[C_2mIm]^+$-based IL solvents[30], no such covalent interactions were found for the phosphonium-based ILs, that is, no high-lying occupied orbitals have significant inter-molecular character. Finally, the moderate complexation energy calculated for $\mathbf{MC_{BSP}}$ with both IL ions simultaneously is not expected to be sufficient to overcome the required disruption of the extended alkyl chain network in the long-tail phosphonium-based ILs, and so the ionic liquid nano-structuring is preserved; this hypothesis is supported by the calculated electronic structures, existing diffusion[26, 27] and Walden plot data[1, 10] and the experiments described below.

5.3.6 Measured polarity and solvatochromic effects

The electronic structures described above serve to rationalise some known features of IL structures and IL-probe interactions as described above, together with some new physicochemical experiments performed as part of this study to determine the thermal relaxation of $\mathbf{MC_{BSP}}$. Taken together, the calculations and measurements help elucidate the processes at work within the ILs. **BSP** was added to each ionic liquid and irradiated to examine the immediate environment presented to the $\mathbf{MC_{BSP}}$

form in each liquid (Table 5.2). It is found that both the $[P_{6,6,6,14}][NTf_2]$ and $[P_{6,6,6,14}][Cl]$ liquids presented similar non-polar environments with a λ_{max} shift to 574nm while $E_T(30)$ values were found to vary in each liquid with values of 46.1 kcal.mol^{-1} and 43.8 kcal.mol^{-1} for $[P_{6,6,6,14}][NTf_2]$ and $[P_{6,6,6,14}][Cl]$, respectively. Such $E_T(30)$ values were expected since the stronger the ion pair, the more the binary system begins to resemble a single neutral solvent molecule. The bulkier $[NTf_2]^-$ anion results in less stable associations between ion pairs and so presented a more 'ideal' ionic system with the individual ion charge becoming more apparent than occurs in the $[Cl]^-$ system. The result of this is that Reichardt's Dye 30 senses a more polar environment and thus the value is increased. While the solvatochromic shifts in the same general region of ~570 nm may be attributed to the common phosphonium cation, the lack of variation may be attributed to the dependence of the interaction of the anion with the **MC$_{BSP}$**. The calculated strong interactions for $[P_{6,6,6,6,14}]^+$ with $[Cl]^-$ results in the $[Cl]^-$ becomming somewhat embedded between the alkyl chains of the phosphonium cation (figure 5.2a). As a result it becomes difficult for the **MC$_{BSP}$** to interact with the anion and thus produce a stabilisation and solvatochromic effect. Although the $[NTf_2]^-$ is a bulkier anion and does not reside as close to the phosphonium cation as the $[Cl]^-$ anion, the more diffuse nature of the ion charge and the lack of any hydrogen bond donor sites reduces its ability to stabilise the **MC$_{BSP}$** phenolate oxygen and the bulky nature of the anion restricts interaction with the positive region of the **MC$_{BSP}$**.

5.3.7 Measured thermodynamic and kinetic parameters

Samples were irradiated and thermodynamic and kinetic parameters were determined using procedures outlined previously (chapter 1, section 1.4.2) using equations **(10)**, **(11)**, **(12)** and **(13)**. The rates of thermal relaxation were recorded at 298K and summarised in Table 5.2. The thermal relaxation of $[P_{6,6,6,14}][Cl]$ is almost half that of $[P_{6,6,6,14}][NTf_2]$ at 1.0 s^{-1} and 1.9 s^{-1}, respectively. As with the solvatochromic parameters previously discussed, the calculated ability of the chloride ion to associate closer to the positive charge of the $\mathbf{MC_{BSP}}$ serves to explain the observed enhanced stability (increased lifetime) of the open form. Similarly, the charge of the chloride ion is much more concentrated because it is a single atom. In the case of the $[NTf_2]$, the charge is more delocalised and the point strength of the negative charge is diminished and dispersed conseqently, this provides less counter-charge to the positive site of the $\mathbf{MC_{BSP}}$ zwitterion and the strength of the interaction is reduced leading to faster thermal relaxation of $\mathbf{MC_{BSP}}$ to its ground non-zwitterionic state. Additionally, the enhanced liquid ion pairing with $[Cl]^-$ may provide a more rigid ionic liquid network around the probe moleclue which would in turn restrict the thermal relaxation of the $\mathbf{MC_{BSP}}$ to its closed form.

The resulting entropies of activation $\Delta S^{\ddagger}$ of -96.13J.K^{-1}.mol^{-1} and -14.59 J.K^{-1}.mol^{-1} for $[P_{6,6,6,14}][Cl]$ and $[P_{6,6,6,14}][NTf2]$ respectively indicate that the chloride based IL does indeed present a more rigid solvent system than that of $[NTf2]^-$ based ILs, consistent with the arguments previously put forward by Fraser *et al* during their initial investigation into the formation of liquid ion-pairing.[10] Under this hypothesis, the small size of the chloride ion drives the ion-pairing that structures the ionic liquid. The quaternary nature of the cations coupled with the length of the side-chains, (e.g. $[P_{6,6,6,14}]^+$), results in the formation of a hydrophobic mesh dotted with paired charged head-groups, resulting in a rigid liquid structure. **MC_{BSP}** is a bulky molecule which requires significant reorientation during thermal relaxation and its conformational space may become restricted within this rigid liquid structure, prolonging the lifetime of the zwitterionic isomer. The bulkier $[NTf2]^-$ anion means that ion-pairing is weaker (Table 5.1) and so the formation of a more 'ideal' IL occurs, with reduced rigidity in the liquid structure, as reflected in the more positive values of the measured $\Delta S^{\ddagger}$ values and lower k values, resulting in a faster thermal relaxation time, τ, of the **MC_{BSP}** to its closed form. Similarly, lower enthalpies of activation $\Delta H^{\ddagger}$ (22.63 $kJ.mol^{-1}$ difference) imply that for chloride based ILs the level of energy for the relaxation process at the transition state of the **MC_{BSP}** is less than that of $[NTf_2]^-$. Such reductions would be expected in the more rigid chloride system where less interaction through solvent reorientation occurs between **MC** and the ions in solution.

Interestingly, activation energies appear counterintuitive in relation to the kinetic parameters reported. The faster relaxation time of $[P_{6,6,6,14}][NTf_2]$ is associated with *higher* activation barriers (Table 5.2) which would normally result in slower thermal relaxation as observed in molecular solvents. This therefore is believed to indicate that the key feature is the enhanced IL ion-pairing with $[Cl]^-$ (Table 5.1; ion:ion complexation energies) provides a more rigid, restrictive IL network around the probe molecule associated with extensive van der Waals interactions involving the alkyl chains of the cation. This is reflected in both the higher entropy of activation and the lower activation energy that reflects a possible decrease in the *frequency* of anion-probe interactions. This agress with previous conclusions in chapter 2 where it is believed that the pre-exponential factor, A, may encorpourate a process critical to the thermal relaxation of spirocyclic compounds which is not quantified by the activation energy. For the bulkier $[NTf_2]^-$ based ILs the resulting ion-ion dissociation results in dispersion of the cations as the anions now act as barriers between alkyl chains and thus reduce the levels of van der Waals interactions available. The resulting structure is therefore less rigid than that of $[Cl]^-$ based systems (reflected in more positive entropy of activation values). The apparent contradiction in activation energies may also be rationalised through the strength of LIP formation. The more dissociated $[NTf_2]^-$ system results in a liquid structure that is based on two distinct charged species. These are both able to to interact with the **MC**$\mathbf{MC_{BSP}}$ form and thus create a larger activation energy barrier to thermal relaxation. The $[Cl]^-$ based ILs, with far stronger LIP binding energies (table 5.1) result in a liquid system that appears almost like a neutral solvent system due to the close association of the cation-anion pair. The association of the ionic liquid with the $\mathbf{MC_{BSP}}$ form is restricted primarily to the phosphonium cation and stabilisation is therefore inhibited through lack of anion interaction with the $\mathbf{MC_{BSP}}$ positive site. As such, the activation energy barrier is found to be lower. It is concluded that while activation energies are an important factor influencing the overall $\mathbf{MC_{BSP}} \rightarrow \mathbf{BSP}$ thermal relaxation process, it appears that the physical structure of the ionic liquids and the ordering of the system mediates the process of a non linear relationship between E_a and k. This appears to be a unique effect previously observed uniquely in phosphonium based ILs and is believed to be an integral part of what has become known as the 'ionic liquid effect'.[4, 31] However, deviations in thermodynamic parameters may also be contributed to by the proposed loss of solvent equilibrium during the chemical process as described by Chiappe *et al.*[32] Such effects would be related to the complex ion-ion interactions which result in unique structuring but also physical parameters such as viscosity. The formation or lack of ion pairing and the apparent charge this endows upon the liquid system may therefore mediate these effects and be imporrtant for the formation of unique effects observed in ionic liquids.

Equilibrium of activation values, $K^{\ddagger}$, may also be explained by the calculated electronic structures, it may also be explained by the thermal relaxation of **MC$_{BSP}$.** The greater steric hindrance caused by the more rigid chloride based IL structures obstructs the smooth transition from open to closed forms and results in longer lived **MC$_{BSP}$** species and thus shifts the equilibrium of activation towards the open **MC$_{BSP}$** form.

Table 5.2 Thermodynamic and kinetic parameters of **BSP** in ionic liquids. Reference values from Fraser et al.[10]

	$E_T(30)$ *(kcal.mol^{-1})*	**λ_{max}** *(nm)*	**k_{20}** *(x10^{-3}s^{-1})*	**S.D** *±(x10^{-5})*	**E_a** *(kcal.mol^{-1})*	**$\Delta S^‡$** *(J.K^{-1}.mole^{-1})*	**$\Delta H^‡$** *(kJ.mol^{-1})*	**$\Delta G^‡_{20}$** *(kJ.mol^{-1})*	**$K^‡$** *(x10^{-5})*	**ΔW^{10}**	**$\Delta E_{disp}{}^{10}$** *(kJ.mol^{-1})*
[$P_{6,6,6,14}$][Cl]	43.8	574	1	1.04	71.51	-96.13	59.76	87.93	2.47	1.4	-46.00
[$P_{6,6,6,14}$][NTf2]	46.1	574	1.9	1.39	84.94	-14.59	82.39	86.66	7.28	0.7	0.00

5.4 Conclusions

The investigation of the formation of even smaller scale, atom-centered inter-ion interactions that mediate the formation of the nano-structures and their contribution to the properties the liquids has allowed greater understanding of the discrete features which contribute to the formation of ionic liquids unique effects. The ability to influence structuring, and thus control the transport properties, could allow for the creation of novel liquids with more predictable properties. In the present study computed electronic structures suggest that non-covalent ion-ion electrostatic and van der Waals's interactions promote the formation of liquid ion pairs in phosphonium based ILs. When ions have dense concentrated charges (e.g the chloride anion) tightly bound liquid ion pair systems are generated leading to liquids that exhibit atypical, off-Walden plot, ionic liquid properties. In contrast, larger molecular anions such as $[NTf_2]^-$ have a more diffuse charge distribution, which gives weaker liquid ion pairing and so a more typical ionic liquid system. In addition to this, the actual size of the anion compared to that of atomic anions such as chloride would also result in more diffuse interactions. The experimental measurement of physical properties in the liquids via addition of the photo-chromic spriropyran probe molecule yielded thermodynamic and kinetic data that supported the theoretical models. The simulations and experiments imply that the zwitterionic form of the probe may be unable to significantly disrupt ionic liquid nano-structuring in phosphonium-based ILs. It is proposed that the calculated IL-probe complexation energy may not be sufficient to surmount the barrier to disruption of the extended alkyl chain network, a hypothesis supported by the calculated electronic structures, physicochemical experiments and known diffusion and Walden plot behaviour.

It may be anticipated that rational engineering will allow the use of systems that incorporate the balance between polar and non-polar interactions into their molecular design. For example, ionic liquid nano-structuring may be ruptured by (a) the introduction of more polar headgroups that would allow switching from the moderate to strong headgroup-mediated probe stabilisation coupled with (b) shorter non-polar tails to switch from the large to moderate hydrophobic tail-mediated diffusion barrier. While route (a) could possibly be controlled dynamically via *in situ* electrochemical shifts, the ionic liquid hydrophobic tails, route (b), may serve as the first point for rational design of IL solvents that strongly influence molecular photochromism, given that the electrostatic interactions that stabilise the zwitterionic probe also promote IL nano-structuring (in a three-site anion-zwitterion-cation "tug-of-war"). Consequently, tuning of charged sites will require careful consideration of all ion-ion and IL-probe interactions.

The formation of Liquid Ion Pairs therefore appears to be a critical precursor to the formation of ionic liquid structure and thus the unique and favourable bulk properties associated with this class of solvents. Prediction of the strengths of ion-pair interactions could therefore possibly be used to predict liquid properties and tailor solvent structure to produce task specific liquids and control the 'ionicity' of ionic liquids. The ability to compromise this 'ionicity' through the formation of solvent-solute interactions may also prove to be a key design feature of next-generation photo-rheological systems will be the incorporation of ionic materials that can make and break multi-site interactions, in a controllable manner (such as light) via switchable polar and/or non-polar interactions, to create probe-sensitive changes in conductivity and viscosity.

5.5 References

1. D. R. MacFarlane, M. Forsyth, E. I. Izgorodina, A. P. Abbott, G. Annat and K. Fraser, *Physical Chemistry Chemical Physics*, 2009, **11**, 4962-4967.
2. J. P. Hallett, C. L. Liotta, G. Ranieri and T. Welton, *ECS Transactions*, 2009, **16**, 81-87.
3. S. P. Coleman, R. Byrne, S. Minkovska and D. Diamond, *Physical Chemistry Chemical Physics*, 2009, **11**, 5608-5614.
4. R. Byrne, S. Coleman, K. J. Fraser, A. Raduta, D. R. MacFarlane and D. Diamond, *Physical Chemistry Chemical Physics*, 2009, **11**, 7286-7291.
5. R. Byrne, K. J. Fraser, E. Izgorodina, D. R. MacFarlane, M. Forsyth and D. Diamond, *Physical Chemistry Chemical Physics*, 2008, **10**, 5919-5924.
6. C. S. Consorti, P. A. Z. Suarez, R. F. de Souza, R. A. Burrow, D. H. Farrar, A. J. Lough, W. Loh, L. H. M. da Silva and J. Dupont, *The Journal of Physical Chemistry B*, 2005, **109**, 4341-4349.
7. K. Iwata, H. Okajima, S. Saha and H.-o. Hamaguchi, *Accounts of Chemical Research*, 2007, **40**, 1174-1181.
8. T. Pott and P. Meleard, *Physical Chemistry Chemical Physics*, 2009, **11**, 5469-5475.
9. J. N. A. Canongia Lopes and A. A. H. Padua, *The Journal of Physical Chemistry B*, 2006, **110**, 3330-3335.
10. K. J. Fraser, E. I. Izgorodina, M. Forsyth, J. L. Scott and D. R. MacFarlane, *Chemical Communications*, 2007, 3817-3819.
11. M. J. Frisch, G. W. Trucks, H. B. Schlegel, G. E. Scuseria, M. A. Robb, J. R. Cheeseman, J. J. A. Montgomery, T. Vreven, K. N. Kudin, J. C. Burant, J. M. Millam, S. S. Iyengar, J. Tomasi, V. Barone, B. Mennucci, M. Cossi, G. Scalmani, N. Rega, G. A. Petersson, H. Nakatsuji, M. Hada, M. Ehara, K. Toyota, R. Fukuda, J. Hasegawa, M. Ishida, T. Nakajima, Y. Honda, O. Kitao, H. Nakai, M. Klene, X. Li, J. E. Knox, H. P. Hratchian, J. B. Cross, V. Bakken, C. Adamo, J. Jaramillo, R. Gomperts, R. E. Stratmann, O. Yazyev, A. J. Austin, R. Cammi, C. Pomelli, J. W. Ochterski, P. Y. Ayala, K. Morokuma, G. A. Voth, P. Salvador, J. J. Dannenberg, V. G. Zakrzewski, S. Dapprich, A. D. Daniels, M. C. Strain, O. Farkas, D. K. Malick, A. D. Rabuck, K. Raghavachari, J. B. Foresman, J. V. Ortiz, Q. Cui, A. G. Baboul, S. Clifford, J. Cioslowski, B. B. Stefanov, G. Liu, A. Liashenko, P. Piskorz, I. Komaromi, R. L. Martin, D. J. Fox, T. Keith, M. A. Al-Laham, C. Y. Peng, A. Nanayakkara, M. Challacombe, P. M. W. Gill, B. Johnson, W. Chen, M. W. Wong, C. Gonzalez and J. A. Pople, *Gaussian 03 Revision C.02*, (2004) Gaussian Inc, Wallingford, CT.
12. A. D. Becke, *The Journal of Chemical Physics*, 1993, **98**, 5648-5652.
13. P. F. Flükiger, *Molekel: Molecular Visualisation Software*, University of Geneva Geneva.
14. A. E. Reed, R. B. Weinstock and F. Weinhold, *The Journal of Chemical Physics*, 1985, **83**, 735-746.
15. E. I. Izgorodina, U. L. Bernard and D. R. MacFarlane, *The Journal of Physical Chemistry A*, 2009, **113**, 7064-7072.

16. I. G. Kaplan, *Intermolecular Interactions: Physical Picture, Computational Methods and Model Potentials*, John Wiley & Sons Ltd, Chichester, 2006.
17. A. K. Burrell, R. E. D. Sesto, S. N. Baker, T. M. McCleskey and G. A. Baker, *Green Chemistry*, 2007, **9**, 449-454.
18. C. B. Aakeroy, T. A. Evans, K. R. Seddon and I. Páinkó, *New Journal of Chemistry*, 1999, **23**, 145-152.
19. P. J. Newman and D. R. MacFarlane, *Zeitschrift für Physikalische Chemie*, 2006, **220**, 1473–1481.
20. Cytec, *CYPHOS IL 101 phosphonium ionic liquid*, 2005.
21. Cytec, 2005.
22. J. U. Calderon, B. Lennox and M. R. Kamal, *Applied Clay Science*, 2008, **40**, 90-98.
23. P. Hunt, A., B. Kirchner and T. Welton, *Chemistry - A European Journal*, 2006, **12**, 6762-6775.
24. O. Hofft, S. Bahr, M. Himmerlich, S. Krischok, J. A. Schaefer and V. Kempter, *Langmuir*, 2006, **22**, 7120-7123.
25. K. Kanai, T. Nishi, T. Iwahashi, Y. Ouchi, K. Seki, Y. Harada and S. Shin, *Journal of Electron Spectroscopy and Related Phenomena*, 2009, **174**, 110-115.
26. C. D. Bain, E. B. Troughton, Y. T. Tao, J. Evall, G. M. Whitesides and R. G. Nuzzo, *Journal of the American Chemical Society*, 1989, **111**, 321-335.
27. G. Gannon, J. A. Larsson, J. C. Greer and D. Thompson, *Langmuir*, 2008, **25**, 242-247.
28. D. J. Abdallah, R. E. Bachman, J. Perlstein and R. G. Weiss, *The Journal of Physical Chemistry B*, 1999, **103**, 9269-9278.
29. J. Dupont, *Journal of the Brazilian Chemical Society*, 2004, **15**, 341-350.
30. B. I. Ipe, S. Mahima and K. G. Thomas, *Journal of the American Chemical Society*, 2003, **125**, 7174-7175.
31. R. Byrne, S. Coleman, S. Gallagher and D. Diamond, *Physical Chemistry Chemical Physics*, 2010, **12**, 1895-1904.
32. C. Chiappe, M. Malvaldi and C. S. Pomelli, *Pure and Applied Chemistry*, 2009, **81**, 767-776.

6

Integration Effects of a Novel Photo-Functional Spiropyran Cation upon Imidazolium Based Ionic Liquid Nanostructures

6.1 Introduction

Following the interesting interactions of spiropyran in ionic liquids related to their migration within structured domains, it is proposed that integration of the spiropyran into the liqid structure itself may allow for the formation of liquids with photoswitchable properties. Several groups have proposed the synthesis of 'task specific ionic liquids' based upon such liquids.[1-3] Ohno reviewed the functional design of ionic liquids.[4] Of particular interest was the use of zwitterionic compounds to form ionic liquids.[5] Preceeding Chapters investigating structuring within ionic liquids employed zwitterion forming spiropyran derivatives with polar and non-polar functional groups to encourage specific location within the liquid domains.[6] It was found that the interactions with the ions allowed for the spiropyran moiety to be located in distinctly different regions and report on them through thermodynamic and kinetic parameters. Following these studies and the ability to form zwitterionic liquids it is therefore intuitive to attempt to produce similar liquids using spiropyran with a functional group compatable with the ionic liquid ions to allow integration into the liquid structure.The effect of integration by a novel spiropyran derivative, **SP$_{\mathbf{Im}}$** compound into the ionic liquid structure was examined and compared to **BSP**.

The **MC-SP** isomerisation of both **BSP/SP$_{\mathbf{Im}}$** provides distinctive polar and non-polar systems dependent upon the form of the spirocyclic molecule. As thermal relaxation occurs, the **MC$_{\mathbf{BSP}}$** is believed to migrate from polar regions, to non-polar regions, as the charged isomer reverts to its **BSP** form. This diffusion effect has been observed by spectroscopic monitoring of lipid bilayers in water.[7] The similarity between this ordering and the proposed ordering of imidazolium based ILs makes this migration process another possible method to examine the existence nano-structuring and their effects on photochromic systems. Ionic liquids are believed to form distinct nano-domains containing both polar and non-polar regions. It is proposed that the dispersion and corresponding expansion of polar regions arising from dissociation of imidazolium head groups by alkyl side-chains mediates the structure of ionic liquids which in turn regulates the stabilisation of the $\mathbf{MC_{BSP}}$. Since the **MC** isomer is believed to interact with polar regions, changes to the liquid structure (increasing side-chain lengths for example) could possibly influence the equilibrium by favouring the a particular form of the molecule.

Chapter 4 investigated the application of designer molecular probes to locate themselves within specific nano-domains to examine the properties of each. The following study expands upon this basis using a specialised molecule, imidazolium functionalised spiropyran, $\mathbf{SP_{Im}}$. It is hypothesised that the imidazolium functional group attached to the spiropyran may interact and possible integrate into the ionic liquid nano-structure. The imidazolium group should, in theory, associate and order itself within these polar nano-structured regions of the ionic liquid, and thus orientate the spiropyran fragment into the non-polar region. This integration should in theory produce an inherently photoswitchable ionic liquid as the photochromic compound is now essentially a component of the ionic liquid itself. Furthermore, the integration of the imidazolium group may associate the spiropyran fragment within the non-polar region of the ionic liquid nano-structure which is not favourable for **MC** formation while simultaneously inhibiting its ability to migrate between regions of the ionic liquid.

BSP has minimal complimentary associations with the IL structure and so is believed to be relatively free to migrate between polar and non-polar domains upon photoswitching. The ionic liquid structure may therefore be somewhat preserved since the **BSP** molecules are able to interact within the existing nano-structured domains of the liquid. Thermodynamic and kinetic studies were carried out to examine the effect the integration of the photochromic compound into the ionic liquid structure has upon on rates of thermal relaxation, solvent reordering and the overall stability/equilibrium of both forms of the spiropyran derivatives. Cations with increasing chain lengths as found in Chapter 3 were chosen to examine the effect of increasing cation-cation interactions and dispersion of polar regions as proposed by Lopes *et al*[8] upon the thermodynamic and kinetic parameters of the integrated $\mathbf{SP_{Im}}$ molecules and comparison to **BSP** from similar experiments[9]

6.2 Experimental

Ionic liquids were synthesised and purified by metathesis of imidazolium cation and bis(trifluorosulfonyl)imide salts ($[C_4mIm]^+$-$[C_{12}mIm]^+$ and $[NTf_2]^-$) obtained from Sigma-Aldrich using previously reported techniques.[10] Ionic liquids were stored under argon due to the hygroscopic nature of these liquids. Spectrometric studies were carried out using a Perkin Elmer Lambda 900 spectrometer (Foss Ireland) with Perkin Elmer PTP-1 temperature controller. Samples were irradiated with UV light at 375 nm by UV LEDs (Roithner Lasertechnik, Vienna, Austria). Conductivity measurements were determined by electrochemical impedance between 10 MHz and 0.1 Hz on a Solartron SI 1296 Dielectric interface and Solartron SI 1270 frequency response analyzer. Viscosity measurements were determined using an Anton Paar AMVn rolling ball viscometer. 6-nitro-1',3',3'-trimethylspiro[2H-1-benzopyran-2,2'-indolin] 1',3'-dihdro-1',3',3'-trimethyl-6-nitrospiro (**BSP**) (Sigma-Aldrich chemicals) was used as purchased and used with no further purification. Additional synthesis and characterisation was supplied in Appendix A-3.

6.3 Results and discussion

6.3.1 Solvatochromic Properties

Samples were analysed at 298K in a temperature controlled UV-Vis spectrometer and irradiated at 375nm to induce ring opening and **MC** formation. **BSP** compounds were previously found to be solvatochromic due to solvent-solute interactions and resulting in the ability to estimate the solvent polarity based upon the extent of the shift observed (figure 6.1). Both probes exhibited about 10nm shifts on increasing side chain length from 4 carbons to 12. The similarity of solvatochromic shifts for each probe is believed to be due to the **MC** forms observing similar environments within each IL and that each spiropyran derivative locates in a specific region within the ionic liquids. Slight shifts in **MC** λ_{max} are believed to be due to increasing influence of the surrounding non-polar side chains upon the stabilisation of the **MC** charge sites.

MC λ_{max} of $\mathbf{SP_{Im}}$ is observed to be red shifted to around 576 nm which would indicate that the region the compound was experiencing is non-polar (table 6.1) This agreements with the postulation that $\mathbf{SP_{Im}}$ is unable to migrate between the IL nano-structured domains due to its imidazolium cation functional group. The integration of this functional group into the liquid structure is believed to restrict the compound and the ordering within the liquid would be expected to arrange the photoswitchable fragment within the non-polar side chain domains. **BSP** however is believed to be free to migrate between these regions depending on whether the **SP** or **MC** isomer is predominant (**SP** preferring non-polar regions, **MC** preferring polar regions) and so can position itself in regions within the liquids which best suit the form of the compound and stabilisation of each form.

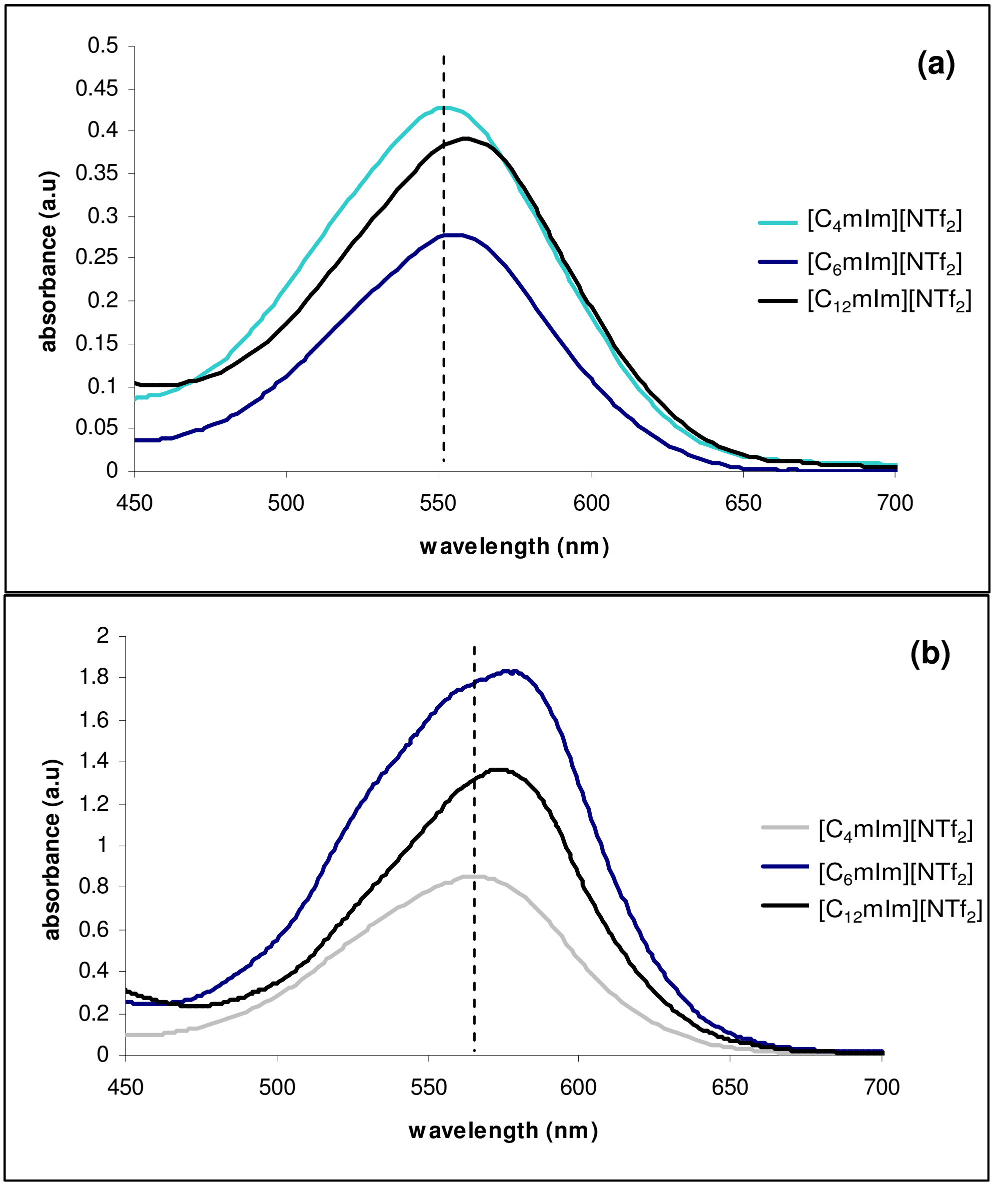

Figure 6.1 UV-Vis spectra showing solvatochromic shift of **MC** form of (a) **BSP** and (b) **SP**$_{\mathbf{Im}}$. Samples irradiated for 30 seconds at 375nm at 298K.

6.3.2 Kinetic Parameters

After irradiation, the resulting first order decay curves (figure 6.2) were analysed using equation (**14**) (chapter 2, section 2.3.2) to determine the rates of thermal relaxation, *k*, at 298 K (table 6.2). Rates are found to be approximately an order of magnitude faster and relatively constant for $\mathbf{SP_{Im}}$ at around $13.5\text{x}10^{-3}\text{s}^{-1}$ in each of the ILs, compared to that of **BSP** which had rates slightly increasing from $1.0\text{x}10^{-3}\text{s}^{-1}$ to $2.0\text{x}10^{-3}\text{s}^{-1}$ from [C_4mIm][NTf_2] to [C_{12}mIm][NTf_2]. Once again, these results can be interpreted in terms of its ability to migrate between the IL nano-structured regions. As **BSP** is believed to be relatively mobile it can migrate to more polar regions within the ILs and thus stabilise the charge sites through electrostatic interactions and hydrogen bonding to the phenolate oxygen.[11] The increase in rate constants for $\mathbf{MC_{BSP}} \rightarrow \mathbf{SP_{BSP}}$ may be due to the cation inter-chain interactions, which at longer side-chain lengths, are believed to put strain upon the mutual interactions of the polar head groups. The result is that the weakened polar regions dissociate, reducing the overall charge density within the region to accommodate the solute molecules in addition to the region being expanded by the solute itself upon its introduction.[12-14] This would lead to a reduction in the liquid's polar region to facilitate the $\mathbf{MC_{BSP}}$ and stabilise the compound in this form. The large increase in relaxation rates observed for $\mathbf{SP_{Im}}$ (approx $13.5\text{x}10^{-3}\text{s}^{-1}$) is believed to be attributed to the functionalisation of spiropyran with the imidazolium ring. The ring would be expected to associate with the neighbouring rings through π-stacking, anion-cation associations and hydrogen bonding. As a result, the spiropyran fragment would be expected to become located within the non-polar regions of the ionic liquid through organisation similar to that seen in the bulk liquid where head group interaction results in the remaining side chains organising into separate domains.

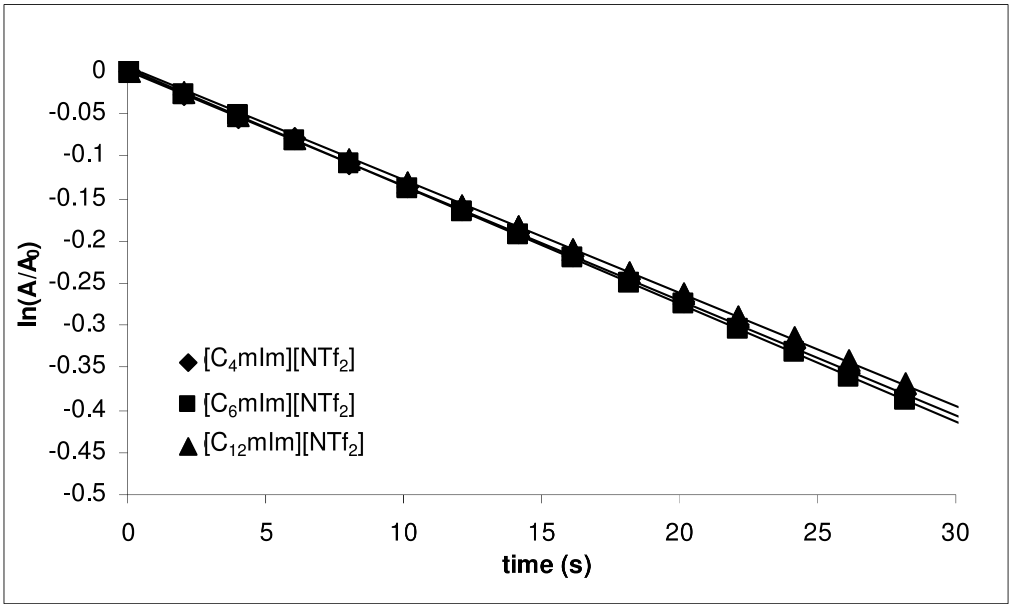

Figure 6.2 First order plots of thermal relaxation on $\mathbf{SP_{Im}}$ in imidazolium based ILs.

Non-polar molecular solvents shift the equilibrium of spiropyran to its closed form due to lack of charge stabilisation and similar effects are seen for $\mathbf{MC_{SPIm}}$ with the aliphatic side-chains of the ionic liquids with resulting order of magnitude increase in kinetics would appear to support this reasoning. In addition to the large increase in rates of thermal relaxation it is also found that the rate of relaxation did not vary significantly; remaining at around $13.5\text{x}10^{-3}\text{s}^{-1}$ for each ionic liquid with for $\mathbf{SP_{Im}}$. This differed from **BSP** with rates observed to double from $1\text{x}10^{-3}\text{s}^{-1}$ to $2\text{x}10^{-3}\text{s}^{-1}$ from [C_4mIm][NTf_2] to [C_{12}mIm][NTf_2] respectively. If $\mathbf{SP_{Im}}$ is immobilised within the non-polar regions of the ionic liquids then the environment it observes has little variation beyond increasing chain lengths which is not detected by the molecules and so the level of interaction remains similar in each ionic liquid.

BSP appears to retain the ability to migrate within the regions resulting in a compound that is more sensitive to the subtle changes in liquid structuring. Since **MC$_{\mathbf{BSP}}$** will preferentially associate with polar regions, changes in the system are believed to affect these regions which would in turn be expected to alter the relaxation of the compound to its closed form. As side chain length increases and polar regions become dispersed this decreases their ability to interact and stabilise the **MC$_{\mathbf{BSP}}$** to the same extent. Also, as side chain lengths increase it would be expected that the increasing size of the non-polar regions would have an increasing attraction to the relaxing molecules (which are returning to the uncharged spiro form) and facilitate faster closure.

6.3.3 Thermodynamic Parameters

Thermodynamic properties were determined by Arrhenius and Eyring plots (figure 6.3) based upon equations **(11)**, **(12)**, **(13)** and **(14)** (chapter 2, section 2.3.2) allowed for the manipulation of the Eyring dependency to derive the transition state equilibrium.[15] Samples were heated between 283K and 303K and results are summarised in table 1. **BSP** values were determined previously in Chapter 3.[11]

The entropy of activation, $\Delta S^{\ddagger}$ values for both derivatives were found to increase with chain length. **BSP** values are found to be larger, ranging from 13.79 - 46.15kJ.mol^{-1}, compared to **SP$_{\mathbf{Im}}$** with values of -7.86 to 29.87kJ.mol^{-1} and overall reductions in $\Delta S^{\ddagger}$ of around 10-15 J.K.mol^{-1} in each IL for the latter. The slight negative entropy of activation is observed for **SP$_{\mathbf{Im}}$** in [C$_4$mIm][NTf$_2$] of -7.86kJ.mol^{-1} implies that the IL-**SP$_{\mathbf{Im}}$** systems are more rigid than that of **BSP** and this complied with the initial hypothesis that the imidazolium fragment of **SP$_{\mathbf{Im}}$** integrated into the cation ordering of the ILs. This integration into the system initially adds rigidity by becoming part of the liquid structure itself while the tethering of the spiropyran fragment to the cation ensured that any diffusion properties of the spiropyran fragment were limited or eliminated. Locating the spiropyran fragment in the non-polar region also reduced the ability of the **MC** form to interact with polar regions and thus reducing the polar region reorientations observed in response to such interactions.

Table 6.1 Physicochemical properties of **BSP** and **SP$_{\mathbf{Im}}$** compounds in molecular solvents and ionic liquids. **BSP** values from Chapter 3.[11]

BSP

				Arrhenius		*Eyring*			
IL	*λ_{max} MC (nm)*	*k_{25} ($x10^{-3}$ s^{-1})*	*ET_{30} ($kcal.mol^{-1}$)*	*E_a ($kJ.mol^{-1}$)*	*A*	*$\Delta S^{\ddagger}$ ($J.K^{-1}.mol^{-1}$)*	*$\Delta H^{\ddagger}$ ($kJ.mol^{-1}$)*	*$\Delta G^{\ddagger}_{25}$ ($kJ.mol^{-1}$)*	*$K^{\ddagger}$ ($x10^{-16}$)*
$[C_4mIm][NTf_2]$	552	1.0	52.4	96.93	8.71×10^{13}	13.79	94.49	90.38	1.65
$[C_6mIm][NTf_2]$	554	1.0	53.3	98.84	2.67×10^{14}	21.48	96.41	90.01	1.65
$[C_8mIm][NTf_2]$	556	1.7	51.2	103.34	2.18×10^{15}	40.55	100.90	88.82	2.71
$[C_{10}mIm][NTf_2]$	558	1.8	51.6	106.68	1.02×10^{16}	52.42	104.24	88.62	2.96
$[C_{12}mIm\ ][NTf_2]$	559	2.0	51.2	105.27	5.73×10^{15}	46.15	102.14	88.39	3.22

SP$_{\mathbf{IM}}$

				Arrhenius		*Eyring*			
IL	*λ_{max} MC (nm)*	*k_{25} ($x10^{-3}$ s^{-1})*	*ET_{30} ($kcal.mol^{-1}$)*	*E_a ($kJ.mol^{-1}$)*	*A*	*$\Delta S^{\ddagger}$ ($J.K^{-1}.mol^{-1}$)*	*$\Delta H^{\ddagger}$ ($kJ.mol^{-1}$)*	*$\Delta G^{\ddagger}_{25}$ ($kJ.mol^{-1}$)*	*$K^{\ddagger}$ ($x10^{-15}$)*
$[C_4mIm][NTf_2]$	564	13.5	52.4	83.84	6.45×10^{12}	-7.86	81.40	83.75	2.17
$[C_6mIm][\ NTf_2]$	572	13.9	53.3	88.72	4.87×10^{13}	8.96	86.28	83.61	2.23
$[C_8mIm][\ NTf_2]$	572	14.6	51.2	96.70	1.35×10^{15}	36.58	94.26	83.36	2.35
$[C_{10}mIm][\ NTf_2]$	576	13.6	51.6	95.72	8.22×10^{14}	32.45	93.29	83.62	2.19
$[C_{12}mIm][\ NTf_2]$	574	13.3	51.2	95.33	7.96×10^{14}	29.87	92.90	84.00	2.14

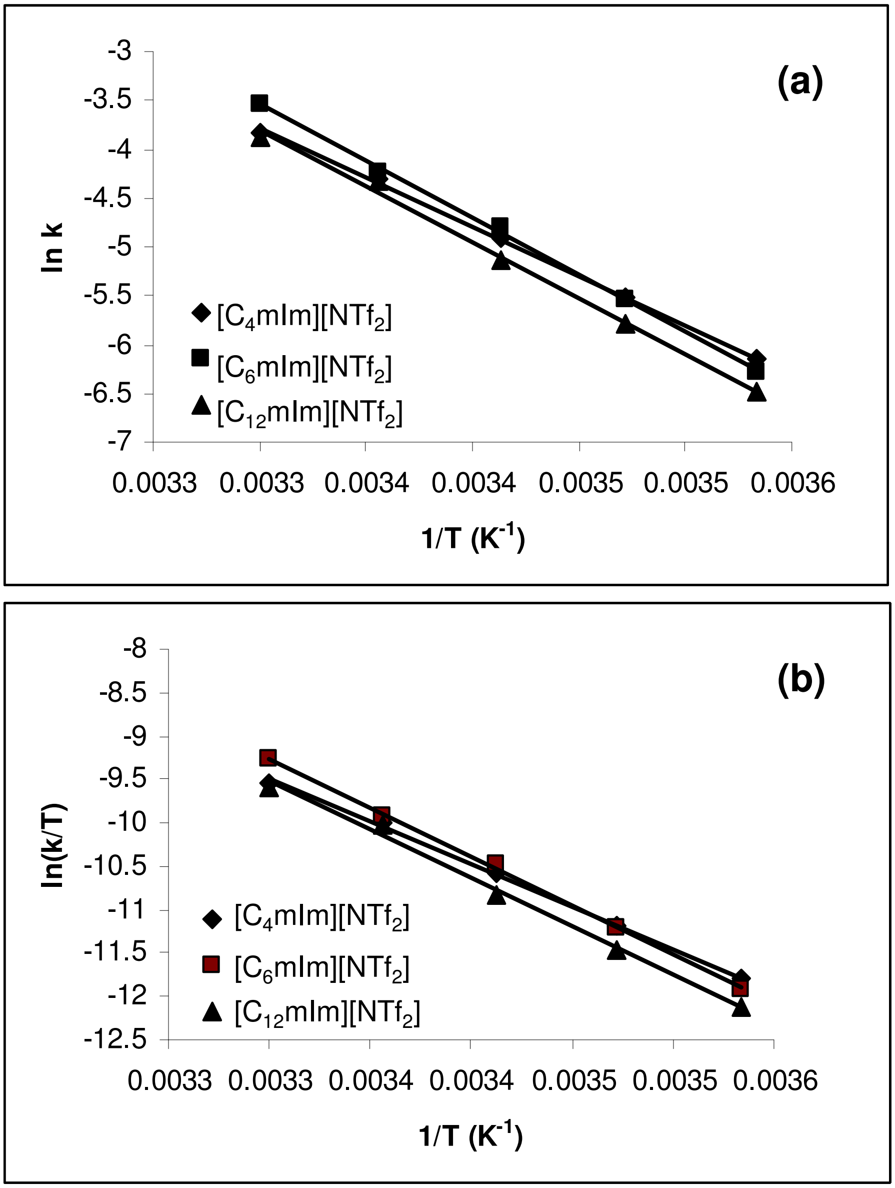

Figure 6.3 Arrhenius (a) and Eyring (b) plots of **SP$_{Im}$** in imidazolium based ILs.

Similarly, activation energies (E_a) are found to decrease about 10 kJ.mol^{-1} when the imidazolium fragment is introduced to the spiropyran molecule (table 6.1). **BSP** is found exhibit activation energies ranging from 96.93 – 105.27 kJ.mol^{-1} while **SP$_{Im}$** has lower energies at 83.84 – 85.33kJ.mol^{-1} for [C_4mIm][NTf_2] to [C_{12}mIm][NTf_2] respectively. Reduction in energies at transition states would imply that much of the solvent interaction had occurred at equilibrium upon integration into the ionic liquid due to **SP_{Im}** becoming immobilised within the liquid nano-structure. The thermal relaxation process that follows therefore involves less interaction of the between **MC_{SPIm}** and the IL ions and therefore the energy barriers observed where not as large as those seen for the thermal relaxation of **MC_{BSP}.** Since **BSP** is free to move within the ionic liquid structure, allowing the molecules to interact to a certain degree with the polar regions at equilibrium. The ring opening process may also result in the formation of solvent-solute interactions which did not exist when **BSP** is in its closed form. These interactions therefore create increased stabilisation and increased energy barriers to be overcome during the thermal relaxation process. Interestingly the reduction in activation energies are relatively small when compared to the resulting increase in rates of thermal relaxation between **BSP** and **SP_{Im}**. This may indicate that the spiropyran molecule is sensitive to such energy requirements and the influence of such barriers may be critical to the control of thermal relaxation and thus stabilisation of the photochromic compounds in either form. Lower enthalpies of activation $\Delta H^{\ddagger}$ and Gibbs energy of activation $\Delta G^{\ddagger}$ of about 10 $kJ.mol^{-1}$ and 5 $kJ.mol^{-1}$ respectively are also observed in **SP_{Im}** when compared to BSP (table 6.1). For $[C_6mIm][NTf_2]$ **SP_{Im}** was found to have a $\Delta H^{\ddagger}$ of $86.28kJ.mol^{-1}$ compared to $96.41kJ.mol^{-1}$ for **BSP** and $\Delta G^{\ddagger}$ values of $83.61kJ.mol^{-1}$ and $90.01kJ.mol^{-1}$ respectively. Since these parameters are analogous to that of activation energy, such reductions would be exepected and provided further insight into the system's overall role in the relaxation process.

The equilibrium of activation, $K^{\ddagger}$,was examined for both **MC** forms to determine the stability of the charged forms of the derivatives and their ability to return to the more stable ground state/closed forms. **SP$_{\mathbf{Im}}$** is found to exhibit $K^{\ddagger}$ values an order of magnitude larger than the equivalent **BSP** indicating that **SP$_{\mathbf{Im}}$** favours conversion to the **SP** form from the transition state more than **BSP** (table 6.1). For example, in [C_6mIm][NTf_2] $K^{\ddagger}$ is found to be $2.23x10^{-15}$ for **SP$_{\mathbf{Im}}$** and 1.65x10-16 for **BSP**. This further supports the hypothesis that the ability to migrate freely within the ILs is critical for stabilisation of the **MC/SP** form. Integrating **SP$_{\mathbf{Im}}$** in the cation-cation association structures and the resulting restriction of the spiropyran molecule produces unfavourable conditions for **MC$_{\mathbf{SPIM}}$** formation which in turn shifted the equilibrium towards the closed form. $K^{\ddagger}$ values agree with such hypothesis with equilibrium of activations around ten times larger for **SP$_{\mathbf{Im}}$** than that of **BSP**. Such values imply that at the transition state the solvent-solute interactions are less for **SP$_{\mathbf{Im}}$** than **BSP** which results in less stabilisation of the **MC$_{\mathbf{SPIM}}$** form.

6.3.5 High concentration effects

Addition of 1 mol% of each derivative to the ILs allows for optical determination of the extent of solvent-solute interactions and equilibrium effects (figure 6.4). The addition of the imidazolium side chain in **SP$_{\mathbf{Im}}$** and its restrictive properties upon the spiropyran fragment is confirmed by the formation of colourless/yellow liquids which indicates that the **SP$_{\mathbf{Im}}$** exists primarily in the **SP** form of the compound due to the established lack of solvent mediated stabilisations by the non-polar side-chains and the spiropyran fragment.

Figure 6.4 Equilibrium of each derivative clearly visible. **BSP** is stabilised towards its coloured **MC** form while **SP**$_{\mathbf{Im}}$ exists in its closed, colourless **SP** form.

BSP in imidazolium based ILs is found to exist in its coloured **MC**$_{\mathbf{BSP}}$ form indicating that **MC** stabilisation in the polar regions enhances the open form of the compound. Since **BSP** is free to associate with all regions within the ionic liquid depending on the form (**BSP**↔**MC**) it is possible that the compound could easily associate at specific locations within the liquid which would stabilise the compound. As shown previously, the attraction to charged/polar regions would be greater than that of the non-polar domains since specific interactions such as hydrogen bonding present in the polar regions would be greater than that of diffuse/non-specific van der Waals forces and thus encourage ring opening.[16]

The effects observed are similar to those found for spiropyran compounds in polar protic molecular solvents.[17] Non-polar solvents are found to enhance the formation of the closed form at equilibrium while the rates of thermal relaxation are quite large. Conversely, in polar solvents the stabilization of the **MC** form results in increased lifetimes of this form and measurable concentrations of **MC** at equilibrium. However, in molecular solvents, such shifts in equilibrium are only observed in each case by changing the molecular solvent itself. In the case of ionic liquids, the changes were observed within the same ionic liquid in each case. It is believed that this is due to the differing interactions the spiropyran derivatives experience within the liquids and thus influence which region the spirocyclic component resides in. This agrees with the proposed migration of spiropyran between the regions of the ionic liquids and further supports the existence of such nano-structuring within the ionic liquids. Interestingly, such large shifts in the equilibrium of the photochromic compounds may provide insight into the creation of photoswitchable systems with enhanced lifetimes of both closed and open states. The addition of tailored functional groups may allow the compounds to be 'trapped' within the ionic liquid region of choice extending the existence of either form for longer periods of time. The irradiation of UV/visible light could provide the energy required to switch between each state and locate the compound in specific regions thereby stabilising the particular isomer. Functional groups could then interact with the reciprocal regions thus 'hooking' the spiropyran molecules to the region of initial affinity and limit the diffusional effects of the molecules, extending the lifetimes of each form.[6]

6.3.5 Viscosity and conductivity effects

Addition of higher concentrations of the spiropyran derivatives (1mol%) also allows for the effect of photoswitching upon ionic liquid viscosity and conductivity to be examined (table 6.2). Previous studies of **BSP** in phosphonium based ILs at similar and higher concentrations (5mol%) have found that the introduction and photoswitching of the compound can result in light mediated rheological and conductivity changes to the ionic liquids themselves.[18] The addition of spirocyclic compounds to ionic liquids is believed to induce disruption of the liquid structure due to the bulky nature of the photochromic compound. It has been suggested that the anion-cation association within polar regions form worm-like ion channels[8]. Photoswitching of spirocyclic compounds and the resulting migration of the compound into these domains could therefore be disrupting these sensitive structures critical to the physical properties of the ionic liquids and so inducing changes in viscosity and conductivity. Positive $\Delta S^{\ddagger}$ values imply that solvent reoganisation occurs upon **MC** formation which supports the belief that photoswitching the compound would further affect the overall properties of the ionic liquids and their structuring. $\Delta S^{\ddagger}$ values are found to be consistently lower for **SP$_{Im}$** which implies that the system observed is more rigid. Since the photoswitchable moiety is immobilised within the cation structure, it would be expected that the molecules are restricted and unable to migrate between domains and so results in less disruption. Comparison of **BSP** and **SP$_{Im}$** can therefore determine the proposed importance of the restriction/freedom of solute migration upon the physical properties of ionic liquids.

Table 6.2 Rheological properties of imidazolium based ILs containing **BSP** and **SP$_{Im}$**

	BSP					**SP$_{Im}$**			
IL	η *(mPa.s)*	*% change*	σ *(Scm^{-1})*	*% change*	**IL**	η *(mPa.s)*	*% change*	σ *(Scm^{-1})*	*% change*
C_4mIm NTf$_2$	50.91	-	3.97x10^{-3}	-	***C_4mIm NTf$_2$***	50.91	-	3.97x10^{-3}	-
1mol% SP	50.73	-0.4	3.92x10^{-3}	-1	*1mol% SP*	52.51	+3	3.8x10^{-3}	-3
1mol% MC	50.2	-1	3.93x10^{-3}	-1	*1mol% MC*	52.67	+3	3.88x1^{-3}	-2
C_6mIm NTf$_2$	64.28	-	2.25x10^{-3}	-	***C_6mIm NTf$_2$***	64.28	-	2.25x10^{-3}	-
1mol% SP	67.89	+6	2.14x10^{-3}	-5	*1mol% SP*	67.87	+6	2.07x10^{-3}	-8
1mol% MC	66.37	+3	2.08x10^{-3}	-8	*1mol% MC*	67.88	+6	2.03x10^{-3}	-10
C_8mIm NTf$_2$	93.47	-	1.28x10^{-3}	-	***C_8mIm NTf$_2$***	93.47	-	1.28x10^{-3}	-
1mol% SP	94.7	+1	1.22x10^{-3}	-5	*1mol% SP*	91.14	-2	1.20x10^{-3}	-6
1mol% MC	94.3	+1	1.19x10^{-3}	-7	*1mol% MC*	91.93	-2	1.17x10^{-3}	-9
C_{10}mIm NTf$_2$	119.85	-	8.31x10^{-4}	-	***C_{10}mIm NTf$_2$***	119.85	-	8.31x10^{-4}	-
1mol% SP	117.02	-2	7.75x10^{-4}	-7	*1mol% SP*	112.2	-6	9.35x10^{-4}	+13
1mol% MC	114.36	-5	7.51x10^{-4}	-10	*1mol% MC*	111.92	-7	9.50x10^{-4}	+14
C_{12}mIm NTf$_2$	151.37	-	5.86x10^{-4}	-	***C_{12}mIm NTf$_2$***	151.37	-	5.86x10^{-4}	-
1mol% SP	144.85	-4	6.11x10^{-4}	+4	*1mol% SP*	-	-	4.50x10^{-4}	-23
1mol% MC	143.29	-5	5.29x10^{-4}	-10	*1mol% MC*	-	-	4.61x10^{-4}	-21

Analysis of viscosity effects found that negligible changes in the properties are observed upon addition and photoswitching of both **BSP** and **SP_{Im}**. At 1 mol% the concentration of the photoswitchable compound is still relatively small compared to that of the bulk liquid which could result in the liquid itself masking the rheological effects as any changes related to photoswitching would be localised and dispersed within the ionic liquid system. Initial addition of the spiropyran derivatives should result in increased solvent-solute interactions such as hydrogen bonding and electrostatic interactions with the subsequent formation of the **MC** forms further increasing the available sites for said solvent-solute interactions. Such cohesive nature of the interactions should in theory result in a decrease in solvent freedom and the reduction in movement and an increase in viscosity. The lack of apparent changes with photoswitching is most likely again due to 1 mol% concentrations being insufficient to affect the bulk properties of the ionic liquids. This could also explain inconsistencies in results such as slight positive results where negative results were expected. Interestingly, conductivity effects yielded some unexpected results whereby the reduction in conductivity due to **BSP** is smaller than that of **SP_{Im}** introduction. The largest effect for **BSP** is a decrease of around 10% in conductivity in [C_{12}mIm][NTf_2] which is about 13% less that that of **SP_{Im}** in the same ionic liquid. Since **SP_{Im}** is believed to integrate within the ionic liquid structure, it is possible that the extent of **SP_{Im}** ordering and restriction within the liquids may be integral to conductivity effects. **BSP,** with its lack of interactive functional groups is envisaged to have much more freedom within the ionic liquid systems and as such should be able to interact with both polar and non-polar regions more readily than that of the tethered derivative. **BSP** appeared to cause negligible changes to both viscosity and conductivity both with introduction and photoswitching. In contrast, the introduction $\mathbf{SP_{Im}}$ is found to steadily decrease the conductivity of the ionic liquids with increasing side chain lengths. This could be attributed a dispersal of the ion channels with increasing sizes in non-polar domains. The addition of spiropyran, due to its bulky nature, could disrupt the side-chain, van der Waals interactions and as such may 'push' the cations further apart producing a more dispersed ionic liquid system. The augmentation of the ionic liquid nano-structure could result in an increase in anion-cation distances and so lowering the efficiency of electron transfer and the resulting conductivity of the liquid.

The viscosity of the imidazolium based ILs is found to be considerably lower than that of the phosphonium based ILs where photorheological effects were previously observed for **BSP**.[18] Since increasing the side-chain lengths of the imidazolium cations was also found to correspond to an increase in viscosity, the corresponding increase in conductivity effects observed with $\mathbf{SP_{Im}}$ addition may imply that the liquids inherent viscosity is important for the ability to produce or detect such physical changes. In addition to the lower viscosity of the imidazolium based liquids, positive entropies of activation imply that the ions themselves have the ability to move when the derivaties are added and photoswitched within the ionic liquids. This may reduce the ability of the spiropyran derivatives to disrupt the ion channels and the transport system may even be able to 'move around' the spiropyran molecules. As viscosity increases this freedom is reduced and so the introduction of the molecules and their effects become more apparent. Indeed, in $[C_{12}mIm][NTf_2]$ the reduction in conductivity with $\mathbf{SP_{Im}}$ addition is found to be almost 25%.

Changes due to **BSP** were not as large and it is found that the entropies of activation are reduced by around 15 J.K-1.mol^{-1} in $[C_{12}mIm][NTf_2]$ when $\mathbf{SP_{Im}}$ is added compared to **BSP**. This is probably due to the increase rigidity that results from the integration of the $\mathbf{SP_{Im}}$ molecules into the ionic liquid itself and the more direct changes it has upon the liquid structure. Since more impressive photorheological effects produced in previous studies[18] were observed in ionic liquids with far higher viscosities and much more negative entropies of activation, we propose the rigidity of the phosphonium based systems described be these physical and thermodynamic properties allow this class of ionic liquids to exhibit the light mediated properties which cannot be seen in imidazolium based ILs. Finally, the solubility limit of imidazolium based ILs for the spiropyran derivatives is reached at 1 mol% additions and so it is unclear whether concentration increases would have any effect to enhance the photorheological effects such as those found for 5 mol% concentrations of **BSP** in phosphomium based ILs.

6.4 Conclusions

Based upon evidence of structuring within ionic liquids, the extent to which interaction with such ordering could have upon the photoswitching properties of spiropyran derivatives. It was found that the integration of the spirocyclic compound, **SP_{Im}** into the liquid results in a significant shift in equilibrium towards the closed (**SP**) form. This is believed to be due to enhanced interactions between the ionic liquid cations and the imidazolium groups covalently attached to the spiropyran molecules resulted restriction of the compounds movement and permanent orientation of the spiropyran fragment into the non-polar region of the ionic liquid. The compound was unable to move to regions which stabilise the open (**MC**) form and resulted in lower activation energies and faster relaxation times. Such effects would appear to support the existence of nanostructured polar and non-polar domains. Addition of the derivatives to ionic liquids with increasing side-chain length resulted in moderate changes to thermodynamic parameters.

Comparison to ionic liquids containing **BSP** suggests that this molecule may dynamically transfer between the polar and non-polar nano-structured domains within ionic liquids and aid in the stabilisation of each form (**SP/MC**) of the compound. Slower rates of thermal relaxation implied that the **BSP** form was more stabilised than that of **SP_{Im}** and that **BSP** has stronger interactions with the polar regions of the ionic liquids. Thermal relaxation rates were found to be similar for **SP_{Im}** in all of the ionic liquids indicating that the environment showed little variation. **BSP** exhibited increasing rates with chain length which implied that polar regions and the interaction of the compound with non-polar regions was more influential. Equilibria of activation values were similar regardless of the ionic liquid cation chain length for **SP$_{\mathbf{Im}}$**, which suggests that stabilisation effects are similar for each form of the probe molecule in each ionic liquid. This further supported the belief that similar structuring was observed within non-polar regions in each ionic liquid and that the effect of increasing side-chain length may be limited to polar regions. The lack of significant variation in activated complex parameters reinforces this interpretation, as similar interactions would logically result in similar levels of stabilisation of the respective forms of the spirocyclic compound. Positive $\Delta S^{\ddagger}$ values mean that the compound undergoes significant reordering within the solvent system during thermal relaxation. This implies that the spirocyclic probe disrupts the ionic liquid nano-structure and when **BSP** was introduced and positions itself dynamically within each of the nanostructured regions. The process is not observed to the same extent for **SP$_{\mathbf{Im}}$** with lower entropy values found in all ionic liquids. This is believed to be because of the restriction of the molecules due to the integration of the imidazolium functionalisation into the ionic liquid structure. Previous studies have found that phosphonium based ionic liquids present rigid systems with negative entropies of activation, which suggests that the structuring of imidazolium based ILs is due to π-π stacking and various non-specific interactions. This in contrast to that of phosphonium based ILs, whose interactions like van der Waals forces generate stronger inter-molecular bonds, which is reflected in the higher viscosities observed for these ionic liquids. Addition of 1 mol% of spiropyran derivatives to ionic liquids produced minimal rheological effects. Conductivity effects were found to increase significantly (up to 23%) for **SP$_{Im}$** with increasing side chain lengths. Smaller effects were found for **BSP** addition with decreases in conductivity up to 10% found in [C$_{12}$mIm][NTf$_2$] while neither compound was found to endow photoswitchable rheological effects. Slight trends observed for **SP$_{Im}$**-IL systems due to increasing chain length, viscosity and decreases in ionic liquid entropies (compared to **BSP**) may provide insight into the future creation of photoactive rheological fluids similar to those observed in phosphonium based IL systems.

6.5 References

1. A. E. Visser, R. P. Swatloski, W. M. Reichert, R. Mayton, S. Sheff, A. Wierzbicki, J.H. Davis and R. D. Rogers, *Environmental Science & Technology*, 2002, **36**, 2523-2529.
2. H. Ohno and Y. Fukaya, *Chemistry letters*, 2009, **38**, 2-6.
3. L. Elizeo, F. d. S. Wladmir , F. Bauer and D. Jairton, *ChemSusChem*, 2009, **2**, 962-964.
4. H. Ohno, *Bulletin of the Chemical Society of Japan*, 2006, **79**, 1665-1680.
5. A. Narita, W. Shibayama and H. Ohno, *Journal of Materials Chemistry*, 2006, **16**, 1475-1482.
6. R. Byrne, S. Coleman, S. Gallagher and D. Diamond, *Physical Chemistry Chemical Physics*, 2010.
7. C. J. Wohl and D. Kuciauskas, *Journal of Physical Chemistry B*, 2005, **109**, 21893-21849.
8. J. N. A. Canongia Lopes and A. A. H. Padua, *The Journal of Physical Chemistry B*, 2006, **110**, 3330-3335.
9. S. Coleman, R. Byrne, S. Minkovska and D. Diamond, *The Journal of Physical Chemistry B*, 2009.
10. A. K. Burrell, R. E. D. Sesto, S. N. Baker, T. M. McCleskey and G. A. Baker, *Green Chemistry*, 2007, **9**, 449-454.
11. S. P. Coleman, R. Byrne, S. Minkovska and D. Diamond, *The Journal of Physical Chemistry B*, 2009.
12. J. Dupont, *Journal of the Brazilian Chemical Society*, 2004, **15**, 341-350.
13. U. Schroder, J. D. Wadhawan, R. G. Compton, F. Marken, P. A. Z. Suarez, C. S. Consorti, R. F. d. Souza and J. Dupont, *New Journal of Chemistry*, 2000, **24**, 1009-1015.
14. M. G. Del PoÌpolo, C. L. Mullan, J. D. Holbrey, C. Hardacre and P. Ballone, *Journal of the American Chemical Society*, 2008, **130**, 7032-7041.
15. K. J. Laidler and J. H. Meiser, *Physical Chemistry*, 3rd edition edn., Houghton Mifflin, Boston, 1999.
16. R. Byrne, K. J. Fraser, E. Izgorodina, D. R. MacFarlane, M. Forsyth and D. Diamond, *Physical Chemistry Chemical Physics*, 2008, **10**, 5919-5924.
17. X. Song, J. Zhou, Y. Li and Y. Tang, *Journal of Photochemistry and Photobiology A: Chemistry*, 1995, **92**, 99-103.
18. K. J. Fraser, Monash University, 2008.

7

Conclusions and Future Work

7.1 Conclusion

Fundamental to all liquids are the diffuse interactions which result in moderate cohesive effects between solvent molecules. One of the most common molecular solvents, water, is an example of extensive interactions whereby hydrogen bonding results in a weak network resembling a mesh formation when a 2-D cross section of the liquid is examined. While polar protic and polar aprotic molecular solvents exhibit varying strengths of interaction, the small size of the solvent molecules and unimolecularity of the system results in an homogeneous system with similar properties throughout. This is generally accepted as common property for the majority of molecular solvents. Solvatochromic probe dyes utilise this homogeneity through the interaction of their permanent dipoles analyse the chemical properties of the liquid environment. Since the system is assumed to be homogeneous, the properties are also assumed to be similar throughout the entire solvent. Ionic liquids, however, present far more complex systems which require a new approach to fully understand their unique properties. Chapter 2 investigated the obstacles of ionic liquid characterisation by comparing polarity parameters found in ionic liquids to those established in molecular solvents using traditional solvent probes and examining the solvent sensitive, thermal relaxation properties of spirocyclic compounds. The resulting lack of correlation with traditional probe dye parameters and spirocyclic thermal relaxation confirmed that ionic liquids present far more complex systems than molecular solvents. The large molecular size and asymmetric distribution of charge across the ions results in ordering of the liquid components into several regions with unique and contrasting characteristics which differentiate them from homogeneous molecular solvents. The lack of correlation for traditional probe dyes in ionic liquids was concluded as the probes being ‘trapped’ within one particular region of the liquid and due to the size of this region all probe dyes appeared to situate in the same domain. Deviations from expected trends such as polarity $E_T(30)$ and rate constants (k_f) in ionic liquids, observed by addition of spirocyclic compounds to ionic liquids containing a diverse range of cation and anions, concluded that the ordering within each system may be significantly different. The result is distinctly varied liquid structures and highly varied chemical properties. As such, it was proposed that spirocyclic probe dye characterisation may only be able to compare and contrast ionic liquids containing a common base structure such (as a common cation structure like an imidazolium ring) and monitor the effect of changes to system ordering resulting from the alterations to the cations such as functionalisation. It was also concluded that such deviations may also be related to the loss of solvent-solute equilibria during the thermal relaxation of the spirocyclic compounds. Examination of the data presented in this thesis appears to compliment these findings and would appear to define ionic liquids as super-associating liquids due to the prevalence of internal structure and void spaces within the highly charged environment. However, the combination of physical properties such as higher viscosities and the strength of interactions which mediate the formation of IL nano-structuring may result in a more rigid solvent system which cannot fully appreciate changes in solutes/reactants in the time scale required for thermodynamic parameters to be accurately quantified by established equations (Eyring and Arrhenius). Although these equations are not in essence incorrect, it is proposed that possible additions of another component to the equations to compensate for the unique equilibrium of ionic liquids and the interactions not normally significant in molecular solvents may help to rectify this inconsistency and accurately describe the ionic liquid process.

Chapter 3 examined the effects of cation side-chain length and found interesting correlations between thermodynamic and kinetic parameters and increasing alkyl-chain lengths. This implies that spirocyclic compounds are sensitive enough to detect structural effects of the liquids within close proximity to their location. It is found that the photoswitching of the compound results in conformation changes and the formation of distinct charge sites which are mediated by the solvent system. It is believed that the spirocyclic compounds are therefore able to migrate between the different nano-domains depending on the form (**BSP/SO–MC$_{\mathbf{BSP/SO}}$**) of the compound. In addition to this, the solvents ability to reorder around the spirocyclic compounds upon photoswitching becomes a critical factor as it is the effect upon thermal relaxation observed by this stabilisation that is related to the strength of inter-ion interactions which is indicative of the formation of bulk structuring within the ionic liquids. These changes in the thermodynamic parameters are thus related to the *physical* properties of the liquid which are believed to be central to the unique properties of the liquids and traditional probe dyes were unable to detect. However, spirocyclic still appeared to fail in becoming truly dynamic probes as they still did not possess the ability to effectively probe the *global* properties of the liquids as the interaction involved migration within certain regions which provided the best stabilisation for the spirocyclic compounds. Less stable regions, particularly frontiers between each nano-domain may also exist with their own local properties (a mixture of both domains influences) but are ignored by the probes as they migrate to the more stable regions.

Chapter 4 examined the possibility of overcoming this problem by pre-positioning of the probe within each region of the liquid through covalent attachment of functional groups which preferentially interact with the desired regions within nano-structured system. Distinct changes in thermodynamic properties for the thermal relaxation of spiropyran in the same ionic liquids implied that such processes were effective in examining each domain and comparison of the effects allows for a global 'map' of the properties of the liquids. Unfortunately, to examine different classes of ionic liquids it would be expected that many derivatives of spiropyran would be required to be synthesised and due to the large number of possible ionic liquids, this may not be feasible. For this reason it is concluded that either a 'universal' probe which can effectively migrate within the domains of an ionic liquid or three generic probes which interact with the 'polar', 'non-polar' and 'intermediate' domains thru similar interactions in each class of ionic liquid allowing for the a somewhat uniform method of analysis.

While the effectiveness of spirocyclic compounds is largely due to the ability of the compounds to disrupt the structuring of the liquids, it appeared that the strength of ion-ion interaction, specifically Liquid Ion Pair (LIP) formation, and the ability of the liquid to resist the disruption of such interactions is a critical parameter for determination of the overall properties of the ionic liquids as found in Chapter 5. It has therefore become apparent from this study that the ‘ionicity’ of ionic liquids appears central to these atom-scale properties. The formation of ion pairs can be seen to drastically effect the ability of the liquids to act as charged environments and strong ion paired liquids may even be said to approach almost molecular solvent like with neutral solvent components. The ability of the liquid to form these ion pairs directly affects the ability of the liquid to form the bulk structures observed in the liquids which in turn mediate the chemical processes or ‘ionic liquid effect’ found within these solvents. While spirocyclic compounds have been found to be far more sensitive at detecting these parameters by somewhat probing several regions within the liquids, the compounds still lack the ability to effectively interact with sufficient changes to allow so the formation of an ionic liquid scale. However, the unique characteristic that provides spirocyclic compounds as successful initial probes in ionic liquid characteristics is their ability to essentially observe both ‘ionicity’ and ‘ionic liquid effects’ simultaneously. The rate at which the compound thermally relaxes to its closed form is dependent upon the stabilisation of the **MC** forms of the compounds. Omitting the obvious steric effects, this is based upon interactions such as hydrogen bonding and van der Waals forces which are chemical processes or the ‘ionic liquid effect’. The disruption of ordering within the ionic liquids and the changes in the thermodynamic properties of the system is also related to the transport properties of the liquid and the strength of the ion-pairs present within the liquid environment. The ability of spirocyclic compounds to quantify such effects can be used as a method of parameterisation of the ‘ionicity’ of ionic liquids.

For effective molecular probe analysis, they must be able to dissociate even the strongest ion pairs to some degree. In addition to this, molecules must be somewhat neutral to the differing bulk structures which are primarily cation-cation interaction dependent and this may be possible by the future probe molecules interacting very closely with an individual ion pair (or a very limited number) and reporting this interaction. Successful probing of the bulk structures of ionic liquids would still probably require the use of specific derivatives of the molecules with methods proven in Chapter 4 whereby the creation of spirocyclic compounds that integrate into the liquid structure in different locations of the liquids. The creation of such probes should be more defined with liquid models first devised to show the ion pairing (Quantum mechanical) and bulk order (Molecular Dynamics) to determine the number of different regions and were the probe should be placed to return the maximum amount of data. As such, the traditional method of solvent characterisation under a single parameter such as polarity appears outdated for ionic liquids. To characterise these liquids it appears that the creation of a table describing regional characteristics for each containing multiple parameters for each will establish the clearest picture of ionic liquid properties and the ability to chose liquids with ideal characteristics for chemical processes and predict the properties when a new ionic liquid is formed.

Spirocyclic compounds, particularly **BSP**, have been shown to allow for a complete analysis of ionic liquids. However, further work in the tailoring of such compounds to associate with all regions (polar, non-polar and their intermediates/frontiers) of the liquids to ensure all physicochemical properties are appreciated. The ability to integrate the spirocyclic moiety into the ionic liquid structure may be of interest for the production of liquids containing photoswitchable control over parameters such as transport and rheological properties. The control of such effects may be due to the ability to disrupt the Liquid Ion Pair (LIP) formation of the liquids and not solely the bulk structure as previously thought. LIP formation is now believed to be more critical to ionic liquid properties as these interactions appear to be the basis of the formation of several, if not all, unique and advantageous properties attributed to ionic liquids. The ability to augment or disrupt such processes may therefore allow for the formation of ionic liquid based smart materials and the generation of a novel class of phase changeable liquids.

7.2 Future work

The following section represents recommendations to future directions of studies following the work outlined in Chapters 2-5. In addition to probing the interactions of the liquid with photoactive probe molecules to determine characteristics of each domain, the interactions may possibly be optimised to allow for the creation of functionalised ionic liquids whereby the transport properties may be altered my photoswitching of the spiropyran functionalised liquid structure.

Further work would be benificial in the synthesis of more specific photochromic molecules which can interact more dramatically with the ionic liquid structure. As discussed in Chapter 5, the ability to disrupt LIP formation and the abilty to physically disrupt the bulk structure, believed to be observed throughout this study with spirocyclic compounds, it may be possible to create photoswitchable ionic liquids. Such liquids could endow ‘catch and release’ mechanisms for sensors or drug delievery as well as the formation of molecular switches. Focus should be on the formation of compounds that can more effectively compete with the components of the liquid structure such as being more attractive to the anion that tne liquid cation when the compound is in a particlar state. Increasing the compatability of the compounds with the liquids will also allow for higher concentrations to be dissolved within the liquids and thus increase the effects initally observed above. Parallel to sensor formation, the creation of more sensitive probe dyes appears important to ensure that all features of ionic liquids are appreciated. Current probes have been optimised for molecular solvents and then applied to ionic liquids. The formation of a novel probe specifically for ionic liquids and possibly alteration of existing thermodynamic equations may allow for further increased unerstanding of these interesting materials.

The electroactive nature of ionic liquids also presents a promising avenue for suture research into ionic liquid properties and their future application within devices such as sensor systems. The possibility of field effects upon the liquids themselves, in addition to their to facilitate current through ionic conductivity may open up may possibilities as valuable transduction systems. Tailoring of the IL ions may allow for specific interactions which in turn can alter the electrical properties of the liquid which in turn is manifested as a change in a measurable paramter such as voltage or current. The ability to create almost ‘limitless’ variations of these materials combined with their green potential bodes well for their future within chemistry and potential for ionic liquids to become a major contributer to modern science and commercial application.

Appendix

A-1 Cleaning of ionic liquids

It has been observed that ionic liquid purity is subject to scrutiny due to its inability to form liquids of spectroscopic grade. Although levels of impurities are below 1% and typically not detectable[1] it has been found that they are still nonetheless a significant source of interference when used as solvents for spectroscopy. Since characterisation of the solvents themselves and solutes dissolved within the ionic liquids was the goal of this study, it was important for the ionic liquids to have no interference effects. Probe dye absorbance maxima may become shadowed by peaks formed due to these impurities and result in an inability to measure these parameters. In addition to this, the inclusion of impurities may cause inaccuracies due to competing interactions between these impurities and the solute.

'Crude' ionic liquids (Commercially available ILs or ILs produced without cleaning pre-metathesis salts) resulted in coloured liquids which absorbed below 400nm. Previous studies have found that the impurities found in the ionic liquids were not of concentrations sufficient for NMR detection and so gave 'clean' spectra.[1] However, optically, the liquids were found to be visibly contaminated and clearly discoloured. Imidazolium based ILs were found to exhibit yellow colourations. Examination of the precursor compounds found that this impurity was found in the pre-metathesis cation salt.

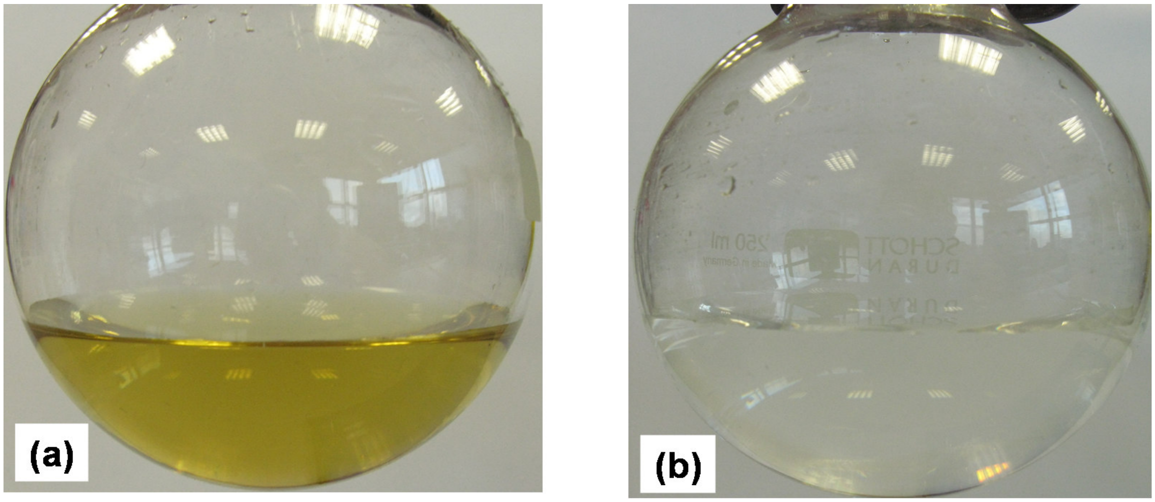

Figure A-1.1 Cleaning of pre-metathesis ionic salts. **(a)** [C_2mIm][Cl] as purchased. **(b)** [C_2mIm][Cl] after cleaning.

Although imidazolium salts appeared highly coloured, ILs such as alkyl ammonium based liquids appeared colourless to the naked eye but still absorbed at lower wavelengths resulting from similar impurity effects in the near UV region. Careful cleaning of the ILs found that the impurities were sufficiently removed that this absorbance was shifted to approximately 350nm with a large reduction in absorption intensity. Figure A-1.2 below shows the effects of cleaning [$N_{1,8,8,8}$][NTf_2] and the ability to use Kamlet-Taft probe dyes to examine solvent properties.

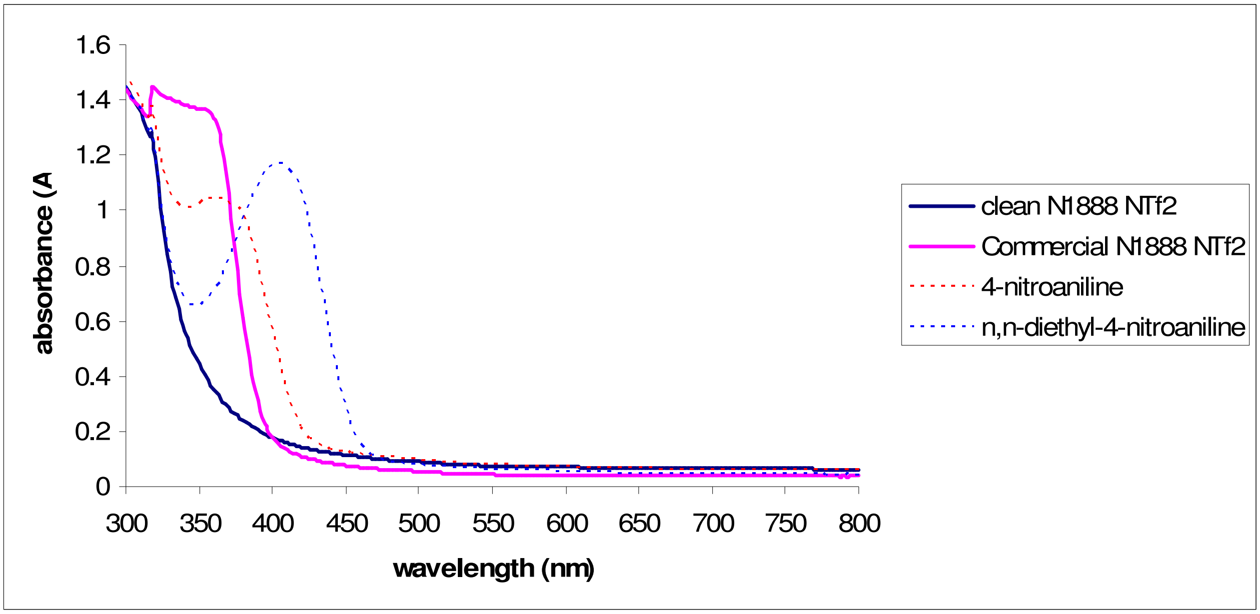

Figure A-1.2 Spectra of $[N_{1,8,8,8}][NTf_2]$. Commercial quality and lab synthesised (cleaned). Dotted lines represent probe dye absorbance maxima in clean IL. n,n-diethyl-4-nitroaniline would be shadowed completely without cleaning

Due to the hygroscopic nature of ILs. All liquids synthesised were dried thoroughly by heating to 65°C under high vacuum for 24 hours. The resulting dried liquids were then stored under nitrogen to exclude absorption of atmospheric water which could act as an interferent to the IL itself or solute molecules within it.

A-2 Reproducible irradiation of Ionic Liquids

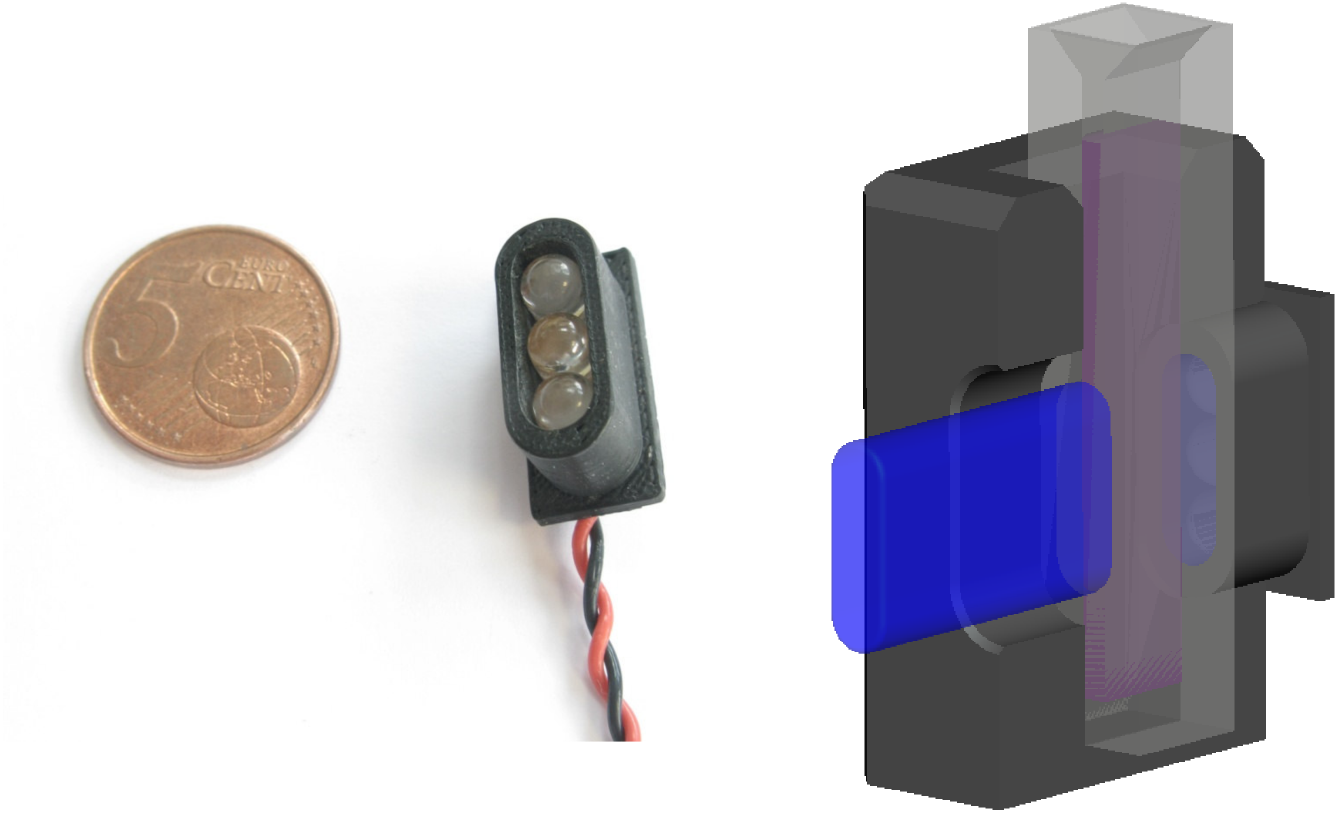

Figure A-2.1 Fabricated UV LED system and its placement within the Cuvette holder within spectrometer

3 LED UV light system (375nm) was designed and constructed with kind help with Dr Stephen Beirne of CLARITY on a Dimension sst 768 3D printer system using Pro Engineer CAD software. The resulting holder fit into the thermostat light path window exactly and due to precision design, allowed for irradiation of each sample reproducibly.

A-3 Example of Excel Plots for determination of kinetic and thermodynamic parameters

To accurately determine kinetic parameters during this study, thermal relaxation rate constants were collected at varying temperatures (10-30°C in 5°C increments). Each sample was heated to required temperature and allowed to equilibrate for ten minutes. Samples were irradiated with UV light for one minute and subsequently the thermal decay curves were collected. Using equation **(14)** (chapter 2, section 2.3.2) the linear portion of the curves was used to find the first order rate constant (figure A-3.1). To ensure accurate results, linearity less than 0.995 R^2 was excluded.

Thermodynamic parameters were determined using five rate constants collected for each solvent containing the spirocyclic probes and were plotted according to the Arrhenius (equation **(10)**) and Eyring (equation **(12)**) equations (chapter 1, section 1.4.2). The points yielded linear plots (figures A-3.2 and A-3.3) from which thermodynamic parameters were found. Linearity of less than 0.995 R^2 was generally rejected to maintain accuracy of data collected. The following figures display sample dates for determination of these parameters for **BSP** in [C_2mIm][NTf_2].

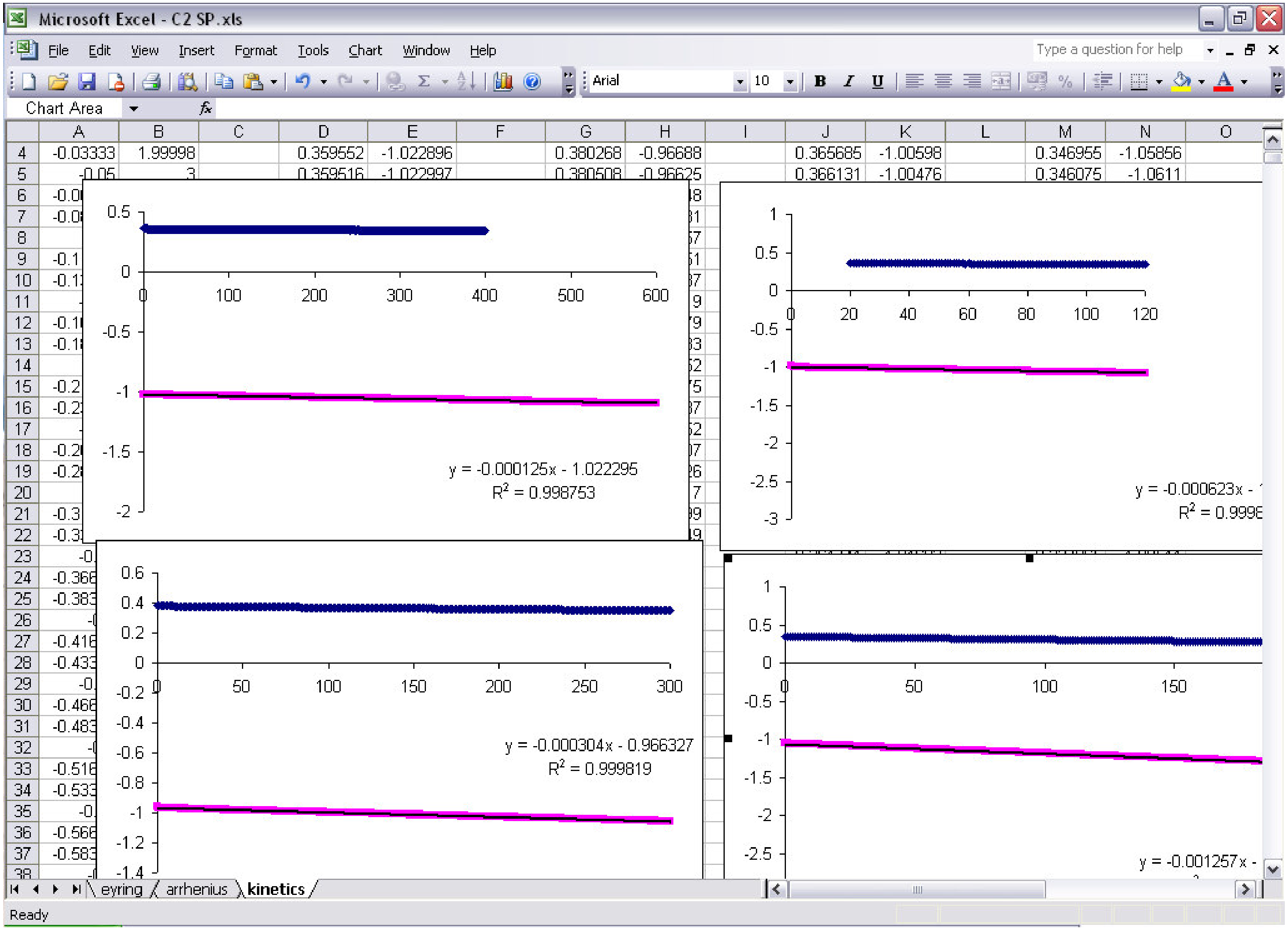

Figure A-3.1 Sample first order plots of **BSP** thermal relaxation at various temperatures in [C$_2$mIm][NTf$_2$].

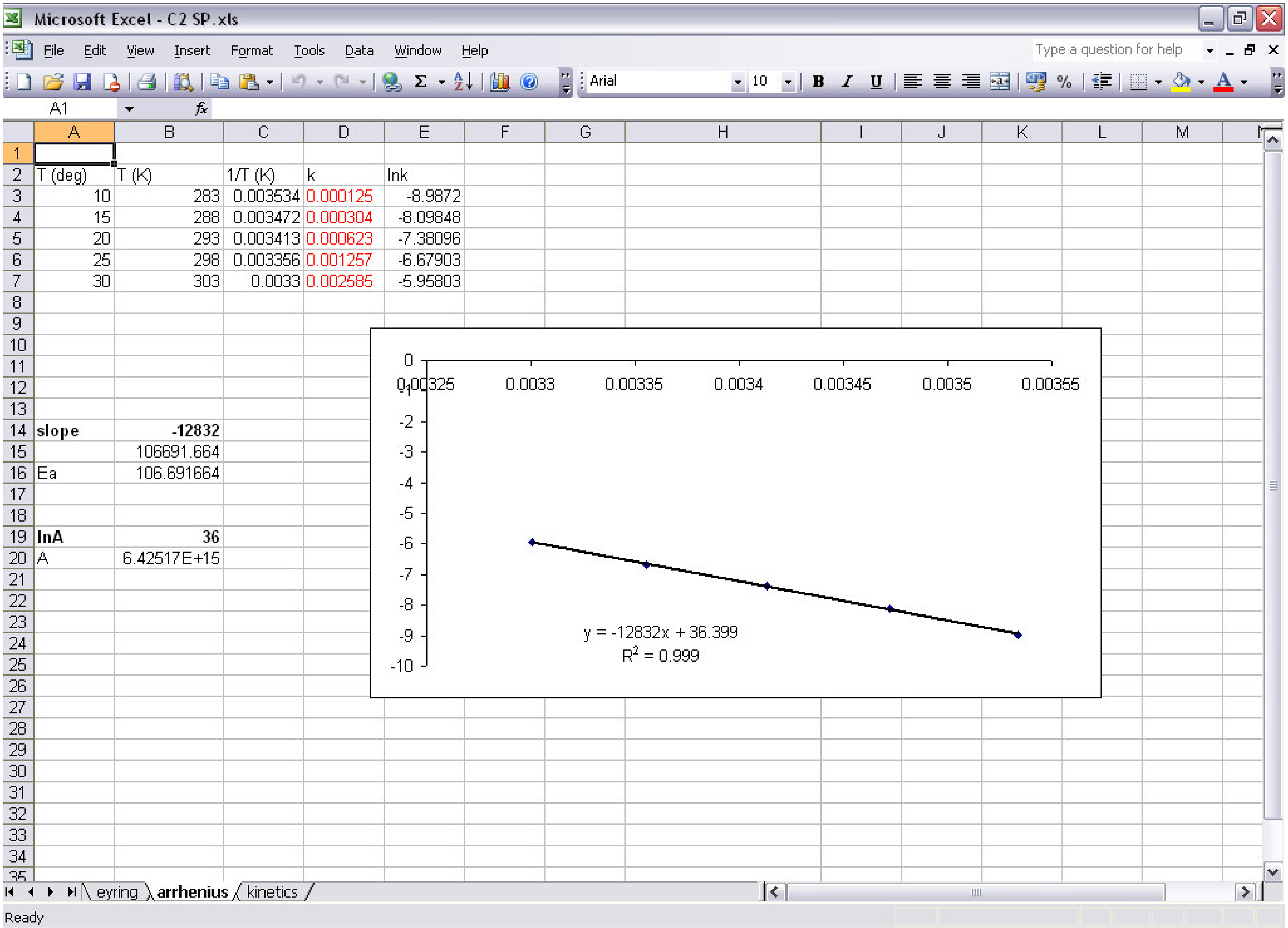

	A	B	C	D	E
2	T (deg)	T (K)	1/T (K)	k	lnk
3	10	283	0.003534	0.000125	-8.9872
4	15	288	0.003472	0.000304	-8.09848
5	20	293	0.003413	0.000623	-7.38096
6	25	298	0.003356	0.001257	-6.67903
7	30	303	0.0033	0.002585	-5.95803
14	**slope**	-12832			
15		106691.664			
16	Ea	106.691664			
19	**lnA**	36			
20	A	6.42517E+15			

Figure A-3.1 Sample spreadsheet of Arrhenius plot for thermal relaxation of **BSP** in $[C_2mIm][NTf_2]$

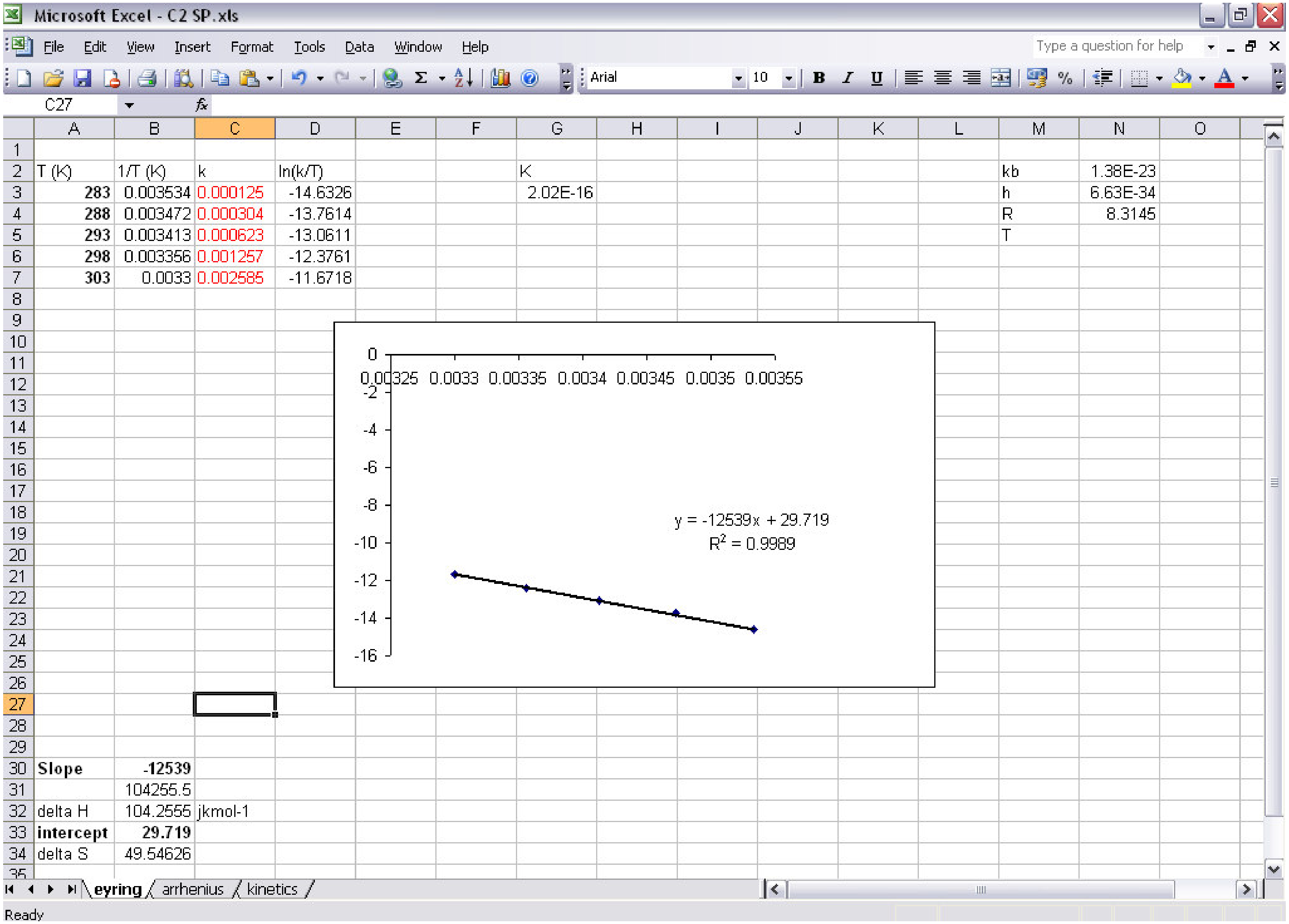

	A	B	C	D	G	M	N
2	T (K)	1/T (K)	k	ln(k/T)	K	kb	1.38E-23
3	**283**	0.003534	0.000125	-14.6326	2.02E-16	h	6.63E-34
4	**288**	0.003472	0.000304	-13.7614		R	8.3145
5	**293**	0.003413	0.000623	-13.0611		T	
6	**298**	0.003356	0.001257	-12.3761			
7	**303**	0.0033	0.002585	-11.6718			
30	**Slope**	**-12539**					
31		104255.5					
32	delta H	104.2555	jkmol-1				
33	**intercept**	**29.719**					
34	delta S	49.54626					

Figure A-3.3 Sample spreadsheet of Eyring plot for thermal relaxation of **BSP** in [C_2mIm][NTf_2]

A-4 Isokinetic plots of BSP and SO in ionic liquids

A method of ensuring that reaction mechanisms remain constant regardless of changes to the ionic liquid ions and thus changes in solvent structure is the preparation of isokinetic plots.[2, 3]

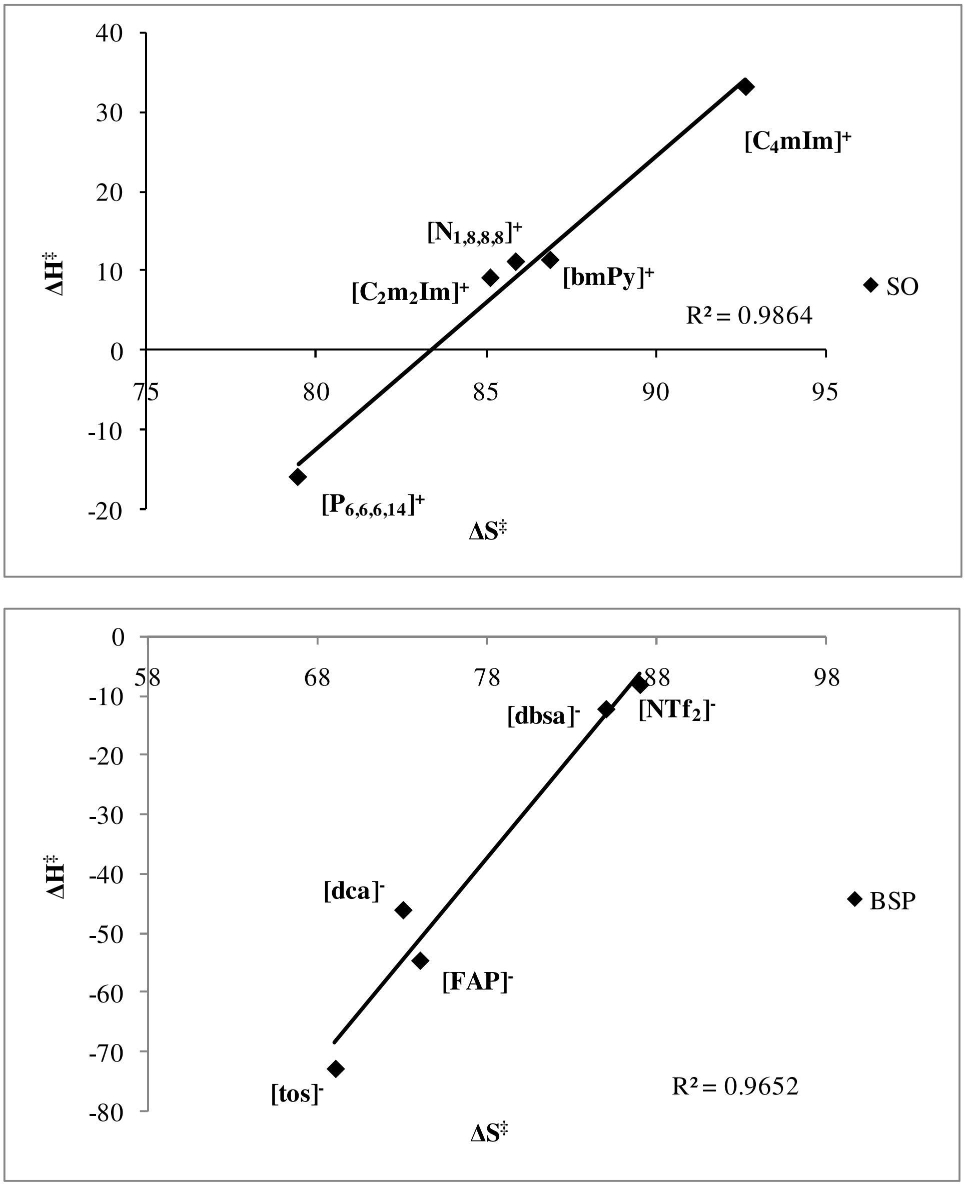

Figure A-4.1 Enthalpy-Entropy plots of thermal relaxation of **SO** (a) and **BSP** (b) in ILs with differing ions studied in Chapter 2.

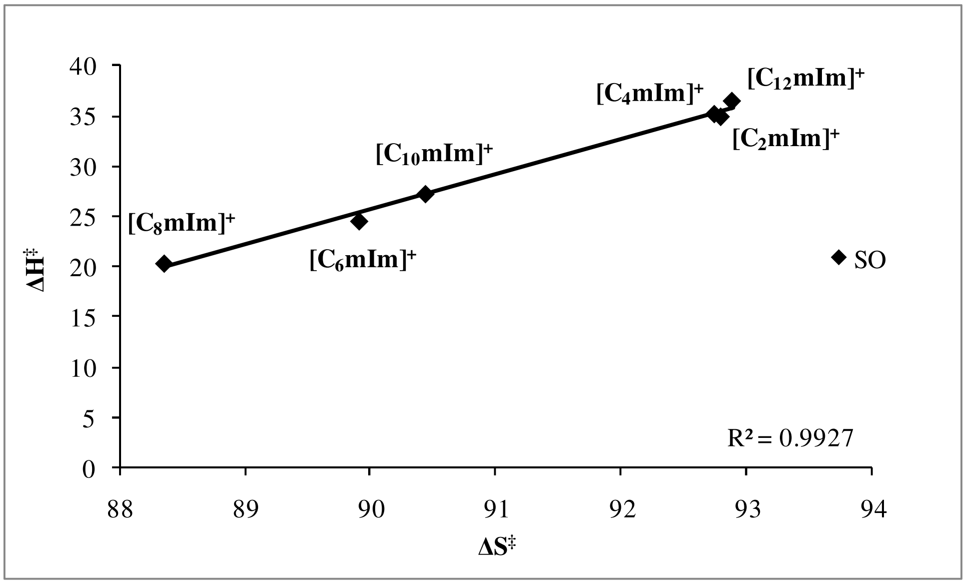

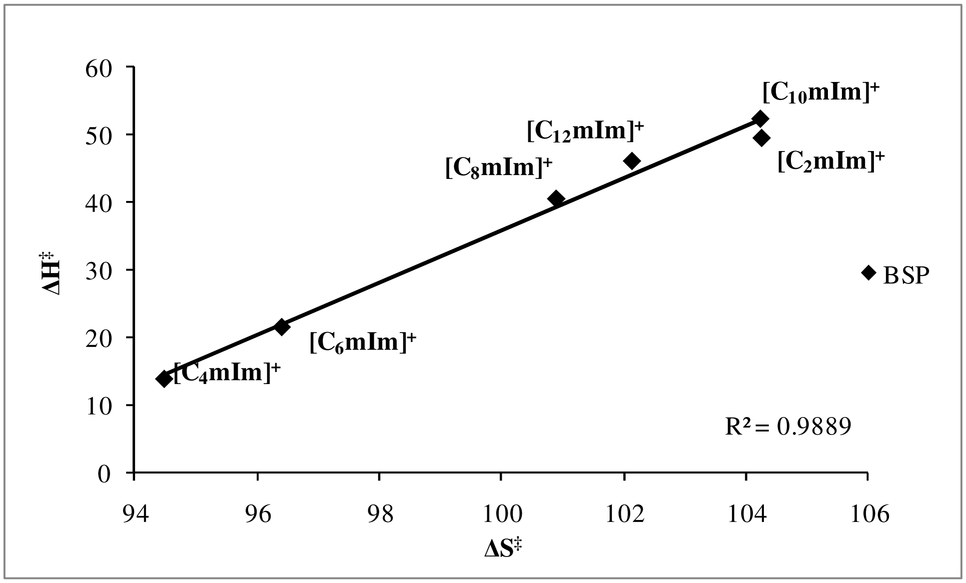

Figure A-4.2 Enthalpy-Entropy plots of the thermal relaxation of **SO** (a) and **BSP** (b) in imidazolium based ILs studied in Chapter 3.

Thermodynamic data collected for chapters 2 (ion change) and chapter 3 (functional chain length) was analysed in this manner to examine its effects upon the thermal relaxation mechanism and thus the ability to compare results. The plots are found to be linear which concluded that such changes in solvent structure and properties appeared to not have any detectable effect on the thermal relaxation mechanism of **SO** or **BSP**. As such it is therefore assumed that changes in thermodynamic parameters were related to changes within the solvent system and it is possible to compare results probed by observation of a similar mechanism in each liquid.

A-5 Characterisation of SP_{Im}

NMR spectra were carried out on a Bruker AVANCE instrument using XWINMR software processed on a Silicon Graphics O2 workstation. The instrument operated at 400 MHz for ^{1}H NMR and 100 MHz for ^{13}C NMR. Mass spectra were recorded on Bruker ESQUIRE LCMS instrument. TGA analysis was conducted using a Perkin-Elmer Pyris TGA in a flowing dry nitrogen atmosphere (50 mL / min.) between 25 and 800 °C with a heating rate of 10 °C / min. DSC traces are presented using the convention of endothermic as up and exothermic as down. All scans were carried out at a heating/cooling rate of 10 ^{o}C /min in the range of -150 ^{o}C – 200 ^{o}C using a TA Q100 series calorimeter.

A. **1-(3-bromoethyl)-2,3,3-trimethylindolenium bromide** was synthesized according to previously published procedure.[4]

B. **1́ - (3″-bromoethyl) - 3́,3́ – dimethyl - 6 -nitrospiro –[2*H*-1-benzopyran-2,2́-indoline] (SP-Br)**

A solution of 1-(3-bromoethyl)-2,3,3-trimethylindolenium bromide (2g, 5.76 mmol) and ethanol (15 ml) was added slowly to a suspension of 5-nitrosalicylaldehide (1g, 5.76 mmol) in ethanol (5 ml). To the reaction mixture was added triethyl amine (0.63g, 5.76 mmol). The reaction mixture was stirred and refluxed over 4 h under nitrogen. The solvent was removed under vacuum and the resulting crude dark brown compound was purified by silica/hexane:ethylacetae 10:1 to afford a bright light yellow compound, 0.23g, yield-10%. Analytical data; ^{1}H NMR (400 MHz) δ ($CDCl_3$): Analytical data; ^{1}H NMR (400 MHz) δ ($CDCl_3$): 1.11 (s, 3H, CH_3), 1.20 (s, 3H, CH_3), 3.31-3.61 (m, 4H, 2 x CH_2), 5.86 (d, H, *J* = 10.4 Hz, CH), 6.52 (d, H, *J* = 7.6 Hz, Ar-H), 6.67 (d, H, *J* = 9.2 Hz, CH), 6.85 (m, H, Ar-H), 7.04 (d, H, *J* = 7.2 Hz, Ar-H), 7.12-7.16 (m, 3H, Ar-H), 7.95 (m, 2H, Ar-H), ^{13}C NMR ($CDCl_3$) δ (ppm): 19.83, 25.88, 29.83, 45.60, 53.00, 106.29, 106.54, 115.61, 118.48, 120.24, 121.75, 122.13, 122.88, 126.06, 127.90, 128.58, 135.84, 141.19, 145.95, 159.16. (m/z ion) calculated for 415.06 $(M+H)^+$ and found 415.2 $(M+H)^+$.

C. **1́ - (3″-methylimidazolioethyl) - 3́,3́ – dimethyl - 6 -nitrospiro –[2*H*-1-benzopyran-2,2́-indoline] bromide (SP-Imidazolium)(9)**.

1́ - (3″-bromoethyl) - 3́,3́ – dimethyl - 6 -nitrospiro –[2*H*-1-benzopyran-2,2́-indoline] (SP-Br) (1.11g, 2.67 mmol) was treated with 1-methyl imidazole (0.87g, 10.69 mmol) in (acetonitrile: DMF, 1:1) (15 ml). The reaction solution was heated to 100 ºC, and left to stir over 15 h. The resulting dark red solution was cooled down and washed with ether several times to remove starting material. The resulting light brown solid was filtered off and purified by silica/chloroform:methanol, 3:1, to afford a red neat compound, 0.8 g, yield -60 %. Analytical data; ^{1}H NMR (400 MHz) δ ($CDCl_3$): 1.07 (s, 3H, CH_3), 1.16 (s, 3H, CH_3), 3.64 (t, 2H, CH_2), 3.93 (s, 3H, CH_3), 4.50-4.65 (m, 2H, CH_2), 5.78 (d, H, *J* = 12 Hz, CH), 6.37 (d, H, *J* = 4 Hz, Ar-H), 6.63 (d, H, *J* = 8 Hz, CH), 6.76 (m, H, Ar-H), 6.92 (d, H, *J* = 8 Hz, Ar-H), 6.98-7.02 (m, 3H, Ar-H), 7.52 (s, H, Ar-H), 7.61 (s, H, Ar-H), 7.85-7.89 (m, 2H, Ar-H), 10.01 (s, H, Ar-H). ^{13}C NMR ($CDCl_3$) δ (ppm): 19.92, 26.02, 36.65, 44.38, 49.22, 52.61, 106.24, 106.48, 115.47, 118.44, 120.83, 121.13, 122.12, 122.97, 123.20, 123.54, 125.92, 127.83, 129.07, 135.71, 137.33, 141.04, 146.03, 158.99. (m/z ion) calculated for 497.11 $(M+H)^+$ and found 497.00 $(M+H)^+$, 417 $(M-Br)^+$, 335.20 (M-Imidazolium ring)$^+$.

Differential scanning calorimetry

m.p: 138.6ºC

Thermogravimetric analysis

Degradation temperature: 292ºC

Water content: 4.4%

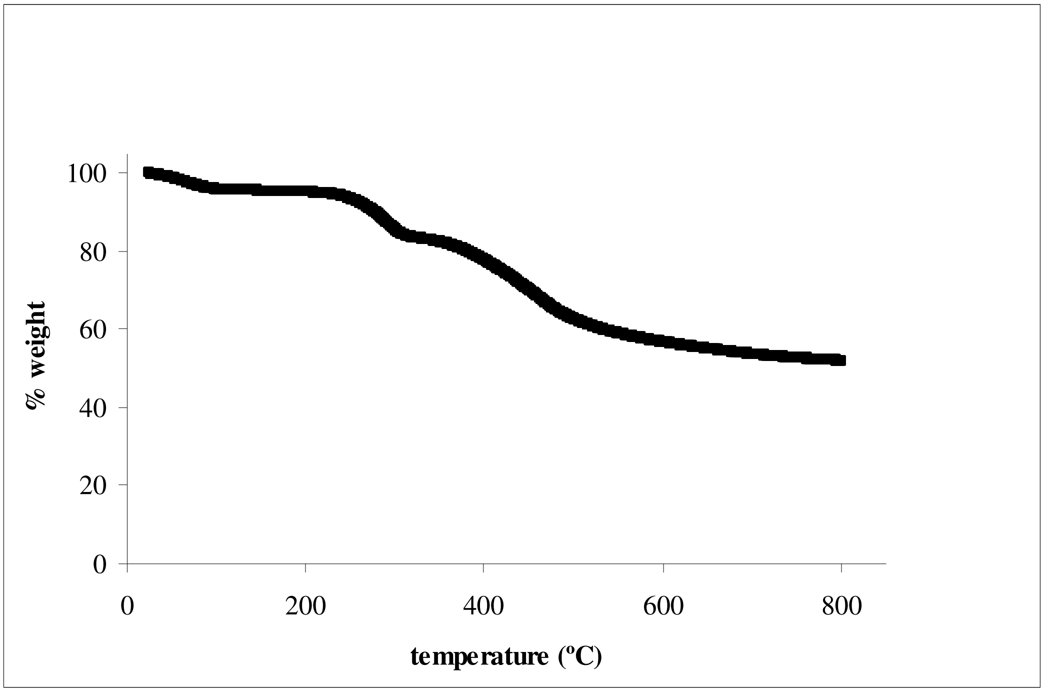

Figure A-5.1 Thermogravimetric analysis of $\mathbf{SP_{Im}}$

A-6 MP2 calculations of MC_{BSP}-ion interactions

*Comparison of B3LYP and MP2 calculated anion-**MC** complexes:* While the post-Hartree Fock MP2 method provides stronger dispersion forces than the HF-DFT hybrid B3LYP functional and so larger magnitude ΔE values (Table A-6.1), the general features of the probe-ion complex geometries are preserved (Figures A-6.1-A-6.3) and the anion-dependent complexation energy difference ΔΔE is similar for both methods, -0.18 eV for MP2 (Table A-6.1) compared with -0.25 eV for B3LYP.

Table A-6.1 Anion-probe complex properties calculated with the MP2 wavefunction.

Complex	Close contact distances (Å)	ΔE (eV)	Δq (a.u)
$[\mathrm{Cl}]^-$: $\mathrm{MC}_{\mathrm{BSP}}$	3.1 ($Cl : H_{N\text{-}CH3}$); 2.6 ($Cl : H_{CH3}$) 3.1 ($Cl : N$)	-1.38	-0.03
$[\mathrm{NTf}_2]^-$: $\mathrm{MC}_{\mathrm{BSP}}$	2.3 ($O_{=S} : H_{CH3}$); 2.8 ($O_{=S} : H_{C6H6}$) 2.7 ($N : H_{N\text{-}CH3}$); 3.1 ($N_{NTf2} : N_{\mathrm{MC}}$)	-1.21	-0.02

Geometries and electronic structures calculated with MP2/6-311++G** model chemistry, as described in the main text. ΔE is the binding energy of the complex, as computed from the MP2 energy of the complex relative to the MP2 energies of the isolated species.

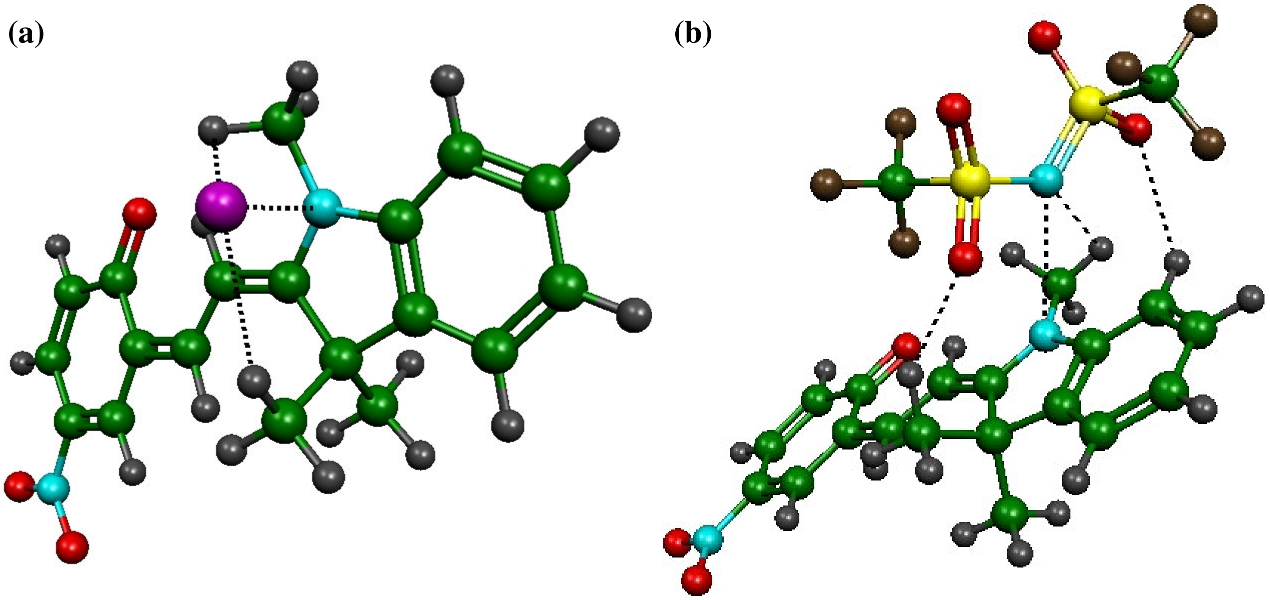

Figure A-6.1 Complexation geometries with close contacts (given in Table A-4.1) marked by dashed lines for charged ion-probe complexes, panel **(a)** the anionic complex with [Cl]$^-$ and **(b)** the anionic complex with [NTf$_2$]$^-$; carbon atoms are green, hydrogens grey, chlorines magenta, nitrogens cyan, oxygens red, sulphurs yellow and fluorine atoms are brown.

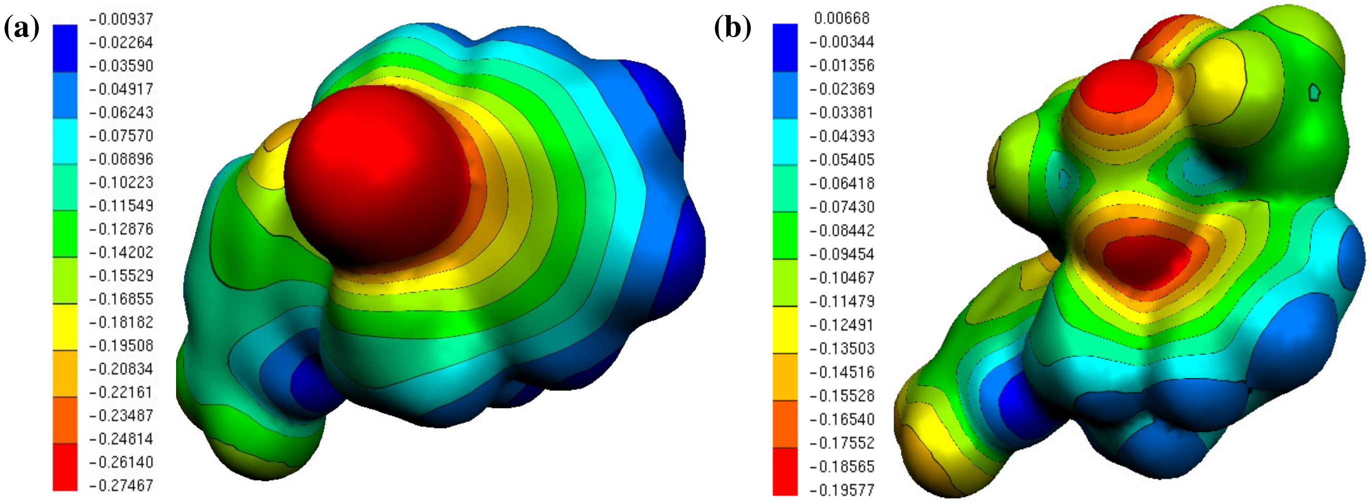

Figure A-6.2 Computed Molecular Electrostatic Potential (MEP) surfaces generated as described in the main text and with surfaces coloured according to regions of net charge as marked in the scale bars, with the scale set in each case according to the largest net negative and net positive sites in each charged ion-probe complexes, panel **(a)** the anionic complex with $[Cl]^-$ and **(b)** the anionic complex with $[NTf_2]^-$.

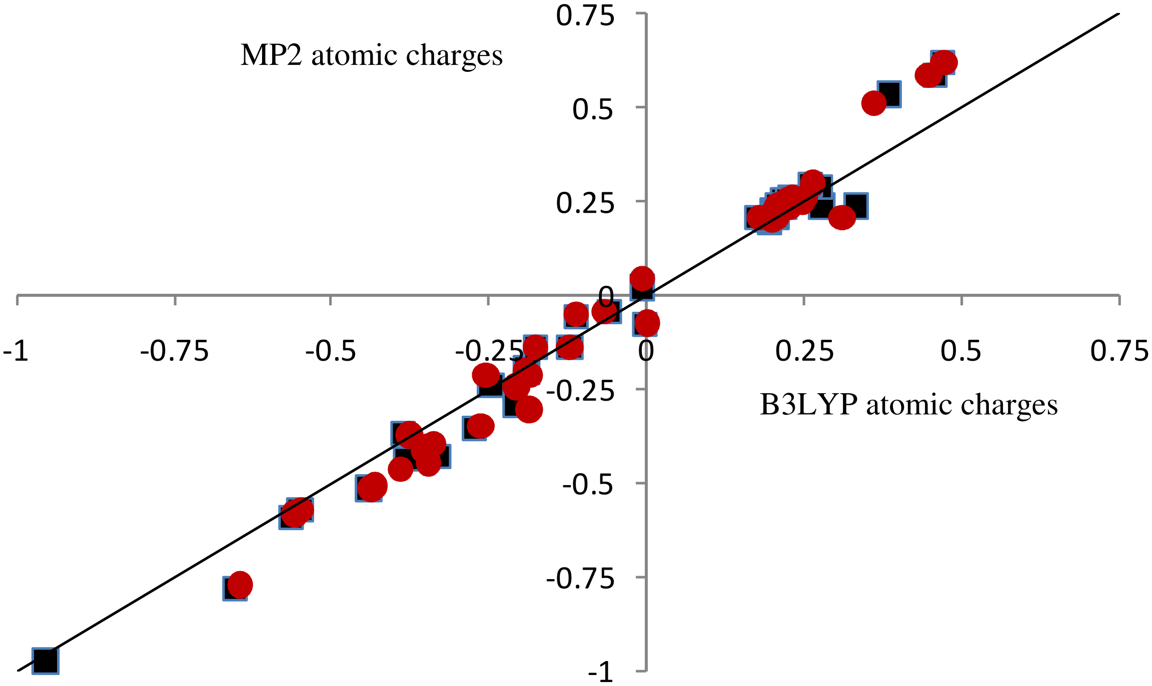

Figure A-6.3 Plots of MP2 vs. B3LYP natural population (see main text) atomic charges computed for **(blue squares)** the anionic **MC$_{BSP}$**:[Cl]$^-$ complex and **(red circles)** the anionic **MC$_{BSP}$**:[NTf$_2$]$^-$ complex. The *y*=*x* black line is included to guide the eye; the magnitudes of the atomic charges are generally slightly larger in the MP2 calculations and both datasets would fit *y*=1.1*x* lines (not shown) with R^2 > 0.95.

Computed [C_2mIm][NTf$_2$] and [C_2mIm]$^+$:MC complexes:

Panel (a) of Figure A-6.4 shows the computed geometries and electrostatic potential surfaces for the [C_2mIm]$^+$ cation paired with the [NTf$_2$]$^-$ anion. The [C_2mIm]$^+$ complex with [Cl]$^-$ is given in Figure 5.2 of the main text. Panel (b) of Figure A-6.4 shows the computed geometries and electrostatic potential surfaces for the EMIm$^+$ cation coordinating the **MC** probe. The corresponding 3-site complexes describing probe stabilisation by the [C_2mIm]-based ILs are given Figure 5.4 of the main text. Figure A-6.5 gives the near-Fermi MO diagram for [C_2mIm][NTf$_2$] together with the MO surfaces that serve to explain some of the observed features in the experimental valence band spectrum.

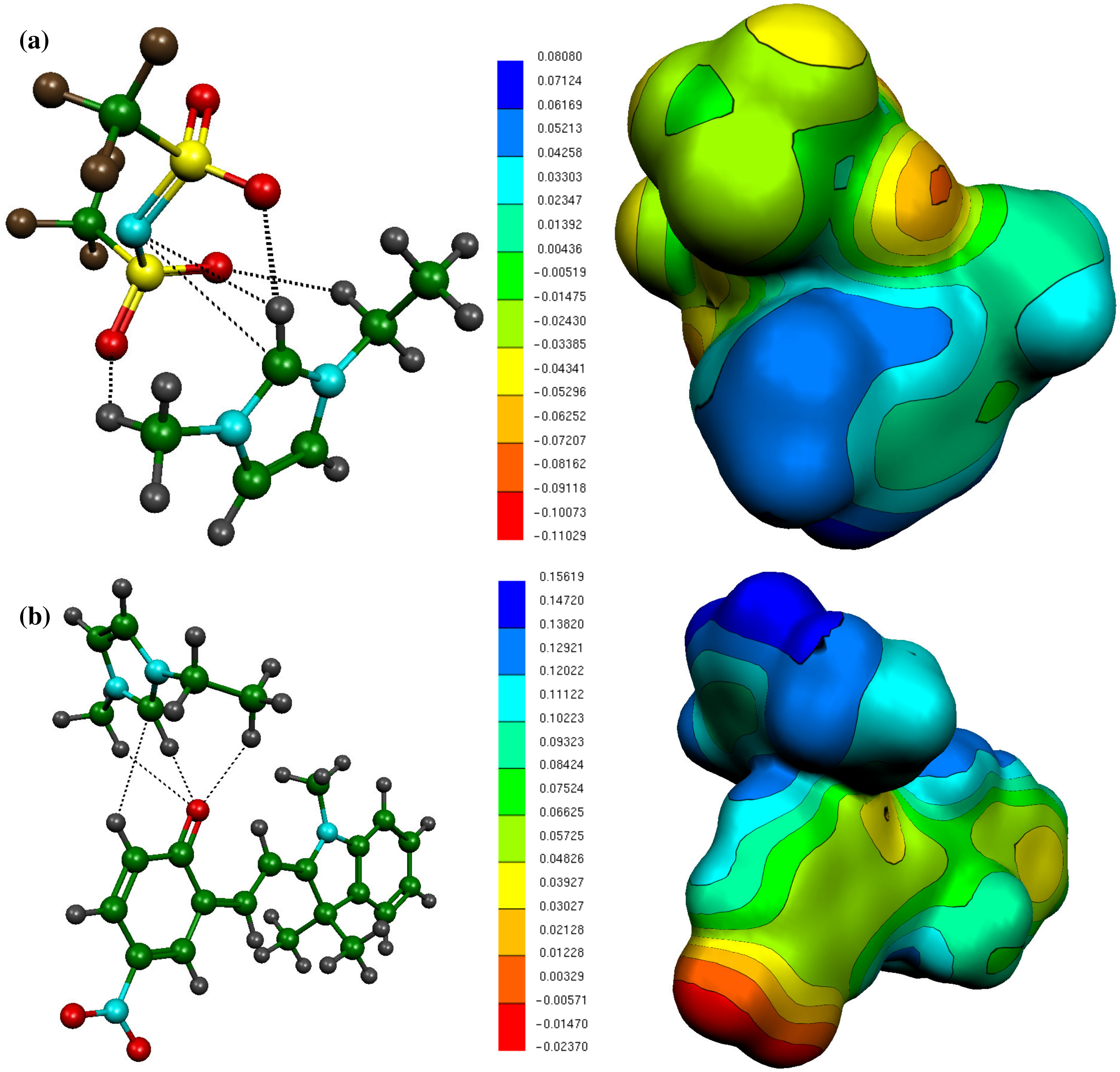

Figure A-6.4 Complexation geometries with close contacts (the corresponding distances are given in Table A-4.1) marked by dashed lines for **(a)** net neutral [C_2mIm][NTf_2] and **(b)** the cationic [C_2mIm]$^+$:**MC**$_{\mathbf{BSP}}$ complex; carbon atoms are green, hydrogens grey, chlorines magenta, nitrogens cyan, oxygens red, sulphurs yellow and fluorine atoms are brown. Also shown are computed Molecular Electrostatic Potential (MEP) surfaces generated as described in the text and with surfaces coloured according to regions of net charge as marked in the scale bars, with the scale set in each case according to the largest net negative and net positive sites in each complex.

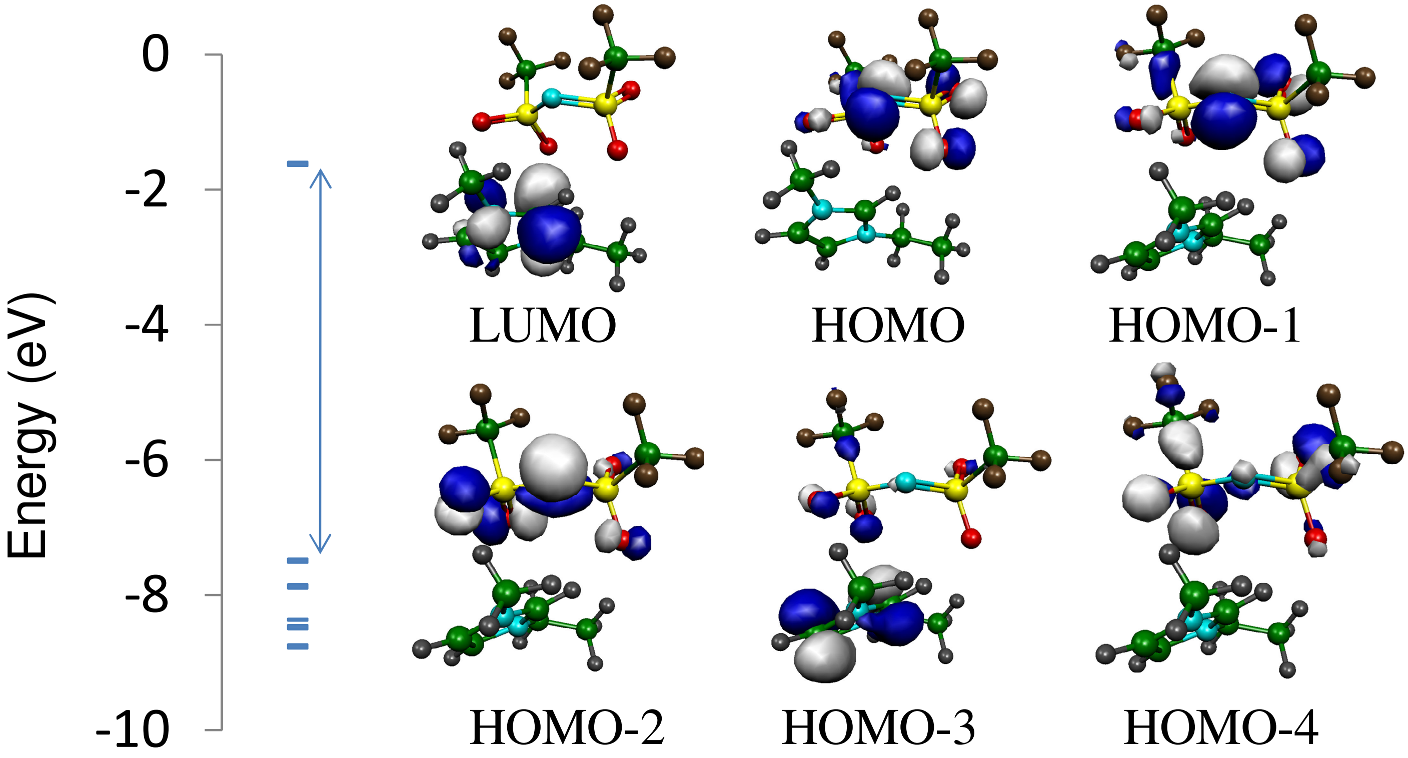

Figure A-6.5 MO diagram with HOMO-LUMO gap as marked, and selected MO surfaces (LUMO, HOMO, HOMO-1, HOMO-2 and HOMO-3) for the net neutral [C_2mIm][NTf_2] complex; carbon atoms are green, hydrogens grey, chlorines magenta, nitrogens cyan, oxygens red, sulphurs yellow and fluorine atoms are brown.

*Control IL:probe simulations replacing **MC**$_{\mathbf{BSP}}$ with the closed **BSP** isomer:* The solvent-perturbed probe photochromism described in this work relies on the stronger interaction of the IL medium with the zwitterionic **BSP** isomer **MC**$_{\mathbf{BSP}}$. Reported below are computed complexes for $[Cl]^-$, $[NTf_2]^-$ and $[C_2mIm]^+$ with the closed **BSP** isomer, together with the corresponding 3-site complexes featuring full IL ion pairs complexed to **BSP**. Table A-6.2 and Figure A-6.6 show the interactions with the closed state; as shown in Figure 1 in the main text, the closed **BSP** isomer features regions of net negative charge centered on the "elbow" between the indoline ring nitrogen and pyran ring nitrogen (maximum negative electrostatic potential is -0.08 a.u., lower than the -1.00 a.u. for the open **MC**$_{\mathbf{BSP}}$ form) and net positive charge centered on the phenyl hydrogens on the nitrobenzene moeity (maximum positive electrostatic potential is +0.05 a.u., lower than the +0.07 a.u. for the open **MC**$_{\mathbf{BSP}}$ form). These weaker interactions for the closed state are reflected in the lower complexation energies given in Table A-6.2, the individual ion interactions with **BSP** are only approximately ¼ (cation interactions with the sterically-constrained N--O "elbow") and ½ (anion interactions with the phenyl hydrogens of the nitrobenzene group) that of the corresponding **MC**$_{\mathbf{BSP}}$:ion binding strengths given in Table 5.1 in the main text. The net complexation energy available for the full IL:probe complexes, subtracting the LIP energy from the IL:probe complexation energy, is at best approximately ⅓ that available with the **MC**$_{\mathbf{BSP}}$ zwitterion, illustrating that the primary effect of the IL medium will be in prolonging the lifetime of the zwitterion with a smaller effect on the stability of the closed form. In essence the calculations support the chemical intuition that the IL will have a much larger influence on the forward, rather than backward, rate of the **MC_{BSP}↔BSP** photoswitch.

Table A-6.2 Calculated **BSP**:ion and **BSP**:IL complex properties.

Complex	**Close contact distances (Å)**	**ΔE (eV)**	**%ΔE vs. MC**
$[Cl]^-$: BSP	2.3 ($H_{Ph}:Cl$)	-0.56	57
$[NTf_2]^-$: BSP	2.3 ($O:H_{CH3N}$); 2.5 ($O:H_{CH3C}$); 2.5 ($O:H_{Ph}$)	-0.37	51
$[C_2mIm]^+$:BSP	2.4 ($H_{CH3}:N$); 2.5 ($H_{CN2}:O$)	-0.20	26
$[C_2mIm]^+$:BSP:$[Cl]^-$	3.0 ($H_{CH3}:Cl$); 2.7 ($C_{CN2}:Cl$); 2.6 ($H_{CN2}:Cl$); 2.9 ($H_{CH2}:Cl$); 2.6 ($H_{Ph}:Cl$)	-0.20	32
$[C_2mIm]^+$:BSP: $[NTf_2]^-$	3.2 ($C_{CN2}:O$); 2.4 ($H_{CH3}:O$); 2.0 ($H_{CN2}:N$); 2.7 ($H_{CN2}:O$); 2.3 ($H_{CH2}:O$); 2.6 ($H_{Ph}:O$); 2.5 ($H_{CH3C}:O$); 2.5 ($H_{CH3N}:O$)	-0.19	30

Geometries and electronic structures calculated with B3LYP/6-311++G**, as described in the main text. ΔE calculated as for the **MC_{BSP}** complexes, comparing two-species complexes with isolated species and full IL:probe three-species complexes with isolated probe and liquid ion pairs. %ΔE values compare complexation energies with closed **BSP** to those calculated for open **MC_{BSP}** (Table 5.1 in the main text).

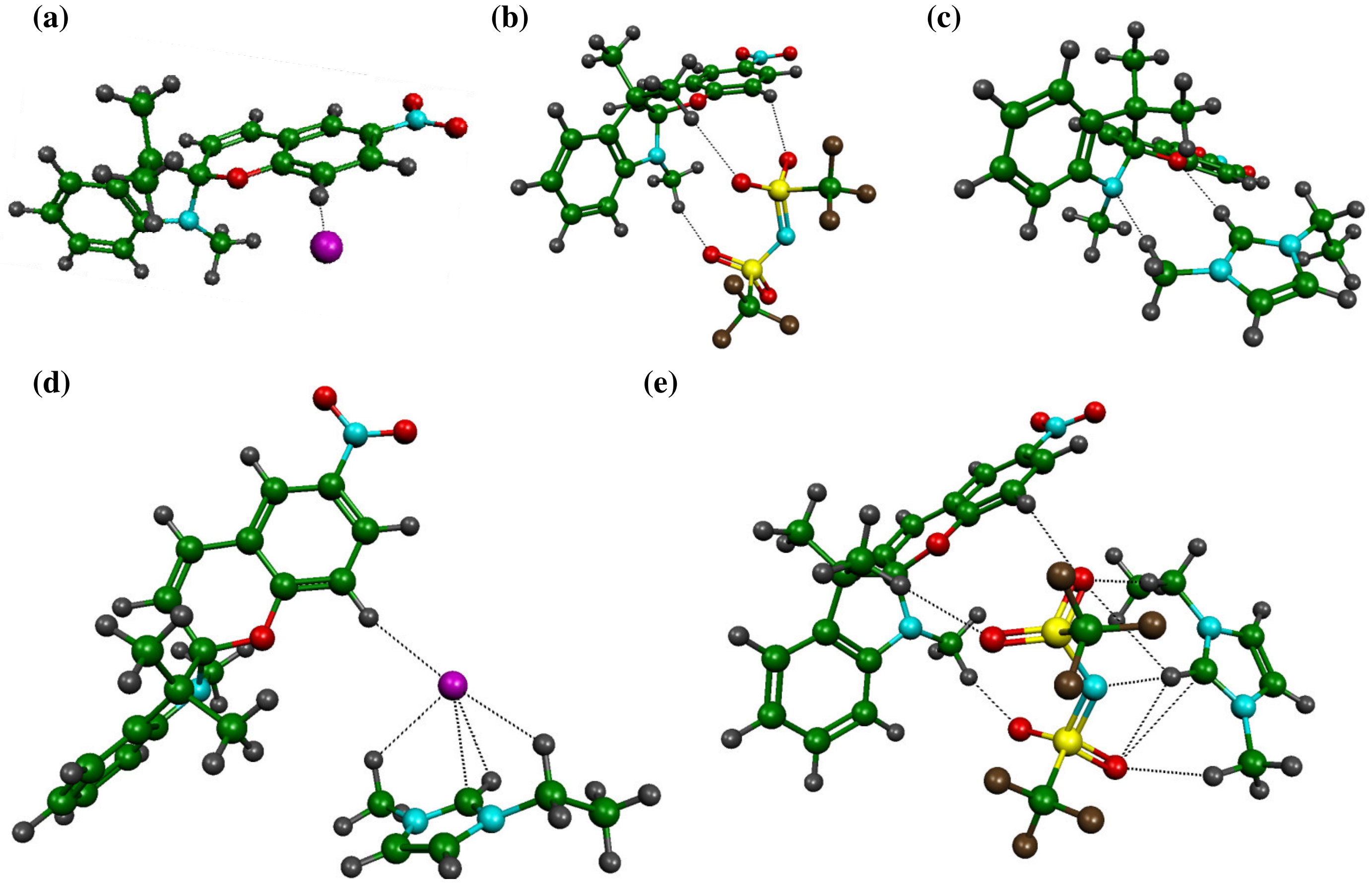

Figure A-6.5 Complexation geometries with close contacts marked by dashed lines and distances given in Table A-4.2 for **(a)** the anionic $[Cl]^-$:**BSP** complex, **(b)** the anionic $[NTf_2]^-$:**BSP** complex, **(c)** the cationic $[C_2mIm]^+$:**SP** complex, **(d)** the net neutral $[C_2mIm]^+$:**BSP**:Cl^- complex and **(e)** the net neutral $[C_2mIm]^+$:**BSP**: $[NTf_2]^-$ complex; carbon atoms are green, hydrogens grey, chlorines magenta, nitrogens cyan, oxygens red, sulphurs yellow and fluorine atoms are brown.

References

1. A. K. Burrell, R. E. D. Sesto, S. N. Baker, T. M. McCleskey and G. A. Baker, *Green Chemistry*, 2007, **9**, 449-454.
2. J. E. Leffler, *The Journal of Organic Chemistry*, 1955, **20**, 1202-1231.
3. D. C. Wigfield and D. J. Phelps, *The Journal of Organic Chemistry*, 1976, **41**, 2396-2401.
4. Y. Hirshberg, *Journal of the American Chemical Society*, 1956, **78**, 2304-2312.